Neuroinflammation and Defining Gene Therapy Approaches for Ovine CLN6 Batten Disease

---

A thesis
submitted in partial fulfilment
of the requirements for the Degree of
Doctor of Philosophy

At
Lincoln University

By

Lucy Anne Barry

Lincoln University
2011

Abstract of a thesis submitted in partial fulfilment of the
requirements for the Degree of Doctor of Philosopy

Neuroinflammation and Defining Gene Therapy Approaches for Ovine CLN6 Batten Disease

By

Lucy Anne Barry

The neuronal ceroid lipofuscinoses (NCLs, Batten disease) are a group of fatal inherited childhood diseases which result in severe cortical atrophy, blindness, seizures, and the accumulation of fluorescent lysosome derived organelles in neurons and most other cells throughout the body. A number of naturally occurring animal models of NCL have been found, the most informative being the CLN6 form in New Zealand South Hampshire sheep. Previous studies in ovine CLN6 have shown a strong correlation between glial activation and subsequent neuronal loss, suggesting that it has a primary role in the development of disease pathology. This thesis describes changes in the expression of inflammatory mediators in affected animals, neuropathological changes that take place in chimeric animals and the implications that these findings have for future therapeutic options.

Quantitative real-time PCR revealed significant increases in the expression of pro- and anti-inflammatory cytokines, TNF-α, IL-1β, TGF-β and IL-10, in the brains of affected animals compared to normal controls. Expression of all four cytokines was significantly increased in affected animals at all ages analysed, including 6 months of age, prior to clinical disease manifestation. These results validate the central role that neuroinflammation is proposed to play in disease pathogenesis and indicates that an atypical, dysregulated inflammatory response is ongoing in affected animals.

Chimeric animals were generated by mixing homozygous affected and homozygous normal blastomeres. Genotypic and histological examination of the resulting chimeric animals indicated a good degree of colonisation of both cell types in the brain and evidence of cross-cell communication. CAT scans revealed that the brain volumes of two chimeras were within the normal brain volume range, whilst three animals had progressively recovering brain volumes. All normal and recovering-like chimeras presented with reduced or absent disease associated glial activation, no evidence of neurodegeneration, normal cortical thickness and

laminar organisation of cells, and no loss of vision, long after these symptoms had progressed to terminal disease in affected animals.

PSA-NCAM staining indicated extended neurogenesis in chimeric animals. Individual PSA-NCAM positive cells were present throughout all cortical layers in chimeric animals, in contrast to affected animals in which newly generated cells are largely confined to cellular aggregates in upper cortical layers. Genotyping brain regions of these animals indicated up to 75% of cells were genotypically affected. Despite this storage bodies were rarely observed indicating that storage had been cleared from most cells. These studies indicate that given the correct environmental milieu newly generated and affected cells can survive and are amenable to correction by normal cells in CLN6 NCL, resulting in an amelioration of disease pathology.

GFP lentiviral vectors injected into the sheep brain resulted in stable cell transductions evident up to 80 days post-injection. Incidental leakage of the vector into the lateral ventricles resulted in GFP expression in ependymal and subependymal cells along the extent of the ventricular surface. Transduced cells included those likely to be type B astrocytic cells, thought to be the *bona fide* adult NSCs. Future therapies targeting this zone of extended neurogenesis in affected animals could lead to the widespread distribution of transduced cells and cross-correction of affected cells in the brain.

Keywords: Batten disease, neuronal ceroid lipofuscinosis, lysosomal storage disorder, animal models, sheep, inflammation, cytokines, microglia, neurodegeneration, chimeras, neurogenesis, neural stem cells, gene therapy.

Acknowledgements

Firstly, I would like to thank my supervisor, Prof. David Palmer, for all of your support and encouragement throughout my PhD, for always having an open door and guiding me through the complicated world of Batten disease. I've certainly had a few ups and downs over the past few years but your positive outlook and expertise have been invaluable in getting me to where I am today. I really appreciate the time and effort you have put into helping me, especially in the past few months when so many other events have been going on. Thanks too for all the fun times and the many stories and tales you've entertained us all with. Thanks also to the very patient Jeanette for opening up your home to me and putting a roof over my head. You made my move to New Zealand a whole lot easier and I really appreciate it.

Thanks to Dr. Jon Cooper for introducing me to the Battens world and accommodating me at the PSDL in London. It was a pleasure to spend time there with the great people in your lab. I'd like to thank Dr. Graham Kay for all of your advice on experimental techniques and design. You always made time to answer my questions and give advice, and I really appreciate it. Thanks to Dr. Tom McNeilly for spending the time to teach me about qPCR and for very kindly donating the plasmids required for these experiments. Thanks to Dr. Stephanie Hughes for putting me up in Dunedin and working on the gene injection trials, and helping with confocal images. Thanks also to Nigel Jay for his help with the sheep, Richard Sedcole for statistical analyses, Manfred Ingerfeld for taking the confocal microscopy images and everyone else that has helped me at some stage throughout my studies.

I'm very grateful to those who provided financial support during my studies. The National Institutes of Health, Neurological Foundation of New Zealand, Pub Charity, the Batten Disease Support and Research Association, and the Massey-Lincoln and Agricultural Industry Trust, without whom this PhD would not have been completed.

Thanks to Nadia Mitchell for being the most organised, helpful, enthusiastic reseacher/ technician a PhD student could ask for. Nothing was ever too big or too small for you to give a hand with and I really appreciate the time that you have spent teaching me techniques, discussing ideas and experiments, and just having a general chat and a moan about things. Thanks also to Karl for all of your help, and to eveyone that's come and gone through our lab over the past few years. There's been a lot of morning teas and a lot of food eaten, but it's been great.

Big thankyou to all my flatmates at Strickland St, Oakford Close and Hagley Ave. You've all offered plenty of encouragemt and at least pretended to be interested in the murky world of neuroscience. And thanks to all my friemds at home in Ireland and here in New Zealand for all the fun, non-PhD times over the past few years, I would have gone crazy without them. Special thankyou to Robin and Gill and all the Muirs for being my kiwi family! I've really enjoyed all the skiing, water-skiing, Tekapo trips, dinners (and especially cheesecakes). It has meant a lot to me and my parents that you've been so generous and welcoming. I hope we can repay the favour some time.

Very special thankyou to my wonderful family. Its not everyone's parents that would support them to move to the other side of the world to do a PhD but you've always encouraged me and allowed me to follow my dreams. Thankyou so much for all the support and making the effort to visit, I've had a great time exploring New Zealand with you. Thanks to Conor and Deirdre, Alan and Fanny, Liz and all my family for your encouragement and the many, many chats, photos and videos to make me feel not quite so far from home.

Last but by no means least, thankyou Matt. You have been a rock over the past four years and it has been so great to have someone who knows exactly how the PhD woes feel. Thanks for putting up with the tantrums and keeping me going, especially in the past few months when I definetly have not been the easiest person to be around! Thankyou so much for showing me around this beautiful, albeit shaky island. You've made New Zealand home for the past four years and I'm looking forward to seeing where we end up next.

Table of Contents

List of Figures

List of Tables

List of Abbreviations

AAV	adeno-associated virus
AD	Alzheimers disease
AFI	amaurotic familial idiocy
ANCL	adult NCL
ATPase	α subunit of the ATPase (Na+/K+) pump
BBB	blood-brain barrier
BDNF	brain-derived neurotrophic factor
BDSRA	Batten Disease Support and Research Association
CAT	computed axial tomography
CLN	NCL causing gene
CNS	central nervous system
COX	cyclo-oxygenase
CSF	cerebrospinal fluid
CTSD	cathepsin D
DAB	3, 3'-diaminobenzadine
DCX	doublecortin
DNA	deoxyribonucleic acid
EDTA	ethylenediaminetetraacetic acid
ER	endoplasmic reticulum
ERT	enzyme replacement therapy
ESC	embryonic stem cells
GABA	γ-aminobutyric acid

GAPDH	glyceraldehye-3-phosphate dehydrogenase
GDNF	glial cell-derived neurotrophic factor
GFAP	glial fibrillary acidic protein
GFP	green fluorescent protein
GnRH	gonadotrophin-releasing hormone
GROD	granular osmiophilic deposits
GSB4	Griffonia simplicifolia isolectin type I-B4
HD	Huntingtons disease
HO-1	heme oxygenase-1
HRP	horseradish peroxidase
ICM	inner cell mass
IFN	interferon
IGF-1	insulin-like growth factor-1
IL	interleukin
INCL	infantile NCL
iNOS	inducible nitric oxide synthase
Jak/STAT	janus kinase/signal transducers and activators of transcription
JNCL	juvenile NCL
LDS	lithium dodecyl sulphate
LINCL	late infantile NCL
LPS	lipopolysaccharide
LSD	lysosomal storage disease
MAPK	mitogen-activated protein kinase
MFSD8	major facilitator superfamily domain containing eight
MHC	major histocompatibilty complex

MND	myeloid sarcoma virus
MPS	mucopolysaccharidosis
MRI	magnetic resonance imaging
MS	multiple sclerosis
NCBI	National Centre for Biotechnology Information
NCL	neuronal ceroid lipofuscinoses
NF	normalisation factor
NF-κB	nuclear factor-κB
NGF	nerve growth factor
NGS	normal goat serum
NO	nitric oxide
NPC	neural progenitor cell
NSC	neural stem cell
PAGE	polyacrylamide gel electrophoresis
PBS	phosphate buffered saline, pH 7.4
PBST	phosphate buffered saline, pH 7.4, containing 0.3% Triton X-100
PCR	polymerase chain reaction
PD	Parkinsons disease
PPT1	palmitoyl protein thioesterase 1
PSA-NCAM	poly-sialated neural cell adhesion molecule
qPCR	quantitative real-time polymerase chain reaction
REML	restricted maximum likelihood method
RNA	ribonucleic acid
RNAi	RNA interference
ROS	reactive oxygen species

RPLPO	large ribosomal protein PO
RT	room temperature
SAP	sphingolipid activator proteins
SNP	single nucleotide polymorphism
SOCS	supressor of cytokine signalling proteins
SVZ	subventricular zone
TBS	Tris buffered saline, pH 7.4
TEMED	tetramethylethylenediamine
TGF	transforming growth factor
TNF	tumour necrosis factor
TNF-R1	TNF-receptor type I
TNF-R2	TNF-receptor type II
TPP1	tripeptidyl peptidase I
vLINCL	variant late infantile NCL
VSV-G	vesicular stomatitis virus glycoprotein
ZSF	zinc salt fixation

Chapter 1
Literature Review

1.1 Neuronal ceroid lipofuscinosis - An overview

The neuronal ceroid lipofuscinoses (NCL, Batten disease) are a group of fatal inherited childhood diseases that collectively constitute one of the most common types of inherited neurodegenerative diseases in childhood. They are inherited mainly as autosomal recessive traits and affect up to 1:12,500 live births worldwide (Rider and Rider, 1988). Onset is usually during childhood and adolescence, but rare cases of adult and newborn onset have been reported. Affected children start life normally but develop clinical symptoms, characterized by progressive mental and motor deterioration, blindness and behavioural changes. They sleep poorly, suffer nightmares and hallucinations, and fits and seizures, which are difficult to control, while the rare adult-onset forms are characterized by psychological problems and/or dementia (Goebel et al., 1999a; Mole et al., 2011). Different mutations in different genes underlie the NCLs but all forms are morphologically identified by the near-ubiquitous accumulation of fluorescent lysosome derived organelles (storage bodies) in neurons and most other cells throughout the body (Goebel et al., 1999b), as well as progressive and selective loss of neurons, predominantly from the cerebral and cerebellar cortices. This loss is coupled with astrocytic proliferation and hypertrophy, and macrophage infiltration. All NCLs are currently untreatable and usually lead to an early death between 7 years of age and early adulthood (Mole et al., 2005).

These are relentlessly progressive disorders which constitute a significant emotional, psychological, physical and financial burden on families with affected children. Patients live in a progressively deteriorating state, from several years to as long as 43 years, depending on the age of onset (Rider and Rider, 1999). The NCLs include three classic childhood-onset forms: infantile (INCL, CLN1), late-infantile (LINCL, CLN2), and juvenile (JNCL, CLN3); as well as four LINCL variants (vLINCL): CLN5, CLN6, CLN7 and progressive epilepsy with mental retardation (northern epilepsy, CLN8). In addition, there is a congenital (CLN10) form and proposed adult-onset (ANCL, CLN4) and CLN9 forms. Each CLN protein is present within the endosomal-lysosmal system and there is evidence that they are all either trafficked through or present in the endoplasmic reticulum (ER)-Golgi system (Weimer et al., 2002). The symptoms and storage body composition similarities between each form of NCL strongly indicates that disruption of a common process is a key event.

NCL has a worldwide distribution and a number of widespread common mutations have been identified for most forms, although certain forms have country-specific mutations such as INCL in Finland and JNCL in Germany, Norway, Scotland and the USA (Claussen et al., 1992; Augestad and Flanders, 2006; Crow et al., 1997; Rider and Rider, 1999). The incidence and distribution of variant forms, CLN5, 6, 7 and 8, are increasing rapidly following genetic advances leading to better diagnosis and an increased awareness of the disease amongst the medical profession. It was traditionally thought that these were minor variants but it is now clear that they are probably as common as the CLN1, 2 and 3 forms (Aiello et al., 2009; Cannelli et al., 2006, 2007, 2009).

1.2 Classification of NCL

The current NCL nomenclature was adopted in 1969 when Zeman and Dyken coined the term "neuronal ceroid lipofuscinoses". The first NCL genes were not identified for a further 25 years and since then eight NCL genes have been identified and characterized. During this period, NCLs were classified based on the age of onset and ultrastructure of the storage material, leading to four main forms: INCL (CLN1), LINCL (CLN2), JNCL (CLN3) and ANCL (CLN4). In some countries they were also known by their eponyms, according to who originally described them, e.g. Haltia-Santavuori, Jansky-Bielschowsky, Spielmeyer-Vogt or Batten disease, and Kufs disease respectively (Haltia et al., 1973a, 1973b; Santavuori et al., 1973; Jansky, 1908; Bielschowsky, 1913; Spielmeyer, 1905; Vogt, 1905; Batten, 1903, 1914; Kufs, 1925). The existence of variants became increasingly recognised, such as late infantile variants, particularly in Finland, and early juvenile in the UK and other countries, leading to a more complicated nomenclature. In addition, the term 'Batten disease' has been used to refer to NCL cases of juvenile onset but is also the accepted term for the complete collection of NCL conditions, further confusing the nomenclature system.

1.2.1 Genetic classification

The NCLs have now been reclassified on the basis of recent molecular genetic and biochemical studies, which have provided evidence of far more overlap for the different genetic variants than previously suggested by the clinical phenotypes (Mole et al., 2004). This progress and an increasing knowledge of NCLs required a revision of the traditional classification to incorporate the increasing number of NCL related genes, identification of the genetic loci and their mutations (Goebel, 2000; Wisniewski et al., 2001). The human NCLs now currently consist of mutations in at least eight characterized human genes (Table 1). Although these genes have been identified and cloned, the pathogenic mechanisms of this

disorder remain unknown. Approximately 280 NCL causing mutations have been found in the eight human genes (http://www.ucl.ac.uk/ncl/; 2010) and many more are likely to be discovered.

The genes underlying two further variants, *CLN4* (ANCL) and *CLN9* are yet to be identified. However, evidence that CLN9 is a distinct variant is currently lacking and it is possible that new mutations in an already characterised *CLN*-gene may result in the development of this variant form of NCL. Mutations in the uncharacterized *CLN4* gene were initially proposed to cause an adult onset form of the disease. This form of NCL has both recessive (Martin, 1991) and dominant (Josephson et al., 2001; Burneo et al., 2003; Ivan et al., 2004) modes of inheritance along with a highly variable age of clinical onset (Martin et al., 1999). It has since been proposed that mutations in other NCL-causing genes that leave some functionally active gene product may be responsible for certain delayed onset forms of NCL (Van Diggelen et al., 2001; Mazzei et al., 2002) and more recently adult onset forms caused by muations in *CLN6* have been described (Arsov et al., 2011). In rare cases it is possible to have a minor mutation in the *CLN1* gene that is mutated in INCL, which results in adult onset cases (Van Diggelen et al., 2001; Ramadan et al., 2007). Furthermore, late onset cases have now been linked to the gene previously designated as *CLN5* (vLINCL) (Pineda-Trujillo et al., 2005; Cannelli et al., 2007). Hence, it is likely that many CLN4 cases may be attributed to previously characterised NCL genes with less severe mutations rather than to an independent gene. Similarly, some CLN7 (vLINCL) cases were shown to be the result of mutations in two already characterised NCL genes; *CLN6* (Siintola et al., 2005) and *CLN8* (Mitchell et al., 2001; Ranta et al., 2004). However, the major facilitator superfamily domain containing eight (*MFSD8)* gene has now been characterised in some patients and constitutes a genetically distinct form of vLINCL; CLN7 (Siintola et al., 2007).

Overall, it has become increasingly clear that mutations in a number of genes can result in similar clinical and histopathological phenotypes (genetic heterogeneity) but also that in an increasing number of NCL cases, different mutations in the same gene can result in markedly different clinical phenotypes (allelic heterogeneity). Additionally, the same genetic mutation within a family can also result in a markedly varied clinical phenotype (Williams et al., 2006) and a number of cases do not fit with any of the known genes suggesting that there may be more to be discovered.

1.2.2 Gene product classification

The NCLs can also be divided into two groups dependent on the *CLN* gene products. These products fall into two distinct categories; either soluble lysosomal proteins (CLN1, CLN2, CLN5 and CLN10) or predicted membrane proteins of unknown function (CLN3, CLN6, CLN7 and CLN8). The NCLs are lysosomal storage diseases (LSDs) in that protein is stored in lysosome derived organelles and subunit c of mitochondrial ATP synthase (subunit c) is the major stored protein in most forms (reviewed in Palmer and Tammen, 2011), except CLN1 and CLN10 in which the sphingolipid activator proteins (SAPs) A and D are stored (Tyynelä et al., 1993; Siintola et al., 2006a). *CLN1* encodes a soluble lysosomal enzyme, palmitoyl protein thioesterase (PPT1) (Vesa et al., 1995) and *CLN2* encodes a soluble lysosomal enzyme called tripeptidyl peptidase 1 (TPP1) (Sleat et al., 1997). *CLN10* encodes the classical lysosomal proteinase cathepsin D (CTSD) (Siintola et al., 2006a) and is involved in proteolytic degradation, cell invasion and apoptosis (Steinfeld et al., 2006). Lack of activity of cathepsin D causes a congenital form of NCL in sheep and children (Tyynelä et al., 2000). *CLN5* encodes a soluble lysosomal glycoprotein of unknown function (Sleat et al., 2005, 2006, 2007).

A second group of NCL associated proteins are putative membrane proteins of unknown function, residing in the lysosomal membrane or in pre-lysosomal organelles. *CLN3* probably encodes an integral membrane protein of the lysosome in most cell types (Ezaki et al., 2003; Kyttälä et al., 2004; Lerner et al., 1995). The CLN8 protein may recycle between the ER and ER-Golgi intermediate compartments (Lonka et al., 2000). Studies indicate that *CLN6* encodes an ER-resident protein and modulates the endocytosis of exogenous proteins (Heine et al., 2004a; Mole et al., 2004). vLINCL caused by mutations in the *CLN7* gene, *MFSD8*, encodes a putative lysosomal transporter (Siintola et al., 2007).

More recently, NCL like disease has been described in mice caused by defects in the chloride channels 3, 6 and 7 (CLCN3, CLCN7, CLCN7) (Yoshikawa et al., 2002; Poët et al., 2006; Kornak et al., 2001; Kasper et al., 2005) but they do not cause NCL like disease in humans. Despite the identification of disease causing mutations, very little is known about how these mutations actually cause the resulting disorder.

Table 1 Gene product, location and structure of the eight genetically characterised NCL forms (derived from http://www.ucl.ac.uk/ncl/; 2011)

Gene	Gene product	Locus	Protein structure	No. of mutations	No. of polymorphisms
CLN1	PPT1	1p32	Soluble	48	6
CLN2	TPP1	11p15	Soluble	72	22
CLN3	CLN3	16p12	Membrane bound	50	5
CLN4	?	?	?	?	?
CLN5	CLN5	13q21-q32	Soluble	27	9
CLN6	CLN6	15q23	Membrane bound	55	4
CLN7	MFSD8	4q28.1-q28.2	Membrane bound	23	2
CLN8	CLN8	8p23	Membrane bound	16	2
CLN9	?	?	?	?	?
CLN10/CTSD	Cathepsin D	11p15.5	Soluble	4	0

1.3 Pathology

1.3.1 Storage body accumulation

Despite the varying ages of onset and clinical course of disease, all forms of NCL share unifying pathological features, the most profound being accumulation of fluorescent, periodic acid-Schiff, Luxol-fast blue and Sudan black positive granules, which are resistant to lipid solvents and accumulate in the lysosomes of most nerve cells, and of many other cell types. Hence, pathologically the NCLs are considered LSDs due to this accumulation of lysosome derived storage material. The lysosomal inclusions, as seen by electron microscopy, are granular osmiophilic deposits (GRODs), curvilinear, fingerprint, or rectilinear profiles, depending on the NCL phenotype and tissue (Table 2). Storage bodies largely accumulate in the perikarya of nerve and glial cells, the granules grouping, resulting in considerable enlargement, and even ballooning of the cell body. The storage bodies give a brownish hue unstained, stain red with periodic acid-Schiff and blue with Luxol-fast blue, and have an enhanced acid phosphatase activity, which is the marker enzyme for lysosomes (Jolly et al., 1980, 1982, 1988, 1989; Cook et al., 2002). They all stain immunohistochemically for

subunit c, some staining solidly while others stain only around the periphery, leaving a translucent area in the middle (Westlake et al., 1995a; Oswald et al., 2005). The specific storage of subunit c in all forms, except CLN1 and CLN10, was unequivocally established by direct protein sequencing (Chen et al., 2004; Fearnley et al., 1990; Palmer et al., 1989a, 1992; Tyynelä et al., 1997) and inferred from immunohistochemical studies. Despite ubiquitous storage, only some of the neurons of the central nervous system (CNS) are selectively destroyed.

The accumulation of fluorescent storage bodies in ovine NCL has been well documented by Oswald et al., (2005), with storage deposits evident in the cerebral cortex from 12 days of age in affected animals becoming more pronounced with age. Significant storage material is evident throughout layers I-VI of all cortical regions and accumulates more rapidly than in the cerebellum, hippocampus, striatum and white matter. However, by 19 months there is comparable storage body accumulation within both the neocortex and subcortical regions. The mechanism of accumulation of these highly hydrophobic proteins and their relation, if any, to clinical symptomatology and neuronal death still remains unsolved (see section 1.8 for further detail). However, due to the pathological similarities of the NCLs it has been suggested that the NCL proteins may play roles in a common biological pathway, especially important in neuronal cell function.

Table 2 Age of onset and pathological features of storage material in NCL

Gene	NCL type	Age of onset (years)	Storage protein	Ultrastructural features
CLN1	Infantile	0-38	SAP A and D	GROD
CLN2	Classical late infantile	2-8	Subunit c	CL
CLN3	Classical juvenile	4-10	Subunit c	FP
CLN4	Adult	15-35	Subunit c	FP, granular
CLN5	Variant late infantile	4-7	Subunit c	RL, CL, FP
CLN6	Variant late infantile	1.5-8	Subunit c	RL, CL, FP
CLN7	Variant late infantile	1-6	Subunit c	RL, CL, FP
CLN8	Northern epilepsy	5-10	Subunit c	CL
CLN9	Juvenile	4-10	Subunit c	CL, FP, GROD
CLN10/CTSD	Congenital	Birth	SAP A and D	GROD

Granular osmiophilic deposit (GROD), curvilinear (CL), rectilinear (RL), fingerprint (FP) profiles.

1.3.2 Neurodegeneration

The second definitive hallmark of NCL is profound brain atrophy. The disease selectively manifests in the CNS and there is progressive cell loss well documented in all human NCL forms (Haltia, 2003) and in ovine NCL (Mayhew et al., 1985; Jolly et al., 1989; Oswald et al., 2001, 2005, 2008). Neuronal degeneration predominates in the cerebral cortex and cerebellum and may commence in the dendritic tree, finally proceeding to neuronal loss (Williams et al., 2006). Neuronal degeneration correlates with age of onset and disease duration, usually being most pronounced in INCL, moderate in JNCL and relatively mild in ANCL. Early studies by Braak and Goebel (1979) showed that small neurons in layer II and V of the cerebral cortex appear to be more affected than other layers, suggesting a discordant onset and progression of neuronal degeneration amongst different cell populations. Little is known about subcortical and peripheral nerve degeneration. Traditionally it has been thought that neurodegeneration is a direct consequence of the accumulation of storage material and lack of the enzyme activity in lysosomes but recent studies in the ovine CLN6 model revealed a close association between glial activation and subsequent neurodegeneration but not with storage body accumulation (Oswald et al., 2005).

Hence, a fundamental question about NCL is why is there selective cell death of neurons? Apoptosis has been suggested as one mechanism of cell death in NCL and many NCL proteins have been shown to have anti-apoptotic properties (Mitchison et al., 2004; Berchem et al., 2002; Persaud-Sawin et al., 2002; Guarneri et al., 2004; Persaud-Sawin and Boustany, 2005; Kim et al., 2006; Hachiya et al., 2006; Zhang et al., 2006). It has also been hypothesized that autophagic pathways are involved in the development of NCL. Autophagy is the major cellular pathway responsible for cellular turnover of proteins and organelles. Fusion between the autophagosome and the lysosome is a crucial step in this process (Mizushima et al., 2002) and lysosomal storage may affect the fusion efficiency. Signs of autophagy have also been recorded in several mouse models of NCL (Deiss et al., 1996; Koike et al., 2005; Mitchison et al., 2004; Shacka and Roth., 2007). Inflammation has also been suggested as a possible explanation for neuronal cell death and is discussed further in section 1.3.3.

Excitotoxicity has also been postulated to be involved in pathology of the NCLs (Walkley et al., 1995). Populations of γ-aminobutyric acid (GABA)ergic interneurons have been shown to be consistently affected in both human, sheep and mouse NCLs (Cooper et al., 1999; Oswald et al., 2001; Bible et al., 2004; Pontikis et al., 2004; Kielar et al., 2007). Studies in the ovine CLN6 model revealed a severe loss of parvalbumin positive interneurons, which paralleled other

degenerative changes and preceded somatostatin, calbindin and calretinin positive interneuron loss. Remarkable regional variation was revealed, with losses starting and progressing fastest in areas first affected by neurodegeneration and clinical symptoms, the visual and parieto-occipital cortices (Oswald et al., 2008). A metabolomic study confirmed these findings, showing that relative concentrations of GABA and glutamate changed in parallel to or in consequence to neurodegeneration (Pears et al., 2007). There was no evidence for any imbalance or metabolic disturbance that could lead to the onset of neurodegeneration.

1.3.3 Glial activation

Consistent and regionally specific patterns of astrocytosis and microglial activation are associated with the different NCL forms and are regarded as a generalised response to neurodegeneration (Haltia, 2003). However in NCL, glial activation appears to precede neuronal degeneration (Oswald et al., 2005, Kay et al., 2006) and remains significant in even severely depleted cortical regions. Immunohistochemical studies in ovine CLN6 have implicated a primary role for glial activation in pathogenesis, with activation apparent in prenatal, presymptomatic sheep brain prior to any neurodegeneration (Oswald et al., 2005; Kay et al., 2006). CLN3 mice also exhibit glial activation prior to the appearance of symptoms, suggesting that neuronal cell loss occurring later in the disease is preceded by neuroinflammation (Pontikis et al., 2004). In the ovine model, proliferating perivascular macrophages and activated astrocytes were revealed to be present at 20 and 40 days before birth, respectively. Focal clusters of activated microglia and astrocytes were present in cortical regions at birth. This activation proceeded in a progressive, regionally specific manner and preceded the future neurodegeneration in these regions suggesting a central role for glial activation in NCL pathogenesis (Oswald et al., 2005).

This chronic inflammatory response can be damaging to neurons (Raivich et al., 1999; Streit et al., 2004) and it is still not known what causes the initial activation or when this cascade becomes fatally damaging to neurons. The regionally defined glial activation is in contrast to the widespread storage body accumulation and indicates that both events are independent manifestations of the disease (Oswald et al., 2005). Glial activation is evident in many other neurodegenerative disorders, such as Alzheimers (AD) and Parkinsons disease (PD), amyotrophic lateral sclerosis and ischemia (Hunot and Hirsch, 2003; Neumann, 2001; Sheng et al., 1998; Troost et al., 1993) and it is generally thought that these responses are initiated by dying neurons or abnormally deposited protein, such as β-amyloid (Minagar et al., 2002). Other LSDs also indicate a pathogenic role for inflammation, with the progressive involvement of glial cells, evident in Tay-Sachs disease, mucopolysaccharidoses (MPS) and gangliosidoses

(Jeyakumar et al., 2003; Ohmi et al., 2003). Glial activation has also been investigated in mouse models of NCL (Cooper, 2003; Pontikis et al., 2004; Chang et al., 2008) but so far has not been investigated at very early and prenatal stages. Wada et al., (2000) found that neurodegeneration was suppressed in a mouse model of Sandhoff disease, due to suppression of microglial activation, a side effect of bone-marrow transplantation. Depletion of macrophage inflammatory protein (MIP-1α) produced the same result, directly implicating inflammation in pathogenesis (Wu and Proia, 2004).

It remains to be seen whether prenatal or early glial activation is a common occurrence amongst all NCL types and if so whether it is in response to some stress or other signal within the brain and is an insufficient attempt at repair or whether it is actually initiating the cascade of neurodegenerative changes.

1.4 Diagnosis

Advances in the understanding of the genetic and biochemical pathogenesis of NCL have greatly influenced diagnosis of this group of disorders. Prior to the identification of the disease causing genes, diagnosis was largely based on histopathological techniques. Age of onset, order of symptoms and the use of electron microscopy to evaluate storage material morphology allowed classification into one of the three main childhood NCL types (Williams et al., 2006). It has since become apparent that the classification of the NCLs is in fact very complex and confusing. Disease phenotype can be very similar in mutations in different genes or very varied in different mutations in the same gene (see section 1.2.1). The spectrum of NCL subtypes makes an accurate diagnosis complicated and in most cases relies on a combination of histological and ultrastuctural analyses, enzyme assays, clinical presentation and mutation analysis. Presently a biochemical and/or genetic diagnosis can be made for the majority of families affected by one of the NCLs but in cases where genetic information is still not available, treatment and care can still proceed on the basis of ultrastuctural findings. The genotype-ultrastructural morphology correlation of storage bodies is very strong, with CLN1 demonstrating a granular phenotype, CLN2 a curvilinear pattern, and CLN3, CLN5, CLN6 and CLN7, fingerprint, curvilinear and rectilinear profiles in nervous tissue (Table 2) (Williams et al., 2006). Since lipopigment accumulation is near-universal in extracerebral tissue it is an easy, non-invasive, useful morphological diagnostic target for some forms of NCL. In addition, the range of samples that can now be utilised for genetic, biochemical and ultrastuctural diagnostics allows much easier diagnosis in testing centres outside of countries where the facilities and expertise would not be available for such diagnoses to be made.

Visual failure is usually the leading symptom in JNCL and these early retinal signs although subtle may be one of the first signs recognised. A reduced retinogram and normal evoked potential (Eksandh et al., 2000) is suggestive of an NCL diagnosis and can prompt further biochemical and genetic testing (Weleber et al., 2004). Varying magnetic resonance imaging (MRI) results can also initiate diagnosis of different forms of NCL, for example LINCL exhibiting severe cerebellar atrophy (Peterson et al., 1996). Genetic and biochemical assays are however the mainstay of diagnosis. The *CLN1*/PPT1, *CLN2*/TPPI and *CLN10*/CTSD genes encode enzymes that catalyse specific chemical reactions. Enzyme activities can be measured using fresh blood (Van Diggelen et al., 1999), dried blood spots (Lukacs et al., 2003) or saliva samples (Kohan et al., 2005) allowing relatively easy and rapid diagnosis. An affected person will have very low activity, an unaffected person normal activity, and a carrier a level of activity approximately half-way in between. A diagnosis can be confirmed by mutation analysis of the corresponding *CLN1*, *CLN2* or *CLN10* gene.

If the age at disease onset is "juvenile" (about 5-8 years old), a blood smear is examined for lymphocyte vacuoles. The presence of vacuolized lymphocytes in combination with typical clinical NCL symptoms leads to the diagnosis of JNCL and is confirmed by mutation analysis of the corresponding *CLN3* gene (Goebel and Wisniewski, 2004). If no mutation in the *CLN3* gene is found, NCL is still not ruled out, as some milder mutations in the *CLN1* or *CLN2* gene may cause the clinical signs of JNCL (Williams et al., 2006). The presence of lysosomal storage material, demonstrated by electron microscopy confirms the diagnosis of NCL and examination of the specific ultrastructure of the storage material can help to distinguish between the NCL variants. Mutation analysis of the other recently discovered NCL genes, *CLN5*, *CLN6*, *CLN7* or *CLN8* can also be performed to confirm one of these NCL types. However, DNA testing is not effective for a number of NCL-like cases which have no association with known disease-causing mutations.

Despite all of these advances, diagnosing NCL is still a prolonged and difficult process, the biggest hurdle being clinical recognition of the disease as an NCL. Better awareness and education of the disease and its clinical manifestation amongst healthcare professionals would aid earlier diagnoses and subsequent therapeutic options. Genetic diagnosis is not available for all NCL genes but the most common mutations can be screened for at a number of European and North American centres (Zhong, 2001). Still, diagnostic testing can now be directed and focused, with prioritisation of the NCL genes to be investigated depending on age of onset, pattern of clinical features and the ethnicity of the family. This can in some cases lead to a faster diagnosis, which will become more vital as therapeutic options become

available. It is predicted that therapies beginning before there is significant progression of disease will offer the most benefit, but presently the majority of cases are still diagnosed only after the disease has progressed considerably.

Enzyme assays can be performed for carrier testing of other family members and for prenatal diagnosis (Das et al., 2001). This is particularly useful for families where an affected child has a 'mild' mutation. It will enable planning for future disease-related needs as well as planning for family life, education, housing and community help. For newly diagnosed families, counselling is fundamentally important in dealing with the reality of a fatal genetic disorder. Organizations such as the Batten Disease Support and Research Association (BDSRA, http://www.bdsra.org/) provide invaluable support and information to affected families, as well as researchers and health care professionals.

1.5 CLN6 NCL

The *CLN6* gene is located on human chromosome 15q23 and contains 7 exons, encoding a putative 311 amino acid protein. Two independent studies, using subcellular fractionation and immunocytochemistry, have suggested that it is an ER-resident protein (Mole et al., 2004; Heine et al., 2004a). The CLN6 protein contains an N-terminal cytoplasmic domain, seven transmembrane domains and a luminal C-terminus. *CLN6* has no homology with other known proteins but the sequence is highly conserved across mammalian species (Heine et al., 2004a).

Most mutations in the *CLN6* gene cause a variant of LINCL that clinically resembles classical LINCL but has a later age of onset, usually between 4-5 years of age (Williams et al., 1999). The age of onset and the rate of disease progression do vary however, with onset being reported anywhere between 18 months and 8 years of age. Recently a number of adult onset cases have also been described (Arsov et al., 2011). Nevertheless, the order in which symptoms develop in younger patients is generally consistent, with seizures, ataxia, and myoclonus presenting early, between 4 and 10 years of age, and visual impairment developing later (Mole et al., 2005). Patients usually die in the second or third decade of life and currently there are no effective therapies available. Computed axial tomography (CAT) and MRI scans reveal severe cortical loss, most prominent in the occipital lobe and especially within layer V of the cortex. Granular cells of the cerebellum are depleted, while Purkinje cells are retained to some extent. At autopsy the brain weighs from 600-900g, compared with a normal human brain weight of ~1400g, emphasising the extent and severity of degeneration (Haltia, 2003). The ultrastructure of storage bodies in neurons consist of a mixture of rectilinear and fingerprint profiles, whereas sweat gland epithelium, smooth muscle and endothelial cells may contain both rectilinear, fingerprint and curvilinear profiles (Lake and Cavanagh, 1978; Elleder et al., 1999; Williams et al., 1999). A

series of experiments established that protein, specifically subunit c, is the major component of storage bodies in this form (Palmer et al., 1986a, 1986b, 1989a; Fearnley et al., 1990).

Originally is was thought that the CLN6 form of NCL was restricted to a narrow set of founder mutations in European gypsies and Costa Ricans but it is now evident that it is much more widespread, with cases identified in France, Italy, Brazil, Turkey and South America (Sharp et al., 2003; Siintola et al., 2005; Teixeira et al., 2003; Sharp et al., 2003). *CLN6* is a highly mutable gene, with 55 mutations reported in different populations (http://www.ucl.ac.uk/ncl/; 2011), including southern (Portugal and Turkey) and Eastern Europe (Czech Republic), the Indian sub-continent and Costa Rica (Mole et al., 2005). The majority of these mutations include a frameshift or nonsense change, resulting in a premature stop codon (Siintola et al., 2006b). Some mutations are more common amongst certain populations such as the c.214G > T (P.Glu72Stop) nonsense mutation in patients of Costa Rican origin but some appear to be unique (Siintola et al., 2006b). Sharp et al., (2003) suggest that a second disease allele that permits some residual function of CLN6 may reduce the severity of the disease. Thus, it is highly likely that mutations in *CLN6* not yet identified could cause disease that is not clinically diagnosed as vLINCL (Mole et al., 2005). Furthermore a number of adult onset NCL cases have recently been attributed to mutations in the *CLN6* gene (Arsov et al., 2011).

Mutations may affect the structure and stability of the protein, or they may interfere directly with its expression, function or intracellular site of action (Mole et al., 2004). Cell biology studies in human, sheep and mice fibroblast cells have indicated that lack of CLN6 does not affect the transport, sorting or processing of newly synthesised lysosomal enzymes from the ER to the lysosome and the role of CLN6 in the ER remains unclear (Heine et al., 2004a). In contrast however, mutant CLN6 results in an increase in the uptake of the lysosomal enzyme, arylsulfatase A, via the plasma membrane mannose-6-phosphate receptor and reduced intracellular degradation (Heine et al., 2004a) suggesting that a lack of CLN6 may affect pre-lysosomal vesicular transport.

1.6 Animal models of NCL

The systematic study of early pathological changes in NCL is only possible in animal models of the disease. These fall into two classes, colonies derived from naturally occurring cases, and constructed gene knock-out and knock-in models. A number of spontaneous NCL forms have been discovered in animals, including dogs (Jolly et al., 1994), cats (Bildfell et al., 1995; Green and Little, 1974; Weissenbock and Rossel, 1997), sheep (Cook et al., 2002; Jolly et al., 1994), goats (Fisk and Storts, 1988), cattle (Harper et al., 1988), horses (Url et al., 2001) and mice (Bronson et al., 1993, 1998). Amongst these are naturally occurring animal models of

CLN6 , the most informative being the ovine model diagnosed in New Zealand South Hampshire sheep over two decades ago (Graydon and Jolly, 1984; Jolly and Palmer, 1995; Jolly et al., 1980, 1982, 1988, 1989, 1992; Mayhew et al., 1985). The gene responsible for this ovine form is 90% homologous with human *CLN6* (Broom et al., 1998), FLJ 20561, on human chromosome 15q21-23 (Gao et al., 2002a; Wheeler et al., 2002) but the disease causing mutation has not yet been identified (Tammen et al., 2006). Ovine CLN6 caused by a different mutation was recently discovered in Australian Merino sheep (Cook et al., 2002; Tammen et al., 2006) and CLN5 forms have also been discovered in New Zealand Borderdale sheep (Jolly et al., 2002, Frugier et al., 2008) and in Australian Devon cattle (Harper et al., 1988; Houweling et al., 2006).

The best characterized of all these models, especially at the biochemical level, is the ovine CLN6 form in South Hampshire sheep (Jolly and West, 1976; Jolly et al., 1980, 1982). The pathology in these sheep is well described and closely matches that in the human disease, particularly in the severe cortical atrophy, profound neuronal loss and retinal degeneration. Affected sheep develop clinical symptoms between 10 and 14 months of age, the most notable being blindness due to atrophy of the occipital cortex and loss of photoreceptors in the retina (Jolly et al., 1989; Mayhew et al., 1985). Affected animals rarely survive past 24 months of age due to disease severity, in contrast to normal unaffected animals which have a life expectancy of 10 to 12 years. *Post mortem* studies by Oswald et al., (2005) revealed that the development of affected CLN6 sheep brains progressed normally for the first four months after birth, after which it progressively regressed. Atrophy of the cerebral cortex was apparent from 6 months of age, notably in the occipital lobe, and by 12 months cortical atrophy was apparent in all regions (Figure 1). In contrast, subcortical nuclei and the cerebellum of affected brains retained a normal appearance, even at advanced stages of disease. Together with the gross brain atrophy, studies further revealed glial activation that precedes neuronal death (see section 1.3.3), and the presence of fluorescent storage bodies in neurons and most cells throughout the body (see section 1.3.1) (Oswald et al., 2001). Additionally, studies of interneuron changes have shown that these follow the pattern of glial activation (see section 1.3.2) (Oswald et al., 2008), whereas the specific loss of gonadotrophin-releasing hormone (GnRH) secreting neurons of the hypothalamus, are not associated with glial activation or storage body accumulation (Kay et al., 2011). Hence, location and connectivity, not phenotype, seem to determine neuronal survival in ovine CLN6.

Figure 1 Cortical atrophy in ovine CLN6 compared to normal control animals
Marked atrophy of the cerebral cortex is evident in ovine CLN6 at 12 months, which is more pronounced at 19 months, especially in the visual cortex (modified from Oswald et al., 2005).

Isolation and analysis of storage bodies from affected sheep revealed that the predominant storage material was subunit c (Fearnley et al., 1990; Palmer et al., 1986a, 1986b, 1989a), which was subsequently observed in the human CLN2, CLN3, CLN5, CLN6, CLN7 and CLN8 forms (Palmer et al., 1989a, 1989b, 1992; Hall et al., 1991; Kominami et al., 1992; Kida et al., 1993; Tyynelä et al., 1997; Herva et al., 2000). Storage bodies display a variety of ultrastructures *in situ*; multi-lamellar, finger-print and curvilinear arrays, all being observed (see section 1.3.1).

Although mouse models of NCL have proved to be informative, the disease in these models are generally milder than in the human or large animal forms and they have other disadvantages compared with the sheep model. Sheep are economical to use as research subjects, live in flocks outdoors and therefore do not require specialized housing, and are relatively easy to care for and cheap to maintain. Sheep are domesticated, normally docile and pose little risk to the investigator. They are long lived compared to rodents and therefore suitable for long-term study. Their brains are similar to human brains and both have gyrencephalic cortices.

The New Zealand South Hampshire colony is well established and the colony provides animals with the same genetic lesion and no sign of disease has ever been noted in heterozygotes, which thus form an ideal control population. Adult sheep brains are also large, weighing about 140g compared to 1400g for humans (Figure 2), meaning that therapeutic strategies requiring direct delivery into the brain can be tested in sheep and translated directly

to humans. In addition, the prolonged disease course enables analysis of the clinical effectiveness and longer term consequences of potential therapies for this devastating disease.

Figure 2 Comparison of human, sheep and mouse brain sizes

1.7 History of NCL

In 1826 Otto Christian Stengel reported the first clinical description of NCL in a case-study (Goebel, 1995). He described four Norwegian siblings displaying rapid deterioration of vision and intelligence, with mental disturbances, convulsions and other neurological symptoms, who died prematurely. Although no pathological studies were performed the clinical descriptions are so succinct that it is believed to be the first description of NCL in the literature. Around the turn of the 20th century, Sachs (1896) introduced the term "amaurotic familial idiocy" (AFI), to describe a group of diseases with infantile onset, characterised by blindness, psychomotor deterioration, and early death. From then until the 1960s the NCLs were grouped under this term. In the intervening period reports of the disease by clinicians such as Batten (1903, 1914) after whom the disease was named, Spielmeyer (1905), Schaffer (1905), Vogt (1905), Jansky (1908), Bielchowsky (1913) and Sjögren (1931) described different forms of the disease. Studies by Klenk (1939) and Svennerholm (1962) indicated that there was an increase in the amount of gangliosides in the Tay-Sachs form of AFI but not in the juvenile form. This suggested that the AFI group was biochemically heterogeneous. Furthermore, comparative histochemical and electron microscopic studies in the 1960s demonstrated that the intra-neuronal storage in late infantile and juvenile AFI (Zeman and

Donahue, 1963; Zeman et al., 1970) radically differed from that in the Tay-Sachs form (Terry and Korey, 1960). Hence, in order to distinguish these forms of AFI from Tay-Sachs disease and other gangliosidoses, Zeman and Dyken (1969) proposed the new term "neuronal ceroid lipofuscinoses", based on the histochemical and electron microscopic similarities of the storage material to ceroid and lipofuscin.

1.8 Storage body accumulation and composition

Storage bodies are often called lipopigments due to their apparent similarities to ceroid and lipofuscin (age pigment), which are considered indicators of cell damage and responsible for impaired cellular performance and cell death. The fluorescence of lipofuscin was postulated to be due to the accumulation of products of lipid peroxidation because it had similar fluorescent spectra to material generated *in vitro* by reacting protein and peroxidised lipids (Chio et al., 1969). The lipofuscin-like fluorescence and similar ultrastructure of the NCL storage bodies to age pigment led to the term "neuronal ceroid lipofuscinoses" (Zeman and Dyken, 1969) and these features initiated the hypothesis that storage body accumulation and pathogenesis were caused by a lack of control of peroxidation. This mechanism would require the loss of polyunsaturated fatty acids to lipid peroxidation but this was soon disproved, due to the development of techniques to isolate storage bodies from an ovine model of NCL. These studies showed that there was no evidence for peroxidative damage or metabolic disruption of other lipids, leading to storage body accumulation (Palmer et al., 1985, 1986b, 1988; Hall et al., 1989). The lipids present in storage bodies were those which would be expected in lysosome derived organelles and included large amounts of lysobisphosphatidic acid, a lysosomal marker. Additionally, large proportions of the fatty acids in this lipid were polyunsaturated, indicating no significant loss due to peroxidation.

Soon after, the stored material was discovered to be subunit c (Palmer et al., 1989a; Fearnley et al., 1990). This recognition that subunit c is the major stored species rather than the originally perceived, peroxidised lipid/protein polymer led to a major conceptual change in NCL research (Fearnley et al., 1990) and development of the lysosomal proteinoses concept. Analysis of storage bodies isolated from fresh sheep tissue also indicated an absence of any "characteristic fluorophor" (Palmer et al., 1986a, 1988). Further studies determined that the "autofluorescence" observed in storage bodies is an array property, as solutions of storage bodies dissolved in 1% lithium dodecyl sulphate (LDS) lack any fluorescence and in addition the observed fluorescence is photo-fast, indicating lack of a chemical fluorophor (Palmer et al., 1993, 2002). Thus, the *in situ* fluorescence is a consequence of packing of protein into

subcellular organelles, the interference of light diffracting from the protein array causing the observed fluorescence (Palmer et al., 2002).

Subunit c accumulation has since been identified in other animal models (Fearnley et al., 1990; Martinus et al., 1991; Jolly et al., 1994; Palmer et al., 1997; Url et al., 2001; Cook et al., 2002; Katz et al., 2005; Melville et al., 2005; Frugier et al., 2008) and in the majority of the characterised human NCLs (CLN2, CLN3, CLN5, CLN6, CLN7 and CLN8) (Palmer et al., 1989a, 1989b, 1992; Hall et al., 1991; Kominami et al., 1992; Kida et al., 1993; Tyynelä et al., 1997; Herva et al., 2000). In the CLN1 and CLN10 forms the main storage materials are SAP A and D, which are small heat-stable glycoproteins required for the hydrolysis of sphingolipids in lysosomes (Mehl and Jatzkewitz, 1964; O'Brien and Kishimoto, 1991; Tyynelä et al., 1993; Siintola et al., 2006a).

Storage is specific to subunit c and subunit c storage is specific to the NCLs, and none of the other 16 ATP synthase subunits or any other inner mitochondrial membrane proteins are stored (Chen et al., 2004; Fearnley et al., 1990). Mass spectrometry analysis of accumulated subunit c has shown that both the normal and stored subunit c share a 42-43kDa modification arising from trimethylation of lysine 43 (Chen et al., 2004). Subunit c is coded for on three nuclear genes, P1, P2 and P3, and initially it was considered that mutations in either or both of these genes may be responsible for the accumulation of subunit c in the NCLs. However Medd et al., (1993) revealed that the genes and their levels of expression are normal in affected sheep. This eliminated the possibility that mistargeting of subunit c away from the mitochondria, over-expression of the gene products so that it accumulates in lysosomes or abnormal trimming of the extended mitochondrial import sequences, were the cause of accumulation (Fearnley et al., 1990; Palmer et al., 1995a).

In LINCL, the accumulation of subunit c is caused by a lack of TPP1, a lysosomal protease which may be involved in its degradation (Sleat et al., 1997; Ezaki et al., 1999; Warburton and Bernardini, 2000). The specific mechanism that causes accumulation of subunit c in the other forms of NCL is not known since the primary deficiency is not that of a protease. It has been suggested that the *CLN* gene products may function in a specific subunit c turnover pathway, disruption of which would lead to accumulation but there is no knowledge of the mechanisms of this process (Palmer et al., 1995a, 1997). Alternatively, suboptimal turnover conditions may lead to lysosomal deposition of the highly hydrophobic subunit c, which has a tendency to form aggregates. This may be a result of disturbed pre-lysosomal membrane trafficking, which has been observed by Fossale et al., (2004) in a CLN3 neuron culture model. Subunit c accumulation has also been reported in other LSDs, like Niemann-Pick

types A and C, GM1 and 2 gangliosidoses and MPS I, II and III, (Elleder et al., 1997; Kida et al., 1993; Lake and Hall, 1993). However the degree of storage is much lower and less uniform than in NCL suggesting that the neuronal accumulation of subunit c is especially amplified in NCL. Furthermore, the specificity of the NCL storage process is shown by the fact that lysosomes of non-neuronal cells in NCL also intensely accumulate subunit c, in contrast to other LSDs in which there is minimal accumulation (Elleder et al., 1997).

There are several hurdles to understanding the inter-connections between the gene lesions, subunit c storage and neurodegeneration that need to be resolved to understand the pathobiology of these diseases. Storage bodies accumulate in nearly all cells of NCL patients, but only certain populations of these cells are selectively damaged and degenerate. Healthy cells, packed full of storage material can be observed, such as Purkinje cells of the cerebellum in ovine CLN6 tissue, giving no indication that storage body accumulation is damaging. Thus, it has been hypothesized that neurodegeneration is a separate consequence to the genetic mutation causing subunit c accumulation (Palmer et al., 2002).

1.9 Current treatments and therapeutic potentials

Currently, there is no cure for Batten disease or treatments available to halt or even slow the disease progression. Presently, the only treatments are directed towards a symptomatic care of secondary complications such as controlling seizures and to provide a good quality of life for as long as possible. Physical and occupational therapies are utilized to slow the progression of physical deterioration.

Dietary supplementation has been proposed as a potential therapeutic treatment. Studies assessing the validity of antioxidants (vitamin B_2, vitamin $B_{6,}$ vitamin C, vitamin E, methionine, butylated hydroxytoluene and sodium selenite) were carried out either individually or in a cocktail to treat JNCL patients (Santavuori et al., 1989; Westermarck et al., 1997). The initial findings of these studies suggested that antioxidant treatment seemed to slow, but not stop disease progression (Westermarck et al., 1997). However, these findings were based on comparing the age of clinical onset and disease progression between control and supplemented individuals. This can vary considerably between individuals suffering from the same NCL variant, hence using clinical course to estimate therapeutic efficacy is not a reliable or useful method. Further analysis revealed little if any benefit from these treatments. Finding that the storage material does not result from lipid peroxidation (see section 1.8) required for these treatments, accounts for the failure of such therapies. In addition, studies by Bennet et al., (1988) in which patients were supplemented with fish oil extracts revealed no

significant clinical, psychometrical or neurophysiological changes. Unfortunately, none of the dietary therapies attempted for the treatment of NCL have altered the disease progression or symptoms but they are still used as a substitute for any effective treatment.

Therapeutic options for the NCLs bear an additional hurdle due to the profound CNS involvement and are for now untreatable (Beck, 2007; Sondhi et al., 2001). Additionally, easy comparisons cannot be made between the size of the human brain when compared to rodents, in which the majority of animal model studies are carried out. Although the genes for eight known NCL variants (CTSD, CLN1, CLN2, CLN3, CLN5, CLN6, CLN7 and CLN8) have been identified and cloned, the pathogenic mechanisms of this disorder remain unknown further limiting the development of treatment options.

Collectively, this emphasises the instrumental role that support groups such as the BDSRA play in providing information to affected families and clinicians, and leading to advances in genetics, diagnosis, management and therapies. The BDSRA was formed in 1987 by the parents of three children suffering from Batten disease and aims to provide medical referrals, information, education and emotional support to affected children and their families (http://www.bdsra.org/index.html). The BDSRA is the largest support and research organization for Batten disease in North America and currently supports over 1,200 families in the USA, Canada, South America, Australia, New Zealand and South Africa amongst others. There are similar family support groups throughout Europe and the world which are closely aligned to the BDSRA, including Lysosomal Diseases New Zealand (www.ldnz.org.nz/) and the Batten Support and Research Trust (http://www.bsrt.org.uk). In addition, financial support is provided for research initiatives associated with Batten disease via fundraising events, which also raises awareness of the disorder in both the public and medical field.

1.9.1 Pharmaceutical and small molecule therapy

A hallmark of NCL is the accumulation of lysosomal storage material, hence one target of therapy has been the removal of this material. Pharmaceutical and small molecule intervention appears to be successful for some LSDs but it is likely to have most therapeutic benefit when combined with other therapies. The high specificity of small molecule interactions requires an in-depth knowledge of the pathology and eitology of each disorder, something which is currently lacking for the NCLs. Hence, due to this lack of knowledge surrounding the disease process, the mechanistic benefits of many pharmaceutical agents are unknown. Cysteamine (Cystagon) has gained attention in the treatment of INCL but little benefit has been

demonstrated (Lu et al., 2002; Hobert and Dawson, 2006). Despite this, a phase II clinical trial (http://clinicaltrials.gov/show/NCT00028262) is now nearing completion, in which ten INCL patients have been treated with Cystagon combined with N-Acetylcysteine (Mucomyst). Small molecule therapy may have potential for the treatment of NCL but for real benefit to be sought a better understanding of the disease process is required. It would likely play a role in reducing the impact of negative pathological events in conjunction with other approaches which can address the causative mutation of the disorder.

1.9.2 Enzyme replacement therapy

Enzyme replacement therapy (ERT) first became clinically available for Gaucher disease with Food and Drug Administration (FDA) approval in 1991 (Barton et al., 1991). Following promising clinical trials, intravenous administration of enzymes showed therapeutic activity in LSDs such as Pompe, Fabry and Gaucher disease (Desnick et al., 1980; Desnick, 2004), the latter being the first LSD to be successfully treated for non-neurological symptoms via this method. ERT has had success in halting the progression and reducing disease burden in certain disease affected tissues (Barton et al., 1991; Grabowski et al., 1995; Ramaswami et al., 2007; Banikazemi et al., 2007; Wraith et al., 2004) but has little effect on brain and skeletal tissue. This underlies a persistent problem with the treatment of the CNS component of these disorders, the inability of systemically delivered enzyme to cross the blood-brain barrier (BBB) in therapeutic quantities. Additional drawbacks associated with ERT include the potential for an allergic reaction and the development of neutralizing antibodies (Heese, 2008), as well as the requirement for a consistent source of purified enzyme. It also requires frequent, often weekly infusions to prevent disease reoccurrence and costs between US$90,000 to US$565,000 per annum creating extreme financial stress for affected families (Burrow et al., 2007; Beutler, 2006). These huge costs are driven by the enormous financial risk and investments which pharmaceutical companies take in researching and developing therapies for very rare disorders. A small portion of these developmental costs and FDA approval fees are covered by the Orphan Drug Act (1983). However, the protection against competition also provided by this act, designed to make the production of orphan drugs commercially viable, eliminates competition, resulting in astronomical drug prices (Beutler, 2006). It is hoped that with better and earlier diagnoses and understanding of disease mechanism the drug costs will decrease as therapies move from developmental to curative. The inability of soluble protein to cross the BBB has resulted in few studies of ERT for the treatment of NCLs, in which there is a dominant CNS involvement. Hence, to overcome these issues alternative delivery systems are being investigated. There are recent reports of

neurological improvement in a mouse model of CLN2 following intraventricular delivery of TPP1 (Chang et al., 2008). Less invasive intrathecal injection of enzyme is also being investigated and has shown promising results (Kakkis et al., 2004). Like systemic ERT however, these procedures would still require regular treatments and are likely to be more effective for soluble lysosomal protein defects than for membrane bound protein defects. For CNS pathology components of these diseases, optimization of enzyme titre needs to be a major focus and treatment will likely need to be combined with additional therapies such as gene therapy or cell transplant and pharmacological agents that reversibly permeate the BBB (Desnick, 2004; Beck, 2007).

1.9.3 Cell mediated therapy

Stem cell transplant therapy bridges the applications of ERT and gene therapy; hence it may prove to be an efficient method of treating NCL. Since transplants rely on the secretion of enzyme or other soluble factors to correct a deficit, it is proposed to be particularly applicable for those NCLs with a soluble enzyme deficiency. Current work on cell mediated therapy for the NCLs is concentrated on the delivery of therapeutic agents *in vivo* such as the corrected gene product, neurotrophic factors or anti-inflammatory agents, in an effort to prevent neuron degeneration altogether. Cell transplants have been tested in several models of NCL and in a number of cases has progressed to human clinical trials, providing a positive outlook for this therapeutic approach.

Bone marrow transplants have been evaluated in INCL (CLN1; PPT1) and LINCL (CLN2; TPP1) but the disease course was not significantly altered in any cases (Lake et al., 1997; Lonnqvist et al., 2001). Some studies have suggested that a limited number of bone-marrow derived stem cells can cross the BBB, integrate in the brain and differentiate into neural cells (Tanaka et al., 2003; Bae et al., 2007; Sostak et al., 2007) but not in sufficient quantities to correct the deficit. Hence, treatment may need to be combined with the use of agents that reversibly alter the BBB permeability or direct cell transplants into specific regions of the brain may be required.

Promising clinical trials have been carried out using human neural stem cells (NSC) which have been transplanted into the brains of children with NCL. Human clinical trials led on from preclinical studies in several animal models of INCL and LINCL in which human CNS stem cells migrated extensively and produced sufficient enzyme levels to alter the neuropathology (Tamaki et al., 2009). Accordingly, phase I clinical trials have been completed in six patients with advanced stages of INCL and LINCL

(http://clinicaltrials.gov/show/NCT00337636). Cells were transplanted directly into multiple sites within the brain and followed by 12 months of immunosuppressant therapy. Transplants were well tolerated by all patients, however clinical efficacy was hard to determine as treatment was started at such an advanced stage of disease and brain atrophy was so severe that only a limited number of cells remained to protect. Due to the favourable safety profile, a second clinical trial has been proposed to further assess safety and efficacy in patients with less advanced disease state and brain atrophy, and is currently awaiting approval by the US FDA.

The efficacy of many such treatments may well be obscured in early clinical trials as treatment is usually trialled on patients with advanced stages of the disease and progression of the disease can vary greatly between individuals suffering from the same NCL variant. This emphasises the need for careful consideration of the timing of intervention as demonstrated in a study by Escolar et al., (2005). They observed significant neurological improvements in patients with the LSD, globoid cell leukodystrophy, who received umbilical cord blood transplants pre-symptomatically but not in patients who received them post-symptomatically. However survival rates were not significantly altered. Although promising results have been demonstrated for cell transplants, they are not without associated risks and so far do not provide a competent therapeutic option for the treatment of NCL.

1.9.4 Gene therapy

Gene therapy can pertain to either the *ex vivo* genetic modification of donor cells or to the introduction of the correct copy of a gene to host cells *in vivo*. In 1993 the first clinical trial using gene therapy was carried out on a child with severe combined immunodeficiency syndrome. Lymphocytes were transduced *ex vivo* and transplanted back into the patient with therapeutic success (Thompson, 1993). However repeated transplants were required due to the short survival of modified lymphocytes. Due to the diverse nature of NCL, gene therapy has a number of hurdles to overcome. These include surmounting the BBB, obtaining adequate amounts of the gene product in tissue and maintaining and regulating *in vivo* expression. For the NCL forms resulting in mutation of transmembrane proteins there is an added caveat. The possibility of cross-cell correction is not a feasible option unless membrane protein defects involve the processing of diffusible agents, such as neurotrophic factors which can rescue neighbouring cells. Despite this, gene therapy using viral vectors is being investigated in a number of forms of the disease as a potential treatment, and sufficient expression of the unmutated form of the protein could compensate for the disease related deficiency. As little as 1-5% of the normal cellular protein concentration can achieve patho-physiological benefits

and correct the abnormal accumulation of undegraded substrates (Porter et al., 1971; O'Brien et al., 1973; Skorupa et al., 1999; Vogler et al., 2005; Wang et al., 2009).

Recombinant viral vectors have been tested in several LSDs including NCL animal models (Cachon-Gonzalez et al., 2006; Passini et al., 2007; Brooks et al., 2002; Griffey et al., 2005). Adeno-associated virus (AAV)2 and AAV5 vectors have been used to deliver the *TPP1* and *PPT1* gene to the CNS of CLN2 and CLN1 mice models respectively (Passini et al., 2006; Griffey et al., 2004). A reduction in fluorescent material and partial histological and morphological improvement was observed and there was no evidence of adverse effects (Hackett et al., 2005; Sondhi et al., 2005). Further studies by Cabrera-Salazar et al., (2007) and Sondhi et al., (2008) have emphasized the greatly increased possibility of therapeutic benefits of presymptomatic/neonatal intervention. In both cases, viral vectors administered to mouse models of CLN2 at the earliest time caused a significant recovery and a higher concentration and wider distribution of protein, compared with later injections.

On the basis of the above preclinical trials, a phase I human clinical trial is ongoing (http://clinicaltrials.gov/show/NCT 00151216) with the aim of studying the safety and clinical efficacy of such treatments. This study comprised direct intracranial administration of an AAV2 vector encoding the human *CLN2* gene to ten children with LINCL. Preliminary results, 18 months post injection, reported no unexpected serious adverse events which could be unequivocally attributed to the vector and a significantly reduced rate of neurological decline compared with untreated controls suggested a slowing of disease progression (Worgall et al., 2008). However as mentioned previously using clinical course as a means to estimate efficacy needs to be approached with caution. This study also lacks statistical significance due to experimental design and small sample size but the authors have proposed additional studies to assess the safety and efficacy of AAV-mediated gene therapy for LINCL.

Limitations exist with each of the treatments discussed and it is likely that no single treatment will suffice but that a combination of therapies will be required. Gene/cell mediated therapies that provide long-term availability of enzyme and pharmacological agents that reduce neuroinflammation or the abnormal build up of lysosomal storage bodies will probably provide the best therapeutic outcome. From all of the potential treatments discussed, it is apparent that the earlier therapeutic intervention begins the better the prognosis. Neonatal treatment offers many advantages and studies suggest that early detection and treatment may be essential for maximal therapeutic benefit for childhood diseases affecting the CNS. Hence, there is a need for earlier and more rapid diagnosis of NCL, as significant damage occurs between onset of initial symptoms and diagnosis and in some cases even before clinical signs

appear. This has implications for supporting newborn screening programs of NCL. Currently, carrier, prenatal and pre-genetic embryo (IVF) testing is available for the more common forms of NCL and the pre-symptomatic testing of younger children is possible using blood screening or rectal biopsy, when the diagnosis in an older child has been confirmed with similar tests. Early diagnosis and intervention before the onset of irreversible pathology would provide a substantial benefit to the newborn as well as enabling parents to receive genetic counselling and provide them with reproductive choices in the future. Until new-born screening becomes more widely available, this will impose an added limitation on therapeutic options.

1.10 Neuroinflammation

The CNS is considered to be immune-privileged due to the BBB and cerebrospinal fluid (CSF) which restrict the entry of plasma proteins and immune cells, and a lack of dendritic cells and lymphatic vessels in the brain (reviewed by Perry, 1998). These features, combined with perivascular macrophages and resting microglia which constantly survey the CNS and help to maintain homoeostasis, limit immune related events in the brain. Following damage, the activation of microglia and astrocytes within the brain, aided by infiltrating peripheral macrophages and lymphocytes, initiate an inflammatory response. These immune cells release a plethora of pro- and anti-inflammatory cytokines, neurotransmitters, chemokines and reactive oxygen species (ROS). Consequently these factors disrupt the BBB and recruit monocytes and lymphocytes to cross the BBB (Hickey, 1999; Taupin, 2008). Subsequently these cells become activated, releasing further inflammatory factors, creating a positive feedback loop which can result in neuronal damage (Das and Basu, 2008). The severity of inflammation can vary from mild acute to chronic uncontrolled inflammation, and the profile of inflammatory mediators differs between these two extremes, resulting in different effects (Whitney et al., 2009).

Microglial activation is a feature of many brain diseases and typically has been regarded as a reaction to cell death or infection within the brain, working to remove cellular debris (Vila et al., 2001). However, mounting evidence has indicated that microglial activation may be actively involved in neurodegeneration or neuroprotection (Vila et al., 2001). Microglial cells can mediate cell death via free radical, ROS, prostaglandin or cytokine production (Hunot and Hirsch, 1999; Beal, 2001). Alternatively, microglia can be neuroprotective by scavenging free radicals, secreting trophic factors and anti-inflammatory cytokines (Vila et al., 2001). This release of cytokines can in turn contribute to the modulation of microglial activation.

1.11 Cytokines and neuroinflammation

Cytokines are mostly glycoproteins that play crucial roles in cell-to-cell signalling and are involved in numerous processes including communication of systemic injury to the brain, infection and inflammation, control of behaviour, sleep and synaptic plasticity, and initiation and progression of neurodegeneration (Merrill and Benveniste, 1996). In the CNS they are mainly produced by microglia and astrocytes but can also be expressed in neurons. They can act on cells in intracrine, autocrine and paracrine manners but can also act as endocrine signals (Turrin and Plata-Salamán, 2000). Cytokines are expressed during normal development and in resting physiological conditions within the CNS but their expression is greatly increased at the onset of an inflammatory response (Griffin, 1997; Benveniste, 1998). Functionally cytokines have been classed as either pro- or anti-inflammatory but they do exhibit pleiotropy and redundancy (Turrin and Plata-Salamán, 2000). Furthermore, the role of specific cytokines during inflammation or injury can shift from beneficial to deleterious depending on the pathological state and cells involved (Akaneya et al., 1995).

Neuroinflammation has been determined to play a pivotal role in chronic neuropathological diseases such as AD, PD and multiple sclerosis (MS) (Minghetti, 2005; Eikelenboom et al., 2006). Studies of *post-mortem* brain tissue from patients and animal models have shown increased numbers of activated microglia and increased expression of pro-inflammatory cytokines compared to control tissue (Hunot and Hirsch, 2003; Cooper and Isacson, 2004; Greenberg and Jin, 2007; Zaremba and Losy, 2001; Sargsyan et al., 2005). Elevated expression of tumour necrosis factor-α (TNF-α) is evident in AD (Cacquevel et al., 2004) and PD (Mogi et al., 1994). The inhibition of harmful inflammatory processes via non-steroidal anti-inflammatory drugs (NSAIDs) or antibodies directed against pro-inflammatory cytokines have resulted in attenuation of neuronal loss, delay of onset and progression of disease, and even functional recovery in animal models of PD and AD (Gao et al., 2003; Sastre et al., 2006) indicating a pivotal role for these inflammatory mediators in neurodegeneration.

Similarly, brain inflammation is a common feature of all LSDs with CNS pathology. Numerous studies indicate that the inflammatory process contributes to pathogenesis (Jeyakumar et al., 2003; Smith et al., 2009), with inflammation predating the onset of clinical signs and even originating prenatally before any neurodegeneration is observed (Jeyakumar et al., 2003; Kay et al., 2006). In GM1 gangliosidosis and Sandhoff disease mouse models, concentrations of the pro-inflammatory cytokines TNF-α and interleukin-1β (IL-1β), and anti-inflammatory transforming growth factor-β (TGF-β), were found to increase with disease

progression and correlate with increased expression of the major histocompatibility complex (MHC)-II, a marker of immune upregulation (Jeyakumar et al., 2003).

1.11.1 Pro-inflammatory mediators of inflammation

Two of the most extensively studied cytokines produced during brain damage are TNF-α and IL-1β, considered to be mainly pro-inflammatory mediators (Viviani et al., 2004). Both are produced as biologically inactive precursors (pro-TNF-α and pro-IL-1β) and must be enzymatically cleaved to release the active form (TNF-α and IL-1β).

1.11.1.1 IL-1β

The inactive IL-1 precursor (pro-IL-1, 31kDa) requires enzymatic cleavage by IL-1 converting enzyme to produce the 17.5kDa active form. IL-1β acts on two receptors, type I (IL-1R1) which mediates most of the biological actions of IL-1, and type II (IL-1R2) which is not coupled to signal transduction mechanisms and may act as a 'decoy' receptor that neutralises IL-1 action (Sims, 2002). Once IL-1 binds the receptor IL-1R1, an accessory protein (IL-1RAcP) is recruited to form a receptor complex necessary for signal transduction. This complex, along with the adaptor molecule, MyD88, recruits several kinases, including IL-1 receptor kinases (IRAK) which can act via TNF receptor-associated factor (TRAF)-6 to activate transforming growth factor-activated kinase (TAK), resulting in activation of the transcription factors nuclear factor-κB (NF-kB) and activator protein-1 (AP-1), and mitogen-activated protein kinases (MAPKs) (Figure 3) (Viviani et al., 2004).

Figure 3 Signalling pathways modulated by IL-1R1
(Viviani et al., 2004).

1.11.1.2 TNF-α

TNF-α can be present as both a homotrimer transmembrane protein (tmTNF) or enzymatically cleaved to form a 51kDa soluble circulating trimer (solTNF), both of which are biologically active (Idriss and Naismith, 2000). Once TNF-α has been released it can interact with two different receptors, TNF receptor types I and II (TNF-R1, TNF-R2 or p55, p75) (MacEwan, 2002). TNF-R1 is expressed in most cell types and can be activated by binding of either solTNF or tmTNF. TNF receptor associated death domain protein (TRADD) interacts specifically with TNF-R1 and triggers caspase-8 via the Fas-associated protein with death domain (FADD) leading to apoptosis, and also associates with TRAF-2 to activate the transcription factors NF-κB and AP-1. In addition TRADD activates MAPKs and the ceramide/sphingomyelinase signalling pathway, and induces intracellular Ca^{2+} to increase (MacEwan, 2002), resulting in responses including inflammation, proliferation, cell migration, apoptosis and necrosis (Figure 4) (Ware, 2005; Eissner et al., 2000, 2004). TNF-R2 is thought to mediate fewer biological effects compared to TNF-R1 and is expressed primarily by cells of the immune system and is preferentially activated by tmTNF (Grell et al., 1995).

Figure 4 Signalling pathways modulated by TNF-RI

(Viviani et al., 2004).

1.11.2 Anti-inflammatory mediators of inflammation

Microglia also produce cytokines with anti-inflammatory activity, IL-4, IL-10, IL-13 and TGF being the most widely studied. They can inhibit the expression of inflammatory mediators via the regulation of transcription factors and cell signalling molecules.

1.11.2.1 TGF-β

TGF-β belongs to the TGF-β superfamily which also includes bone morphogenetic proteins (BMPs) and activins (Herpin et al., 2004). They are a family of cytokines with neurotrophic and immunosuppressive properties and modulate cell proliferation, differentiation, apoptosis, adhesion and migration of various cell types (Dennler et al., 2002). TGF-β is synthesized as a precursor which is proteolytically processed to the mature protein and dimerizes to produce a 25kDa active molecule (Herpin et al., 2004). It initiates intracellular signalling by binding to and bringing together type I and type II receptor serine/threonine kinases on the cell surface, which then initiate intracellular signalling by phosphorylation of Smad proteins (Itoh et al., 2000). It is not clear how TGF-β protects neurons, but several mechanisms have been postulated. For example, TGF-β contributes to the phosphorylation and thus inactivation of Bad, a pro-apoptotic protein, by activation of the Erk/MAP kinase pathway (Zhu et al., 2002). On the other hand, TGF-β increases production of the anti-apoptotic protein Bcl-2 (Prehn et al., 1994). TGF-β has also been shown to synergize with neurotrophins and/or be necessary for at least some of the effects of a number of important growth factors for neurons (reviewed in Unsicker and Krieglstein, 2000, 2002). In addition, TGF-β increases laminin expression (Wyss-Coray et al., 1995) and is necessary for normal laminin protein concentrations in the brain (Brionne et al., 2003) thought to provide critical support for neuronal differentiation and survival and which may be important for learning and memory (Luckenbill-Eds, 1997; Venstrom and Reichardt, 1993).

1.11.2.2 IL-10

IL-10 is one of the most important regulators of the immune system. It is a homodimeric, glycosylated polypeptide of two 17-21kDa monomers (Moore et al., 1990) which binds to two receptors, IL-10 receptors type I and II (IL-10R1 and IL-10R2). Although IL-10 is known to have many different roles in immune reactions, it is a powerful member of the anti-inflammatory cytokine family. It suppresses the NF-κB signalling pathway, which plays a critical role in stimulating expression of pro-inflammatory mediators (Ehrlich et al., 1998). IL-10 also induces expression of the suppressor of cytokine signalling (SOCS) family of proteins, resulting in inhibition of inducible nitric oxide synthase (iNOS) expression (Qasimi et al., 2006), and induction of anti-oxidant enzymes which regulate the production of ROS

and nitric oxide (NO) (Lee and Chau, 2002). In addition, IL-10 interrupts pro-inflammatory cytokine signalling by down-regulation of pro-inflammatory cytokine receptor expression (Sawada et al., 1999).

1.11.3 Other regulators of brain inflammation

In addition to anti-inflammatory cytokines several other negative regulators are expressed in order to modulate brain inflammation mechanisms. These include antioxidant enzymes and SOCS family proteins, which are negative feedback regulators of inflammation (Alexander and Hilton, 2004). SOCS-mediated regulation of inflammatory responses can occur via at least three mechanisms. They can suppress the janus kinase/ signal transducer and activator of transcription (Jak/STAT) pathway activated by inflammatory mediators (Yasukawa et al,. 1999) as well as suppressing activation of the transcription factor NF-kB, that plays a critical role in stimulating expression of pro-inflammatory mediators (O'Keefe et al., 2001). SOCS also inhibit p38MAPK which is significantly activated in response to lipopolysaccharide (LPS) or TNF (Kinjyo et al., 2002).

In addition, apoptosis of activated inflammatory cells is an important regulator of inflammation (Tidball and St.Pierre, 1996). Factors including Fas/Fas ligand and NO are responsible for inflammatory cell death. Furthermore, inflammation can induce apoptosis of activated microglia via the production of secondary mediators rather than direct activation of cell death pathways (reviewed in Yang et al., 2007).

Antioxidant enzymes including superoxide dismutase (SOD) and heme oxygenase-1 (HO-1) induced by anti-inflammatory cytokines such as IL-10 and TGF-β, can down-regulate inflammatory responses via the reduction of ROS (Yang et al., 2007; Kutty et al., 1994; Lee and Chau, 2002) another major signalling factor induced by inflammatory mediators. Prostanoids synthesized from arachidonic acid via the cyclo-oxygenase (COX) pathway are also important regulators of inflammation. Prostaglandin E2 is thought to have a protective role due to its ability to inhibit macrophage pro-inflammatory functions. It also inhibits microglial production of pro-inflammatory cytokines and nitric oxide as well as expression of MHC class II and co-stimulatory molecules (reviewed by Levi et al., 1998). These findings suggest that prostaglandin E2 production by activated glial cells may be another factor that contributes to the local regulation of inflammatory and immune responses. Increased concentrations of prostanoids and COX-2 have been demonstrated in several CNS inflammatory pathologies (Aloisi, 2001).

It is evident that diverse mechanisms co-operate to regulate the duration and extent of brain inflammation and disruption of this homeostasis can result in an uncontrolled inflammatory response and may contribute to neurodegenerative events (Yang et al., 2007). Hence, understanding which steps in the inflammatory cascade are disturbed in the NCLs could be crucial for understanding disease pathogenesis and potential therapeutic options.

1.12 Adult neurogenesis

Neurogenesis is the process by which new neurons are formed from populations of neural stem or progenitor cells residing in the CNS (Gage, 2000). It occurs in four main stages: 1) stem or progenitor cell proliferation, 2) migration, 3) differentiation into specific neuronal cell types, and 4) integration of these newly formed cells into existing neuronal networks (Abdipranoto et al., 2008). For over 100 years a central assumption in the neuroscience field had been that the generation of neurons occurs primarily during development and that new neurons are not added to the adult mammalian brain; thus it is incapable of regeneration.

> *In adult centres the nerve paths are something fixed, ended, immutable. Everything may die, nothing may be regenerated. It is for the science of the future to change, if possible, this harsh decree. S.Ramoin y Cajal (1928).*

In 1962 Joseph Altman challenged these beliefs with the first observations of adult neurogenesis which was followed by the studies of Kaplan and Hinds (1977). These received predominantly negative reactions with few researchers considering it a possibility. Thus it was not until the discovery of neurogenesis in birds in the 1990's and later in the mammalian hippocampus that adult neurogenesis was considered a possibility (Goldman and Nottebohm, 1983; Eriksson et al., 1998). Thereafter, the long-held dogma that we are born with a limited number of neurons and that the brain cannot regenerate or renew itself was undermined.

The adult brain contains two neurogenic regions, the subgranular zone of the hippocampal dentate gyrus and the subventricular zone (SVZ) of the lateral ventricles (Eriksson et al., 1998; Curtis et al., 2007). It has been estimated that 30,000 cells are generated bilaterally daily in the mouse SVZ and between 3,000 and 9,000 in the dentate gyrus of adult rats depending on age (Cameron and McKay, 2001; Lois and Alvarez-Buylla, 1994). Newly generated neurons of the subgranular zone migrate into the granular cell layer where they differentiate into neuronal cells and extend axonal projections to the CA3 region of the hippocampus, indicative of a role in learning, memory and mood regulation (Cameron et al., 1993). The progenitor cells of the SVZ migrate via the rostral migratory stream to the olfactory bulb, where they differentiate into interneurons, granule and periglomerular neurons

involved in olfactory discrimination and memory (Lois and Alvarez-Buylla, 1994; Abrous et al., 2005). Subsequently the newly generated neurons of the olfactory bulb and dentate gyrus establish synaptic contacts and functional connections with neighbouring cells (Markakis and Gage, 1999; Carlen et al., 2002).

The frequency of adult neurogenesis is reported to decrease with age and low levels of neurogenesis have been reported in older primates (Kornack and Rakic, 1999), including humans (Eriksson et al., 1998). Adult neurogenesis is regulated via a range of hormones, intrinsic growth factors and environmental conditions. It is reported that neurotrophic factors, such as brain-derived neurotrophic factor (BDNF), fibroblast growth factor-2 (FGF-2), insulin-like growth factor-1 (IGF-1) and vascular endothelial growth factor (VEGF) are involved in enhancement of adult neurogenesis either by direct effects on neuronal generation or indirectly via the promotion of newly generated neuron survival (Lee et al., 2002a; Palmer et al., 1995b; Aberg et al., 2000; Jin et al., 2002). Additionally, it has been reported that neurogenesis may be stimulated by such things as increased exercise, dietary restriction and an enriched environment, whereas stress, glucocorticoid overexposure and lack of sleep may inhibit neurogenesis (van Praag et al., 1999a, 1999b; Lee et al., 2002b; Kempermann et al., 1997; Mirescu et al., 2006, Sheline et al., 2003).

1.13 Neurogenesis in the diseased and injured brain

Adult neurogenesis is further influenced by pathological conditions affecting the brain. The resulting deficits arising from injury and disease are primarily due to the damage and death of neurons, but the disruption of endogenous neurogenesis may also contribute to the neurological deficits and hinder recovery from insults to the CNS (Krathwohl and Kaiser, 2004 a, 2004b; Kaul, 2008). The upregulation of neurogenesis is a well studied phenomenon in acute brain disorders (Carmichael, 2006; Wiltrout et al., 2007) with conditions such as status epilepticus and stroke inducing neurogenesis in the subgranular zone and SVZ (Parent et al., 1997; Arvidsson et al., 2001) as well as site-directed migration of newly generated cells outside of these germinal zones (Parent, 2002; Yanamoto et al., 2005). This has also been reported in human brain tissue with evidence for stroke-induced neurogenesis (Jin et al., 2006). Although this may be the case, a major problem is that only a small fraction of the newly generated neurons will survive long-term. It has been estimated that about 80% of stroke generated neurons die within two weeks of formation (Arvidsson et al., 2002), most likely because of the pathological environment into which the neurons are born. There are also many conflicting reports regarding neurogenesis in chronic neurodegenerative disorders,

with reports of increased and reduced neurogenesis in AD, PD and Huntingtons disease (HD) (Jin et al., 2004; Donovan et al., 2006; Curtis et al., 2003, 2005; Hoglinger et al., 2004).

Furthermore there is evidence for extended neurogenesis in ovine CLN6. Initially the persistence of small calbindin and calretinin positive granule cells were observed in the SVZ, white matter and cerebral cortex of affected animals (Oswald et al., 2008). Cells were found to span the rostral-caudal extent of the lateral ventricle and small granular and bipolar cells in the white matter and cerebral cortex had a radial orientation and were much more apparent in affected animals (Oswald et al., 2008). More recent studies have further implicated increased neurogenesis in ovine CLN6 (Dihanich et al., 2009, article in preparation) with poly-sialated neural cell adhesion molecule (PSA-NCAM) and doublecortin (DCX) staining of newly generated and migratory neurons markedly increased along the SVZ in affected animals at all ages. Moreover, spherical structures containing newly generated neurons observed in degenerating cortical regions are postulated to represent ectopic proliferation or aggregates of neuroblasts that have migrated to these sites.

Adult neurogenesis is finely tuned and any alteration in the microenvironment of the stem or progenitor cells may allow ectopic neurogenesis to occur (Nakatomi et al., 2002). Interestingly, ischaemia-induced neurogenesis was found to give rise to neurons not only in the traditional neurogenic regions but also in non-neurogenic regions, such as the striatum and cortex (Lindvall and Kokaia, 2008). These recent observations suggest that damaged brain regions, whether they are neurogenic or not, may be able to initiate regenerative responses and hence that neurogenesis can occur outside of the classical neurogenic regions. There are conflicting reports of neurogenesis occurring in the substantia nigra, neocortex and amygdala of non-human primates (Zhao et al., 2003; Frielingsdorf et al., 2004; Gould et al., 1999; Bernier et al., 2002; Koketsu et al., 2003), although the site of origin of these newly generated cells is unclear. It is postulated that they may be generated in the SVZ and migrate to neocortical regions (Gould et al., 1999, 2001) or they may be recruited from local progenitor cells which are awaiting some stimulus to induce neurogenesis in these non-neurogenic regions (Magavi et al., 2000; Zhao et al., 2003). Whether these newly generated neurons survive and incorporate into existing circuits in the diseased and damaged brain remains unclear. If the local microenvironment is not supportive, regenerative responses will not be successful. Nevertheless, the possibility that rare neurogenesis can take place outside of the normal neurogenic niche areas during the course of disease or brain injury cannot be ruled out.

1.14 Inflammation and adult neurogenesis

There is an emerging link between inflammation, neurogenesis and neurodegenerative diseases. Recent studies have demonstrated that microglial activation can impair neurogenesis, therefore it is possible that suppression of neurogenesis contributes to cognitive dysfunction in aging, dementia, epilepsy, and other conditions leading to brain inflammation (Ekdahl et al., 2003; Monje et al., 2003). Collective evidence suggests that acute and chronic inflammation which are major components of the pathological state of the diseased brain affects neurogenesis via the dysregulation of cytokines, chemokines, neurotransmitters and ROS produced by the mediators of inflammation; activated macrophages, microglia and reactive astrocytes (Whitney et al., 2009). Dependent on the severity of inflammation, the unique profile of inflammatory mediators can have contrasting consequences on neurogenesis and may influence several of the steps of adult neurogenesis; proliferation, survival, migration and differentiation.

Activation of microglia has been shown to have an inhibitory effect on brain repair (Monje et al., 2003; Ekdahl et al., 2003). *In vitro* studies have indicated that acute LPS-activation of microglia reduces NSC and neuronal differentiation (Cacci et al., 2008). This was further emphasised in a study by Ekdahl et al., (2003), in which the administration of the microglial inhibitor minocycline to a rodent model of status epilepticus increased the production of neurons whilst simultaneously decreasing the microglial population, indicating that uncontrolled inflammation is detrimental to neurogenesis. Pro-inflammatory factors such as TNF-α, IL-1β, IL-6 and IL-8 produced by activated microglia appear to induce these detrimental effects on neurogenesis (Liu et al., 2005a; Wang et al., 2007; Monje et al., 2003). Studies by Monje et al., (2003), revealed that IL-6 and TNF-α decrease *in vitro* neurogenesis dramatically, whilst IL-1β and interferon-γ (IFN-γ) effects were not significant. Conversely studies by Ben-Hur et al., (2003) showed a detrimental effect of IFN-γ on neurogenesis but contradictory findings that microglia stimulated with low levels of IFN-γ actually support neurogenesis have been reported (Butovsky et al., 2006). Therefore the influence of IFN-γ may well be concentration dependent or influenced by the presence of other inflammatory mediators, such as TNF-α.

Furthermore the receptors employed appear to influence neurogenesis, at least in the case of TNF-α. Iosif et al., (2006), indicated that TNF-R1 acts as a suppressor of neural progenitor cell (NPC) proliferation in the adult mouse hippocampus, whereas TNF-R2 can improve proliferation and survival of newly formed neurons. Certainly findings have varied between

studies depending on the models used; hence this is an area of research that requires further study to provide a concrete role for these mediators in neurogenesis.

There are many conflicting reports regarding the impact of inflammation on neurogenesis. Inflammatory factors released during acute inflammation are postulated to stimulate neurogenesis, whereas the factors released by uncontrolled chronic inflammation are thought to create an environment which is detrimental to neurogenesis (Whitney et al., 2009). Conversely, studies by Bonde et al., (2006), reported that new neurons which survived acute deleterious microglial activation in a rodent model of status epilepticus subsequently survived long-term, indicating a neuroprotective function of a chronic microglial response. Additionally, following stroke TNF-α production is increased in the SVZ of mice and acts as a negative regulator of NSCs (Iosif et al., 2006, 2008) but following the acute microglial response, the number of neuroblasts increases, suggesting a possible change in the role of TNF-α at later time points (Heldmann et al., 2005). Therefore, early detrimental actions of microglia after acute injury may sometimes be converted to a supportive state during the chronic microglial response.

Ultimately, it appears that microglial activation and inflammation are not pro- or anti-neurogenic as such, but that the net outcome is dependent on the balance between the pro- and anti-inflammatory secreted molecules (Ekdahl et al., 2009). Understanding the contribution and involvement inflammation may have in modulating neurogenesis will have implications for therapy, as pro- or anti-inflammatory treatments may be essential components of therapeutic strategies involving cellular or gene based therapies.

Chapter 2
Experimental Rationale

2.1 Research objectives

It was originally thought that neurodegeneration in the NCLs was a direct consequence of storage body accumulation in cells but studies in ovine CLN6 have revealed a close association between glial activation and subsequent neurodegeneration but not with storage body accumulation (Oswald et al., 2005; Kay et al., 2006). Glial activation was found to begin prenatally and preceded neurodegeneration. Whilst the underlying mechanisms resulting in this phenomenon are unknown, it does suggest that inflammation may be primarily involved in the pathogenesis of this disease. Hence understanding the cascade of activation/inflammatory events in ovine CLN6 and defining the pathogenic parts of the process could allow early and more accurate targeting of therapeutic suppression before significant neurodegeneration has occurred.

Furthermore, it has generally been considered that NCLs resulting from defects in soluble enzymes can be treated differently from those in which the defect is in a membrane bound protein (Bou-Gharios et al., 1993). The majority of studies support the hypothesis that therapies for LSDs, including NCLs, benefit significantly from cross-correction, whereby affected cells take up soluble enzymes from the surrounding environment (Frantantoni et al., 1969; Neufeld and Fratantoni, 1970; Neufeld and Muenzer, 1995). Exogenous enzyme could be provided via ERT, stem cell or gene therapy (see section 1.9), providing a continuous supply of functional enzyme. Once secreted, they can be endocytosed by other cells via mannose-6-phosphate receptors in the plasma membrane of most cells (von Figura and Hasilik, 1986; Neufeld, 2004) and as long as a small proportion of cells express the corrective gene, they can continuously supply the surrounding tissue with corrective enzyme via cross-correction (Shihabuddin and Aubert, 2010).

In contrast, these methods have not been assumed practical for NCLs resulting in deficits of membrane bound proteins, including CLN6, which are anticipated to be entirely intracellular. However in ovine CLN6, although there is widespread storage body accumulation, implying that the underlying pathological insult may be similar in all cells, severe degeneration is confined to the CNS and is regionally defined. Location and connectivity, not phenotype, seem to determine neuronal survival, indicating that intercellular interaction may be possible. Hence, although *CLN6* encodes a membrane bound protein, it may be involved in the processing of some soluble factor, which may be able to influence neighbouring cells.

Hence, therapeutic options based on cross-cell correction may be warranted even in the case of membrane bound protein defects. One such option is gene-therapy and studies such as these in the ovine brain are particularly important for advancing therapies to the clinic and do not have the same problems of scaling up to a large brain as those associated with small lissencephalic rodent brains.

2.2 Research aims, hypotheses and scope

The first aim of this study was to analyse whether differences in cytokine expression were occurring in the ovine CLN6 model compared to normal animals, and how these differences changed with increasing age and disease progression. Quantitative real-time polymerase chain reaction (PCR) was used to quantify pro- and anti-inflammatory cytokine expression, described in Chapter 3. The following hypotheses were tested:

- Differences in inflammatory cytokine expression exist between normal and diseased sheep.

- These differences implicate a central role for neuroinflammation in disease pathogenesis and represent potential therapeutic targets.

The second aim was to indicate whether normal cells can influence affected cells in the ovine CLN6 brain and what effect this has on disease progression and pathogenesis. Chimeric animals generated from blastomere exchange of normal and affected embryos were analysed for neuronal loss, glial activation, neurogenesis and storage body accumulation as indicators of modified disease pathology, and genotype analysis revealed the extent of normal and affected cell colonisation in the brain, as described in Chapter 4. The following hypotheses were tested:

- Normal cells can influence affected cells in the ovine CLN6 brain.

- Therapies based on cross-cell correction are an option even in NCLs resulting in membrane bound protein defects.

Lastly, Chapter 5 describes an experiment to test lentiviral-mediated green fluorescent protein (*GFP*)-gene transfer to the ovine CLN6 brain. Histological analysis revealed successful transduction of cells and stable expression of the GFP protein in the ovine brain. This tested the following hypotheses:

- Ovine CLN6 is an appropriate large-animal model for development of gene-therapy for the human NCLs.

- Targeted gene injections with selected vectors enhance the possibility of effective viral vector mediated gene therapy.

Chapter 6 provides a general discussion and conclusion, as well as future directions to carry on this research.

Chapter 3
Biochemical Analysis of Cytokine Expression

3.1 Introduction

Cytokines are multipotent, pleiotropic, low molecular weight proteins secreted by many different cell types, most prominently by cells of the immune system (Budhia et al., 2006). They include interleukins (ILs), interferons (IFNs), tumour necrosis factors (TNFs), chemokines and growth factors. Expression can be low or undetectable in the normal brain but can rise after some specific physiological stimulation, or become highly elevated in disease (Vitkovic et al., 2000). Cytokines are involved in the modulation of major immune responses such as lymphocyte activation, proliferation, differentiation, survival and apoptosis. They are also able to initiate, mediate and propagate numerous cellular inflammatory responses. Hence, some cytokines are thought of as "pro-inflammatory" whereas others are considered "anti-inflammatory", processes generally viewed as being neurotoxic and neuroprotective respectively.

Cytokines in the CNS have two possible origins. Either they originate from the peripheral immune system and cross the BBB or they are produced by glial cells and certain neurons within the CNS. Glial cells are both the primary source and target of many cytokines in the CNS, and they can release both neuroprotective (growth factors) and neurotoxic (ROS) substances in response to cytokine activation (Du and Dreyfus, 2002; Raivich et al., 1999). Hence neuronal viability depends on both the cytokine profile and the different substances released by glial cells in response to those cytokines. Cytokine expression is tightly regulated and they are usually produced only after cell activation in response to an induction signal. Both pro- and anti-inflammatory cytokine concentrations increase following brain injury or with the development of diseases like AD (Wang et al., 2007; Paganelli et al., 2002; Rota et al., 2006). These inflammatory responses are usually characterized by an early and pronounced activation of glia, aimed to inhibit the neurodegenerative process. However, if an uncontrolled inflammatory response is established it can promote neurodegenerative events (Viviani et al., 2004). The sustained release of inflammatory mediators works to perpetuate the inflammatory cycle, activating additional microglia, promoting their proliferation and resulting in the further release of inflammatory factors (Frank-Cannon et al., 2009).

The most extensively studied cytokines produced within the CNS following damage are TNF-α and IL-1β (see section 1.11.1). These are the two main pro-inflammatory cytokines with

pleiotropic and overlapping functions, produced largely by microglia and blood-derived macrophages during CNS inflammation. However, IL-1β and TNF-α should not be considered as neuroprotective or neurotoxic *a priori*, rather the question being under what conditions do these cytokines become neuroprotective or neurotoxic. Increases in both of these cytokines have been observed before neuronal death occurs (Viviani et al., 2004) and inhibition of IL-1β or TNF-α, via the IL-1 receptor antagonist (IL-1ra) or the soluble TNF receptor respectively, markedly attenuates several forms of neuronal damage (Loddick and Rothwell, 1996; Nawashiro et al., 1997). Although considerable, the evidence that pro-inflammatory cytokines like IL-1β and TNF-α are neurotoxic is still controversial. They do not cause neuronal death in healthy brain or normal neurons (Rothwell, 1997) although few studies indicate a neuroprotective role (Strijbos and Rothwell, 1995; Bruce et al., 1996). Ultimately, the type, duration and extent of cellular activity induced by cytokines can be influenced considerably by the micro-environment, depending on the type of neighbouring cells, cytokine concentration, the combination of other cytokines present and the temporal sequence of cytokine action on a cell. Hence, a single cytokine may transmit diverse signals (Viviani et al., 2004).

Microglia also produce cytokines with anti-inflammatory activity, such as TGF-β, IL-10 and IL-1ra (see section 1.11.2) which down-regulate inflammation in a number of ways. They can inhibit the expression of inflammatory mediators via the regulation of transcription factors and cell signalling molecules. In addition, they can regulate the production of ROS via the expression of antioxidant enzymes. Both TGF-β and IL-10 inhibit microglial activation through their ability to inhibit antigen presentation and by inhibition of pro-inflammatory cytokines and chemokines (Frei et al., 1994; O'Keefe et al., 1999). However increased expression and accumulation of TGF-β in the brains of AD patients points to an involvement of this cytokine in AD (Peress and Perillo, 1995). Thus it is important to remember that effects of cytokines such as TGF-β are dependent on the cell type and its differentiation state as well as on the combination of surrounding cytokines (Letterio and Roberts, 1998).

There are several neurodegenerative diseases in which microglial activation and function may play a more significant role in disease pathology than just protecting neurons (Kim and Joh, 2006). For example, inflammatory activity is one of the significant features of PD and concentrations of cytokines such as TNF-α, IL-1β and IFN-γ are elevated by 7-15 fold in the brain of PD patients (Mogi et al., 1994; Hirsch et al., 1998). Neurodegenerative CNS disorders, including MS, AD, PD, HD and amyotrophic lateral sclerosis are associated with chronic neuroinflammation and elevated expression of several cytokines (Block and Hong, 2005; McGeer and McGeer, 2007; Mrak and Griffen, 2005; Nagatsu and Sawada, 2006). In some

cases neuroinflammation may begin prior to significant neuronal loss and be driven by cytokines which play a role in modifying disease progression. For example, IL-1 is overexpressed in AD brains and induces microglial reactivity and astrocyte activation, which are part of the underlying pathophysiology of AD (Mrak and Griffen, 2001; Akiyama et al., 2000).

Numerous studies have also implicated immune system irregularities in LSDs, such as globoid cell leukodystrophy in which IL-6 and TNF-α have been reported to be upregulated in the CNS of the twitcher mouse model (Wu et al., 2001). Bone marrow transplant in these mice reduced cytokine expression and improved pathology, demonstrating that cytokine expression contributes to pathogenesis. IL-1β has also been reported to be upregulated in human and murine JNCL (Castaneda et al., 2008). Similarly, in Gaucher disease TNF-α and IL-1β have been reported to be increased and a correlation between the severity of clinical symptoms and concentrations of IL-1β and IL-6 in patients has been described (Allen et al., 1997; Barak et al., 1999). Hence, inflammation induced by activated microglia has the ability to exacerbate brain damage, emphasising the importance of understanding how the extent and duration of brain inflammation is controlled.

Cytokines have multiple actions in the CNS that can be important in neurodegenerative disease. The cytokine response can be detrimental or beneficial depending on the magnitude of activation, temporal profile and balance between pro-and anti-inflammatory molecules (Plata-Salaman, 2002). There is significant overlap in functions between different cytokines and their roles can change over time, with early expression after injury contributing to pathology, whereas later expression may assist in repair and recovery, or vice versa (Allan and Rothwell, 2003). The effects of cytokines also depend on which cell types they act upon and whether this is a direct or an indirect effect (Allan and Rothwell, 2001).

The balance between pro- and anti-inflammatory cytokines is crucial in the escalation and resolution of the inflammatory cascade. Hence, failure or dysfunction of the anti-inflammatory control mechanisms may play a role in the establishment of chronic neuroinflammation and neurodegenerative disease. Previous studies by Oswald et al., (2005) and Kay et al., (2006) revealed prominent early glial cell activation within the ovine CLN6 brain, which precedes neurodegeneration. Given the earliness of the first response it is surprising how long the development of the affected sheep brains follows a normal growth path. The underlying molecular cues responsible for this early activation are unknown but glial cells are a major source of cytokines within the CNS. Hence, in this study the expression of key pro- and anti-inflammatory cytokines at different stages of disease development was investigated to gain an insight into changes in the cytokine expression profile with disease progression. Determining

which step in the cascade becomes fatally damaging to neurons will be important for timing and targeting of therapeutic interventions.

3.2 Materials and methods

3.2.1 Animals

The sheep used in experiments described here and in ensuing chapters were part of a unique flock of a sheep model of CLN6 NCL that provides off-spring and samples for subsequent experimental analysis. This model was first described by Jolly & West (1976) in two affected rams from a flock of South Hampshire sheep. An experimental flock providing affected animals has since been developed and maintained by crossing homozygous affected rams with heterozygote carrier ewes, resulting in 50% affected and 50% carrier off-spring each year. An out-breeding program in recent years has introduced heterozygous ewes attained from crosses between normal Friesian, Finn and Coopworth ewes, and affected South Hampshire rams to improve the health and reproductive performance within this sheep colony.

Since 2004 all offspring are diagnosed at 2-3 months of age by an A/G restriction enzyme test on DNA extracted from blood. The non-disease causing allelic variation exploited for genotyping occurs in the coding region of *CLN6*, 111bp downstream of the 5´ end of exon 7, with either A or G (c.288G>A) being the third base of the codon triplet both coding for alanine. The flock is structured so that all affected sheep carry only the A allele, control animals carry only the G allele and heterozygote South Hampshire animals carry both. This variation provides a differential cut site for the restriction enzyme *Hae*II which cuts GGC**G**CT but not GGC**A**CT (Tammen et al., 2006). Amplification from genomic DNA, enzymatic cleavage of the GCG form and gel separation of the products allows allele analysis and is therefore used as an indirect DNA test on the South Hampshire sheep. This diagnosis method was originally tested against brain biopsies (for storage body accumulation) and subsequent development of clinical signs on 292 sheep over three seasons and established as perfectly reliable. No sign of disease has ever been noted in heterozygous animals, therefore these or homozygous normal animals were used as controls. All animals were maintained under standard New Zealand pastoral conditions on university farms and animal procedures carried out in accordance with the New Zealand Animal Welfare Act, 1999.

3.2.2 Immunohistochemistry

3.2.2.1 Tissue collection and processing

Brain tissue from affected sheep aged 18 and 24 months was used in conjunction with age-matched unaffected control tissue for formalin fixation. Sheep were sacrificed under ketamine/diazopan anaesthesia by exsanguination. The brain was fixed by perfusing the head via the carotid arteries, firstly with phosphate buffered saline (PBS, pH 7.4, 37ºC) to clear the blood followed by 200-300ml warm 10% formalin in 0.9% NaCl. The spinal cord was cut, the brain removed intact and left in fixative for seven days at room temperature (RT). Fixed brains were then bisected along the midline and re-equilibrated in a solution of 30% sucrose, 10% ethylene glycol and 0.9% NaCl, and stored frozen at -80^{o}C for subsequent tissue sectioning.

Sequential 50µm sagittal sections were cut through the medio-lateral extent of the right hemisphere using a sliding microtome (MICROM International, Walldorf, Germany). Sections were collected, one per well, into 96-well plates containing cryoprotectant (PBS containing 30% ethylene glycol, 15% sucrose and 0.05% sodium azide) and stored at -20^{o}C until required.

Brain tissue was collected for zinc salt fixation (ZSF) from a 24 month old affected animal and an age-matched control, sacrificed by exsanguination. The spinal cord was cut and the brain removed intact and immediately placed on ice. Duplicate 1cm^3 samples were dissected from the frontal, parietal and occipital lobes, and from the cerebellum. Samples were placed in freshly prepared zinc salt fixative (Appendix A.1) (Gonzales et al., 2001), trimmed after 6 h and placed in fresh fixative for a further 36 h. Samples were then paraffin wax-embedded and 5µm sections serially cut from each block and mounted on superfrost plus glass slides (Gribbles Veterinary Pathology, Christchurch, New Zealand).

Mesenteric lymph nodes from an animal infected with the parasitic gastrointestinal nematode *Trichostrongylus colubriformis*, shown to increase cytokine expression in infected animals (Pernthaner et al., 2005), were also collected and either formalin or ZSF fixed, and processed as above for use as positive control tissues for cytokine expression.

3.2.2.2 Immunohistochemistry

Antibodies used were mouse anti-bovine TNF-α (1:500, monoclonal, AbD Serotec, Kidlington, Oxford, UK), mouse anti-bovine IL-10 (1:500, monoclonal, AbD Serotec), mouse anti-sheep IL-1β (1:500, monoclonal, AbD Serotec), and mouse anti-sheep/human TGF-β (1:500, monoclonal, Abcam, Cambridge, UK). Mouse anti-parvalbumin (1:2000, monoclonal, Swant, Bellinzona, Switzerland) was used to detect interneurons as a positive control for the histochemical reagents and protocol. All antibodies were diluted in 10% normal goat serum

(NGS) in PBST (PBS, pH7.4, containing 0.3% Triton X-100). Slides were blocked for 30 min with 1% H_2O_2 in PBST to quench endogenous peroxide activity and for 60 min in 15% NGS in PBST to remove non-specific tissue antigens. All steps were followed by three washes in PBST. Chromogenic detection of primary antibodies was performed via two methods.

1) The avidin-biotin amplification system linked to horseradish peroxidise (HRP) was used on formalin-fixed sagittal brain sections. Sections were processed simultaneously, stained floating in 6-well plates and all steps were performed on a rocking platform. Antigen retrieval was performed by microwave pre-treatment of the fixed tissue as described previously (Fritschy et al., 1998). The tissue sections were incubated overnight in 0.1M sodium citrate buffer, pH 4.5, at 4°C, then transferred to 6-well plates, 10ml of fresh buffer per well, and irradiated in a household microwave oven at 650 W for 30 s. After cooling to RT, sections were blocked with H_2O_2 and NGS as above, then incubated with primary antibody, overnight, 4°C. Immunoreactivity was detected using the secondary antibody, biotinylated goat anti-mouse IgG (1:1000, Sigma, St.Louis, MO, USA), followed by ExtrAvidin peroxidase (Sigma) made up at least 45 min prior to use, diluted 1:1000 in PBST. Secondary and tertiary reagent incubations were 2 h at RT. Staining was visualised by incubation in 3, 3'-diaminobenzadine (DAB, 0.5mg/ml [Sigma], 0.01% H_2O_2 in PBS) solution for 20 min away from direct light. Sections were rinsed in H_2O (all water used here and in ensuing chapters was deionised by electrodeionization), mounted in a solution of 0.5% gelatine and 0.05% chromium potassium sulphate on custom-made glass slides (Milton Adams Ltd., Auckland, New Zealand), air-dried, dehydrated in 100% ethanol, cleared in xylene and coverslips mounted with DPX (BDH, Poole, England).

2) The EnVision Plus HRP system for mouse immunoglobulins (Dako, Ely, England) was used on paraffin wax-embedded ZSF tissue. Control and affected brain tissue slides of cerebellum, frontal, parietal and occipital lobes, and lymph node sections, were dewaxed and hydrated; 2 x xylene, 2 x 100% ethanol, 1 x 95% ethanol, 1 x 70% ethanol, 1 x 50% ethanol and 2 x H_2O. Excess liquid was removed and sections encircled using a Dako pen (Dako), then transferred to Coplin jars and rinsed in PBS and PBST. Following the blocking steps described above, slides were incubated with primary antibody overnight at 4°C in a sealed container lined with damp tissue. Bound antibody was detected with secondary antibody, peroxidise labelled polymer conjugated to goat anti-mouse immunoglobulins, from the EnVision system kit, applied for 30 min at RT. Conjugate binding was detected with DAB (included in kit), colour allowed to develop for 20 min away from direct light and tissue sections washed with H_2O. Sections were counterstained with haematoxylin (BDH), rinsed, dehydrated in graded ethanol; 1 x 70%

ethanol, 1 x 90% ethanol, 1 x 95% ethanol, 2 x 100% ethanol, cleared for 30 min in xylene and coverslips mounted with DPX (BDH).

Negative control sections, in which either the primary or secondary antibody was omitted, were included in each staining run. In addition sections were incubated with mouse IgG isotype controls (AbD Serotec) appropriate to the isotype of, and at the same dilution, as the respective primary antibody. Isotype control antibodies had no specificity for the antigens in question but had all the non-specific characteristics of the antibodies used in the experiment. Lymph node sections were included as positive controls.

3.2.3 Western blotting

Proteins of homogenates of brain samples from 18 month old affected and control animals were separated by LDS-polyacrylamide gel electrophoresis (PAGE) and analysed by Western blot with spleen tissue and peripheral blood lymphocytes used as positive controls.

3.2.3.1 Peripheral blood mononuclear cell culture

Blood was collected from the jugular vein of an affected and a control 18 month old sheep into vacutainers containing ethylenediaminetetraacetic acid (EDTA) as anticoagulant. Immediate centrifugation of samples for 20 min, 4ºC, 2600rpm, separated the blood into three layers: red blood cells, buffy coat containing leukocytes and platelets, and plasma. The buffy coats were collected into 15ml tubes and 3ml of Roswell Park Memorial Institute medium 1640 (RPMI, GIBCO, Invitrogen, Carlsbad, CA, USA) (Moore et al., 1967) containing 0.075% EDTA pH 8.0, 100U/ml penicillin and 100µg/ml streptomycin (GIBCO) added. Lymphocytes were isolated by floatation over an equal amount of Ficoll-Paque PLUS (GE Healthcare, Uppsala, Sweden) separating buffer and centrifugation for 30 min, RT, 3000rpm, as described by Bøyum (1968). Lymphocytes were collected from the interface of the two resultant phases, washed twice in 5ml of RPMI + EDTA medium and centrifuged for 10 min, 1100rpm, to remove remaining platelets, Ficoll and plasma. Pelleted lymphocytes were resuspended in 2ml of RPMI and 5% fetal calf serum (FCS) (GIBCO) culture medium. Lymphocyte viability was determined using vital dye exclusion. A 1:1 dilution of 0.04% trypan blue (GIBCO) and cell suspensions (1:50, 1:100 and 1:500 dilutions in RPMI medium) were prepared on a haemocytometer and living lymphocytes counted under a light microscope. Cells/ml were calculated using the formula

> Cell counts/number squares counted x (dilution factor of cells) x 2 (trypan dilution factor) x 10^4 = n x 10^6 cells/ml

Subsequently cell suspensions were diluted to 1 x 10^6cells/ml in RPMI and 5% FCS culture medium, and 0.5ml of cell suspension added to wells of a flat bottomed 24-well tissue culture plate (Nunc, Thermo Fischer Scientific, Roskilde, Denmark). Half of the samples were stimulated with 0.5ml culture medium containing 100µl of concanavalin A (ConA) (Sigma) and half unstimulated with 0.5ml of culture medium alone, yielding a final concentration of 5 x 10^5 cells/ml. Plates were incubated at 37°C, 5% CO_2, 95% humidity for three days and checked daily for cell proliferation. Cells and medium were collected from each well and placed into microfuge tubes. Following centrifugation, 10 min, RT, 2000rpm, supernatant was removed and frozen at -20ºC. Pelleted lymphocytes were resuspended in PBS, centrifuged as before, PBS removed and cells frozen at -20ºC.

All *in vitro* procedures were carried out under aseptic conditions in a laminar flow hood in a tissue culture room and reagents were pre-warmed to RT and filtered prior to use, where appropriate.

3.2.3.2 Preparation of protein samples

Two hundred mg of spleen and occipital lobe grey matter tissue from 18 month old affected and control animals were dissected out. Tissue was homogenized in a hand-held homogeniser in 1ml of ice-cold radioimmunoprecipitation assay (RIPA) buffer (Appendix A.2) containing 100µl of complete mini protease inhibitor cocktail (Roche Diagnostics, IN, USA) before being gently passed through a 25G needle to manually homogenise each sample. Homogenates were left on ice for 45 min before centrifugation 40 min, 4ºC, 13,000rpm. Resultant supernatants were kept at -20ºC until required.

The protein concentrations of supernatants and both stimulated and unstimulated lymphocytes, resuspended in 50µl of sterile PBS, were determined using bicinchoninic acid (BCA) (Pierce Biotechnology, Rockford, Il, USA) as per manufacturer's instructions and described by Coligan et al., (1995). All samples were diluted 1:10, 1:50 and 1:100 with H_2O and 10µl samples assayed in triplicate. Samples were incubated for 30 min, 37°C, with 200µl of BCA solution and compared to a standard curve generated using dilutions of a 2mg/ml albumin standard to provide concentrations ranging from 0.0625mg/ml to 1mg/ml. Absorbance at 562nm was measured on a Fluostar plate reader (BMG Labtechnologies, Offenberg, Germany) and blank lysis buffer was analysed to provide a zero value.

3.2.3.3 Polyacrylamide gel electrophoresis

To evaluate the expression of cytokines in brain, spleen and lymphocytes from normal and affected 18 month old animals, two gels were prepared for each sample type. Sample sets were

run in duplicate in each gel and following transfer to the membrane, each membrane was halved and each half incubated with a different primary antibody concurrently.

Proteins were separated by denaturing LDS-PAGE performed using a Bio-Rad Mini Protean II Cell Electrophoresis System (Bio-Rad Laboratories, Hercules, CA, USA). Polyacrylamide gels, 0.75mm x 7cm x 10cm, were prepared after the method of Laemmli (1970), with an acrylamide:bisacrylamide ratio of 29:1 w/w (Bio-Rad) used to make a 15% resolving gel and 4% stacking gel (see Appendix A.3 for gel and electrophoresis buffer constituents).

Protein samples were diluted 1:1 in Laemmli sample buffer (Bio-Rad) containing 0.5% β-mercaptoethanol (Sigma) to a total volume of 20µl, denatured at 98°C for 3 min, spun down and loaded at 20µg total protein/well. Electrophoresis was carried out at RT for 2 h at 100V. Molecular weights of protein were determined by comparison of their migration rates with those of the dual colour Precision Plus Protein standard, 10-250kDa range (Bio-Rad).

3.2.3.4 Western blot analysis

Proteins separated by electrophoresis, as above, were transferred from acrylamide gels to Hybond C-extra nitrocellulose membrane (Amersham Biosciences, Piscataway, NJ, USA) in a Bio-Rad Mini Trans-Blot Electrophoresis transfer cell. Transfer was carried out for 1 h, 100V, 4°C, using cold transfer buffer (Appendix A.3) and a cooling unit. Membranes were rinsed in Tris buffered saline (TBS, 0.1M Tris-HCL, pH 8.0, 0.15M NaCl) and water and stained for 10 min in 0.1% (w/v) Ponceau S (BDH) and 4% (v/v) acetic acid. This reversible stain was used to verify transfer efficiency prior to immunodetection. Lane positions were marked with a pencil, and each membrane cut in half and numbered. Membranes were destained in TBS and blocked for 60 min in 3% (w/v) bovine serum albumin (BSA) in TBS, RT, to block additional binding sites on the membrane. This and all subsequent steps were carried out on a rocking platform and followed by 4 x 5 min washes in TBS containing 0.05% Tween-20. Each sample was immunostained for TNF-α (17.5kDa), IL-1β (17.5kDa), IL-10 (17kDa) and TGF-β (12.5kDa). Antibodies (previously utilised in section 3.2.2.2) were diluted 1:2000 in TBS containing 3% BSA and 0.05% Tween-20. Membranes were incubated in the presence of one primary antibody overnight, 4°C, washed, then 90 min, RT, in biotinylated goat anti-mouse secondary antibody (1:20,000, Sigma). Subsequently, ExtrAvidin peroxidise (Sigma) was diluted 1:3000 in TBS and applied for 30 min, RT. Following four changes in TBS, antigens were detected by enhanced chemiluminescence using the SuperSignal West Pico chemiluminescent substrate (Pierce Biotechnology) according to the manufacturer's instructions. Exposure to BioMax MS Film (Eastman Kodak Company, Rochester, NY, USA) was carried out in an autoradiograph cassette and the exposure time for each antigen was kept consistent for all samples to ensure that

variation in band intensities was not due to differing exposure times between blots. Films were developed with X-ray film developer and fixer solutions (Kodak) and subsequently scanned on a flat bed scanner (CanoScan, Canon, NY, USA) at 600dpi and saved as JPEG files.

3.2.4 Quantitative real-time PCR

Quantitative real-time PCR (qPCR) using the standard curve method determined the relative gene expression of *TNF-α, IL-1β, IL-10* and *TGF-β* in affected and control sheep at 6, 9, 18 and 24 months of age. Each sample was analysed in triplicate and the same batch of cDNA was used to quantitate all genes in order to reduce possible variability from differing reverse transcriptase efficiencies.

3.2.4.1 Sample preparation, RNA extraction and cDNA synthesis

Fresh brains were obtained from two each of 6, 9, 18 and 24 month old affected and control sheep sacrificed by exsanguination. Immediately following sacrifice one hemisphere of each brain was sliced into serial 6mm sagittal slabs that were snap frozen in liquid nitrogen and stored at -140ºC.

RNA was extracted from samples of the most medial slab of each brain. Using a scalpel 30mg of tissue was collected from the frontal, parietal and occipital lobes, as close to the cortical region as possible and with minimal extraction of white matter. Using corresponding slabs from different animals ensured that samples were collected from the same region of each animal. Total RNA was isolated using the Qiagen RNeasy mini kit (Qiagen, Hilden, Germany) according to manufacturer's instructions. Cells were lysed in 600µl of lysis buffer, after which the RNA was immobilized on a silica-gel membrane, washed, DNase I (RNase-Free DNase set, Qiagen) treated to remove any genomic DNA contamination and eluted in 50µl RNase-free water by centrifugation. The optical density $(OD)_{260}$ and 260/280nm ratio was measured using a spectrophotometer (NanoDrop Technologies Inc., Wilmington, DE) for each sample and the RNA factor (40) was used to quantitate the concentration (ng/µl)

$$40 \times OD_{260} \text{ of the sample} = \text{concentration of RNA } (\mu g/ml)$$

RNA integrity was checked by separating 5µl RNA on a 1.5% agarose gel in TBE (Appendix A.4) with 0.5µg/ml ethidium bromide, 30 min, 100V. An image was obtained using a GelDoc XR (Bio-Rad) imaging system and Quantity One v4.5.1 image analysis software (Bio-Rad).

Single stranded cDNA was synthesised from 450ng of total RNA in two 20µl reactions using Superscript III reverse transcriptase (Invitrogen) as per the manufacturer's instructions. RNA was diluted to a total volume of 13µl with RNase free water, 1µl of 10mM dNTPs (Invitrogen)

and 2µl of 50µM random hexamers (Invitrogen) and incubated at 65ºC for 5 min after which samples were submerged in ice for 1 min. A first strand synthesis master mix consisting of 1 X First Strand buffer, 200 U Superscript III polymerase and 40 U RNaseOut Recombinant Ribonuclease Inhibitor (Invitrogen) was prepared and a 7µl aliquot added to each sample. These were then incubated at 25ºC, 5 min, and 50ºC for 50 min followed by inactivation at 70ºC, 15 min. All PCR reactions were carried out on a Mastercycler Gradient PCR machine (Eppendorf, Hamburg, Germany). Following cDNA synthesis, duplicate samples were pooled and 5µl aliquots frozen at -20 ºC.

3.2.4.2 Primer design

Three housekeeping genes for the large ribosomal protein PO (*RPLPO*), the α subunit of the ATPase (Na+/K+) pump (*ATPase*) and glyceraldehye-3-phosphate dehydrogenase (*GAPDH*) were analysed for accurate and comparable quantitation of expression levels of cytokines in the brain.

TNF-α, TGF-β, IL-1 β, IL-10, GAPDH and *ATPase* gene specific internal and external primers were based on the ovine mRNA sequences from previously published data (McNeilly et al., 2008; Pariset et al., 2006; Smeed et al., 2007) (Table 3).

Ovine RPLPO sequence information was incomplete but showed 99% homology with the full length bovine sequence by a BLAST algorithm search using the National Centre for Biotechnology Information (NCBI) GenBank. Therefore primers were designed based on the bovine sequencing information. Internal primers were based on unpublished data (Houweling, 2009). External primers spanning ~500bp were designed using the FASTPCR programme (http://www.biocenter.helsinki.fi/bi/Programs/manual.htm).

All gene specific primers were synthesized and supplied lyophilized (Invitrogen). Each primer was diluted using sterile TE (10mM Tris-HCl, pH 8.0, 1mM EDTA) to a stock concentration of 50µM. Working dilutions of 5µM were diluted with sterile water. All stock and working solutions were stored at -20ºC.

PCR reactions were optimized for annealing temperature (T_m), cycle number and primer concentration to ensure a single gene specific band was produced and the identity of each band confirmed by sequencing prior to qPCR experimentation. A standard 20µl PCR reaction was carried out with 1µl of control ovine brain cDNA (as prepared in section 3.2.4.1) and forward and reverse primer sets for all cytokine and housekeeping genes. Each 20µl reaction contained 0.125µM of forward and reverse primer, 0.125mM dNTPs, 2µl 10x Buffer, 2.5mM $MgCl_2$ and 1U *Taq* DNA polymerase (Qiagen). The cycles used were: 95ºC for 10 min, 35 cycles of 95ºC

for 30 s, 57ºC for 30 s and 72ºC for 30 s, followed by 72ºC for 5 min. A single, clean band of the expected size was observed by fluorescent ethidium bromide binding for all primer sets by separating 10µl PCR products out on 1.5% agarose gels (as per section 3.2.4.1) and calibrated using 5µl of the 1Kb Plus DNA Ladder (1µg/µl, Invitrogen) molecular weight control.

Subsequently, 6ng of PCR product and 5pmol of forward primer were diluted in water to 15µl and sent for sequencing to Allan Wilson Centre Genome Service (AWCGS), Massey University, using Big Dye terminator v3.1 Cycle sequencing (Applied Biosystems, Foster City, CA, USA). Pre-sequencing clean-up was performed with a CleanSEQ Dye-Terminator removal kit (Agencout Bioscience Corporation, Beverly, MA, USA) and samples sequenced on an ABI PRISM 3100-Avant Genetic Analyser (Applied Biosystems). The resulting sequences were aligned against the ovine sequence or the bovine sequence for RPLPO (see Table 3 for accession numbers).

Table 3 Primer sequence information and reaction conditions for qPCR

Gene	NCBI accession number	Primer type	Primer sequence (5'- 3')	Product size(bp)
TNF-α	X55152	External	F, TCC TTG GTG ATG GTT GGT R, CAC TGA CGG GCT TTA CCT C	525
		Internal	F, GAA TAC CTG GAC TAT GCC GA R, CCT CAC TTC CCT ACA TCC CT	238
TGF- β	NM_001009400	External	F, GCC CTG GAC ACC AAC TAC TG R, TCA GCT GCA CTT GCA GGA G	338
		Internal	F, GAA CTG CTG TGT TCG TCA GC R, GGT TGT GCT GGT TGT ACA GG	169
IL-1β	NM_001009465	External	F, CTG TGT TCT TCC CTT CCC TT R, CAA AAA TCC CTG GTG CTG	518
		Internal	F, CCT TGG GTA TCA GGG ACA A R, TGC GTA TGG CTT TCT TTA GG	317
IL-10	NM_001009327	External	F, AGC TGT ACC CAC TTC CCA R, GAA AAC GAT GAC AGC GCC	305
		Internal	F, TGA AGG ACC AAC TGA ACA GC R, TTC ACG TGC TCC TTG ATG TC	160
GAPDH	AF030943	External	F, AAG GCA GAG AAC GGG AAG R, AGT GAT GGC GTG GAC AGT	366
		Internal	F, GGT GAT GCT GGT GCT GAG TA R, TCA TAA GTC CCT CCA CGA TG	265
RPLPO	BT021080	External	F, TCT TCC AGG CTT TAG GCA TCA CC R, ACC TTG GCT GGG GCT GCG GTG GT	494
		Internal	F, CAA CCC TGA AGT GCT TGA CAT R, AGG CAG ATG GAT CAG CCA	226
ATPase	NM_001009360	External	F, GAC GTG GAG GAC AGC TAT GG R, GCT TCG GTG CTT TCC TAC C	501
		Internal	F, GCT GAC TTG GTC ATC TGC R, CAG GTA GGT TTG AGG GGA TAC	168

3.2.4.3 RPLPO plasmid generation

Standard curves for *TNF-α, IL-1β, IL-10*, *TGF-β, GAPDH* and *ATPase* were generated from plasmids of known concentration generously donated by Dr. T.McNeilly, Moredun Research Institute, Midlothian, Scotland.

For generation of the RPLPO plasmid a classical TA cloning protocol was used to insert a fragment of the ovine *RPLPO* cDNA into a plasmid vector. cDNA plasmids are advantageous in that once constructed, they can be easily prepared in large amounts, ensuring that numerous experiments can be performed using the same dilutions of the standard, minimizing interassay variations.

External forward and reverse primers for RPLPO spanning 300-500bp were designed, as outlined in the previous section, to generate a primary PCR product. A PCR was performed on 1µl control ovine brain cDNA (extraction and synthesis as per section 3.2.4.1) in a 20µl reaction, set up and cycling conditions as per section 3.2.4.2.

The resultant PCR product was separated on a 1.5% agarose gel, excised and purified using the AxyPrep DNA Gel Extraction Kit (Axygen Scientific Inc, CA, USA) as per manufacturer's instructions. Under ultraviolet illumination the gel slice containing the DNA fragment of interest was excised and the sample heated to 75ºC in supplied buffer to solubilise agarose. DNA was immobilised on a miniprep column, washed and eluted in 30µl of eluent (2.5mM Tris-Cl, pH 8.5) by centrifugation. Three µl of purified DNA product was run on a 1.5% agarose gel for estimatation of concentration and a sample sent for sequencing (as per section 3.2.4.2), using external RPLPO forward and reverse primers to confirm correct PCR product prior to cloning.

Subsequently, 50ng of product was cloned into the sequencing vector pGEM-Teasy (Promega Corporation, Madison, WI, USA) as per manufacturer's instructions. A 10µl ligation reaction component consisting of a 1:1 ratio of pGEM-Teasy vector and insert, 2 X Rapid Ligation buffer and 3 U of T4 DNA ligase was incubated overnight at 4ºC.

In a microfuge tube, 2µl of ligation mix and 50µl competent cells (*Escherichia coli* JM109, Invitrogen) were placed on ice for 20 min, followed by heat shock at 42ºC, 2 min, then immediately put on ice for a further 2 min. Nine hundred and fifty µl of super optimal broth medium (SOC) (Appendix A.5) was added and the transformation mix incubated in a shaking incubator at 850rpm, 90 min, 37 ºC. Following transformation of competent cells with the ligated plasmid, colonies were obtained by plating 100µl or 200µl of ligated plasmid cells onto lysogeny broth (LB) agar plates (Appendix A.6) including 100µg/ml Ampicillin (Duchefa Biochemie B.V, Haarlam, The Netherlands) and containing 0.5mM isopropyl β-D-1-

thiogalactopyranoside (IPTG) (Sigma) and 50mg/ml X-Gal (Quantum Scientific, Milton, Qld, Australia), and left to grow overnight at 37 ºC. A control LB only plate, plated with 50µl of ligated plasmid cells verified competent cell viability.

Following overnight incubation, a single white colony from one of the LB + Ampicillin plates was used to inoculate a 20µl PCR mix to check correct insertion of the *RPLPO* sequence. PCR set up and cycling conditions were as per section 3.2.4.2. A single band of expected size was observed verifying insertion into the plasmid. A 1ml starter culture consisting of LB broth (Appendix A.7) containing 100ug/ml Ampicillin, was inoculated with the same colony and grown for 4 h, 37 ºC and 500µl of this starter culture added to 5ml of LB broth containing 100ug/ml Ampicillin and grown up overnight at 37 ºC in a shaking incubator at 250rpm. Glycerol bacterial stocks were prepared by mixing 500µl aliquots of this overnight culture with 500µl of sterile glycerol and frozen in cryotubes at -80 ºC for future use.

Subsequently 1.5ml of the remaining culture was centrifuged and the resulting cell pellet processed through the AxyPrep Plasmid Miniprep Kit (Axygen) to isolate plasmid DNA, as per manufacturer's instructions. The pelleted bacterial cells were resuspended in supplied buffer, lysed and centrifuged for 10 min, 12,000rpm, to pellet the bacterial DNA, protein, and cell debris and the resultant supernatant was applied to a spin column, washed and centrifuged to adsorb plasmid DNA to the silica-gel membrane. Plasmid DNA was eluted in 60µl eluent (2.5mM Tris-Cl, pH 8.5) and quantitated spectrophotometrically at 260nm on a Nanodrop, and the corresponding copy number calculated using the equation

$$(X \text{ g/µl DNA} / [\text{plasmid length in bp} \times 660]) \times 6.022 \times 10^{23} = Y \text{ molecules/µl}$$

Sequencing of the insert was carried out using the universal MI3 forward (5′-GTA AAA CGA CGG CCA GT–3´) and reverse (5′-CAG GAA ACA GCT TAT GAC-3′) primers within the vector. A mix consisting of 600ng template and 5pmol of forward or reverse MI3 primer (Invitrogen) was made up to 30µl with water and sent to AWCGS, Massey University for sequencing. Correct insertion of the desired sequence was confirmed by aligning against the bovine *RPLPO* sequence using the GeneDoc multiple sequence alignment program (Nicholas and Deerfield, 1997). Remaining plasmid DNA was diluted to 10^9 copies, aliquoted and stored at -20 ºC. Standard curves for each individual gene were generated from the same 10^9 aliquot of plasmid in order to minimize interassay variability.

3.2.4.4 Quantitative real-time PCR

Real-time PCR reactions were performed using the iCycler iQ real-time PCR detection system (Bio-Rad) real-time PCR machine, on 1µl of cDNA samples and the appropriate internal primer

sets (Table 3). Cycling was performed in 25µl reaction volumes containing 12.5µl iQ SYBRGreen Supermix (Bio-Rad), 9.5µl H_2O and 0.2µM of the appropriate primer set or 0.04µM for RPLPO primers, in 96-well iCycler iQ PCR plates, (Bio-Rad) sealed with iCyler iQ optical tape. Thermo cycling conditions used were; 95^{o}C for 15 min, 40 cycles of 94^{o}C for 30 s, 57^{o}C for 30 s and 72ºC for 30 s. Following the amplification protocol a melt analysis was carried out, which consisted of 10 s incubation at 60^{o}C, followed by a 0.5^{o}C increase in every subsequent cycle to a maximum temperature of 99^{o}C. Serial 1:10 dilutions ranging from 10^8 to 10^2 copies per µl of plasmid containing the gene of interest were run in parallel with each series of samples, allowing the automatic generation of a standard curve by the iCycler iQ Optical System Software 3.0a (Bio-Rad). The amplification efficiency of the qPCR reaction for each gene was calculated from the standard curve using the equation, $E = 10^{(-1/\text{slope})} - 1$ (Wong and Medrano, 2005). Minor differences in PCR efficiency between different runs were corrected for by using the same dilution series of the standard curve. The linearity of the relationship between the C_T and logarithm of the DNA concentrations was monitored from the R^2 value. All standards and samples were run in triplicate in the same plate for each gene and each assay also included a blank. The threshold values for each sample and baseline cycles were set automatically. The copy number per µl of sample was calculated by reading the Ct value for that sample off of its respective standard curve to obtain a log concentration value. The anti-log of that figure gave the relative concentration of the particular gene for that sample. This calculation was carried out automatically by the software.

3.2.4.5 Selection of optimal housekeeping genes and normalisation of cytokine gene expression

The method described by Vandesomple et al., (2002) was followed to assess the stability of the expression of the housekeeping genes under study using the Microsoft *EXCEL* application *geNorm* 3.5, which provides a measure of gene expression stability (*M*), being the mean pair-wise variation between an individual gene and all other tested control genes. To determine if the reference genes *RPLPO, ATPase* and *GAPDH* were constantly expressed, all three genes were analysed in each brain region in animals from each age group and both genotypes. Gene copy numbers per µl of cDNA were entered into *geNorm*, which then ranks the genes based on *M*, where genes with the lowest *M* values have the most stable expression, and following exclusion of the least stable reference gene, *M* values were recalculated. The normalisation factor (NF) was then calculated as the geometric mean of the most stable reference genes (Vandesompele et al., 2002).

Average copy numbers from all sample triplicates were calculated for each gene and the normalised expression level calculated as the ratio between the average copy number per sample and the corresponding NF.

3.2.4.6 Statistical analysis

Normalised cytokine copy numbers were entered into GenStat 12.2 (VSN International Ltd, Hempstead, UK), log transformed and analysed by restricted maximum likelihood method (REML) variance component analysis with Wald and F statistics to determine sources and sizes of variability caused by genotype, brain region, or age. Paired *t*-test analyses in Microsoft *EXCEL* were also performed to determine the variance between genotypes at each time point and the variance between time points in animals of the same genotype. Differences between genotypes and ages were considered significant if probability values of $P < 0.05$ were obtained. Mean and standard error of the mean (SEM) data were back-transformed from the log data for visual representation on scatter plots using SigmaPlot 11.0 (Systat Software Inc., Chicago, IL, USA).

3.3 Results

3.3.1 Immunohistochemistry

Initial histological examination of cytokine expression in ovine brain was performed on formalin fixed tissue. With the TNF-α, IL-β, IL-10 and TGF-β specific antibodies no positive staining was detected in any of the normal or affected brain tissues, or lymph node samples. Lymph nodes are immunologically active tissues and would be expected to contain a wide range of cytokine producing cells. In addition all negative control sections and isotype controls exhibited minimal diffuse background and no specific staining. However, positive parvalbumin staining which is routinely used and well detected in control and affected tissue in our lab, was observed in control and affected tissue, indicating the correct performance of secondary and tertiary reagents and sufficient fixation and processing of tissues. Antigen retrieval techniques did not improve cytokine detection, nor did alterations in the length of blocking or washing steps, antibody concentration or incubation times.

ZSF paraffin wax-embedded tissue displayed apparent intracellular and extracellular staining for TNF-α, IL-1β, IL-10 and TGF-β in normal and affected frontal, parietal and occipital lobe samples and in lymph node control tissue (Figure 5 B-D). However, negative controls in which the secondary antibody was omitted and isotype controls displayed similar reactions (Figure 5 A).

Changing antibody dilutions, incubation times, blocking and wash lengths did not alter the apparent staining. Negative controls in which the primary antibody was omitted had no discernable staining indicating that the apparent staining did not arise from non-specific binding of the secondary antibody. The presence of positive staining in the isotype controls which were used to estimate the non-specific binding of target primary antibodies due to Fc receptor binding or other protein-protein interactions indicated that non-specific binding of the primary antibody was occurring. Possible staining caused by cytokine presence could not be discriminated from non-specific binding of the antibody.

Because of the lack of sensitivity and specificity of this technique due to an incompatibly of antibodies with fixed brain tissue, antibody species specificity or too little cytokine protein present to detect cytokines via this method, alternative techniques were explored to detect differences in cytokine expression.

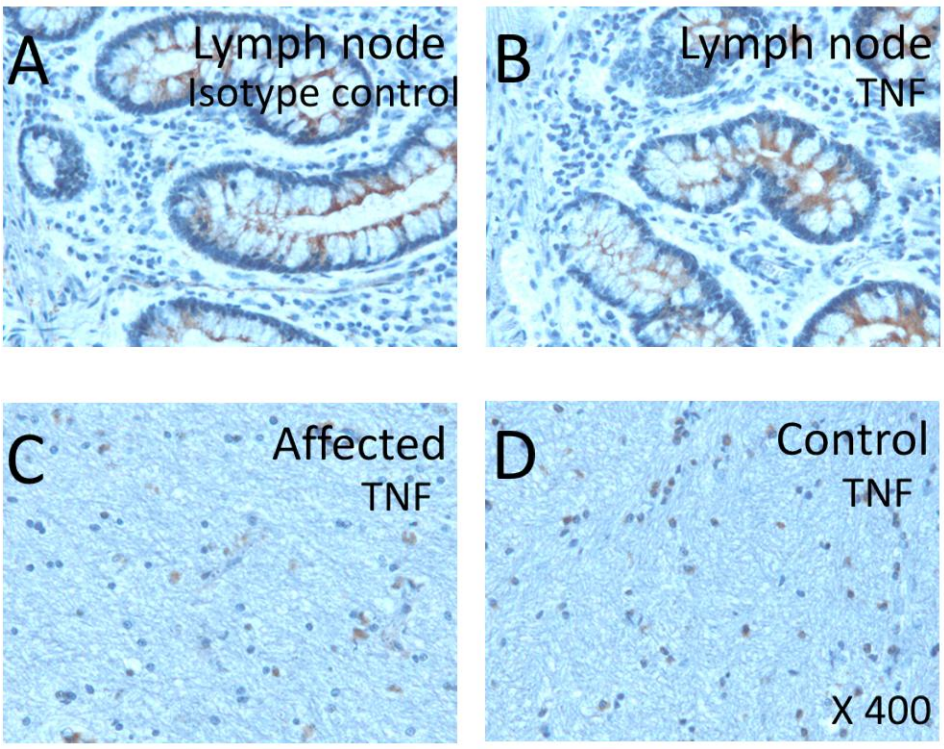

Figure 5 Immunohistochemical detection of TNF-α in zinc salt fixed ovine tissue using the EnVision Plus HRP kit

Lymph node (positive control tissue) displayed positive staining (brown DAB reaction product) (**B**) which was indistinguishable from non-specific staining due to Fc receptor binding or other protein-protein interactions with isotype IgG2b control (**A**). Thus, staining observed in affected (**C**) and control **(D**) ovine brain tissue could not be determined to be cytokine specific nor was there any apparent difference between the staining of normal or affected brain.

3.3.2 Western blotting

Cytokine expression was examined by Western blotting using the same antibodies on spleen, stimulated peripheral blood lymphocytes and brain homogenate from control and affected 18 month old animals. Control and affected spleen, lymphocytes and brain all exhibited TNF-α (17.5kDa), IL-1β (17.5kDa), IL-10 (17kDa) and TGF-β (12.5kDa) cytokine expression and all antibodies generated bands of the predicted molecular weight (Figure 6). Expression was strongest in the stimulated lymphocytes, which acted as a good positive control for cytokine expression but double bands were observed, one at the predicted molecular weight which correlated with the bands observed in spleen and brain tissue samples, and one a minor band 1-2kDa below this. An increased expression of TNF-α and TGF-β in control lymphocytes compared to affected samples was observed. Control and affected spleen samples exhibited similar expression of all four cytokines, with IL-10 having the lowest expression. Staining of occipital lobe homogenates displayed bands which were more intense in affected samples compared to controls, with TGF-β and IL-1β having the strongest expression and IL-10 the weakest.

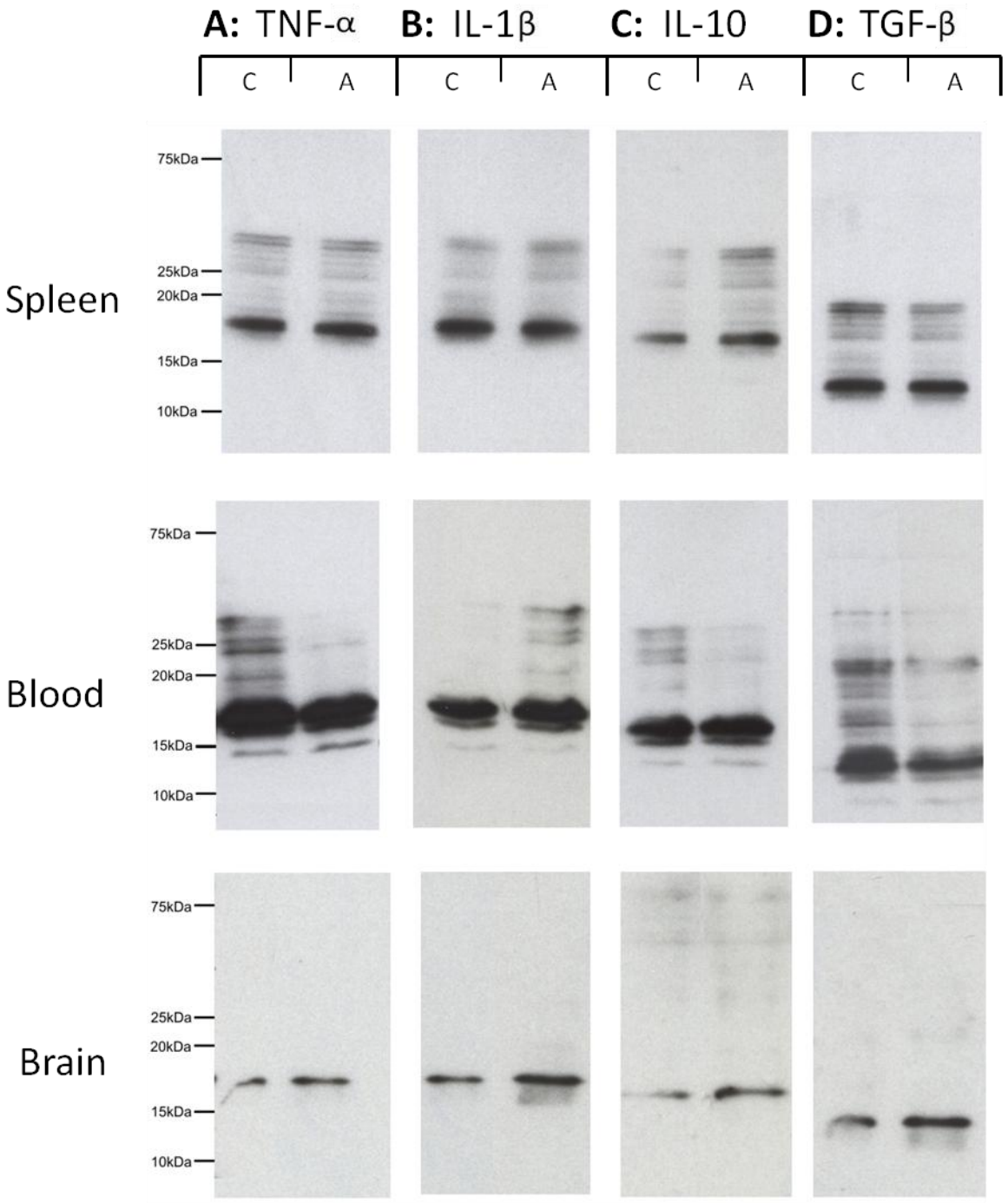

Figure 6 Cytokine detection by Western blotting

Western blots of spleen homogenates, isolated peripheral stimulated blood lymphocytes and occipital lobe homogenates probed with antibodies to (**A**) TNF-α, (**B**) IL-1β, (**C**) IL-10 and (**D**) TGF-β. Blots were carried out on 20µg protein per lane from control (C) and affected (A), 18 month old animals.

3.3.3 Quantitative real-time PCR

These increases in cytokine expression in affected tissue were not amenable to effective quantitation by Western blotting, particularly at different ages and in different brain regions. Therefore qPCR was performed, as it was deemed more likely to be informative, sensitive and a more accurate method for quantitating the expression of cytokines (Wang and Brown, 1999).

Isolation of intact RNA is essential for qPCR gene expression analysis. All RNA samples utilised had an $OD_{260/280}$ between 1.9-2.1 indicative of pristine RNA with minimal protein contamination or RNase activity. The integrity of RNA was revealed by agarose gel electrophoresis and ethidium bromide staining with a clear sharp 28S rRNA band present with approximately twice the intensity of that of a similarly clean 18S rRNA band for all samples, indicative of undegraded RNA. Synthesised cDNA samples were pooled and aliquoted which assured that the same pool of cDNA was used in all subsequent analyses to reduce any variability arising from different efficiencies of RNA reverse transcription to single stranded cDNA.

All qPCR runs accepted for data analysis had PCR efficiencies between 90-100% and R^2 values between 0.98-0.99. Melting curve analysis performed at the end of each PCR run verified that a single specific PCR product was present and no non-specific amplification or primer dimer was observed.

3.3.3.1 Selection of a housekeeping gene

Three housekeeping genes, *GAPDH, ATPase* and *RPLP0,* were analysed with *geNorm* 3.5 software to determine the most stable gene for accurate representation of mRNA expression within three brain regions from control and affected animals at four different ages. Analysis showed that the expression of *GAPDH* and *ATPase* varied the least across all tested ages, brain regions and genotypes, whereas *RPLPO* varied the most. Outputs from the *geNorm* application demonstrated *GAPDH* to be the most suitable single gene, having the lowest *M* value of 0.864 (Table 4) and *GAPDH* and *ATPase* as the most suitable gene combination, with an *M* value of 0.629 (Table 5). A normalisation factor was calculated for each sample based on the geometric mean of the *GAPDH* and *ATPase* expression, and subsequently used for normalisation of cytokine gene expression.

Table 4 Gene expression stability measures (*M*) as determined by *geNorm*

Gene	Stability value (*M*)
GAPDH	0.864
ATPase	0.869
RPLPO	1.104

Table 5 Stability values for combination of two genes determined by *geNorm*

	RPLPO	*GAPDH*	*ATPase*
RPLPO		1.098	1.109
GAPDH	1.098		0.629
ATPase	1.109	0.629	

Figure 7 qPCR analysis of cytokine mRNA expression in the brain of affected and control animals at 6, 9, 18 and 24 months of age

Gene expression of *IL-1β* (**A**), *TNF-α* (**B**), *TGF-β* (**C**) and *IL-10* (**D**) normalised to *GAPDH* and *ATPase.* Changes in expression between affected and control animals of the same age were analysed by paired *t*-test on log-transformed data. Values depict the mean ± SEM for frontal, parietal and occipital brain regions for animals at each time point.

*, significant difference ($P < 0.05$; paired *t*-test); **, very significant difference ($P < 0.005$; paired *t*-test) compared to the value for control animals of the same age.

A: *IL-1β* expression increased progressively in affected animals from 6 to 24 months of age and was significantly increased at all time points compared to control animals. In contrast, control animals displayed a relatively stable *IL-1β* expression, increasing at 24 months but still significantly lower than in affected animals.

B: *TNF-α* expression was very significantly increased at all ages in affected animals compared to age-matched controls. Expression peaked at 18 months after which it decreased at 24 months of age. In contrast, control animals did not display any significant change in expression which remained significantly lower than affected animals.

C: *TGF-β* expression was similar in affected animals at 6 and 9 months of age, after which it increased significantly at 18 months remaining elevated up to 24 months of age. Expression in control animals increased at 18 months compared to all other ages but remained significantly lower than in affected animals.

D: *IL-10* expression in affected animals peaked at 18 months, decreasing at 24 months to quantities similar to those seen at 6 and 9 months of age. Control animals followed a similar pattern of expression with an increase in *IL-10* expression at 18 months, before subsequently decreasing. However, expression was significantly lower than in affected animals at all ages.

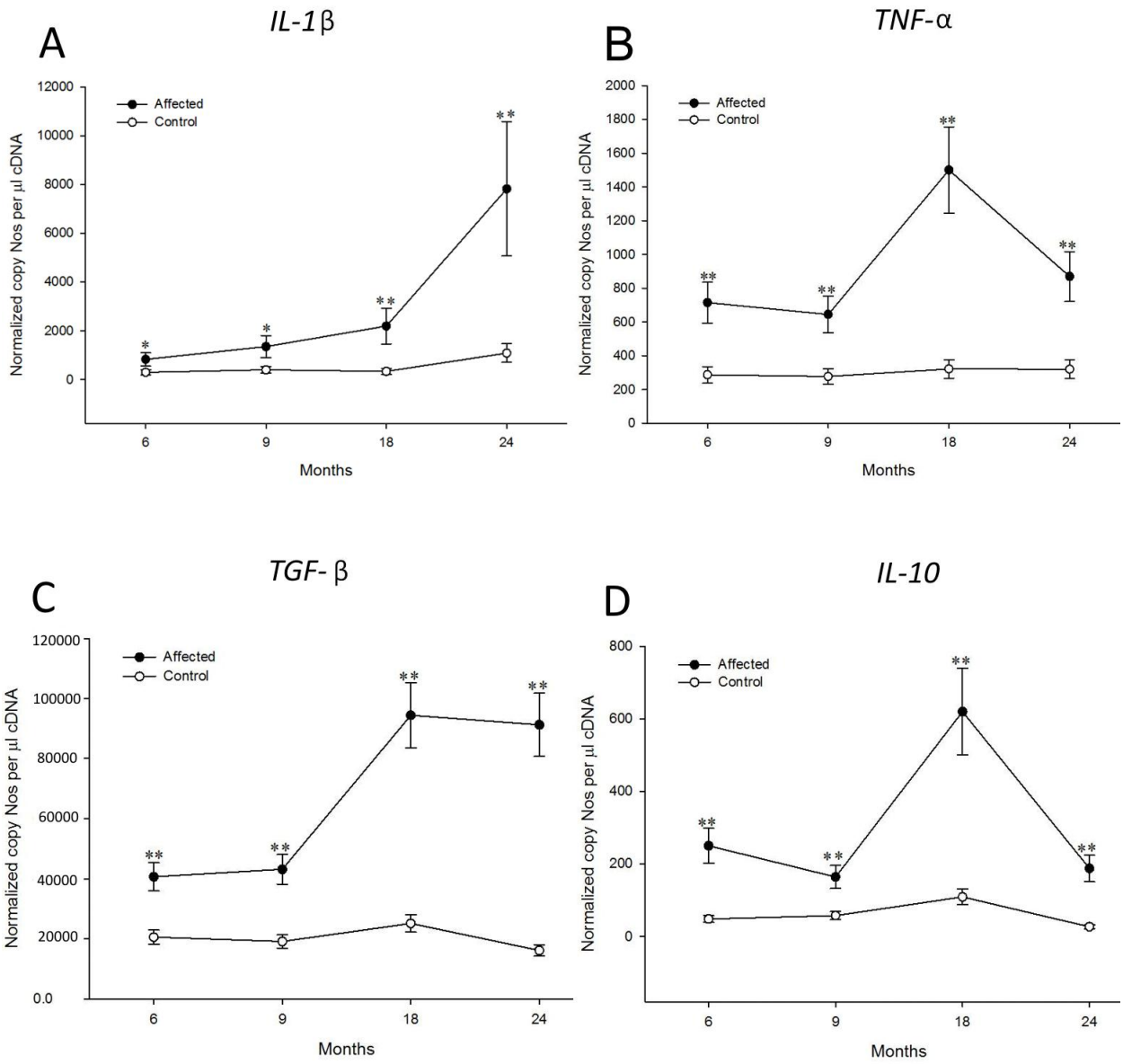
A
IL-1β
Affected
Control
Normalized copy Nos per µl cDNA
Months
B
TNF-α
C
TGF- β
D
IL-10

3.3.3.2 Cytokine expression

REML analysis and accompanying Wald and F statistics indicated that there was no significant difference in cytokine expression between frontal, parietal and occipital brain regions for all affected and control samples for any of the four cytokines analysed (*IL-1β*, *P* 0.433; *TNF-α*, *P* 0.084; *IL-10*, *P* 0.257; *TGF-β*, *P* 0.528). Conversely, a significant difference in expression was found between affected and control samples for genotype (*IL-1β*, $P < 0.001$; *TNF-α*, $P < 0.001$; *IL-10*, $P < 0.001$; *TGF-β*, $P < 0.001$) and age (*IL-1β*, $P < 0.005$; *TNF-α*, $P < 0.05$; *IL-10*, $P < 0.001$; *TGF-β*, $P < 0.001$). Hence, the mean expression values and SEM for all brain regions in animals of a particular genotype (affected or control) at each time point were utilised for graphing the data, and in subsequent paired *t*-tests to analyse differences in cytokine expression between affected and control animals at each time point and between time points in animals of the same genotype.

The expression of all four cytokines was detected at all ages in affected and control brain samples with some dramatic variations observed. Transcript copy number in relation to the two housekeeping genes, *GAPDH* and *ATPas*e, showed that different cytokines are present at very different copy numbers in affected and control brain samples (Figure 7). The largest cytokine expression was detected in affected animals for *TGF-β*, with a peak expression of 94,400 copies/µl cDNA at 18 months of age. This was dramatically higher than *IL-1β* expression which peaked at 7,800 copies/µl cDNA at 24 months in affected animals. Peak *TNF-α* and *IL-10* mRNA expression, 1,500 and 620 copies/µl cDNA respectively at 18 months in affected animals, was greatly reduced compared with the data obtained for both *TGF-β* and *IL-1β* at all ages.

Control brain samples followed a similar pattern to affected samples of increased expression of *TGF-β* at 18 months, 2500 copies/µl cDNA, and *IL-1β* at 24 months, 1080 copies/µl cDNA. However *TGF-β* expression was not dramatically increased compared to *IL-1β*, as was observed in affected samples. Both *TNF-α* and *IL-10* had a considerably lower peak mRNA expression of 321 and 100 copies/µl cDNA respectively, at 18 months of age in control animals. Although control samples did display some variation in the expression of all four cytokines the magnitude of change in expression was considerably lower compared to affected samples. The copy number data demonstrated that different cytokines are present at very different copy numbers in animals of the same genotype and dramatic differences in expression are also evident between different genotypes. These differences were clearly shown when the data was analysed by paired *t*-tests to indicate significance.

Expression of all four cytokines were found to be significantly (*, $P < 0.05$) or very significantly (**, $P < 0.005$) increased in affected animals compared to controls even at 6 months of age before clinical disease is evident (Figure 7). Control animal cytokine expression remained much more stable with increasing age and did not exhibit the significant fluctuations in expression evident in affected animals.

IL-1β expression (Figure 7 A) increased in affected animals from 6 to 18 months of age ($P < 0.05$) and subsequently increased very significantly at 24 months ($P < 0.005$) compared to earlier ages. Conversely, in control animals no significant change in expression was evident up to 18 months of age after which *IL-1β* expression did increase ($P < 0.05$) compared to earlier ages. At no time were control and affected expressions similar, a significant difference (*, $P < 0.05$; **, $P < 0.005$) in expression being evident at all ages.

Affected *TNF-α* mRNA expression (Figure 7 B) peaked at 18 months and was significantly higher ($P < 0.005$ compared to 6 and 9 months, $P < 0.05$ compared to 24 months) than other ages. In contrast, *TNF-α* expression did not significantly change in control animals and remained significantly lower than affected animals at each age (**, $P < 0.005$).

IL-10 mRNA expression (Figure 7 D) followed a similar pattern to *TNF-α* expression in affected animals. Correspondingly, expression was similar at 6, 9 and 24 months of age but peaked significantly at 18 months ($P < 0.005$) compared to other ages. Control animals displayed an increase in expression from 6 to 18 months ($P < 0.05$), subsequently decreasing at 24 months. At all ages, expression in affected animals was significantly (**, $P < 0.005$) increased compared to control animals.

TGF-β expression (Figure 7 C) was relatively stable in affected animals (P 0.52) from 6 to 9 months of age, after which a significant increase in expression was evident at 18 months ($P < 0.005$) and remained elevated up to 24 months. In control animals, an increase in *TGF-β* expression occurred at 18 months which was significantly increased compared to quantities at 6, 9 and 24 months ($P < 0.05$) but at all ages remained lower than in affected animals (**, $P < 0.005$).

3.4 Discussion

Progressive glial activation in ovine CLN6 indicates a role for inflammation in disease pathogenesis. Considering that glial activation is evident in affected animals (Oswald et al., 2005; Kay et al., 2006) prior to the initiation of neurodegeneration it is postulated that an abnormal inflammatory response may be occurring and alterations in cytokine expression could play a central role. The presence of activated glial cells in combination with cytokine expression would solidify the central role that inflammation is proposed to play in the pathogenesis of ovine NCL. Therefore both the transcription and protein expression of some major pro- and anti-inflammatory cytokines was investigated.

3.4.1 Limitations of immunohistochemistry and Western blotting for cytokine detection at the protein level

Cytokine expression in ovine sagittal brain sections was investigated by immunohistochemical analysis in formalin fixed tissue in order to visualise the pathological distribution of cytokine expression in affected and control brain tissue. However, specific, positive staining was not achieved by this technique for any of the four cytokines investigated, TNF-α, IL-1β, IL-10 and TGF-β. This may have been due to a lack of ovine specific antibodies demonstrated to work in immunohistochemistry, an issue which makes it difficult to assay cytokine expression at the protein level (Konnai et al., 2003). Only the TGF-β antibody had been determined to work in ovine (ovarian) tissue in immunohistochemistry (http://www.alzforum.org/res/com/ant/TGF-b/abcamab1279.shtml). In addition, cytokines are normally present in low concentrations in the normal brain, are known to have a short half-life *in vivo* and are subject to rapid degradation following sample collection (Panicker et al., 2007). Hence, by the time adequate tissue fixation has occurred, biologically active and detectable cytokine levels may no longer be present in the tissue or cytokines may be washed out during fixation. Therefore, suitable levels of expression may not have been present or immunohistochemistry may not be sensitive enough a technique for the detection of cytokines in this tissue.

Alternatively, it is known that many antigens are not well demonstrated after fixation in formaldehyde-based fixatives, which establish cross-linking bridges between cells, often masking the cell surface antigens (Fox et al., 1985). Formaldehyde can also react with amino acids adjacent to the epitope of interest, resulting in conformational changes which can be reversed by antigen retrieval techniques. However, antigen retrieval methods did not alter the staining outcome in this experiment, with no positive staining detected in any samples.

Therefore, it is possible that the epitopes of interest had been heavily masked or destroyed by the method of fixation and therefore epitopes remained inaccessible to antibodies.

Due to the possibility of epitopes being sensitive to processing methods, immunohistochemical examination of ZSF sections was investigated. ZSF is a procedure for the detection of fixation-sensitive antigens in paraffin wax-embedded tissue based on the use of a non-aldehyde fixative containing zinc salts (Beckstead, 1994). This method of fixation, followed by paraffin wax-embedding coupled with a highly sensitive method of immunolabelling (EnVision Plus HRP kit) was subsequently demonstrated in ovine tissue for the detection of immune system markers considered to be processing-sensitive (González et al., 2001; Buxton et al., 2002). In addition this method does not require an antigen retrieval step to permit adequate detection of cell surface epitopes. Despite these attributes this method did not work on the ovine brain tissue. Although staining was obtained in sections, isotype controls indicated a non-specific binding of primary antibody to the tissue. Similar instances of non-specific and background staining with isotype controls have been shown in a previous study by Whiteland et al., (1997) in which intracellular and cytoplasmic staining was observed on both frozen and paraffin-embedded sections. Hence specific staining for TNF-α, IL-1β, IL-10 or TGF-β could not be discriminated from non-specific binding of the antibody.

Concurrent to the immunohistochemical study, Western blot analysis of cytokine expression in protein extracts was undertaken to determine antibody specificity and sensitivity. Western blotting is a useful method for the detection of proteins especially those that are of low abundance, and specificity of antibody detection is further characterized by binding to protein bands of the anticipated molecular weight. Fresh or frozen unfixed tissue used for protein extraction eliminates concerns with fixation and epitope masking which can be an issue in immunohistochemistry. Additionally detergent denatured proteins expose more epitopes and thus can provide a better chance of detection. On the other hand denaturation can also modify the epitope conformation rendering it undetectable, which is especially problematic when using monoclonal antibodies. Stimulated lymphocytes and spleen tissue from control and affected animals were utilised as positive controls as these tissues are likely to have strong cytokine expression. Despite possible issues with denaturation it was evident that antibodies were specifically detecting the cytokines of interest, all samples displaying bands of the correct molecular weights (Figure 6). A double band was observed in stimulated lymphocyte samples for all four cytokines. This second minor band was only 1-2kDa smaller than the band of the correct molecular weight and may represent glycosylation or phosphorylation of the protein or may be attributed to overloading of the gel. Alternatively samples may not have

been completely denatured, if disulfide bond breakage is incomplete samples can be detected as a double band with differences of 2-4kDa in apparent mass (Schägger, 2006). Extraneous bands appeared to be proportionate to the amount of protein present as they were not detectable in spleen or brain tissue samples in which less intense protein bands were present. All samples were loaded at the same protein concentration, 20µg, to compare cytokine expression and due to stimulation of the peripheral lymphocytes much higher cytokine expression was obviously present in these samples compared to spleen and brain samples. The concentration of protein loaded was not decreased as this may have resulted in a lack of cytokine detection in brain samples which had much less intense bands than lymphocyte samples.

It is well documented that antibodies that work via one detection method do not necessarily work in another. Cytokines were detected by Western blotting but not by immunohistochemistry. These differences may be accounted for by incorrect or destroyed epitope confirmation in samples used for immunohistochemistry, rendering them undetectable and resulting in a lack of specific staining in immunohistochemistry but presence in Western blotting. Blots indicated an increase in cytokine protein expression in affected brain samples compared to controls, particularly of TGF-β and IL-1β. Accurate quantitation of these differences was carried out by qPCR.

3.4.2 Quantitative real-time PCR

As discussed in section 3.4.1 the investigation into the pathogenesis of ovine NCL is limited by a lack of immunological and biological assays for the detection of ovine cytokines, largely arising from a lack of specific antibodies. Determination of cytokine mRNA expression provides a more direct approach for the detection of ovine cytokines (Budhia et al., 2006). Cytokine expression has been successfully assessed at the mRNA level using techniques such as competitive RT-PCR, Northern blot and PCR (Dunphy et al., 2001; Montagne et al., 2001; Stephens et al., 2003; Woodall et al., 1997). Collectively, qPCR allows more accurate quantitation, demonstrates high sensitivity and provides a wide linear dynamic range, hence is particularly useful for target genes present in low quantities and for small fold changes in expression.

3.4.2.1 Housekeeping genes

Quantitation of any gene is dependent on normalisation of the data obtained to a reference gene. This is to allow for variation in the samples such as cell number, RNA extraction efficiency and transcriptional activity (Vandesomple et al., 2002). Choosing the correct

reference genes is essential to ensure biologically meaningful and credible results and therefore should be investigated thoroughly. An ideal reference gene should be expressed at a constant level in different tissues at all stages of development, and should not be affected by the experimental treatment or disease state being investigated. An endogenous reference such as a constitutively expressed housekeeping gene is usually used (García-Vallejo et al., 2004). However, there are many reports of variation in presumably stable housekeeping genes and there can be no universal reference gene (Schmid et al., 2003; Schmittgen and Zakrajsek, 2000; Radonić et al., 2004; Huggett et al., 2005; Robinson et al., 2007). Because of variation in housekeeping gene expression under differing conditions some studies now recommend examining up to ten different housekeeping genes, using computational programmes such as *geNorm* (Vandesompele et al., 2002) and normalising to the geometric mean of the most stable genes to obtain the most accurate validation of relative gene expression. Vandesomple et al., (2002) demonstrated that errors in expression data up to 20-fold can be generated by the use of a single reference gene.

Three widely used potential reference genes were investigated in this study, *GAPDH*, *RPLPO* and *ATPas*e, for their stability with increasing age and disease progression. *GAPDH* is an abundant glycolytic enzyme present in most cells that participates in many different cellular processes (Giulietti et al., 2001) and is also implicated in apoptosis and neurodegenerative disease (Tatton at al., 2000). Although widely used recent reviews now criticise the use of *GAPDH* as an endogenous control because its expression has been shown to be influenced by experimental treatment or condition in numerous cases (Bustin, 2000; Freeman et al., 1999; Barroso et al., 1999; Suzuki at al., 2000), although others have found *GAPDH* expression to be stable (Backman et al., 2006; Meldgaard et al., 2006) and it has previously been used in ovine NCL tissue (Tammen et al., 2006). Collectively, these concerns emphasise the need to choose and validate optimal housekeeping genes for the specific tissues and conditions of an experiment. *RPLPO* is another housekeeping gene successfully used as a reference gene in previous studies (Szameit et al., 2008; You et al., 2008; Houweling, 2009; Riley et al., 2008), including cytokine analysis in ovine tissue (Fakioglu et al., 2008). The ubiquitous ovine housekeeping gene *ATPase* (Woodall et al., 1997) has also been used as a reference gene in RT-PCR for ovine cytokine expression (Woodall et al., 1997; Knight et al., 2007).

The method described by Vandesomple et al., (2002) was used to determine whether accurate normalisation would require the use of all three housekeeping genes under investigation or whether the use of one or two would provide the most accurate normalisation. *geNorm* analysis showed that *GAPDH* displayed the lowest variation amongst different brain regions,

ages and disease state, with *ATPase* expression similarly stable, whereas *RPLPO* was the least stable. The lowest stability value (*M*) was achieved by the combination of *GAPDH* and *ATPase* (Table 5) and the geometric mean of these two genes was used for normalisation of the cytokine data.

3.4.2.2 Cytokine expression

qPCR analysis of cytokine expression in frontal, parietal and occipital cortical regions at 6, 9, 18 and 24 months, revealed that *IL-1β, TNF-α, TGF-β* and *IL-10* are significantly increased in affected animals compared to controls (Figure 7). These results indicate that an inflammatory response is occurring within affected animals and that the elevated expression of both pro- and anti-inflammatory cytokines is evident by 6 months of age. This correlates with the initiation of neurodegeneration at 4-6 months of age, but is prior to clinical disease manifestation evident at 10-14 months. All four cytokines significantly increased expression at 18 months by which time widespread cortical atrophy and glial activation is apparent. However, whilst *TGF-β* and *IL-1β* expression remained elevated at 24 months of age, both *IL-10* and *TNF-α* expression significantly declined but were still above control values (Figure 7).

The copy number data also indicated that *TGF-β* and *IL-1β* were expressed in much higher quantities than *IL-10* and *TNF-α* in affected animals. Cytokine mRNAs are short-lived due to a nuclease-sensitive consensus sequence in the 3'-noncoding region (Caput et al., 1986), therefore the dramatic differences in the copy number datum for individual cytokines cannot be accounted for by differential half-lives, thus indicating a true increase in expression of *TGF-β* and *IL-1β* compared to *IL-10* and *TNF-α*. However the relationship between mRNA expression and the biologically active cytokine secreted by cells is dependent on factors including mRNA stability, maturation, transport, and rate of release from cells (Lichenstein et al., 1997). The mRNA expression data correlated with the protein expression observed in Western blots in which the TGF-β and IL-1β bands were more intense than IL-10 and TNF-α in affected 18 month old brain samples (

Figure 6), indicating that the stability of mRNA was not an issue. This demonstrates that the observed increased mRNA expression of *TGF-β* and *IL-1β* in affected animals equates to an observable increase in cytokine protein expression. The subsequent effects of these cytokines could differ however depending on the cell type involved, the combination of other cytokines present and the receptor type activated (Buckwalter and Wyss-Coray, 2004).

There is a lack of comparable data available with regards to normal cytokine expression in the ovine brain but many studies in other species noted expression in unstimulated cells (Budhia

et al., 2006) and cytokine detection in control brain samples was not unexpected. Compared with cytokine expression in the ileum of control sheep and those with chronic inflammatory disease of the gut, *TGF-β* expression in affected brain was almost twice as high as that in inflammatory ileum but control brain samples were within the range detected in normal ileum. Conversely, *IL-1β, IL-10* and *TNF-α* expression were considerably lower in affected and control brain samples compared with those seen in ovine ileum tissues (Smeed et al., 2007). However *IL-1β* and *TNF-α* mRNA expression in affected brain was within the range of peak cytokine expression observed in ovine peripheral blood mononuclear cells stimulated with ConA (Budhia et al., 2006). This study also reported that macrophage cytokine expression in response to LPS stimulation was much higher than in peripheral blood mononuclear cells and considerably higher than the expression noted in this study. This highlights the difficulty in comparing results between studies due to differences in cytokine expression between different cell populations and tissues, the cell activation state and the normalisation methods utilised.

This inflammatory profile in the ovine CLN6 brain does not follow a stereotypical chronic inflammatory profile, with *TNF-α, IL-1β, IL-10* and *TGF-β* expression continuously upregulated compared to control animals. The expression of both *IL-10* and *TNF-α* significantly decreased in affected animals at 18 months. These cytokines would not normally be expected to follow a similar expression profile, *TNF-α* considered to be pro-inflammatory and *IL-10* being anti-inflammatory. The reason for a decrease in *TNF-α* and *IL-10* expression but not *IL-1β* or *TGF-β* at 18 months of age is unknown but emphasises the complexity of cytokine networks and the intricacies of cytokine-cytokine interactions of which the net output can be additive, synergistic or antagonistic (Turrin and Plata-Salamán, 2000). Cytokines interacting synergistically can result in an effect significantly greater than the sum of the individual effects. Interestingly, not all properties of a cytokine will be affected in the same way, some effects can be stimulated, while others are inhibited or not affected at all (Turrin and Plata-Salamán, 2000).

Chronic and continued activation and over-expression of microglia and astrocytes, resulting in elevated cytokine expression imply that inflammation is associated with neuronal degeneration in ovine NCL. This alteration in the immune profile before the onset of clinical symptoms, suggests that neurodegeneration is exacerbated by inflammation, a situation which is evident in other neurodegenerative diseases such as AD (Akiyama et al., 2000; McGeer and McGeer, 2001). Furthermore, many neurodegenerative diseases are now associated with altered cytokine expression. In mouse models of Niemann-Pick type C, Tay-Sachs and Sandhoff disease, activation of microglia and astrocytes, and secretion of pro-inflammatory

cytokines, including TNF-α and IL-1 are reported to be increased (Baudry et al., 2003; Jeyakumar et al., 2003) (see also sections 1.10 and 3.1).

In this study *IL-1β* mRNA expression significantly increased in affected animals especially at end stages of disease. IL-1β is typically considered a pro-inflammatory cytokine and has been implicated in the progression of neurodegenerative diseases (Akiyama et al., 2000; Rothwell and Luheshi, 2000). Although there are reports that IL-1β can exert a beneficial effect, this has largely been confined to low concentrations of the cytokine (Basu et al., 2004) and the progressive increase in expression in the affected sheep suggests a mainly pro-inflammatory, detrimental role. Similarly, TNF-α expression was significantly elevated in affected animals at all ages studied, with peak expression observed at 18 months. Although TNF-α is known as a pro-inflammatory cytokine and inducer of apoptosis, there are also reports of positive effects exerted by TNF-α. It can activate the transcription of TGF-β (Tracey and Cerami, 1994), which in turn inhibits the pro-inflammatory cytokines IL-6 and IL-1β, suppressing further activation and proliferation of microglia (Suzumura et al., 1993). Clearly this is not the case in ovine CLN6, as although TGF-β is upregulated so too is IL-1β. Hence a sufficient negative feedback loop is evidently not established.

Anti-inflammatory cytokines also increased in the affected ovine brain and the increased expression of *TGF-β* and *IL-10*, which are also elevated in the CSF of AD patients (Chao et al., 1994), suggest that these cytokines are actively produced for defence against inflammation. The significant and progressive increase in *TGF-β* and *IL-10* in affected animals indicates that an attempt at controlling inflammation is occurring. TGF-β has been shown to promote cell survival or induce apoptosis, stimulate cell proliferation or induce differentiation, and initiate or resolve inflammation (Dennler et al., 2002). IL-10 is a powerful anti-inflammatory cytokine which can suppress many pro-inflammatory cytokines and also interrupts signalling by down-regulation of pro-inflammatory cytokine receptor expression (Sawada et al., 1999). Despite TNF-α and IL-1β, and IL-10 and TGF-β typically being considered to be pro- and anti-inflammatory, respectively, the immunological action of a specific cytokine may be enhanced or masked depending upon the presence of other cytokines (Ostensen et al., 1989; Arend et al., 1987). Hence, the anti-inflammatory action of IL-10 and TGF-β in affected brains may have been limited because of the dramatic intensity of other inflammatory responses.

The site of action could also play a role, as it is possible that different regions of the brain are differentially susceptible to cytokine expression, rendering some regions particularly sensitive. A study by Stroemer and Rothwell (1997) in rats showed that cortico-striatal

projection neurons, which originate in the cortex, can be damaged by neurotoxic levels of IL-1β in the striatum, but not in the cortex. It was suggested that IL-1β in the striatum can initiate a cascade of toxic and/or inflammatory agents that then diffuse to, or indirectly affect other, distal brain regions potentiating damage in the cortex. The degree of the microglial inflammatory response may also determine which cell types are damaged, as certain cell types localized in select brain regions may be preferentially vulnerable to microglia derived insult and expression of cytokines. For example, while a lower grade inflammatory response selectively kills dopaminergic neurons in rats, higher doses of the same toxin (such as LPS) begins to kill multiple cell types (Gao et al., 2002b). A similar mechanism may be responsible for the localised loss of specific interneuron populations and GnRH positive neurons in ovine NCL (Oswald et al., 2008; Kay et al, 2011).

3.4.3 Regional differences in cytokine expression

The lack of a significant difference in cytokine expression amongst different brain regions was not expected as glial activation proceeds in a progressive, regionally specific manner, foremost affected being the visual, parieto-occiptal and somatosensory cortices, followed by the primary motor and entorhinal cortices (Oswald et al., 2005). However, a previous study by Oswald et al., (2008) demonstrated contrasting patterns of GABAergic interneuron loss in different brain regions. These results were not consistent with a generalised metabolic defect which preferentially affects GABAergic cells but indicated that regional functionality and connectivity appear to be better determinants of neuronal susceptibility to degeneration. The numbers of calretinin and calbindin immunoreactive interneurons increased in affected animals, peaking when generalised atrophy of the cerebral cortex was underway and subsequently declining to normal. Similarly, although cytokine expression may be similar in different brain regions, subpopulations of cells and other determining factors may make them more vulnerable to inflammatory-induced decline. Furthermore, the peak expression of cytokines IL-10 and TNF-α at 18 months followed by a significant decline may be associated with the changes observed in specific interneuron populations.

Subpopulations of microglia may also provide secreted factors which cause diverse phenotypic and functional outcomes. A study by Walton et al., (2006) showed differences in the influence of microglia isolated from the SVZ or the cerebellum of adult mice on the rate of neurogenesis. Hence, microglia may have different neuroprotective or inhibitory properties depending on their location. Regional differences in microglial populations and their inflammatory responses also offer a further insight into potential mechanisms mediating the compartmentalization of both neurodegenerative pathology and microglial activation seen in

ovine NCL. Furthermore, brain region differences in microglial regulatory factors, such as astrocyte populations, could also explain how the generalized phenomenon of microglial activation could be localized by brain region (Block and Hong, 2005).

3.4.4 Regulation of the inflammatory cascade

The progressive increase in cytokine expression suggests that an uncontrolled inflammatory response is underway. There are a number of ways by which inflammation is normally controlled and alterations in this process could account for an uncontrolled response. Microglial stimulators activate signalling pathways such as Jak/STAT, NF-κB and MAPK, increasing ROS and pro-inflammatory cytokine production. Simultaneously, these stimulators induce the expression of SOCS, HO-1 and anti-inflammatory cytokines, which hamper the activation of signalling pathways, thus suppressing the production of inflammatory cytokines (see section 1.11 for further details). Hence, disruption of this homeostasis may result in an uncontrolled inflammatory response (Yang et al., 2007). Similarly, prostaglandins which are produced by activated glial cells may be another factor contributing to the local inflammatory response and changes in their expression could lead to inflammatory dysregulation.

Other evidence for a pro-inflammatory response in the ovine brain is the upregulation of MHC-II molecules on activated microglial cells (Oswald et al., 2005) and MHC proteins are reported to be upregulated during disease progression in other LSDs (Drozina et al., 2005). However, pathological conditions are not the only stimuli that alter MHC protein expression, as dysfunction of the lysosome may also cause the upregulation and incorrect expression of MHC-II (Castaneda et al., 2008). Since MHC proteins have a strong immunomodulatory effect upon the activation and suppression of the immune system which depends upon a functioning lysosomal compartment to correctly process and present protein antigens, alterations in this process may result in incorrect processing, loading and expression of MHC-II molecules (Castaneda et al., 2008) which could subsequently alter the cytokine profile.

Pharmacological suppression of inflammation via the chronic administration of minocycline to ovine NCL affected animals has been attempted (Kay et al., article in preparation). Treatment started at 3 months of age and continued for a year but had no observable effect on the development of symptoms, pathology or glial activation, despite pharmacological concentrations of the drug reaching the brain. Although treatment began before neurodegeneration commenced at 4-6 months of age, glial activation is by then already underway in the sheep brain (Kay et al., 2006). The neuroprotection afforded by minocycline

is thought to be associated with its ability to inhibit microglial activation, thereby reducing the levels of cytotoxic factors released by microglia (Sririam et al., 2006). A number of studies in mice have shown that induced pro-inflammatory cytokines such as TNF-α (Zhao et al., 2007; Sriram et al., 2006) decline with minocycline treatment. A potential mechanism by which minocycline exerts its anti-inflammatory actions is inhibition of p38 MAPK, a key regulator of the expression of pro-inflammatory cytokines (Kumar et al., 2003). However, it appears that even by 3 months of age the degree of microglial activation and related cytotoxic factors in the ovine model are too advanced for successful inhibition by minocycline. Similarly, this qPCR data has revealed that by 6 months of age, expression of TNF-α, IL-1β, IL-10 and TGF-β are all significantly elevated in affected animals compared to controls even though neurodegeneration is only commencing at this age.

3.5 Conclusion

Both pro- and anti-inflammatory cytokines are elevated in the ovine NCL brain and clearly point to an involvement of these cytokines in NCL neuroinflammation. This indicates that both trophic and toxic pathways co-exist side by side, but the mechanisms regulating these pathways and the factors resulting in this expression remain unknown. Understanding the effect of normal cells on both the beneficial and detrimental aspects of neuroinflammation in ovine NCL could be especially valuable for future prospects for disease treatment, something which is investigated in the following chapter.

Chapter 4
Chimeras

4.1 Introduction

An individual whose body contains different cell populations derived from different zygotes is defined as a chimera. The different cell populations can be derived from one species (intra-species chimerism) or from two different species (inter-species chimerism). Intra-species chimeras can occur naturally and are quite common in cattle during the development of twins. In cattle there is often fusion of placenta and chorionic blood vessels, leading to exchange of hematopoietic stem cells between the two foetuses, with the resulting haematopoietic chimeras carrying two different cell populations, each derived from the two different haematopoietic stem cells (Jolly et al., 1976). A striking clinical significance is seen when one foetus is a female and one a male. The female foetus can be exposed to hormones from the male resulting in an infertile female animal which has masculinized behaviour and non-functioning ovaries. Such female cattle are called freemartins (Lillie, 1917; Marcum, 1974; Padula, 2005). The degree of masculinization is greater if the fusion occurs earlier in the pregnancy. In about 10% of cases no fusion takes place and the female remains fertile. Freemartinism is a common outcome of mixed-sex twins in cattle species and it also occurs occasionally in other animals including sheep, goats and pigs (Marcum, 1974; Long, 1980; Bosu and Basrur, 1984; Smith and Dunn, 1981; BonDurant et al., 1980; Somlev et al., 1970; Bruere et al., 1968).

Spontaneous human chimerism is extremely rare. It can result from such events as the aggregation of two non-identical twin embryos at an early developmental stage (Bader et al., 2009). Other forms of intra-species chimerism can occur after common medical procedures such as bone marrow transplantation (Thomas et al., 1957) or following transplacental leakage between mother and foetus, resulting in a form of microchimerism only measurable by sensitive techniques, such as PCR (Sykes and Sachs, 2001). According to this definition, blood, bone marrow and organ transplant recipients are chimeras.

Conversely, inter-species chimeras are not believed to occur naturally and have only been artificially generated for scientific or medical purposes, produced by physically mixing cells from two independent zygotes. Originally chimeras were developed out of scientific curiosity but as time has gone on, numerous scientific and medical problems have been addressed by the use of chimera technologies, including studying the developmental, differentiation,

migration and functional properties of different cell types. The formation of animal chimeras was first described by Tarkowski (1961) and Mintz (1962) and involved aggregating two eight-cell mouse embryos. The result was a normal-sized mouse, whose tissues were a mixture of cells derived from the two embryos. Ten years later the same technique was used to produce the first inter-species chimeras between different mouse species, *Mus musculars* and *Mus caroli* (Rossant and Frels, 1980), different bovine species, *Bos indicus* and *Bos taurus* (Williams et al., 1990), mouse and rat (Stern, 1973), and sheep and goat (Fehilly et al., 1984a).

Gardner (1971) extended the technique of creating chimeras by injecting dissociated embryonic cells into blastocysts. This revolutionary new technique opened up a new method for introducing any kind of cell, including genetically-modified cells, into the host embryo. A recent development in technologies to generate chimeras is the use of embryonic stem cells (ESC). These cells were first derived from mouse blastocysts (Evans and Kaufman, 1981) but are now available from other mammals including humans (Thomson et al., 1998). Hence, the creation of animal-human chimeras has now become feasible and can be used in experiments to help clarify human stem cell pluripotency and differentiation *in vivo*, to create *in vivo* models for drug testing and to create donor animals carrying human tissue for transplantation (Bader et al., 2009).

The two stages of development most commonly used for making conventional chimeras are the early morula and the expanding blastocyst still encased in an intact zona pellucida, used for making aggregation and injection chimeras respectively. In both cases the cells from the two embryos assemble to form a single chimera, which when placed in a foster mother can develop to term. Most aggregation chimeras, particularly in mice, are formed at the eight-cell stage, but successful aggregations have been obtained between 16-cell and 32-cell morulae (Stern and Wilson, 1972; Mystkowska et al., 1979), as used in this experiment. However, chimera generation does not always produce a chimeric animal. When two morulae are aggregated, the initial proportions of cells of the two genotypes in the chimeric embryo are 1:1. However, in the majority of chimeric individuals cells from one embryo predominate and some animals are not chimeras at all (Mystkowska et al., 1979). Falconer and Avery (1978) considered that this phenomenon results from two successive segregations of cell material which take place during the early stages of development. Initially, the cells of the morula become arranged into an outer peripheral layer called the trophoblast which forms extraembryonic tissues such as the placenta, and the inner cell mass (ICM) which forms the embryo proper. The next segregation takes place with the differentiation of primary ectoderm

from primary endoderm within the ICM. The blastomeres of the two aggregated embryos can mix to varying degrees, or not mix together at all, before segregation processes begin (Garner and McLaren, 1974). Therefore the ICM could be composed of cells of one type only or of the two types in various proportions, and the contribution of the two partners can be approximately balanced or be very markedly skewed in favour of one or the other.

Chimeric offspring can be recognized in several ways. If they are derived from embryos of pigmented and albino strains, they may have stripes of pigmented skin and patches of pigment in the eye, whereas internal chimerism can be detected by the use of chromosomal or cell surface markers, or genetically determined enzyme variants. In sheep, embryonic chimeras have been produced between cleaving embryos (Fehilly et al., 1984b) and by introducing ICMs to blastocysts (Butler et al., 1987). Polzin et al., (1987) generated sheep-goat embryos, with the resulting offspring resembling sheep, goat and overt sheep-goat chimeras. Similar outcomes were observed by Fehilly et al., (1984a) and Butler et al., (1987) in the production of sheep-goat and sheep-sheep chimeras respectively, emphasising the heterogeneity of chimeric offspring.

Studies indicate that cross-cell correction is an important phenomenon for the treatment of LSDs (Frantantoni et al., 1969; Neufeld and Fratantoni, 1970; Neufeld and Muenzer, 1995). A case of natural chimerism in a calf with mannosidosis which was also a blood chimera, supplied with a population of lymphocytes from its normal co-twin was studied by Jolly et al., (1976). They established that α-mannosidase produced by the population of normal lymphocytic cells influenced the pathology of the disease, with α-mannosidase activity in the lymph nodes either approaching or within the normal range, and reduced storage material in cells of the liver compared to affected control calves. For LSDs, including NCLs, with a CNS disease manifestation, therapy with the gene product should be possible as long as proteins can pass through or bypass the BBB. Cross-correction may be a possibility in the treatment of ovine CLN6, as previously mentioned in Chapter 2 despite the defect being in a membrane bound protein.

In addition, understanding the inter-connections between the gene lesions, subunit c storage and neurodegeneration is limited but pivotal for determining options for therapy. The multiple tissue involvement in NCL also raises the question of whether the disease gene action occurs independently in every affected cell type or whether affected cells are responding secondarily to a deficiency in a circulating factor, and some cell types, such as neurons, are more susceptible to this (Porter et al., 1997). Having normal and affected cells side by side, as in sheep chimeras, is a direct way to study these pathogenic aspects of the disease. It allows

analyses of the pathology and phenotype of cells with different genetic compositions, under the influence of identical environmental factors and any effect the cells have on each other (Sakkas and Vassalli, 1993).

In this study chimeric animals, generated from homozygous control and affected embryos, were compared phenotypically and genotypically to affected and normal control animals. A number of pathological changes have been catalogued in affected animals which indicate the progression of the underlying disease pathology, specifically cortical thinning and decreased brain volume associated with severe neurodegeneration, loss of vision, glial activation, storage body accumulation and extended neurogenesis (discussed in Chapter 1) (Mayhew et al., 1985; Jolly et al., 1989; Oswald et al., 2001, 2005, 2008; Kay et al., 2006). If chimerism fails to override the deleterious effect of the mutation, clinical and pathological profiles of these animals will lie somewhere between those of affected and control animals. Chimeric animals which resemble controls phenotypically but which contain a significant proportion of affected cells would indicate that the presence of normal cells overrides the effect of the mutation and cell transplant or gene therapy is possible. Alternatively, if there is no transport of enzyme, other soluble factors or signalling from normal to affected cells which is beneficial, then enzyme replacement and cell or gene therapy will not be successful.

4.2 Materials and methods

4.2.1 Animals

Fifteen chimeric lambs were generated within our research group over four breeding seasons by Dr. Graham Kay and Nigel Jay. Normal and affected ewes were synchronised with progesterone impregnated controlled intrauterine drug release devices, induced to superovulate using follicle stimulating hormone, then fertilised by laparoscopic insemination (Kay et al., 1999). Embryos at the 16-32 cell stage were collected by flushing the oviducts and uterine horns and half the blastomeres from selected homozygous affected embryos were exchanged for half the blastomeres of selected homozygous unaffected normal Coopworth embryos (Figure 8 A). The resultant hybrid embryos were then re-implanted into synchronised normal recipient ewes for development to term. Initial indications of chimerism in the 15 generated lambs based on observations of coat colour patterns suggested a good degree of chimerism. Affected lambs born with black faces and feet and all white Coopworth controls were used, resulting in ostensibly chimeric lambs having a mix of both coat patterns (Figure 8 B).

The development of the chimeric lambs was compared to normal and affected animals via monitoring with CAT scans to estimate brain volume. Brain atrophy is apparent from 3 months of age in disease affected animals, and by 6 months normal and affected brains differ by about 10ml, the difference increasing to at least 30ml by 18 months of age. Growth rates were compared to normal and affected animal control rates, as affected animals gain less weight resulting in sheep longer boned for their weight than normal control animals. Clinical loss of sight was assessed by a simple obstacle course test and a blink response to bright light (Westlake et al., 1995b). Samples of endodermal (liver, thyroid, pancreas), mesodermal (cardiac muscle, skeletal muscle, kidney, testis, ovary) and ectodermal (brain, skin) origin were collected at *post mortem* for genotyping to estimate the degree of chimerism. Tissue samples were immersion fixed in 10% formalin for histological assessment, or snap frozen in liquid nitrogen and stored at -80°C for DNA or RNA analysis.

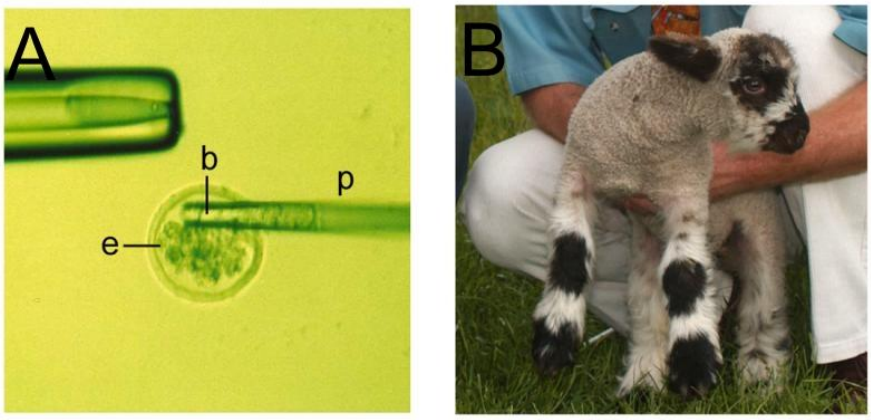

Figure 8 Exchange of blastomeres between homozygous normal and CLN6 affected embryos to create chimeric lambs

A: Blastomeres (b) of an affected embryo positioned in the tip of an aspiration pipette (p) being deposited into a normal embryo (e) after removal of approximately half the blastomeres. **B**: A resultant chimeric lamb.

4.2.2 Immunohistochemistry

4.2.2.1 Tissue collection and processing

Archival tissue from chimeric animals (aged from 17-41 months at *post mortem*) was used for histological examination. Portions of formalin fixed tissue had previously been paraffin wax- embedded, sectioned sequentially at 5μm (Gribbles Veterinary) and mounted on glass slides. Remaining tissue was stored in 10% formalin for subsequent tissue sectioning.

Two affected and two age-matched normal control animals, aged 18 and 24 months were collected as controls. Sheep were sacrificed by exsanguination, the brain removed intact and halved longitudinally. Tissue samples of endodermal, mesodermal and ectodermal origin were immersion fixed in 10% formalin for seven days then placed in fresh solution for a further seven days. Subsequently portions of tissue were paraffin wax-embedded and sectioned as above. Concurrently the remaining brain hemispheres were re-equilibrated (as per section 3.2.2.1) and stored frozen at -80^{o}C for subsequent tissue sectioning.

Sequential 50µm sagittal sections were cut from control and chimeric formalin fixed brains as described previously (section 3.2.2.1). For all subsequent immunohistochemical analyses, matched series of sections from each brain were selected at the previously defined medio-lateral level 5 (Oswald et al., 2005). This was the only level present in all brain samples. Digital images of the tissue, taken at regular intervals whilst sectioning, aided the matching of sections to level 5.

4.2.2.2 Immunohistochemistry

Primary antibodies used were rabbit anti-cow glial fibrillary acidic protein (GFAP, 1:5000, polyclonal, Dako) to detect astrocytes, a biotinylated form of the α-D-galactose specific isolectin I-B4 from *Griffonia simplicifolia* (GSB4, 1:500, Vector Laboratories, Burlingame, CA, USA) and mouse anti-sheep MHC-II (1:2000, monoclonal, Veterinary Preclinical Centre, Parkville, Victoria, Australia) with specificity for HLA-DP molecules (Puri et al., 1987) for activated microglia detection, and mouse anti- PSA-NCAM (1:1000, monoclonal, Chemicon, Temecula, CA, USA) for newly generated and migrating cells.

Routine immunohistochemical detection was carried out via the avidin-biotin amplification system as previously described (section 3.2.2.2, without the use of antigen retrieval) using the appropriate secondary antibodies, biotinylated goat anti-rabbit IgG (1:1000, Sigma) for GFAP, biotin-conjugated affinity purified IgM (1:500, Chemicon) for PSA-NCAM and biotinylated goat anti-mouse IgG (1:500, Sigma) for MHC-II antibody. The optimal incubation period with DAB substrate solution was tested for each antigen (Table 6) and negative control sections, in which either the primary or secondary antibody was omitted, were included in all staining runs.

Digital images of GFAP, GSB4, MHC-II and PSA-NCAM stained sections were acquired with an inverted DMIRB microscope (Leica, Wetzlar, Germany) and a SPOT RT colour digital camera with software (v4.0.9, Diagnostic Instruments Inc., Sterling Heights, MI, USA) using the x 10 and x 20 objectives. The microscope lamp intensity, exposure time, condenser aperture

setting, video camera setup and calibration, and use of neutral density filter were kept constant for capturing all images of a particular immunostain. Digital images were saved as .tif files and figures and photomontages prepared in Corel Photopaint 12 (Corel Co., Ontario, Canada).

Table 6 Primary antibody details and DAB incubation times

Primary Antibody	Concentration	Host	Supplier	DAB incubation time (min)
GFAP	1:5000	Rabbit	Dako	7
GSB4	1:500		Vector	5
MHC-II	1:2000	Mouse	Veterinary Preclinical Centre	20
PSA-NCAM	1:1000	Mouse	Chemicon	3

4.2.2.3 Histology

Luxol-fast blue and Sudan Black histological staining was carried out on paraffin wax- embedded tissue sections for analysis of storage body accumulation. Sections were first dewaxed by clearing in xylene and hydrated through a series of ethanol dilutions; 2 x 100% ethanol, 1 x 95% ethanol, 1 x 70% ethanol, 1 x 50% ethanol and 2 x H_2O. Dewaxed sections for Luxol-fast blue staining were incubated in 0.1% Solvent Blue 38 (Sigma) in 95% ethanol, 24 h, 37°C, in an air-tight container then rinsed in 95% ethanol, followed by water. Destaining was for 6 min with 0.05% lithium carbonate, rinsed 2 x in 70% ethanol, counter stained with filtered haematoxylin (BDH) for 10 min and rinsed in water. Sections were then dehydrated in graded ethanol; 1 x 70% ethanol, 1 x 90% ethanol, 1 x 95% ethanol, 2 x 100% ethanol, cleared for 30 min in xylene and coverslips mounted with DPX (BDH). Sections for Sudan Black were rinsed in water, dehydrated in 100% propylene glycol, 5 min, stained with a solution of 0.7% Sudan Black B (Sigma) in 100% propylene glycol, 7 min, differentiated in 85% propylene glycol, 2 min, rinsed, and coverslips mounted with glycerol. Images were viewed with an inverted DMIRB microscope (Leica).

A corresponding set of paraffin wax-embedded sections dewaxed with xylene and ethanol as above, and formalin fixed unstained sections from animals, were coverslipped with glycerol, sealed, and examined by confocal laser scanning microscopy (Leica TCS SP5) for analysis of fluorescent storage body accumulation. Images were obtained from both cortical and cerebellar sections using a laser excitation peak of 405nm and an emission band pass filter of

535-570nm, and the x 20 (0.7 NA) and x 63 (1.3 NA) objectives. Pinhole size, amplitude offset and detector gain were kept constant for all sections. Confocal images (.lsm) were converted to .tif files using LAS AF lite software (Leica) and figures prepared in Corel Photopaint 12.

For Nissl staining of neurons to analyse cortical thickness and cytoarchitecture, formalin fixed, level 5, sagittal brain sections were dehydrated through a series of ethanol dilutions and cleared in xylene as described above. Sections were then rehydrated through the ethanol gradient, rinsed in water and incubated in a pre-warmed solution of 0.05% cresyl violet acetate (Sigma), 0.05% acetic acid in water, 10 min, rinsed and destained in 95% ethanol, 5 min. Sections were then mounted on glass slides (as per section 3.2.2.2), air-dried, dehydrated through a series of ethanol dilutions and cleared in xylene as above, and coverslips mounted with DPX (BDH). Sections were observed and photographed using an inverted DMIRB microscope (Leica) and SPOT RT colour digital camera with software (v4.0.9). The perpendicular distances between the surface at the pia mater and the boundary between the grey and white matter in the visual cortex were measured. At least 50 measurements were taken at regular intervals. Digital images were saved as .tif files and figures and photomontages prepared in Corel Photopaint 12.

4.2.3 Genotyping

The extent of chimerism was assessed in a range of tissues from each animal using restriction fragment length polymorphic analysis of the single nucleotide polymorphism (SNP) in CLN6 exon 7 (Tammen et al., 2006), described in section 3.2.1. Since genetically normal cells are GG and genetically affected cells AA, the proportion of G:A in tissue from chimeric animals will be indicative of chimerism in that tissue.

4.2.3.1 DNA extraction

DNA was extracted from blood and tissues of endodermal, mesodermal and ectodermal origin from 15 lambs born after blastomere exchange. DNA was extracted from multiple brain sites; frontal and occipital lobe, thalamus, cerebellum, brainstem and spinal cord, where available (see Table 7 for full list of samples for each animal). DNA samples from an affected, South Hampshire heterozygote and Coopworth control sheep were used as controls.

Genomic DNA was extracted from 20mg of tissue using the Axyprep Multisource Genomic DNA Miniprep Kit (Axygen). DNase-rich tissues, liver, pancreas and thyroid, and collagen-rich tissues, skin, cardiac and skeletal muscle, were frozen in liquid nitrogen prior to processing to prevent DNase activation and for more efficient homogenisation, respectively.

Tissue was lysed in 650µl of supplied buffer to release genomic DNA. DNA was purified by a two-phase partition and free DNA bound to an Axyprep spin column and eluted with 200µl of 2.5mM Tris-HCl, pH 8.5. The OD_{260} and 260/280 ratio were measured spectrophotometrically (NanoDrop) for each sample and the double stranded (ds) DNA factor (50) used to quantitate the concentration (ng/µl)

$$50 \times OD_{260} \text{ of the sample} = \text{concentration of DNA } (\mu g/ml)$$

All samples had an $OD_{260/280}$ between 1.9-2.0 indicative of highly purified DNA. Samples were stored at -20ºC until required.

Archival genomic DNA, extracted from blood collected every six months throughout the lifespan of six chimeric animals was also available.

4.2.3.2 RNA extraction and cDNA synthesis

Archival brain tissue samples snap frozen in liquid nitrogen and stored at -80ºC for RNA extraction were available for six chimeric animals, as well as affected, heterozygote and normal controls. RNA was extracted from 30mg of brain tissue using the Qiagen RNeasy mini kit (Qiagen) and RNA concentration and integrity checked as previously described (section 3.2.4.1) All samples had an $OD_{260/280}$ between 1.9-2.1, indicative of pristine RNA. Single stranded cDNA synthesis was carried out on 200ng/µl of RNA in a 20µl reaction, as previously described (section 3.2.4.1) and stored frozen at -20ºC.

4.2.3.3 PCR

All PCR reactions were carried out on a Mastercycler Gradient PCR machine (Eppendorf), in 20µl reactions as described in section 3.2.4.2. Reactions included either 80ng/µl DNA and 0.125µM of the forward E7F1 (5′- GTA CCT GGT CAC CGA GGG-3′) and reverse 7aR (5′-AGG ACT CTA TTG GCT GC-3′) primer, or 1µl of cDNA and 0.125µM of the alternative forward primer 7aF (5′-CTT CAT CCT CTT CAT CTT CAC CTT-3′) and 7aR primer. Standard thermo cycling conditions were utilised, as described in section 3.2.4.2, but with a T_m of 55ºC. Seven µl of PCR product was separated on a 1.5% agarose gel, 30 min, 100V and imaged with a GelDoc XR imaging system and Quantity One v4.5.1 image analysis software. Images were examined to ensure amplification of a single product of the correct size.

Ten µl of the resulting 251bp or 277bp PCR product, was digested with a 10µl mix of 1x NEB4 buffer, 1 x BSA and 10U *Hae*II (New England Biolaboratories, Ipswich, MA, USA), overnight at 37ºC. The resulting DNA fragments were identified by running 12.5µl of the digest on a 3.5% agarose gel (1g MetaPhor agarose [Lonza, Rockland, ME, USA], 0.4g agarose, 40ml TBE [Appendix A.4], 0.5µg/ml ethidium bromide), 40 min, 100V and an image

obtained. Digestion of the products of the E7F1 and 7aR primer set on DNA yields two fragments of 91 and 186bp for homozygous affected "AA" sheep, three fragments of 67, 91 and 119bp for normal, unaffected "GG" sheep and four fragments of 67, 91, 119 and 186bp for heterozygote "GA" sheep (Figure 9). The 7aF and 7aR primer set used on cDNA samples produces bands of 67bp and 184bp for affected DNA, bands of 67bp and 117bp for normal DNA, and 67, 117 and 184bp for heterozygotes (Tammen et al., 2006). Affected, South Hampshire heterozygote and Coopworth control DNA or cDNA was included in all PCR runs. Five µl of the 1Kb Plus DNA Ladder (1µg/µl, Invitrogen) was run in one lane of all gels as a molecular weight control.

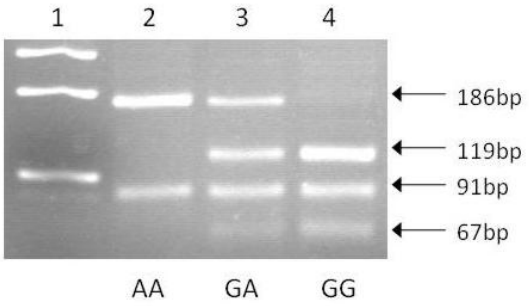

Figure 9 Restriction enzyme detection of the c.822G>A polymorphism using the E7F1 and 7aR primer set

A 277bp PCR product from normal "GG" sheep cleaved with *Hae*II results in three bands of 119, 91 and 67bp shown in 3.5% agarose gels, affected "AA" sheep yield two bands of 186 and 91bp, and heterozygous "GA" sheep four bands of 186, 119, 91 and 67bp. This polymorphism is used as an indirect DNA test in the South Hampshire sheep. Lane 1 contains a size standard with 300, 200 and 100bp bands visible.

Serial dilutions of 80ng/µl affected brain DNA and 80ng/µl normal brain DNA were prepared to provide samples with known affected: normal DNA ratios. PCR and restriction enzyme analysis was performed on these samples as described above. In order to semi-quantify the affected: normal cell ratio, chimera samples were compared visually against these serial dilutions to assign the extent of chimerism as a % of affected DNA present in samples.

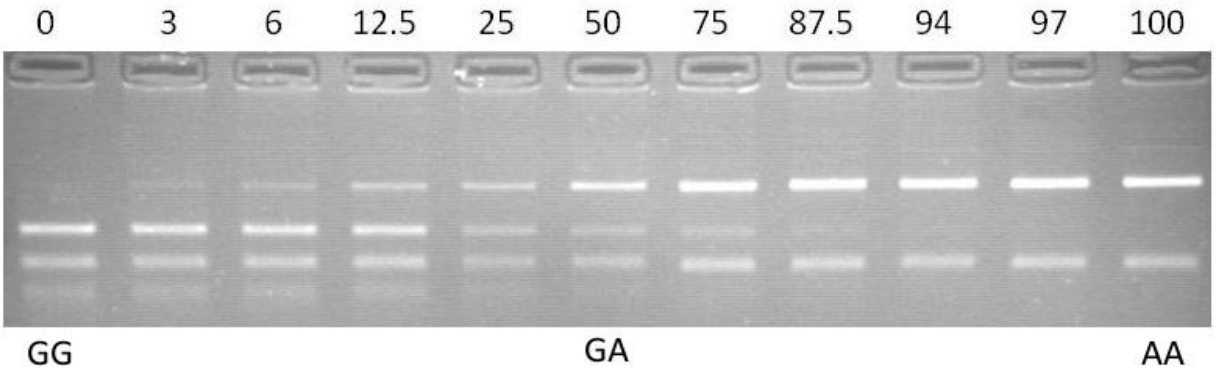

Figure 10 Serial dilution of affected (AA) and normal (GG) DNA

Serial dilution of affected (AA) and normal (GG) DNA digested with *Hae*II enzyme and shown in 3.5% agarose gels. Numbers indicate the affected portion (%).

4.2.3.4 Sequencing

Banding patterns for any samples that were not irrefutable were sent for sequencing, along with normal, heterozygote and affected controls. Fifteen µl of PCR product was separated on a 1.5% agarose gel excised, purified and prepared for sequencing as described in section 3.2.4.2, utilising the forward E7F1 primer. Sequences were aligned against the ovine CLN6, exon 7 sequences and additionally analysed using the Chromas Lite program (Technelysium Pty Ltd, Qld, Australia) to confirm either the presence or absence of an A or G at the SNP site.

4.3 Results

Over four breeding seasons, 74 manipulated embryos were transferred to normal recipient ewes and 15 lambs were born. The resultant lambs were monitored and the extent of chimerism initially assessed, as judged by coat-colour patterns, blood DNA analysis and signs of clinical disease. Based on these initial indications seven of the 15 sheep were classed as chimeric and chosen for further detailed analysis, while six were regarded as 100% normal and two were 100% affected. The extent of chimerism was determined from restriction fragment length polymorphic analysis of the SNP in *CLN6* exon 7 and compared with immunohistochemical examination of glial activation with GSB4 and GFAP staining, neurogenesis with PSA-NCAM staining, and storage body accumulation within the brain. These data were correlated with phenotypic observations and brain volume data to gain an

indication of the influence normal cells have on the progression or course of pathological disease.

4.3.1 Genotyping

Routine amplification from genomic DNA and gel separation of the products after restriction enzyme detection of the c.822 G>A polymorphism was exploited for chimeric assessment of the contribution of normal and affected cells to the genotype of CNS and non-CNS tissues in seven chimeric animals. Ambiguous genotyping results in which the 186bp band was only faintly present, indicative of a mild state of chimerism in which there is a higher proportion of normal cells than affected cells, were validated by sequencing to confirm the presence of both the A and G alleles. Additionally, for animals and tissues for which RNA was available, cDNA amplification and restriction enzyme digest patterns were analysed. Primer set E7F1 and 7aR did not amplify cDNA samples, hence the 7aF and 7aR primer set were utilised. This confirmed that gene presence was reflective of gene expression within a particular tissue. Genotype analysis on serial blood samples collected every six months revealed that the extent of chimerism in haematopoietic cells remained consistent over the life span of all animals.

Genotype analysis on available tissues from seven animals indicated chimerism in the majority of tissues analysed (Table 7), ranging from predominant colonisation of normal or affected cells to more equal proportions of both cell types evident across tissues. In order to determine the proportion of affected: normal cells present in a particular brain region or tissue, gel electrophoresis images were compared visually against serial dilutions of affected and normal DNA. These serial dilutions indicated the gel electrophoresis band pattern and intensities for DNA ranging from 0-100% affected or normal (Figure 11 A). From these results it was clear that the majority of tissues from two animals, 58/02 and 403/04, were dominated by affected cells. All available CNS samples indicated an affected genotype and did not demonstrate the presence of normal cells within the brain. In addition, all blood samples analysed correlated with the tissue genotype.

Chimerism was determined in animals 401/04, 401/05, 402/05, 404/05 and 405/05. All brain regions exhibited affected cell proportions ranging from 3-75% of all cells (Table 7, Figure 11). Similarly, gel-electrophoresis results for non-CNS tissues also indicated chimerism within these tissues (Table 7). Animal 401/05 in particular demonstrated a more equal contribution of affected to normal cells within all brain regions analysed, with the cerebellum displaying a 50:50 proportion. The extent of chimerism within brain regions was relatively constant, compared to non-CNS tissues, in which there was considerable variation in this

animal. The remaining animals, 401/04, 402/05, 404/05 and 405/05, had less equal proportions of both cell types within brain regions, with a more predominant presence of normal cells in most brain regions compared to animal 401/05. Animal 402/05 had a predominant proportion of normal cells in all brain regions, as did animal 401/04 although there was more variation between the different brain regions in this animal. Correspondingly, the non-CNS tissues of these two animals, 401/04 and 402/05, had a prevailing absence of affected cells, with the majority of tissues being 100% normal (Table 7). The remaining two animals, 404/05 and 405/05, displayed a higher contribution of affected cells within non-CNS tissue than animals 401/04 and 402/05, and the extent of chimerism varied to a larger extent, similar to animal 401/05. However, most brain samples had a higher proportion of normal cells but some regions did display dramatic variations, such as the brainstem of animal 404/05 which was 75% affected. In addition, the analysis of multiple blood samples collected every six months revealed the presence of affected DNA in animals 401/04, 404/05 and 405/05 to varying degrees but not animals 401/05 and 402/05 which were 100% normal (Table 7). Tissues of endodermal, mesodermal and ectodermal origin all displayed variation in the extent of chimerism observed.

Figure 11 Restriction enzyme detection of the c.822G>A polymorphism to determine the extent of chimerism

A 277bp PCR product resulting from use of the E7F1 and 7aR primers and cleaved with *Hae*II results in two bands of 186 and 91bp from affected "AA" sheep samples, three bands of 119, 91 and 67bp from normal "GG" samples, and four bands of 186, 119, 91 and 67bp from heterozygote "GA" samples.

A: Serial dilutions of affected and normal DNA for use as a standard to estimate the proportion of affected DNA present in samples from chimeric animals. Samples were compared visually against these dilutions to indicate the proportion of normal and affected cells in tissue samples. Numbers indicate the affected portion (%).

B: The extent of chimerism in animal 401/05 varied noticeably between tissues e.g. kidney is mainly normal (12.5 % affected) whilst liver and pancreas are mainly affected (87.5% affected). There was less variation between different regions of the brain. There is considerable colonisation of affected cells within all brain regions analysed, with an estimated 12.5-50 % affected DNA.

C, D, E, F: All brain regions for animals 405/05, 404/05, 401/04 and 402/05 were chimeric, but there was a higher proportion of normal cells in most brain regions than in animal 401/05 and more variation between different brain regions. Note in particular the dramatic variation in brain samples from animal 404/05, the brainstem exhibiting a much larger contribution of affected cells compared to other samples.

G, H: Brain regions analysed in animals 58/02 and 403/04 were 100% affected indicating a lack of normal cells in the brain and hence no chimerism.

See Table 7 for % affected DNA in different brain regions and non-CNS tissues of all animals.

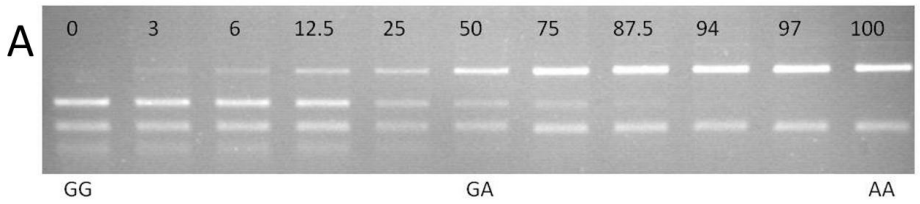
A
0
3
6
12.5
25
50
75
87.5
94
97
100
GG
GA
AA

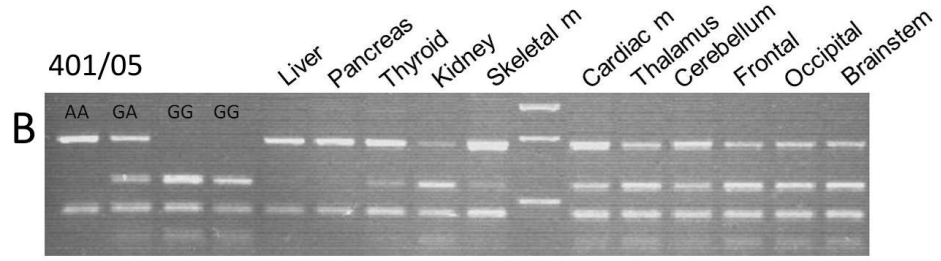
401/05
Liver
Pancreas
Thyroid
Kidney
Skeletal m
Cardiac m
Thalamus
Cerebellum
Frontal
Occipital
Brainstem
B
AA
GA
GG
GG

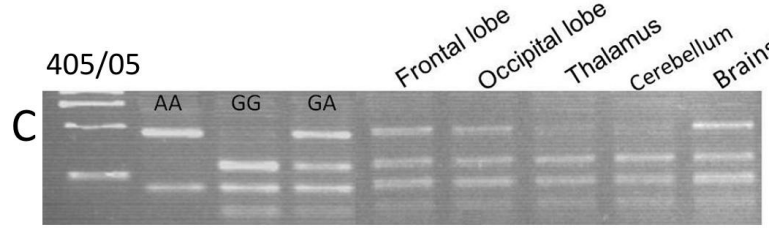
405/05
Frontal lobe
Occipital lobe
Thalamus
Cerebellum
Brainstem
C
AA
GG
GA

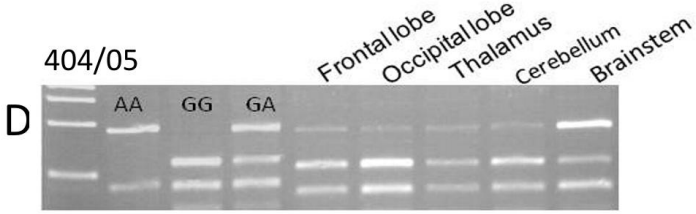
404/05
Frontal lobe
Occipital lobe
Thalamus
Cerebellum
Brainstem
D
AA
GG
GA

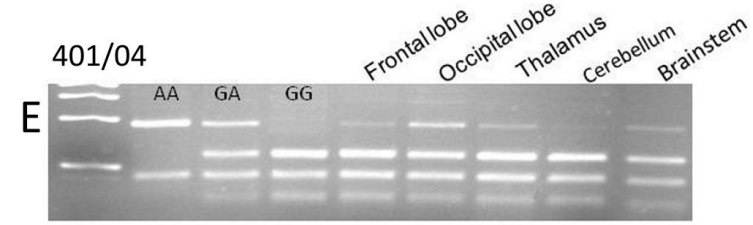
401/04
Frontal lobe
Occipital lobe
Thalamus
Cerebellum
Brainstem
E
AA
GA
GG

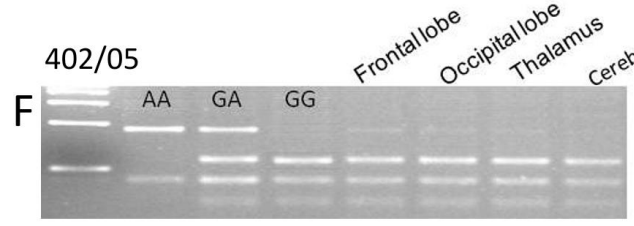
402/05
Frontal lobe
Occipital lobe
Thalamus
Cerebellum
F
AA
GA
GG

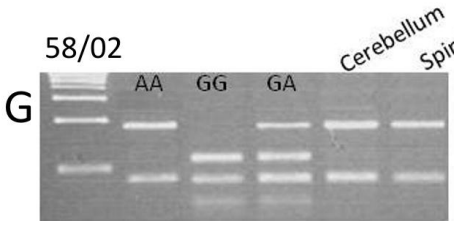
58/02
Cerebellum
Spinal cord
G
AA
GG
GA

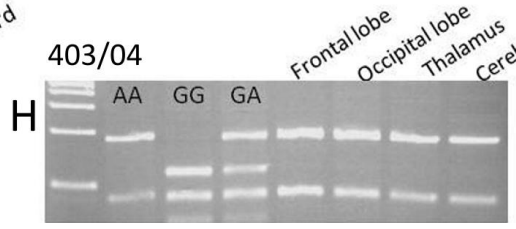
403/04
Frontal lobe
Occipital lobe
Thalamus
Cerebellum
H
AA
GG
GA

Table 7 Genotyping results for DNA samples from tissues of chimeric animals

Genotyping results obtained for each tissue is denoted as the % affected DNA present in each sample, as determined visually by comparison with serial dilutions of affected: normal DNA (see Figure 11).

Animal #	Blood	Frontal lobe	Occipital lobe	Thalamus	Cerebellum	Brainstem	Skin	Liver	Thyroid	Pancreas	Kidney	Skeletal muscle	Cardiac muscle
58/02	100	n/a	n/a	n/a	100	100	25	12.5	100	n/a	100	25	50
403/04	100	100	100	100	100	100	100	100	n/a	n/a	100	100	100
401/04	3	6	25	6	3	12.5	n/a	0	0	0	0	0	50
401/05	0	12.5	12.5	25	50	12.5	n/a	87.5	75	87.5	12.5	75	50
402/05	0	6	6	3	3	n/a	n/a	0	0	0	0	0	3
404/05	13	6	6	25	6	75	n/a	25	25	25	12.5	50	6
405/05	50	25	25	3	3	25	n/a	50	25	25	6	6	75

n/a: tissue sample not available

4.3.2 Brain volume

From 3 months of age, animals were CAT scanned every six months and the brain volume determined. Changes in the brain volume profile of chimeric animals with age were compared to the average changes in brain volume observed in control and affected animals (Figure 12).

A number of chimeric animals had increasing brain volumes, indicating a recovering-like brain. The brain volumes of animals 404/05 and 402/05 were below normal initially but increased progressively and by 600-800 days had increased to within the normal range. A small subsequent reduction in brain volume was observed in animal 402/05 but its brain volume at 800 days was still significantly higher than affected animals which rarely survive past 24 months of age due to disease severity. The brain volume of animal 401/04 was far below the affected line initially at only 60ml compared to ~80ml for affected animals. However, the brain volume progressively increased, surpassing the affected line at 600 days and continued to increase over the following 600 days to approach the normal line. This animal followed a contrasting path to that of affected animals in which brain volume progressively decreases. These three animals survived longer than affected control animals, especially animal 401/04 being sacrificed at 41 months of age. These data in combination with genotype analysis, which revealed the presence of affected cells in all brain regions of these animals (Table 7), indicates a recovering-like brain.

Two animals, 405/05 and 401/05, displayed some fluctuations in brain volume, decreasing slightly at 400 and 600 days respectively and subsequently increasing. However these brain volumes remained above normal at all times, even though genotyping indicated colonisation of affected cells within the brain.

Two animals, 58/02 and 403/04, had brain volume changes that closely followed those of affected animals, decreasing progressively with age to 70-75ml by 24 months of age compared to 110ml for normal control animals. This data indicated that these animals were predominantly affected-like, in agreement with the genotype analyses (Table 7).

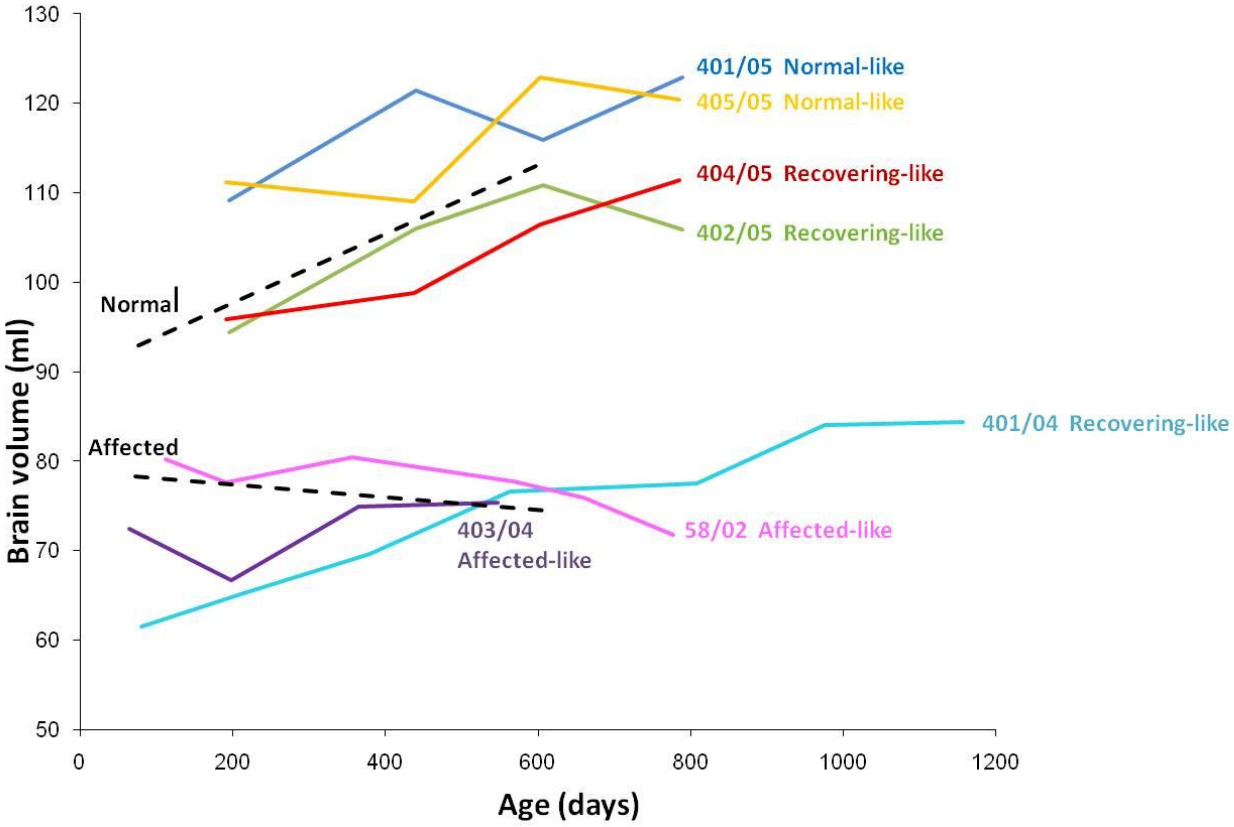

Figure 12 Changes in CAT brain volumes of seven chimeric animals compared to affected and normal controls

Note: affected animals do not usually survive past 24 months of age due to terminal disease and no volume measurements are available for them beyond this age.

4.3.3 Nissl staining to reveal cortical atrophy

This recovery of chimeric brains was also analysed in Nissl stained sections by measuring cortical thickness and general brain atrophy. Atrophy of the cerebral cortex and thinning of the cortical layers was discernable in all regions of the 18 and 24 month old affected sheep brains but not in normal controls, the affected visual cortex thickness being reduced to 48% of normal (Figure 14). Individual cortical layer boundaries had become very difficult to discern in affected animals at 18 and 24 months of age, as the few remaining neurons lacked a visible laminar distribution (Figure 13 D). A striking difference between the affected and control cortices was the appearance of clusters of cellular aggregates observed at the layer I/II boundary throughout all cortical regions of affected sheep but not in controls. Neuronal loss was not exhibited in any of the cortical regions examined in control animals. There was no indication of atrophy in the cerebellum and hippocampus of control or affected animals.

Two affected-like chimeric animals, 58/02 and 403/04, revealed severe neuronal atrophy in all cortical regions of the brain. Their visual cortex thickness was reduced to 48-52% of normal at 24 months, comparable with that of affected animals (Figure 14). Nissl staining revealed a dramatic loss of neurons in all cortical regions in these animals, especially pronounced in cortical layers II-III, where remaining neurons were organised within cellular clusters (Figure 13 E, F). As for the affected controls, cytoarchitecture of the cerebellum and hippocampus were unchanged.

Both the two normal-like chimeras, 401/05 and 405/05, and the three recovering chimeras, 401/04, 402/05 and 404/05, displayed a laminar distribution of cells within all cortical regions, with no apparent loss of neurons or formation of clusters (Figure 13 B, C), regardless of the degree of chimerism in different brain regions as revealed by DNA analysis (Table 7). Cortical thickness measurements consolidated these findings, all animals being within 97-114% of normal at 24 months of age (Figure 14).

Figure 13 Comparison of Nissl stained occipital cortex sections from normal, affected and chimeric animals

Upper lines mark the layer I/II boundary, middle lines indicate the layer IV/V boundary and lower lines mark the layer VI/white matter boundary. Atrophy is advanced in the cortex of severely affected animals (**D**) in which cortical layer boundaries are less distinct and densely packed cellular clusters are evident within layer II. The affected-like chimeric animals 58/02 and 403/04 (**E**, **F**) exhibit clusters and severe neuronal loss, especially pronounced in upper cortical layers. In contrast, clusters are not exhibited in the normal (**A**) or normal-like chimeric animals 401/05 and 405/05 (**B**, **C**), which also display no apparent atrophy or loss of cortical layers. Note: Images B and C are representative of the recovering-like chimeric animals 404/05, 402/05 and 401/04, which also had a normal laminar distribution of cells.

Figure 14 Occipital cortex thickness in normal, affected and chimeric animals

Assessment of cortical atrophy in chimeric brains compared to age-matched normal (n=3) and affected (n=3) controls. Each column represents the mean thickness (n>50) of the visual cortex ± SD. Chimeric animals have been grouped as affected, normal or recovering-like based on genotype, Nissl staining and cortical thickness analyses.

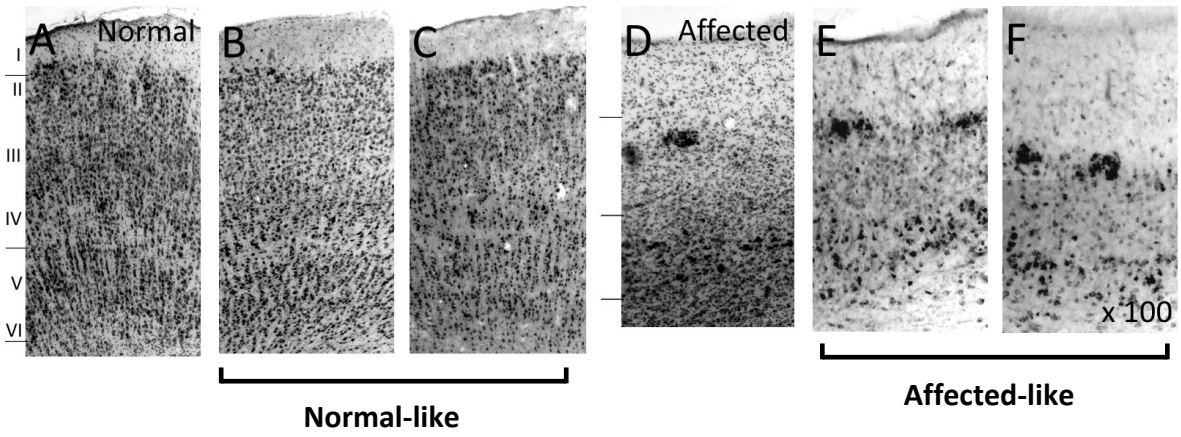

Figure 13 **Comparison of Nissl stained occipital cortex from normal, affected and chimeric animals**

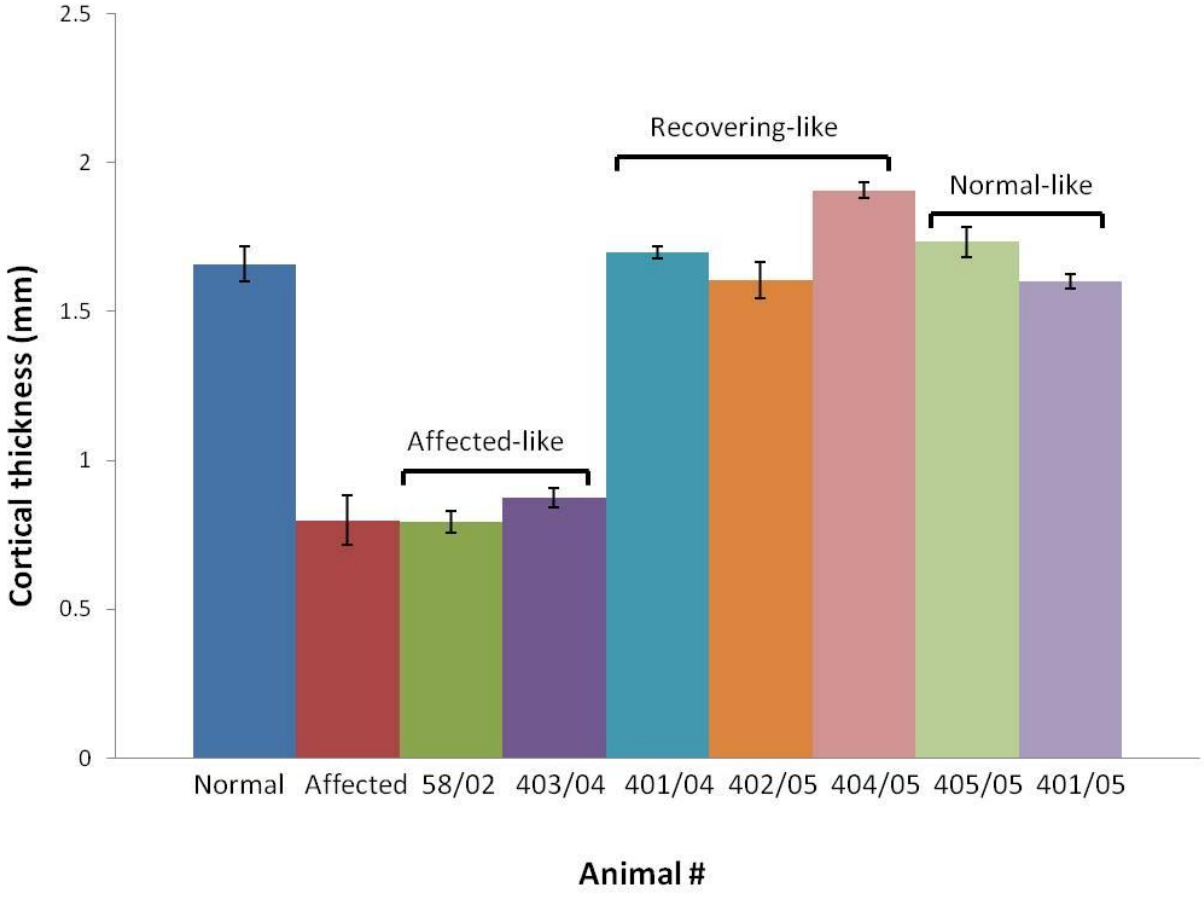

Figure 14 **Occipital cortex thickness in normal, affected and chimeric animals**

4.3.4 Storage body accumulation

To study the accumulation of storage bodies in the brain, sections were stained with Luxol-fast blue or Sudan black, or analysed for the presence of fluorescent storage material. All sections were analysed without knowledge of the genotype or other indicative factors and independently analysed by a colleague. All observations were consistent to both viewers.

Histological studies revealed the presence of storage material in cells of the brain in affected 18 and 24 month old animals. Storage material was fluorescent and strongly stained by both Luxol-fast blue and Sudan black with storage bodies observed throughout neocortical, subcortical and cerebellar regions of these animals. The few remaining large pyramidal neurons of the cortex were densely packed with globular storage body deposits (Figure 15 D) and smaller neuronal and glial like cells were predominantly filled with granules which occupied the entire cytoplasm. In the cerebellum, fluorescent storage bodies were most obvious within the perikarya of large Purkinje cells (n >200, cells viewed), the majority of which contained globular, punctate storage bodies of varying size (Figure 16 D, F). No regional variations in storage material accumulation were observed and many smaller, glial-like cells contained significant deposits. Conversely, normal control animals did not contain storage deposits in any brain regions (Figure 15 A, B; Figure 16 A, B).

The affected-like chimeric animals 58/02 and 403/04, had storage body accumulation consistent with an affected diagnosis. Storage bodies were evident throughout all neocortical regions and similar amounts of fluorescence were observed in both upper and lower cortical layers (Figure 15 E). Similarly, subcortical and cerebellar regions contained storage deposits and no regional variation was observed. Storage bodies had a round, globular morphology and were densely packed within large cortical pyramidal cells (Figure 15 F) and Purkinje cells of the cerebellum (Figure 16 G, H). Many smaller cells contained significant storage, comparable to that of affected controls.

One of the normal-like chimeric animals, 401/05, had an accumulation of some small storage deposits within both large and small cells of all neocortical, subcortical and cerebellar regions but at a significantly lower incidence than observed in affected animals. Cells with globular storage deposits were present alongside cells which showed no accumulation (Figure 15 G, H; Figure 16 I, J) and it was observed that every 20-30th cell exhibited some degree of storage material accumulation. Some cells contained significant storage, resembling that of an affected animal, whilst others contained substantially less with only a few globular deposits present along the periphery of the cell perikaryon (Figure 15 H). No regional variation in

accumulation was observed, with all regions exhibiting the same incidence and degree of storage body accumulation. All storage bodies observed were both Luxol-fast blue and Sudan Black positive and exhibited fluorescence. The reduced accumulation of storage bodies in this animal was interesting as it was older than affected controls, 26 months, whereas affected animals rarely survive past 24 months due to disease severity, therefore, there was much less storage than expected for an affected animal of this age. The remaining normal-like chimera, 405/05, and the three recovering animals, 401/04, 402/05 and 404/05, were exclusively of the normal phenotype, being negative for storage body accumulation in all brain regions.

Figure 15 Accumulation of fluorescent storage material in cortical grey matter
Confocal microscopy of fluorescent storage material (405nm excitation, 535-570nm emission) in the cerebral cortex of normal, affected and chimeric brains. Images were obtained from thin 5µm wax-embedded sections to achieve better resolution for analysing storage body accumulation within cells, but all observations were consistent in both thin and 50µm thick sections.

Low power images (x 20 objective) of cortical grey matter reveal extensive storage body accumulation in an affected (**C**) and an affected-like chimeric animal, 403/04 (**E**). Fluorescent storage bodies are present in the normal-like chimeric animal 401/05 (**G**), albeit at a significantly lower incidence than in affected controls, indicative of the presence of affected cells within the brain. In contrast, storage material is not present in normal control brain (**A**).

Higher power images (x 63 objective, 2 x zoom) reveal large pyramidal cells densely packed with globular storage deposits which fill the entire cytoplasm in an affected and an affected-like animal, 403/04 (arrows, **D**, **F**). Storage deposits in small cortical neurons of the normal-like chimera 401/05 are present peripherally and do not fill the cytoplasm (arrows, **H**). Note the complete lack of storage material in neighbouring cells.

Note: Images of the affected-like chimera 403/04 are representative of the other affected-like chimera 58/02. Images for the remaining normal-like chimeric animal, 405/05, and the recovering-like animals, 401/04, 402/05, 404/05, were not included as no storage body deposits were observed.

Scale bar = 50µm.

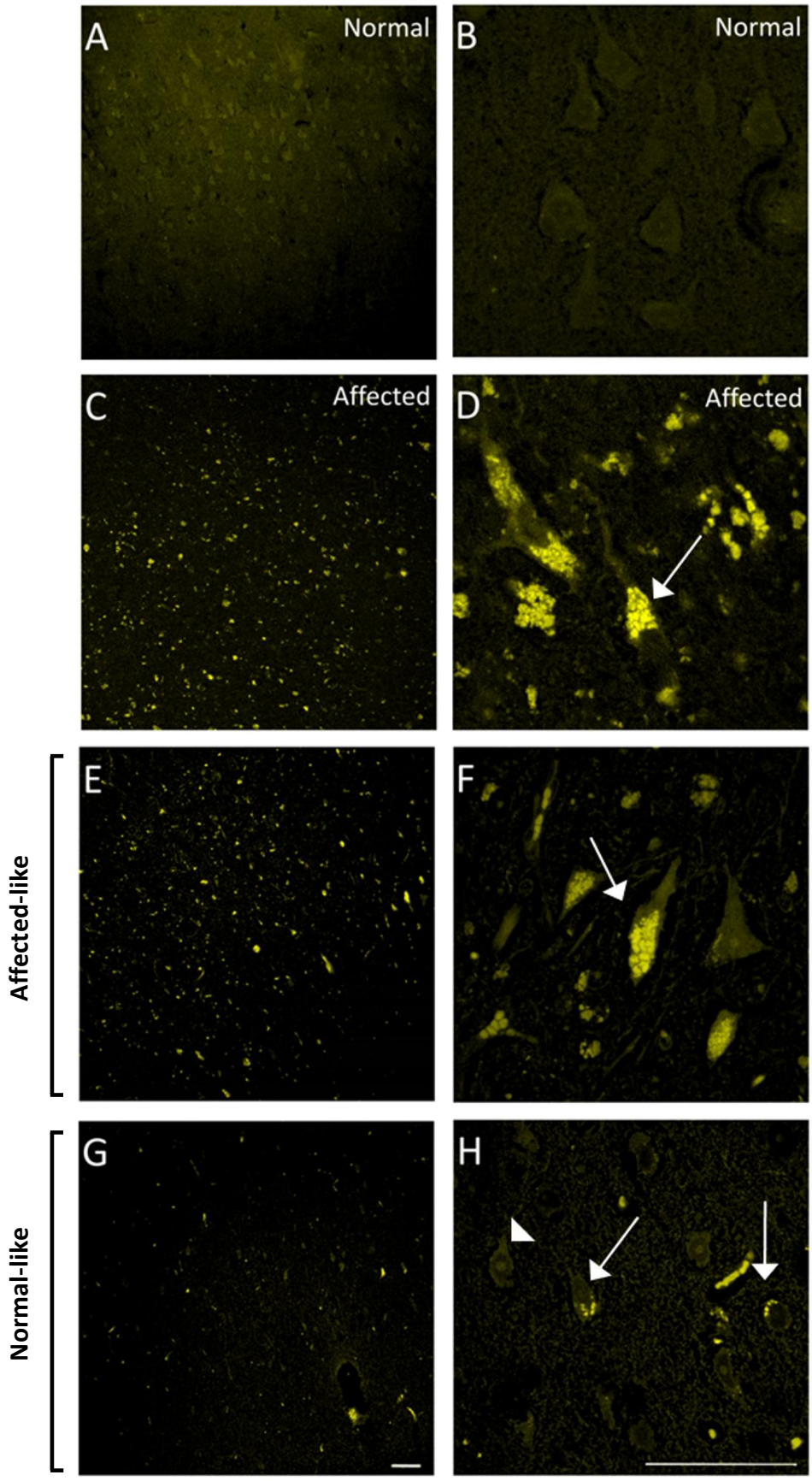
A
Normal
B
Normal
C
Affected
D
Affected
E
F
Affected-like
G
H
Normal-like

Figure 16 Accumulation of fluorescent storage material in Purkinje cells of the cerebellum

Confocal microscopy of fluorescent storage material (405nm excitation, 535-570nm emission) in Purkinje cells of the cerebellum of normal, affected and chimeric brains. As per Figure 15 images were obtained from thin 5µm wax-embedded sections.

The large Purkinje cells of the cerebellum contain punctate, globular storage deposits in affected brain (**C**-**F**). Correspondingly, the affected-like chimeric animal 403/04 (**G**, **H**) contained fluorescent storage deposits in most of the n>200 Purkinje cells viewed, consistent with an affected phenotype. In contrast, storage material was present in only every 20-30th cell viewed in the normal-like chimeric animal 401/05 (**I**, **J**) and deposits appeared smaller than in affected animals. Cells containing storage (arrow, **I**) were present alongside cells which lacked any fluorescent deposits (arrowheads, **I**), whereas the majority of cells in affected control animals contained storage material (arrows, **C**, **E**). Fluorescent storage material was not evident in the normal control brain (**A**, **B**).

Note: Images of the affected-like chimera 403/04 are representative of the other affected-like chimera 58/02. Images for the remaining normal-like chimeric animal, 405/05, and the recovering-like animals, 401/04, 402/05, 404/05, were not included as no storage body deposits were observed.

Scale bar = 50µm.

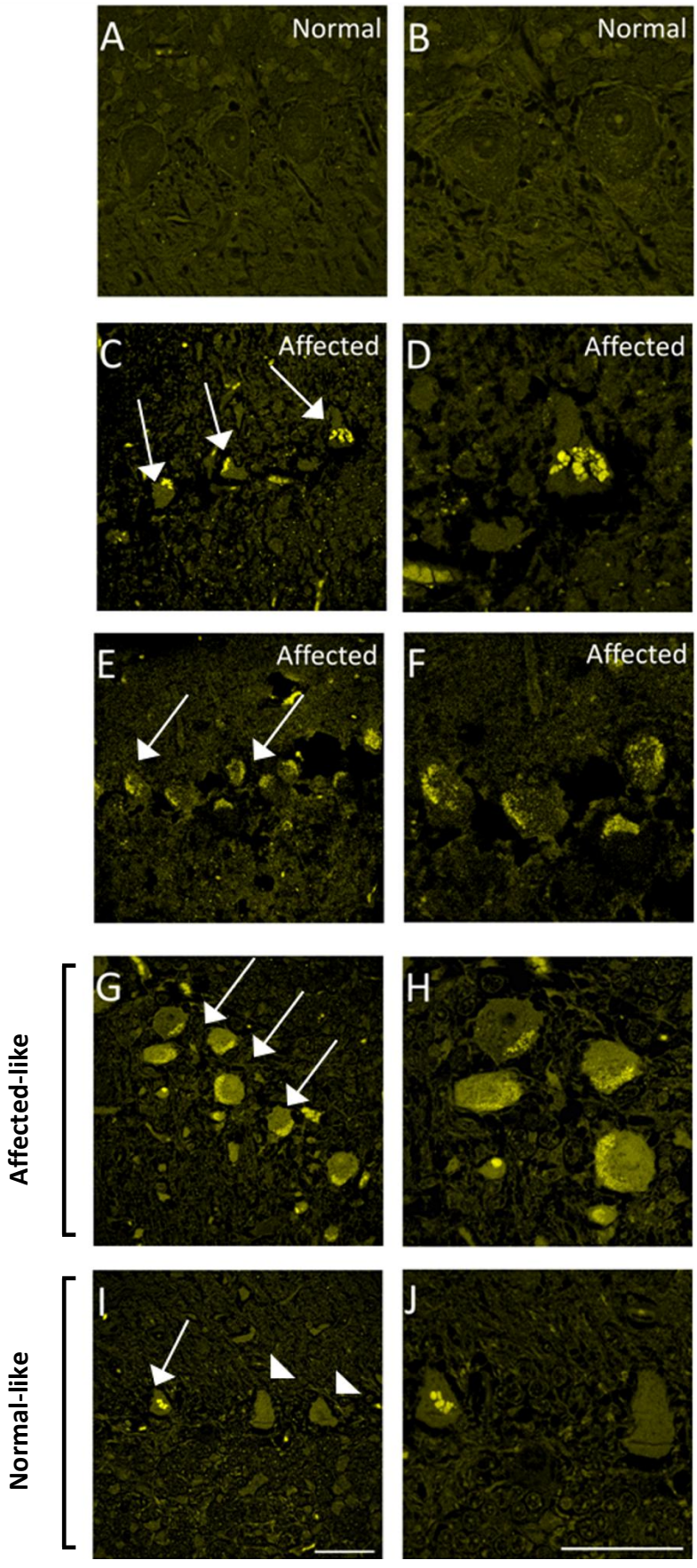
A
Normal
B
Normal
C
Affected
D
Affected
E
Affected
F
Affected
G
H
I
J
Affected-like
Normal-like

4.3.5 Glial activation

Due to the central role that glial activation is proposed to have in the pathogenesis of NCL chimeric animals were examined for any alterations in this response. Activation was assessed by immunostaining for GFAP as a marker for reactive astrocytosis, and GSB4-lectin histochemistry and MHC-II immunoreactivity to detect activated microglia in normal, affected and chimeric brains.

4.3.5.1 GFAP

As expected, GFAP immunoreactivity in affected control 18 and 24 month old animals was intense in the pia mater and both upper and lower cortical layers, where hypertrophic astrocytes formed a dense meshwork (Figure 17 (i)D). Reactivity was more pronounced in the visual cortex compared to parieto-occipital and motor cortices.

In normal 18 and 24 month old control cerebral cortex, GFAP reactivity was found in protoplasmic astrocytes, with short, thick, highly branched processes. Positive cells were distributed uniformly across all cortical layers with no regional variation observed and immunoreactivity was also detected in the pia mater (Figure 17 (i)A).

The two affected-like chimeric animals, 58/02 and 403/04, had GFAP staining intensities similar to affected controls. Staining was intense along the pia mater and a dense meshwork of hypertrophic astrocytes was particularly prominent in upper cortical layers. Immunoreactivity was evident across all cortical layers, albeit at a slightly lower intensity than that in affected controls, suggestive of a less advanced astrocytic response in these animals (Figure 17 (i)E, F).

The two normal-like chimeric animals, 401/05 and 405/05, and the three recovering chimeras, 401/04, 402/05 and 404/05, displayed GFAP immunoreactivity consistent with that of normal control animals, even though genotype analysis did reveal the presence of affected cells in all brain regions of these chimeras. The distribution of protoplasmic astrocytes throughout all cortical layers and regions was similar to that in normal controls (Figure 17 (i)B, C). No significant differences were observed in subcortical or cerebellar regions between normal and affected controls and chimeric animals.

4.3.5.2 GSB4

GSB4 staining which labels extracellular matrix components, blood vessels, perivascular macrophages and activated microglia (Streit, 1990), was markedly increased in 18 and 24 month old affected brains compared to normal controls, with intense GSB4 staining in all cortical grey matter regions and subcortical nuclei. GSB4 positive microglia, with thick

retracted processes and hypertrophied cell bodies were present throughout cortical layers II-VI, forming a conspicuous band especially in upper layers II and III, and lower layers V and VI (Figure 17 (ii)D). No regional variation in cortical staining was observed at these ages. Staining was also present in all white matter tracts at a much stronger intensity than in normal brain but the affected hippocampus remained unstained.

GSB4 positive parenchymal microglia were not present in any cortical layers or regions of normal control animals (Figure 17 (ii)A). Occasionally, capillaries were detected in the cortical grey matter and within white matter tracts, but without activated perivascular macrophages. Diffuse staining was present in white matter tracts and subcortical nuclei but at a much lower intensity than in affected animals and the hippocampus was unstained.

The two affected-like chimeric animals, 58/02 and 403/04, had intense cortical GSB4 staining of brain macrophages, exhibiting rounded cell bodies and thickened processes (Figure 17 (ii)E, F). Staining was present in all cortical layers, albeit at a much lower intensity in layer I than in layers II-VI. The pattern and distribution of staining was comparable to that in affected animals, with no regional variation in staining intensities observed. Positive staining was also present in white matter tracts and subcortical nuclei at a comparable intensity to affected animals.

GSB4 staining of the two recovering, 402/05 and 404/05, and two normal-like, 401/05 and 405/05, chimeric animals did not reveal activated microglia or perivascular cells (Figure 17 (ii)B). General, diffuse staining of capillaries within cortical grey matter was widespread and at a higher incidence than in normal control brain. Elongated, flat perivascular cells were occasionally present and consistent with those found in control brains. However, rounded perivascular macrophages, indicative of activated cells, were not associated with these blood vessels. All four animals had staining intensities within white matter tracts and subcortical nuclei comparable to those in normal control brains. Similarly, the hippocampus was unstained in all animals.

The other recovering chimera, 401/04, displayed GSB4 stained microglia scattered throughout cortical layers I-VI (Figure 17 (ii)C). The majority had a ramified morphology and small cell body, characteristic of resting, non-reactive microglia. Cells with thicker, retracted processes were occasionally observed scattered throughout all cortical layers, indicative of cells transforming to activated brain macrophages. No regional or cortical layer differences in staining amount or intensity were observed. Staining of white matter tracts and subcortical nuclei were comparable with normal animals and the hippocampus was unstained.

4.3.5.3 MHC-II

MHC-II staining which is routinely used to detect activated microglia, perivascular macrophages and brain macrophages (Streit, 1990; Streit and Gaeber, 1993), was intense in the 18 and 24 month old affected control brains. Activated microglia mainly had a macrophage-like morphology and formed a continuous, conspicuous band in layers II-VI in all cortical regions. Staining was absent or minimal in layer I. Immunoreactive cells were also detected in the white matter and subcortical nuclei. In contrast, MHC-II staining of microglia was not observed in the cortical grey matter of the 18 and 24 month old normal control brains. Occasionally macrophages were detected in the meninges and perivascular cells.

No positive MHC-II staining was detected in any of the seven chimeric animals. This would be expected for those animals which also lacked positive GSB4 staining but was unanticipated for the three animals which had displayed moderate to intense GSB4 staining of activated microglial cells.

Figure 17 Glial activation in the occipital cortex of the sheep brain

(i): GFAP positive astrocytic response in the occipital cortex of chimeric animals compared to immunoreactivity in the normal and affected control cortex.

GFAP immunoreactivity was strong throughout all cortical layers but was particularly intense in the pia mater and upper cortical layers of affected brain, where hypertrophic astrocytes formed a dense glial meshwork (**D**). Hypertrophic astrocytes were evident in the affected-like chimeric animals 58/02 and 403/04 (**E**, **F**), forming a prominent band in upper cortical layers. The pia mater was strongly reactive but immunoreactivity in layer I and lower cortical layers was not as intense as affected controls. GFAP reactivity was detected in protoplasmic astrocytes throughout all cortical layers of normal control brain (**A**). Similarly, the normal-like animal 401/05 and recovering animal 401/04 (**B**, **C**), displayed immunoreactive protoplasmic astrocytes throughout all cortical layers, with no evident differences between cortical layers or glial meshwork observed. Note: images of the chimeras 401/04 and 401/05, are representative of the other chimeric animals 402/05, 404/05 and 405/05.

(ii): GSB4-lectin histochemistry in the occipital cortex of chimeric animals compared to immunoreactivity in the normal and affected control cortex.

GSB4-lectin histochemistry stained activated microglia throughout all cortical layers of the affected occipital cortex (**D**). Staining was particularly intense in upper cortical layers II and III, and lower cortical layers V and VI, forming prominent, continuous bands. GSB4 positive cells were typical of brain macrophages, having hypertrophied cell bodies and retracted processes. Comparable staining patterns and intensities were observed in the affected-like animals 58/02 and 403/04 (**E**, **F**), with intensely stained brain macrophages especially notable in upper cortical layers. Conversely, immunoreactivity was not detected in the cortical grey matter of normal control brain (**A**). Immunoreactivity in the cortex of the normal-like animal 401/05 was confined to capillaries (**B**), likely an artefact of prolonged immersion fixation. Occasionally, flattened, elongated perivascular cells were present but no activated, round perivascular macrophages were detected. Staining in the recovering animal 401/04 (**C**) was stronger than normal controls but weaker than affected animals. The majority of cells stained had a ramified morphology and small cell bodies, characteristic of resting, non-reactive microglia. Cells with thicker, retracted processes were occasionally observed scattered throughout all cortical layers, indicative of cells transforming to activated brain macrophages. Note: images of the chimera 401/05 are representative of the other chimeric animals 402/05, 404/05 and 405/05.

(i)

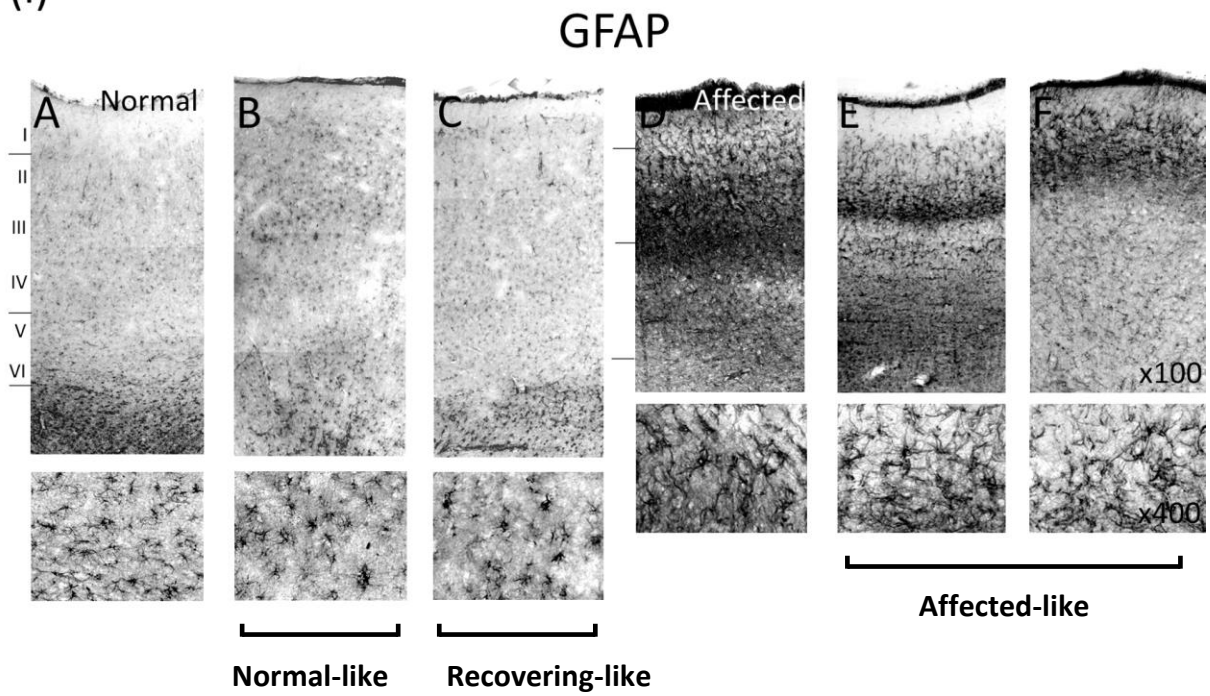
GFAP
A
Normal
B
C
D
Affected
E
F
I
II
III
IV
V
VI
x100
x400
Affected-like
Normal-like
Recovering-like

(ii)

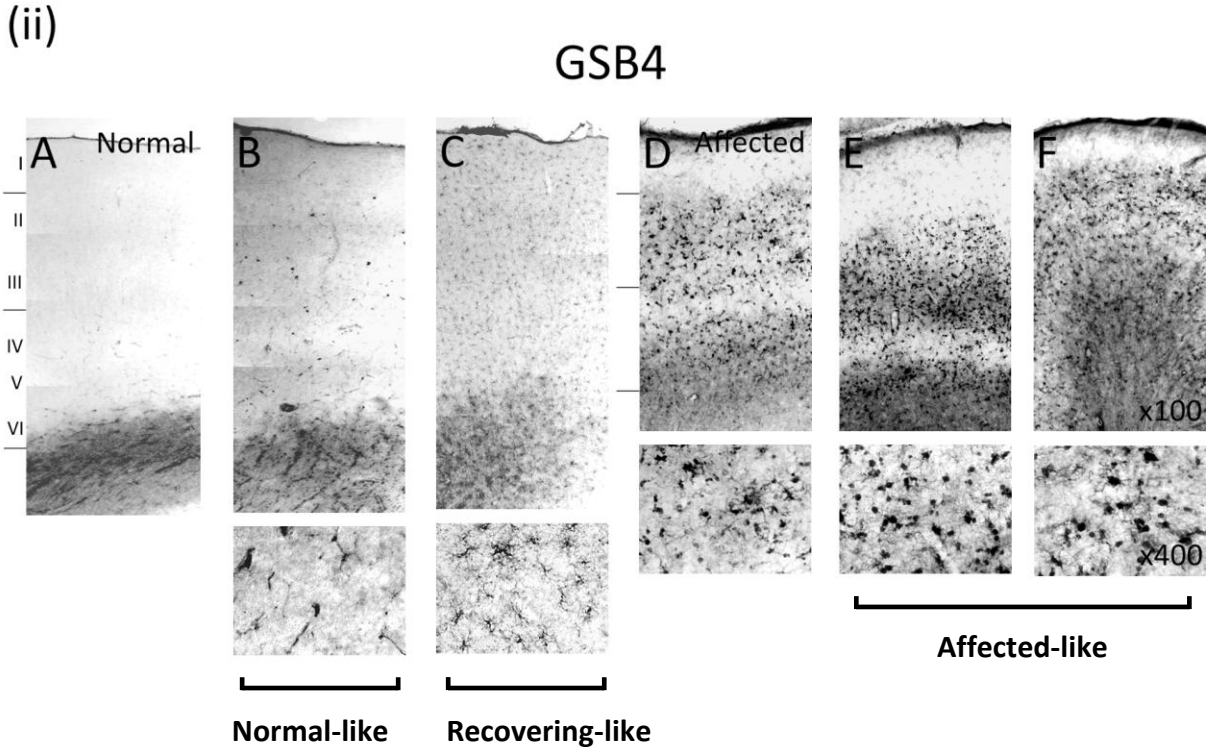
GSB4
A
Normal
B
C
D
Affected
E
F
I
II
III
IV
V
VI
x100
x400
Affected-like
Normal-like
Recovering-like

4.3.6 Neurogenesis

Significant PSA-NCAM positive staining was observed in the 18 and 24 month old affected animals along the entire rostral-caudal extent of the SVZ lining the lateral ventricle (Figure 18 F). A thickened band of intensely stained cells and fibres was evident and especially conspicuous at more rostral regions of the SVZ. These PSA-NCAM positive cells and fibres displayed a tangential orientation, characteristic of the rostral migratory stream to the olfactory bulb. In addition immunoreactive cells and fibres were detected radiating away from the SVZ within white matter tracts, migrating towards the neurodegenerative cortex. PSA-NCAM positive cells were present within all cortical regions in the affected brain and these immunoreactive cells formed prominent, densely packed cellular aggregates in upper cortical layers II-III (Figure 19 (i)F), congruous with the laminar distribution of cellular clusters revealed by Nissl staining.

SVZ neurogenesis was also evident in normal control animals but the band of PSA-NCAM positive cells and fibres was markedly decreased compared to age-matched, affected animals (Figure 18 A). Rarely, individual cells were stained within the corex but cellular aggregates were not present in normal control brains (Figure 19(i)A). PSA-NCAM positive cells were detected within the dentate gyrus of the hippocampus but no differences in the intensity or extent of neurogenesis was noted between affected and normal brains in this region.

All seven chimeric animals displayed higher amounts of PSA-NCAM immunoreactivity than normal control animals. The two affected-like animals, 58/02 and 403/04, had intense staining along the SVZ, with a conspicuous band of cells and fibres comparable with that seen in affected animals (Figure 18 E). Concurrently, cells were observed migrating along white matter tracts and immunoreactive cells were present within all cortical regions of the brain (Figure 19(i)E, (ii)E). These cells had intensely stained perikaryon and multiple dendritic processes, present at a high incidence throughout all cortical layers and were particularly prominent in upper layers. However, cluster formation within the upper cortical layers as seen in affected control animals, was not observed.

The two normal-like chimeras, 401/05 and 405/05, and the three recovering chimeras, 401/04, 402/05 and 404/05, displayed immunoreactivity along the SVZ at a higher intensity than normal controls but less than affected control animals (Figure 18 B-D). Staining was punctate, with many individual small cell bodies evident and less fibrous staining present than in affected animals. Larger cells with multiple processes also stained and had a higher incidence in more rostral regions. All seven chimeric animals had migrating PSA-NCAM positive cells

and fibres with radial orientations present within white matter tracts and intense staining within cortical grey matter regions (Figure 19(i)B-D, (ii)B-D). Immunoreactivity within the cortex was different to that within affected control animals, with numerous cell bodies and occasional apical dendrites stained throughout, possibly indicating their early stage of maturation. Cluster formation was not present in any cortical regions in the chimeric animals but intensely stained cells possessing multiple dendritic processes were present. These cells were numerous at the grey-white matter border and were more abundant in the normal-like animals 405/05 and 401/05, which also appeared to have more of these cells within cortical layers II-VI compared with the recovering animals 401/04, 402/05 and 404/05.

Figure 18 PSA-NCAM immunoreactivity in the SVZ of normal, affected and chimeric sheep

Immunohistochemical staining for PSA-NCAM revealed marked differences in staining between affected (**F**) and normal (**A**) control sheep. The SVZ of affected animals shows increased expression of PSA-NCAM even at late stages of disease and markedly more PSA-NCAM positive cells and fibres can be seen extending away from the SVZ in diseased animals. Comparable PSA-NCAM staining is present in the affected-like chimera 403/04 (**E**) in which a prominent band of immunoreactive cells and fibres are evident along the SVZ and radiating away from this region. The two normal-like animals, 405/05 and 401/05 (**B**, **C)**, and the recovering animal 404/05 (**D**) all display increased expression of PSA-NCAM compared to normal controls but this is not as intense as that in affected animals. Immunoreactive cells and fibres are evident extending away from the SVZ and higher powered images (x 400) reveal the presence of highly branched migratory cells.

Note: Images of the affected-like chimera 403/04 and the recovering chimera 404/05 are representative of the other affected-like chimera 58/02, and recovering chimeras 401/04 and 402/05, respectively.

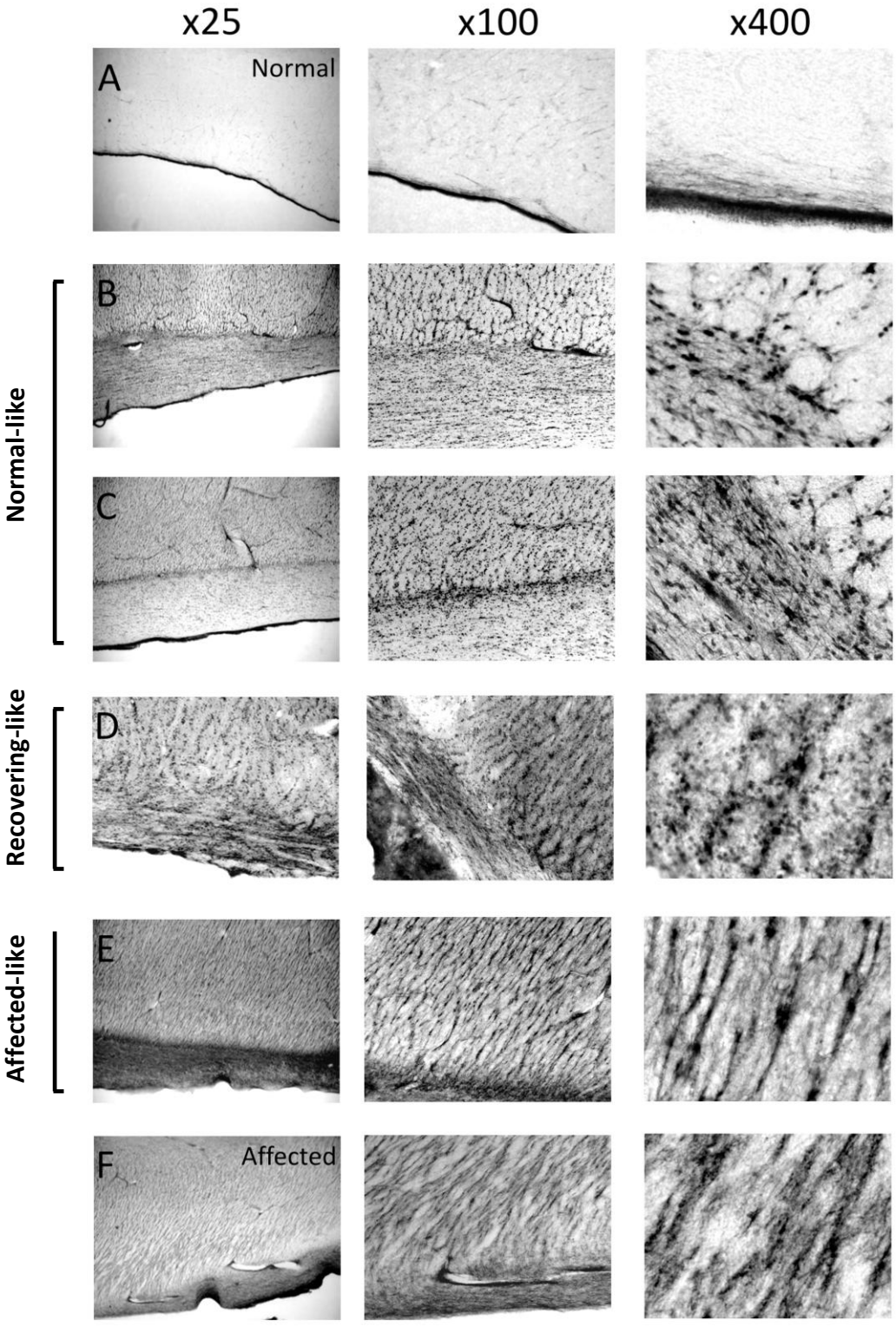
x25
x100
x400
A
Normal
B
C
D
E
F
Affected
Normal-like
Recovering-like
Affected-like

Figure 19 PSA-NCAM staining of cortical grey matter and white matter tracts of normal, affected and chimeric sheep

(**i**)**:** PSA-NCAM staining revealed dense clusters of cellular aggregates within layer II of affected animals (**F**). Aggregates were not present in the normal control cortex and only very rarely were immunostained cells evident (**A**). Conversely, intense PSA-NCAM reactivity was present in the cortex of the affected-like animal 403/04 (**E**). Intensely stained highly branched cells were present throughout the grey matter but more cells were stained in upper cortical layers than in lower layers. The extent of cellular aggregation was not the same as in affected brains. The normal-like animals, 405/05 and 401/05 (**B**, **C)**, and the recovering-animal 404/05 (**D**) also displayed intense immunoreactivity, with prominent staining present throughout all cortical layers. Cells here were larger, with fewer processes, possibly indicating their early stage of maturation.

(**ii**): PSA-NCAM immunoreactivity within the white matter of affected brain revealed PSA-NCAM positive fibres and cells with a highly branched, fusiform morphology (**F**). A similar intensity of staining was revealed within the white matter tracts of the affected-like animal 403/04 (**E**). Immunoreactivity was also detected in the normal-like animals 405/05 and 401/05 (**B**, **C**), and the recovering animal 404/05 (**D**). Many distinct small cell bodies were immunoreactive along with numerous, larger branched cells. These cells were especially prominent near the grey-white matter border, particularly in the normal-like animals 405/05 and 401/05 (**B, C**). In contrast, immunoreactivity was minimal in normal, control white matter tracts (**A**).

Note: Images of the affected-like chimera 403/04 and the recovering chimera 404/05 are representative of the other affected-like chimera 58/02, and recovering chimeras 401/04 and 402/05, respectively.

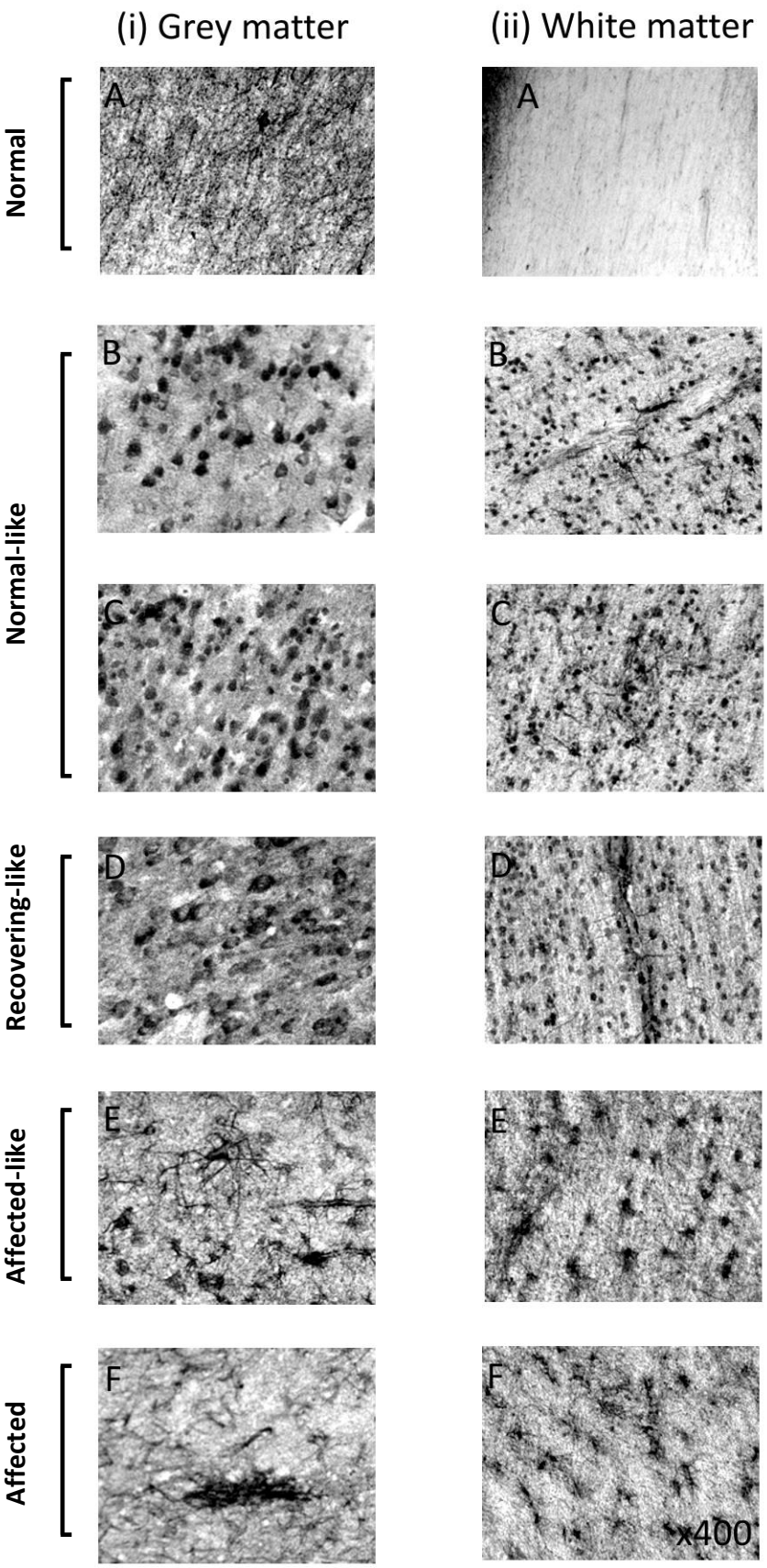
(i) Grey matter
(ii) White matter
Normal
Normal-like
Recovering-like
Affected-like
Affected
A
B
C
D
E
F
x400

Table 8 Phenotypic, genotypic and histological appearance of chimeric animals

	Animal ID	Age at sacrifice (months)	Phenotype		Genotype (% CLN6)			Storage body accumulation	Glial activation[c]	Neurogenesis[c]	Last CT as % normal brain vol.
			Predominant coat pattern	Vision	Blood	Brain[a]	Non-CNS tissue[b]				
Affected-like	58/02	25.5	South Hampshire	Blind	100	100	12.5 - 100	Typical storage	Yes	Yes	73
Affected-like	403/04	19.5	South Hampshire	Blind	100	100	100	Typical storage	Yes	Yes	80
Recovering-like	401/04	41	Coopworth	Normal	3	3 - 25	0 - 50	No storage	Yes	Yes	78
Recovering-like	402/05	26	Coopworth	Normal	0	3-6	0 - 3	No storage	No	Yes	87
Recovering-like	404/05	26	Coopworth	Normal	13	6 - 75	6 - 50	No storage	No	Yes	100
Normal-like	405/05	26	Coopworth	Normal	50	3 - 25	6 - 75	No storage	No	Yes	107
Normal-like	401/05	26	Coopworth	Normal	0	12.5 - 50	12.5 - 87.5	Some atypical storage	No	Yes	103

[a] % CLN6 affected DNA as determined by restriction enzyme analysis of DNA extracted from five regions of the brain; frontal and occipital lobe, thalamus, cerebellum and brainstem samples.

[b] % CLN6 affected DNA as determined by restriction enzyme analysis of DNA extracted from kidney, liver, pancreas, thyroid, skin, skeletal muscle and cardiac muscle.

[c] Glial activation (GFAP, GSB4) and neurogenesis (PSA-NCAM) at higher intensities than observed in normal control animals as determined by immunohistochemical examination.

4.4 Discussion

Sheep chimeras generated by mixing blastomeres from normal and disease affected homozygous embryos, resulted in lambs with tissues being a composite of normal and affected cells, the ratio of which varied between individuals and tissues. Because disease affected and normal cells share the same local environment in the same chimeric individual, animal-to-animal variation and indirect and systemic effects of the gene mutation are minimized. The development of chimeric sheep were compared to normal and affected control animals by CAT scanning to estimate brain volume, growth rates and loss of vision. Pathologically chimeras were compared to normal and affected animals, the latter displaying severe cortical neurodegeneration, accumulation of storage bodies, significant glial activation and extended neurogenesis.

Fundamental questions of interest are whether cells expressing mutant CLN6 damage neighbouring normal cells and whether normal cells can protect cells expressing NCL-causing *CLN6* mutations. Furthermore if normal cells can influence affected cells what effect does this have on disease progression and severity, and what does this mean for the future treatment of CLN6 NCL?

4.4.1 Development and heterogeneity of chimeric animals

The seven animals analysed exhibited a considerable variation in the proportion of normal: affected cells present in tissues, highlighting the extent of heterogeneity of animals constructed by embryo aggregation. This heterogeneity is consistent with the evidence that the relative colonization of bodily tissues by genotypically different cell lineages comprising a chimeric animal can differ from tissue to tissue and animal to animal (Le Dourain and McLaren, 1984; Goldowitz et al., 1992; Kuan et al., 1997). If normal and affected cell mixing has occurred prior to formation of the ICM both cell types can contribute to the ICM and its subsequent differentiation into the ectodermal, mesodermal and endodermal layers, which give rise to all the tissues of the body. Hence, the variation of cell proportions throughout the whole body is dependent on the extent of mixing and proportion of each cell genotype in the ICM (Falconer and Avery, 1978). For the affected-like animals 403/04 and 58/02, it is evident that cells with an affected genotype contributed almost exclusively to formation of the ICM, with the majority of tissues subsequently having an affected genotype.

Where mixing does occur, there have been many reports of the proportion of the two genotypes deviating from 1:1 proportions (Mystkowska et al., 1979; Mintz and Palm, 1969; Mullen and Whitten, 1971). The two normal-like chimeras 401/05 and 405/05, and the three

recovering chimeras 401/04, 402/05 and 404/05, had both normal and affected cells present in most tissues analysed and the proportions of each cell type varied considerably between tissues and were rarely in a 1:1 proportion. This is postulated to arise because of different rates of proliferation of the cells of the two genotypes (Krzanowska, 1967). If one of the cell types has a faster rate of proliferation, the resultant individual will be composed of relatively more cells from the faster proliferating line than were initially present in the ICM. This differential proliferation along with the sampling of progenitor cells can also cause subsequent variation leading to organs arising from the same germ layer having different proportions of the two genotypes, as seen with the chimeras in this study (Table 7). A study by Reiner et al., (2001) demonstrated regional variations in chimeric mouse models in the abundance of Huntington-deficient neurons across all regions of the brain. Similarly, regional variations within brain tissue were observed in most of the chimeras used in this study (Table 7). Conversely, the proportion of affected and normal DNA in blood samples collected every six months remained constant over the life-span of all chimeric animals, indicating that normal haematopoietic stem cells did not replace affected cells over this period.

The extent of cell mixing and subsequent developmental path followed by each animal is different and animals with a similar phenotype, genotype and brain pathology may not necessarily have reached this outcome via the same route. However, common features and histological presentations between different animals allow us to infer the possible roles and implications which each cell type has and how this affects disease progression.

4.4.2 Disease presentation in CLN6 affected animals

One of the most intriguing findings was an increase in neurogenesis in affected animals compared to normal controls. PSA-NCAM is upregulated in newly generated and migratory cells (Ono et al., 1994) and staining indicated markedly increased numbers of newly generated cells in affected animals compared to age-matched normal controls. Staining along the SVZ, one of the two constitutive neurogenic regions in the adult CNS, was evident in affected and normal controls but a much more prominent band of immunoreactive cells and fibres was apparent in affected animals compared to normal controls (Figure 18). Immunostained cells and fibres could be seen extending away from the SVZ and migrating along white matter tracts towards neurodegenerative cortical regions. Intensely stained clusters of cells were present within the degenerating cortex of affected animals but were absent in normal controls (Figure 19).

The identification of cellular clusters in the cortex of affected animals is not confined to this study. Dihanich et al., (2009, article in preparation) showed that these clusters contain immature and mature neuronal cells but not glial cells, hypothesised to indicate a futile attempt at neuronal replacement within the diseased brain. Affected animals were shown to exhibit more prominent neurogenesis along the SVZ with disease progression, suggesting a correlation between the degree of degeneration in the CNS and increased neurogenesis. In contrast normal control animals displayed an age dependent decline in neurogenesis.

There was no correlation between storage body accumulation and neurodegeneration. Neurons in some areas, such as Purkinje cells of the cerebellum, accumulated dense packings of storage bodies but did not degenerate (Figure 16). This indicates that neurodegeneration and storage body accumulation are separate manifestations of the genetic lesion, as has been suggested previously (Jolly et al., 1989; Palmer et al., 2002; Oswald et al., 2005). In addition, the lack of a temporal or regional correlation between storage body accumulation and glial activation argues against the idea that activation occurs in direct response to storage body presence (Kay et al., 2006). The progressive involvement of glial activation in the brain precedes neurodegeneration, implicating a central role for inflammation in disease pathology (Oswald et al., 2005; Kay et al., 2006). Hence, the extent of neurodegeneration, glial activation and neurogenesis appear to be intimately linked and changes in one or more of these parameters could produce subsequent effects on the others.

Although most studies report that the frequency of adult neurogenesis decreases with age (Heine et al., 2004b; Bondolfi et al., 2004), the occurrence of neurogenesis in neurodegenerative disorders is not uncommon. Similarly, whilst inflammation is proposed to contribute to the pathology of both chronic neurodegenerative diseases as well as acute pathologies such as stroke, brain trauma, and meningitis (Eikelenboom et al., 2006; Whitton, 2007; Zipp and Aktas, 2006; Lucas et al., 2006; Block et al., 2007; Wyss-Coray, 2006) there are contradictory reports regarding the impact of neuroinflammation on neurogenesis in the diseased brain (discussed in section 1.13). In the CLN6 ovine model glial activation begins prior to neurodegeneration (Oswald et al., 2005; Kay et al., 2006). Both affected and control animals display a perinatal wave of gliogenesis, necessary for correct brain development. This subsequently declines in normal animals by a process termed programmed cell death, which is fundamental to the regulation of neuronal and glial populations (Ferrer et al., 1992; Oppenheim, 1991). However affected animals do not appear to successfully inhibit this gliogenic phase with a progressive, dysregulated glial activation established and it is surprising how long the affected brain follows a normal developmental path. This suggests

that activation is not solely a response to neuronal insult (Oswald et al., 2005; Kay et al., 2006). Hence, these immune cells may have an early positive effect stimulating one or more processes of neurogenesis and only subsequently becomes detrimental following extended, chronic activation.

Once neurodegeneration is underway, microglia are involved in the process of recognizing and removing damaged neurons by phagocytosis, but in affected animals microglia will carry the *CLN6* mutation and their ability to degrade the endocytosed material may be inhibited. This in turn, could exacerbate the inflammatory response by continuously recruiting microglia to manage the neuronal damage. This expansion of activated microglia could trigger cell death in compromised neurons through the expression of cytokines, and both pro- and anti-inflammatory cytokines have been shown in Chapter 3 to be significantly increased in disease affected animals. Alternatively due to the continuous neurodegeneration in the affected brain, differentiation and development might never be signalled as complete so neurogenesis never gets turned "off". Neurogenesis requires the appropriate micro-environmental signals necessary for neuronal differentiation and survival; hence alterations in the local microenvironment that resemble conditions seen during development could maintain neurogenesis. Therefore changes in the local microenvironment could keep neurogenesis turned on in the diseased brain, effectively maintaining it in a developmental state.

4.4.3 Disease presentation in the chimeric brain

On the basis of the genotypic, phenotypic and histological examination of the seven chimeric animals generated, they were split into three groups, indicative of their pathological and chimera state.

Chimeric animals with an affected genotype, 58/02 and 403/04, displayed increased neurogenesis, intense glial activation, prominent storage body accumulation and severe neurodegeneration within all cortical brain regions, similar to disease affected animals. Consistent with these findings was a progressive decrease in brain volume and cortical thickness, and loss of vision. Although non-CNS tissues did display some extent of chimerism, cumulatively these results indicate a dominance of affected cells in the brain, resulting in a near typical CLN6 disease presentation. Nissl staining revealed widespread neuronal loss and a change from a laminar distribution of cells towards densely packed cellular aggregates (Figure 13). Furthermore, neurogenesis was upregulated even at advanced stages, a phenomenon which is also seen in affected animals. Intense PSA-NCAM staining along the SVZ and within cells and fibres migrating away from the SVZ along white matter

tracts, and immunoreactivity within cells and fibres of upper cortical layers, indicate enhanced neurogenesis within the SVZ and subsequent migration of newly formed cells to cortical brain regions undergoing severe neurodegeneration (Figure 18, Figure 19).

PSA-NCAM immunoreactive cells were not confined to cellular clusters as seen in affected controls, but rather were evident throughout all cortical layers. Reasons for this differential distribution of immunoreactive cells within the cortical grey matter are unknown. GFAP staining also revealed a less advanced astrocytic response in these animals than in affected controls (Figure 17) but GSB4 histochemistry displayed a comparable pattern and distribution of staining to affected animals with widespread staining of brain macrophages, representing the end-stage activation of microglia (Streit, 1990; Streit and Graeber, 1993). It is possible that some brain regions which were not sampled in this study had populations of normal cells present which influenced the inflammatory and neurogenic responses in these animals, resulting in a differential presentation to affected controls. However collectively these animals display findings similar to those from affected controls, indicative of few if any normal cells in the attempted chimeric construction.

Conversely, the two normal-like animals, 401/05 and 405/05, had a genotype indicative of a more balanced presence of normal and affected cells within tissues, suggestive of a chimeric state. There was a distinct lack of glial activation even at advanced ages, in contrast to affected animals in which activation is profound even before this stage. Similarly, storage body accumulation was only evident in some cells in one animal, 401/05, and the extent of storage in these cells was minor compared to storage in cells in affected control animals. This suggests cross-cell correction with the population of normal cells influencing affected cells and resulting in a significant reduction in storage material accumulation in those cells. This phenomenon is also likely in the other normal and recovering-like chimeras, albeit at a more advanced rate so that there was no observable accumulation of storage bodies by the time of sacrifice. Brain volume and cortical thickness findings for these two animals were all consistent with normal controls and there was no loss of vision.

Genotypic analysis of the recovering animals, 401/04, 402/05 and 404/05, indicated a larger proportion of normal cells than affected cells in most brain regions (Table 7). However, dramatic variations were evident in animal 404/05, with the brainstem exhibiting 75% affected DNA. Brain volumes of all three animals were below normal, although animals 402/05 and 404/05 had recovered to about normal volume by advanced age (Figure 12). Similarly, animal 401/04 appeared to have a progressively recovering brain volume, but did not reach the normal line. However, all three animals had normal cortical thickness

measurements (Figure 14), none went blind and there was no evidence of storage body accumulation. Glial activation was only evident in animal 401/04 and was less advanced than in affected controls, with fewer morphologically activated cells stained (Figure 17). This animal was considerably older, 41 months, than affected controls and may be subject to a slower developing disease progression or may be exhibiting age-related glial activation. Although, there was a higher proportion of normal cells within the brains of these animals it is not known which cells were of the affected genotype. Hence, it is possible that the affected cell types in these animals resulted in the lower brain volumes but did not cause a full pathological response. Unfortunately, it is in the nature of such experiments that brain samples cannot be analysed throughout the lifespan and the course of histological and genotypic change within the brain cannot be mapped.

The general diffuse GSB4 staining of capillaries observed within the cortical grey matter of chimeric animals was widespread and more frequent than in normal controls. This may be due to the prolonged immersion fixation of chimeric tissue compared to control tissue, resulting in less efficient clearing of red blood cells and subsequent detection by GSB4 labelling (Streit, 1990). Similarly, the lack of MHC-II staining in chimeras that had displayed GSB4 staining of activated microglial cells was unexpected. Previous studies have reiterated the close relationship between GSB4 and MHC-II staining of activated microglial cells in this ovine model of NCL (Oswald et al., 2005). The prolonged storage of the chimera tissue in formalin may be the cause of these unexpected histological results. The MHC-II antibody has specificity for HLA-DP molecules which are αβ-heterodimer cell-surface receptors and there have been previous reports of difficulty in immunohistochemical detection of HLA-D antigens due to prolonged exposure to formalin masking or destroying the epitope (Mattiace et al., 1990).

Extended neurogenesis was evident in the brains of the two normal-like animals, 401/05 and 405/05, and the three recovering animals, 401/04, 402/05 and 404/05 (Figure 18, Figure 19). All five animals had intense PSA-NCAM staining along the SVZ and evidence of radial migration of cells along white matter tracts with subsequent detection of newly generated cells within the cortical grey matter, which is not seen in normal control animals. Individual PSA-NCAM positive cells were present throughout all cortical layers and this widespread detection of cells within the grey matter is in contrast to affected animals in which newly generated cells are largely confined to cellular aggregates in upper cortical layers. As revealed by Nissl staining affected sheep display laminar reorganisation corresponding to the occurrence of disease symptoms (Jolly et al., 1989; Tammen et al., 2006) and it has been

suggested that the continuous degeneration of the cortex fails to provide the correct signals and microenvironment for successful migration and distribution of cells throughout the cortical layers (Dihanich et al., 2009, article in preparation). However, Nissl staining of these normal and recovering-like chimeras indicated an intact laminar distribution of cells and cortical thickness measurements implied a lack of neurodegeneration, hence newly generated cells likely to originate from normal NPCs may undergo successful migration and be correctly distributed throughout all cortical layers.

In addition, due to a lack of glial activation and inflammatory response in all but one (401/04) of the normal and recovering-like chimeras newly generated cells are being borne into a microenvironment conducive to cell maturation and survival. These hypotheses are reflected in the brain volume data. The two normal-like animals, 401/05 and 405/05, displayed some fluctuations in brain volume but remained above normal whereas the recovering animals initially had lower than normal brain volumes which subsequently increased. These changes may reflect increased neurogenesis and replacement of degenerating cells within the brain with a progressively increasing proportion of normal cells. Obviously the rate or extent of cell loss was low enough for significant replacement to be achieved and hence brain volume was maintained or progressively increased as seen in normal and recovering-like chimeras, respectively.

As all of these animals are chimeras, it is probable that some NPCs will be of an affected CLN6 genotype and some of a normal unaffected genotype. Affected degenerating cells could theoretically be replaced with functional, unaffected cells or with cells carrying the *CLN6* mutation. Therefore, replacement of affected cells by normal, unmutated cells may occur at a slower rate in some animals and in some brain regions depending on the population of NPCs from which the new cells arise. Alternatively, due to the lack of glial activation mutated cells may survive for an extended period of time or even long-term in the absence of a detrimental inflammatory environment.

The animals that had an initial low brain volume and size, 401/04, 402/05 and 404/05, had an apparent high colonisation of normal cells in the brain, as inferred by histological and genotypic analysis. The reduced brain volume may have been a consequence of early affected cell neuronal loss and subsequent progressive replacement by neuroblasts generated from normal unaffected NPCs. Animal 401/04 also displayed microglial activation, albeit at a much lower intensity than affected animals. This less intense glial activation may have caused neuronal death but at a lower and slower rate than in affected animals, hence enabling a progressive rate of cell replacement. Additionally, the reduced body size characteristics in

these three animals could stem from abnormalities in feeding and growth regulation due to colonisation of disease affected cells within neural and extraneural regions critical to these processes as hypothesised by Reiner et al., (2001), in which a similar reduction in chimera body size was noted.

As explained earlier the initial cell proportions and changes in these proportions over time are not known for all of these animals. It has previously been revealed that location and connectivity, not phenotype, seem to determine neuronal survival (Oswald et al., 2008) and it could be that there are critical cell types and brain regions required for normal development, accounting for the differential developmental pathways in these chimeras.

4.4.4 Cross-cell correction and implications for therapy

Chimeric mouse models of neurodegenerative diseases have been informative in determining whether gene defects are cell intrinsic or whether they are extrinsic and amenable to correction by unaffected cells (Mullen, 1977; Herrup and Mullen, 1979; Campbell and Peterson, 1992). Chimeras generated in this study suggest that the phenotype of CLN6 is cell extrinsic, i.e. the cell defect is amenable to external modification via a change in the cellular environment.

Intercellular communication affecting pathology at both the gross and histological level was evident in the two normal-like chimeras, 401/05 and 405/05, and the three recovering chimeric animals, 401/04, 402/05 and 404/05. These animals presented with reduced or absent glial activation and storage body accumulation, no evidence of neurodegeneration, normal cortical thickness measurements and a laminar organisation of cells, enhanced neurogenesis and no loss of vision. Genotyping of different brain regions indicated up to 75% affected cells in some brain regions. Despite this only one animal, 401/05, displayed considerable storage body accumulation and at that a significantly decreased incidence compared to affected animals at younger ages. The lack of storage bodies in the majority of cells suggest loss of affected cells, removal of storage material or a halt in the process leading to storage formation.

Extended neurogenesis had a positive effect in these animals, resulting in normal or recovering brain volumes. This suggests that given the correct environmental milieu disease affected and newly generated cells can survive and are amenable to correction by normal cells, resulting in an amelioration of disease pathology. Conversely, in the affected-like chimeras, 58/02 and 403/04, and in affected control animals, extended neurogenesis is not effective, the newly generated affected cells being born into an inflammatory environment

detrimental to cell survival, and resulting in progressive neurodegeneration and decreasing brain volumes.

This study indicates that targeting neurogenic regions in the brain can but does not always work, depending on whether the right stem cells are corrected and the environmental milieu into which newly generated cells are born. Importantly, these studies show that not all cells need to be corrected for disease amelioration to be achieved. Better targeting of NSCs in the SVZ and correction via methods like gene therapy will be required, possibly in combination with anti-inflammatory therapy, but offers an exciting therapeutic potential.

Chapter 5
Gene Transfer to the CLN6 Affected Sheep Brain

5.1 Introduction

Gene therapy relies on the ability of viruses to infect host cells, delivering unmutated copies of a gene to the cells, and hijacking the host cell machinery to produce viral proteins. Lentiviruses are a subgroup of the retroviruses, which along with AAVs have formed the basis for most gene delivery systems. Lentiviruses are widely used as vectors due to their ability to stably integrate the viral genome into the genome of both post-mitotic and mitotic cells. The vector, once integrated is known as a provirus, remains in the genome and is passed onto the progeny of the cell when it divides. These attributes make them very attractive candidates for stable, long-term gene delivery to neurons and stem cells, with the resultant newly generated cells also carrying the viral genome (Kootstra and Verma, 2003; Wiznerowicz and Trono, 2005). Some of these viruses have been engineered to remove all pathogenicity and ability to replicate, and constructs can therefore be used to deliver corrective copies of a gene safely. Intracerebal gene therapy presents a promising approach for treatment of the CNS component of LSDs and particularly NCL. Not only does it use host cells for protein production, ensuring appropriate post-translational modifications and regulation but has many advantages over other therapies such as ERT and pharmacological agents. It provides long-term production of protein on the parenchymal side of the BBB, providing much longer therapeutic value and eliminates the need for repeated enzyme treatments (Liu et al., 2005b; Chung et al., 2007; Sondhi et al., 2008).

A collaborative study was undertaken with a research group based at Otago University to develop a system for gene transfer in the sheep brain and monitor the efficacy and safety of the lentiviral-mediated gene therapy (Linterman et al., 2011). The majority of gene therpay trials in Batten disease have been carried out in rodent models, which possess a much simpler and smaller brain and exhibit a differing neuropathology to the human disease. Although effects on the progression of pathology have been noted in rodents (refer to section 1.9.4) the increased size of the human brain presents many untested and potentially significant hurdles. Trials have been undertaken in human patients (section 1.9.4), however by the time a correct diagnosis had been made and therapy begun, the disease was too advanced for any reasonable assessment of efficacy and ultimately only the short-term safety of the protocols was tested.

This emphasises the need for a robust animal model for translating advances in viral-mediated gene therapy to the clinic. The problems of scaling up from a small lissencephalic rodent brain to a large one complete with gyri and sulci, include ensuring that transduction and expression is stable and does not adversely affect the brain, and that the target cells are accessible. Multiple injection paradigms to ensure sufficient spread of the virus in large brains present additional complications and thus require the development of much more sophisticated injection and surgical techniques. Large species such as sheep provide an ideal intermediary model in which to assess the tropism and distribution of gene therapy vectors in a similar sized brain to human patients, assessing the many drawbacks and hurdles of large brains for such therapies (Haskins, 2009; Gagliardi and Bunnell, 2009). Additionally, the US Federal Drug Agency now requires large animal model trials before any therapies can progress to human studies, hence sheep may become useful as animal models of other neurodegenerative diseases which may be amenable to gene therapy. Only one previous study has tested viral gene transfer in sheep, targeting RNA interference (RNAi) to the hypothalamus using AAV vectors (Dufourny et al., 2008).

As mentioned previously (section 2.1) NCLs resulting in the loss of soluble enzymes are particularly applicable to the gene therapy approach. As has been demonstrated *in vitro*, transducing a small percentage of cells that subsequently produce and secrete the deficient soluble enzyme and enable cross-cell correction, obviates the need to transfer genes to all affected cells (Haskell et al., 2003; Sondhi et al., 2005). Although the CLN6 protein is an intramembrane protein the analysis of chimeric animals in Chapter 4 suggests that the problem is not as daunting as it seems with evidence for intercellular communication and cross-correction of affected cells by normal cells in the ovine brain. Hence if CLN6 NCL is not a cell intrinsic disease and factors that promote cell survival can be released from corrected cells, gene therapy is a plausible therapeutic option. In addition, the substantial evidence for extended neurogenesis in the SVZ of affected sheep (discussed in section 4.4.2) and humans (Dihanich et al., 2009, article in preparation), represents a potentially exciting and realistic area to target in the CLN6 form of Batten disease. Targeting NSCs within the SVZ with lentiviruses that can integrate into the host cell genome, could give rise to functionally corrected neuroblasts that subsequently migrate to degenerating cortical regions, and facilitate a wide spread of transduced cells within the diseased brain.

5.2 Materials and methods

Sections 5.2.1 to 5.2.3 were carried out by other members within the Batten disease research group based at Lincoln University, and collaborators based at Otago University, Dunedin. This work laid the foundations for the immunohistochemical examination of gene transfer to the sheep brain.

5.2.1 Viral constructs and *in vitro* analysis

Initial studies carried out *in vitro* by Dr. Stephanie Hughes and Kate Linterman (Otago University, Dunedin, New Zealand) demonstrated the ability for a lentivirus containing GFP to transduce sheep neural cells in culture (Linterman et al., 2011). HIV-1 derived lentiviral plasmids encoding GFP under the control of either a viral promoter, myeloid sarcoma virus (MND) or the constitutive human promoter, human elongation factor 1 α (EF1α) were pseudotyped with the vesicular stomatitis virus glycoprotein (VSV-G). The transduction, cell tropism and transgene expression from these two lentiviral constructs were tested in neuronal cultures (confirmed to contain 20% neurons, 24% neuroblasts and 17.5% astrocytes) from both affected and control sheep foetuses (n=3) harvested after 60 days of gestation. GFP expression was observed in all three major cell types in culture; neurons, astrocytes and neuroblasts, five days after transduction from both promoters. Both neurons and neuroblasts were transduced at a significantly higher efficiency than astrocytes and expression was found in both cell bodies and neurites (Linterman et al., 2011). No significant difference was found between the ability of each promoter to drive GFP expression. Subsequently, a lentivirus pseudotyped with VSV-G and expressing GFP under the control of the MND promoter (LV-MND-GFP) was prepared at Otago University, transported to Lincoln University and used to transduce sheep cells *in vivo*.

5.2.2 Animals

Homozygous affected lambs were generated and the genotype determined as previously described in section 3.2.1. Unrelated Coopworth sheep were used as age-matched controls. The *in vivo* viral injections were performed when lambs were 8 months of age. Two stereotactic injections were made into the brains of two affected and two control animals, rostral to the occipital ridge, just dorsal to the lateral ventricle. In addition, virus was injected directly into the CSF at the cistern amagnum of a control and affected animal. Approval for the use of recombinant lentiviral vectors was obtained from ERMA New Zealand (GMD03091) and all animal work was approved by the Lincoln University Animal Ethics Committee.

5.2.3 *In vivo* viral injections

Design and plan of the stereotactic gene injections was performed by a team of Dr. Graham Kay, Dr. Robin McFarlane and Nigel Jay based at Lincoln University. Sheep were fasted overnight and anaesthesia induced with an intravenous administration of a mixture of ketamine (7.5mg/kg live weight) and diazepam (0.3mg/kg live weight). Sheep were then intubated (9.5mm cuffed endotracheal tube) and maintained on a mixture of halothane (2-4%) and oxygen, within a closed circuit system, and placed in the prone position with the head secured for injection in a large animal stereotactic frame (KOPF 1630, TSE-Systems, Germany). The surgical sites were clipped and prepared for surgery by multiple scrubs with 4% chlorhexidine gluconate and polyvinylpyrrolidone iodine followed by draping. A medial skin incision was made and the underlying musculature and fascia retracted. Two 3mm holes were drilled through the frontal bone, 5mm either side of the midline and 47mm rostral to the occipital ridge. A stereotactic micromanipulator was used to drive a 20G needle attached to a fine tube containing a column of sterile saline stained with trypan blue to indicate the positive flow of CSF once the ventricle was reached. This was used to establish the depth to the tissue-ventricle interface. The needle was then withdrawn 5mm and a 10µl Hamilton syringe with a 26G needle was threaded down through the 20G needle so that the tip of the needle was 4mm proud of the end. A total of 10µl of viral solution containing 1.3×10^8 transducing units (LV-MND-GFP) was infused at 1µl/min, starting with 1µl, 1mm superficial to the tissue/ventricle interface. The needle was then withdrawn at 1mm/min before the next 1µl of viral solution was discharged and repeated until all 10µl were injected. The procedure was then repeated on the other side of the brain. The wound was closed with a continuous sub-cuticular suture followed by interrupted skin sutures that were subsequently removed. An analgesic (buprenorphine HCl) was administered intramuscularly (330µg/animal), along with a mixture of procaine and benzathine penicillin (12,000 IU/kg), and the animals observed until a full recovery was made.

An additional affected and control animal were injected with 100µl of viral solution, containing 1×10^9 transducing units, directly into the CSF at the cisterna magnum (Scott, 1993). Treated animals were housed in an indoor custom built Physical Containment level 2 facility and checked daily for any adverse reactions until being sacrificed for tissue collection.

Figure 20 Lentiviral injection site anterior to the occipital ridge in the ovine brain (Linterman et al., 2011)

5.2.4 Tissue collection and immunohistochemistry

Brains were collected from a control and affected pair of animals at 40 and 80 days after the intracortical injections. The animals which received direct injection into the CSF were sacrificed at 40 days post-injection. Brains were collected, formalin fixed and sectioned as described in section 3.2.2.1

All antibodies were diluted in 10% NGS in PBST. To identify the gene injection site and spread of the virus every twelfth section was stained for GFP. Sections were blocked in 15% NGS, 60 min, and incubated in rabbit polyclonal anti-GFP (1:20,000, Abcam) which had been pre-incubated with control sheep brain sections for 1 h to remove non-specific labelling, overnight at 4ºC. Immunoreactivity was detected with fluorescent Alexa Fluor 488 goat anti-rabbit IgG (1:2000, Molecular Probes, Eugene, OR; λ_{ex} max 495nm, λ_{em} max 519nm), 4 h at RT. In other cases the secondary antibody was biotinylated goat anti-rabbit IgG (1:1000, Sigma), 4 h at RT followed by ExtrAvidin peroxidase and DAB (detailed in section 3.2.2.2) applied for 7 min.

Sections adjacent to the injection site and positive for viral spread as determined from GFP staining, were double labelled with GFP and GFAP or the fluorescent Nissl dye, NeuroTrace, as markers of transduced glial cells and neurons respectively. For GFAP and GFP immunofluorescence, sections were blocked as above, then incubated in rabbit anti-cow GFAP (1:1000, Dako), overnight at 4ºC. The secondary antibody, Alexa Fluor 594 goat anti-rabbit IgG (1:1000, Molecular Probes; λ_{ex} max 590nm, λ_{em} max 617nm) was applied for 4 h at

RT. GFP was detected using rabbit anti-GFP, Alexa Fluor 488 conjugated antibody (1:500, Molecular Probes; λ_{ex} max 495nm, λ_{em} max 519nm), overnight at 4 ºC.

Parallel series of sections were stained for GFP with rabbit polyclonal anti-GFP, 1:20,000 (as above) and neurons detected using NeuroTrace fluorescent Nissl stain, diluted 1:150 in PBS (Invitrogen; λ_{ex} max 530nm, λ_{em} max 615nm) and applied for 60 min, RT.

Sections were mounted in a solution of 0.5% gelatine and 0.05% chromium potassium sulphate on glass slides, air-dried overnight and coverslipped using glycerol. Negative control sections, in which either the primary or secondary antibody was omitted, were included in all staining runs.

5.2.5 Microscopy

The detection of fluorescently labelled cells was examined on a Zeiss LSM510 confocal laser scanning microscope and Axioplan 2 Imaging system (Carl Zeiss Ltd., Jena, Germany). A 1.4 N.A objective lens was used to visualize cells labelled for GFP and identify the gene injection site and spread of the virus. Laser excitation light was provided at a wavelength of 488nm and fluorescent emission collected at wavelengths above 530nm. Laser settings, amplification gain and offset, and detector gain were optimised and then held constant for capturing all images. Multitract images were acquired to identify double labelled cells. Serial optical sections were taken every 1.5µm along the z-axis and subsequently integrated in order to obtain a 3-D stack and orthogonal projection. Confocal images were converted to.tif files in Corel Photopaint 12.

5.3 Results

5.3.1 Sheep

The six sheep displayed no adverse reaction to the injections, recovery from the anaesthesia was uneventful and all animals resumed normal eating within 24 h. Rectal temperatures remained normal for the three week observation period after injection. Growth rates, appearance and health remained the same as uninjected controls.

5.3.2 GFP immunoreactivity in viral injected sheep brain

Out of the four animals which received LV-MND-GFP injections to each cerebral hemisphere, three revealed transduced cells expressing GFP along the extent of the needle track within the brain parenchyma (Figure 21 A, B). These were comprised of one control and

affected animal, analysed at 80 days post injection, and one affected animal examined at 40 days post injection. The fourth animal did not display any transduced cells. Intense fluorescence and high cell density displayed at the injection site suggested potent lentivirus infection, which declined further away from the centre of injection. GFP positive cells were detected in the brain parenchyma up to 2.5mm rostral-caudal and lateral to the injection site as revealed by DAB staining. GFP and GFAP or NeuroTrace staining revealed that both astrocytes and neurons were transduced. Intense, homogenous GFP expression was evident within stellate cell bodies, characteristic of mature astrocytes (Figure 22 A, B). GFP expression was not confined to the cell soma, with dense ramifications of astrocytic processes also expressing GFP, albeit at a lower intensity than in the cell soma. A heterogeneous population of neurons were transduced, with numerous multi- and bipolar neurons displaying GFP immunoreactivity. Neurons with spheroid cell somas stained intensely for GFP, with bipolar neurons exhibiting expression of the GFP protein throughout the axon hillock and up to 150µm along axonal and dendritic extensions (Figure 22 C). Multipolar neurons with polygonal cell somas showed successful migration of protein throughout the entire network of axons and dendrites, some with complex, branched processes orientated in multiple directions (Figure 22 D, E). There was no evidence for differences in the efficiency of anterograde or retrograde transport of the protein through axons or dendrites, all processes displaying a similar intensity of GFP expression. These transduced cell types were evident along the extent of the injection site and there were no apparent differences in the proportion of either cell type transduced.

Transduced cells were also revealed up to 3mm lateral to and along the entire rostral-caudal extent of the ependyma lining the lateral ventricle in the subventricular region (Figure 21 C-F). This was particularly evident in one affected animal 80 days post-surgery. This animal also appeared to have a much smaller and less intensely stained region of transduced cells corresponding to the injection site within the brain parenchyma. It is not clear how much of the injection volume was retained in the cerebrum. The injection protocol was designed to inject the vector into the SVZ and it was anticipated that the hole from the needle would close sufficiently to block leakage into the ventricle. However the widespread gene transfer along the rostral, caudal and lateral extent of the ependyma of the lateral ventricle and evidence of less staining within the brain parenchyma indicates that there may have been considerable leakage of vector into the ventricle that transduced these cells. GFP was strongly expressed within the cell soma of cuboidal ependymal cells arranged in a single layer lining the lateral ventricle (Figure 21 D, E). Transgene expression was also observed in subependymal cell bodies in the region of 30µm from the ventricular surface (Figure 21 C-F, arrowheads). This

region contained transduced cells with large cell somas and multiple GFP expressing processes extending vertically above the soma, or radiating laterally from them, and which extended at least another 50μm into the SVZ region. These cell features are typical of type B astrocytes (Figure 21 C-F, arrowheads). Other positive cells were characteristic of immature neuroblasts, displaying a smaller fusiform morphology and shorter processes without any specific orientation (Figure 21 D, arrows). GFP was also expressed in cells with a characteristic, unipolar morphology consistent with migrating neuroblasts. These cells were located deeper within the subependymal region, at a distance of up to 200μm from the ventricular surface. They were not evident along the entire extent of the SVZ, the few revealed by immunohistochemistry being present at more rostral regions (Figure 21 C, arrow).

There was no discernable difference in the number of transduced cells, staining intensity or in cell types transduced in control and affected animals, and no differences were noted between animals analysed at 40 and 80 days post injection. There were no signs of inflammation or other pathology around the injection sites and the GFP expressing cells retained healthy morphologies typical of their type.

Conversely, no transduced cells were observed in the two animals injected directly into the CSF at the cisterna magnum, analysed at 40 days post injection, despite a thorough examination of sagittal sections across the mediolateral extent of each brain hemisphere. No positive immunostaining was observed in any of the negative control sections.

Figure 21 Lentiviral-mediated gene transfer to the sheep brain

A, B: Images of GFP positive transduced cells within the brain parenchyma of an affected animal at 40 days (**B**) and a control sheep brain at 80 days (**A**) post injection. Intense fluorescence and a high density of transduced cells are evident along the extent of the needle track, suggestive of potent lentiviral infection. The enlarged image reveals entire cell somas and processes transduced and expressing GFP protein 80 days post injection. Transduction was largely restricted to the immediate region surrounding the injection site but GFP positive cells were detected up to 2.5mm rostral-caudal and lateral to the injection site.
Scale bar = 200µm, enlarged image = 20µm.

C, D: DAB staining revealed transduced cells along the entire rostral-caudal extent of the ependyma lining the lateral ventricle (LV) in the subventricular region. Transduced cuboidal ependymal cells were evident at the ventricular surface. Transduced subependymal cell bodies were observed up to 30µm from the ventricular surface (arrowheads and 2). These cells possessed multiple processes extending vertically above the soma, as seen in the enlarged image, extending at least 50µm into the SVZ region and may represent type-B astrocytes (NSCs of the SVZ).

Other transduced cells were located deeper within the subependymal region, up to 200µm from the ventricular surface. Immature neuroblasts displayed a smaller, fusiform morphology and shorter processes without any specific orientation (**D**, arrow), and a characteristic unipolar cell morphology consistent with migrating neuroblasts (**C,** arrow and 1) was observed. These cells imply successful transduction of stem cells along the SVZ and subsequent retention of the GFP gene in resulting neuroblasts.
Scale bar = 100µm, 1 and 2 = 20µm.

E, F: Higher power confocal images of immunofluorescently labelled transduced cells along the ependymal and SVZ region. GFP expressing ependymal cells (**E,** arrows) which lack processes are present at the ventricular surface, whilst multi-processed cells (**E**, **F**, arrowheads) are located at a distance of 30µm from the surface. Both the cell soma and processes were transduced, with homogenous GFP expression evident up to 50µm along dendritic processes.
Scale bar = 50µm.

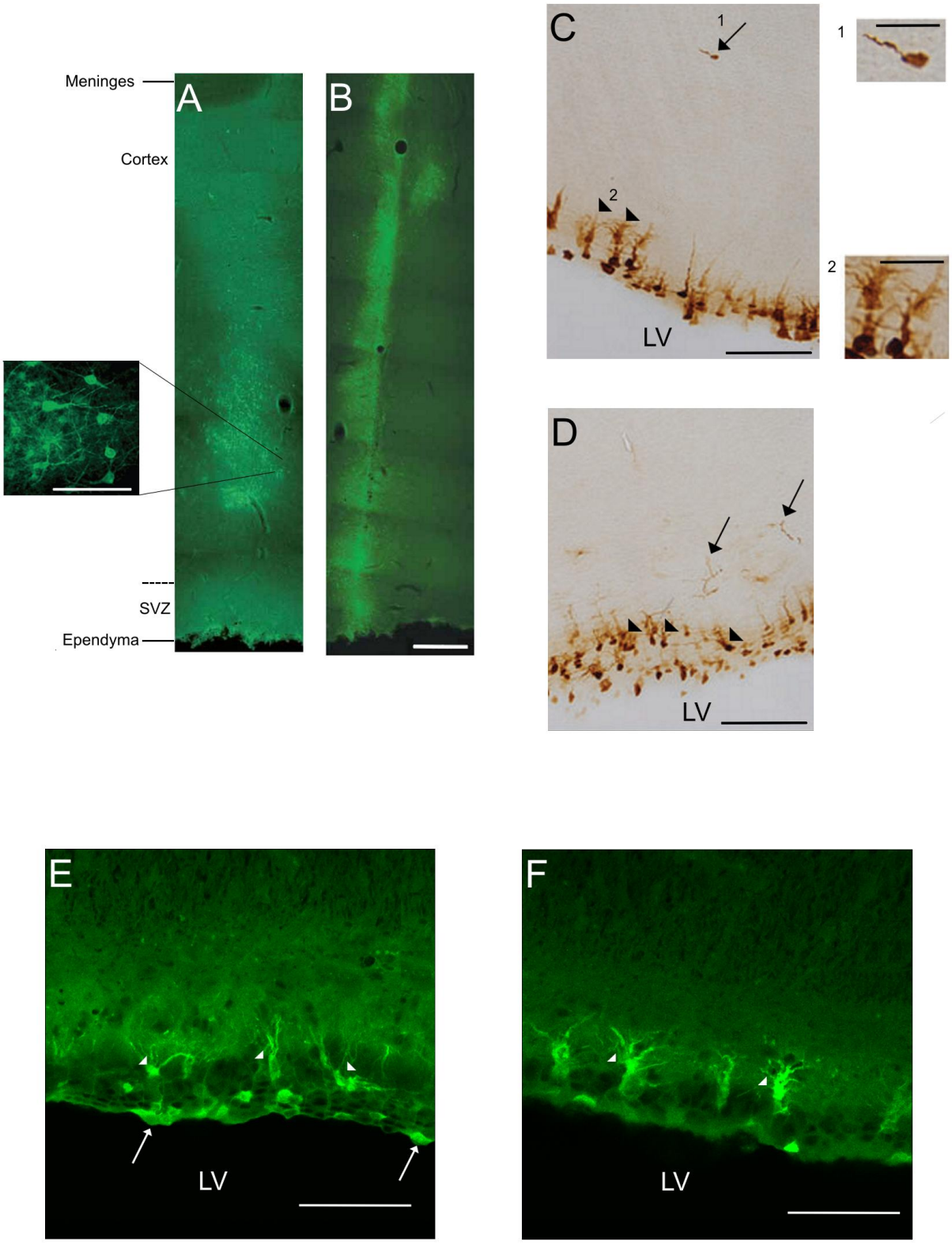
Meninges
A
B
Cortex
SVZ
Ependyma
C
1
2
LV
1
2
D
LV
E
LV
F
LV

Figure 22 Transduced cells in affected and control sheep brain

A,B: Confocal analysis of GFP (green) and GFAP (red) expression in control (**A**) and affected (**B**) sheep brain injected with LV-MND-GFP. Double-labelled cells and processes (yellow) could be found in both genotypes up to 2.5mm rostral-caudal and lateral to the injection site. Staining was intense throughout multiple processes and the entire stellate cell soma, characteristic of astrocytes.

C, D, E: Fluorescent immunolabelling of GFP (green) and NeuroTrace (red) in control (**C**) and affected (**D**, **E**) sheep brain. Colocalization (yellow) revealed transduced multipolar neurons expressing GFP throughout polygonal cell somas and up to 150µm along multiple dendritic and axonal processes. Scale bar = 50µm.

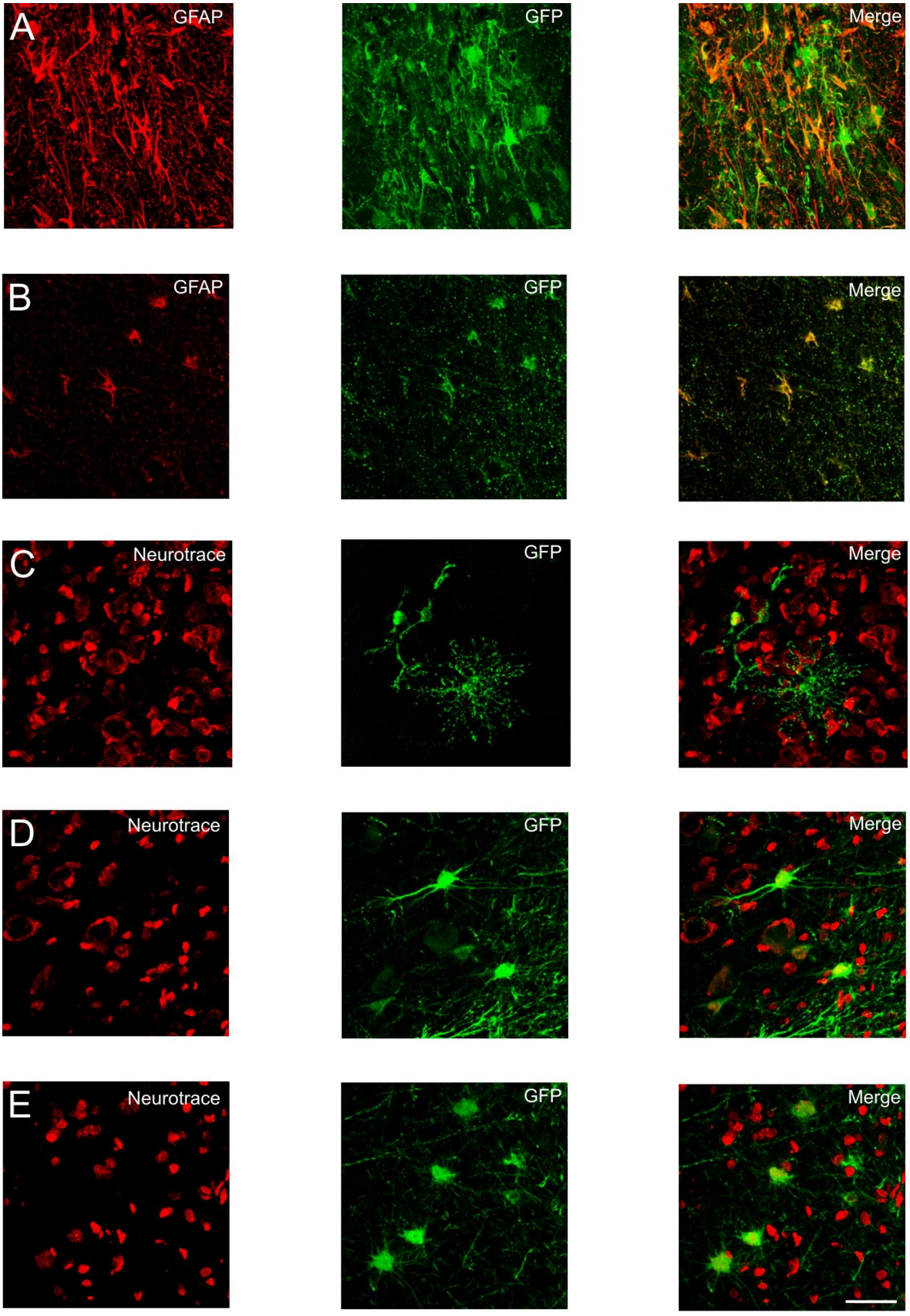
A
GFAP
GFP
Merge
B
GFAP
GFP
Merge
C
Neurotrace
GFP
Merge
D
Neurotrace
GFP
Merge
E
Neurotrace
GFP
Merge

5.4 Discussion

This study aimed to test lentiviral-mediated gene transfer *in vivo*, by direct stereotactic injection into the cerebrum or CSF of 8 month old control and affected sheep. Transductions in the sheep brain were stable, with GFP expressing cells evident up to 80 days post injection. Hence, the GFP gene was not silenced at the transcriptional or post transcriptional level as a result of histone modifications, DNA methylation or RNAi. Additionally, the GFP gene was expressed within stem cell like cells and neuroblasts within the SVZ, indicative of successful expression and stable integration of the gene during proliferation (Figure 21). The cell types transduced *in vivo* correlated with the previous *in vitro* studies (Linterman et al., 2011). Neither the vector nor the expressed GFP appeared to cause any pathology to transduced or neighbouring cells. Expression from the intracortical injections was most intense along the line of the injection site but some cells were specifically labelled up to 2.5mm from this site indicating either migration of transduced cells, or spread of the viral particles from the site of injection. Moreover transgene expression was conspicuous at considerable distances along the axons/dendrites, a factor which would be important for the transfer of soluble transgene metabolites to distal regions of the brain.

Transgene expression in ependymal and subependymal cell bodies along the entire extent of the ventricular surface indicates leakage of the virus into the ventricular space and subsequent absorption from the ventricular surface. It has been suggested by Johansson et al., (1999) that subsets of ependymal cells function as multipotent NSCs in adult mice. Most studies, however, suggest that type B astrocytes in the SVZ are the *bona fide* adult NSCs (Doetsch et al., 1999a; Laywell et al., 2000; Chiasson et al., 1999). Although type B astrocytic cells have their cell bodies located at the apical edge of the SVZ, a subpopulation of them have been reported to occasionally send a process through the ependymal layer to contact the ventricle, which might indicate an activated stem cell (Conover et al., 2000, Doetsch et al., 1999b) and provide a scenario by which vectors present in the lateral ventricle would have physical access to NSCs. The identity of these stem cells has been the subject of intense research and it is now well accepted that some of the GFAP expressing cells are stem cells in rodent and human SVZ. Cells with apparent neuroblast morphology were evident at a distance of up to 200µm from the ventricular surface and imply successful transduction of stem cells along the SVZ and subsequent retention of the GFP gene in resulting neuroblasts (Figure 21 C). Few transduced migrating neuroblasts were evident, perhaps because of the usually quiescent state in which stem cells exist and the infrequency of division, only every few weeks. Alternatively only a few stem cells may have been transduced and vectors that more

specifically target this region and cell type might improve this outcome. One animal which received injections to each cerebral hemisphere did not display any transduced cells, despite a thorough examination of brain sections. As discussed above, the injection protocol did not work as planned in all animals, with incidental leakage of the vector into the lateral ventricle evident. In this animal the vector may have leaked back into the larger needle during the injection protocol resulting in an absence of vector in the brain parenchyma.

Lentiviral vectors can be powerful agents for gene transfer to the brain and they show high transduction efficiency and long-term expression in the CNS (Naldini and Verma, 2000). Therapeutic benefit of lentiviral vectors has previously been demonstrated in animal models of severe CNS disorders, including PD and HD (Kordower et al., 2000; Trono, 2000; Regulier et al., 2002). Lentiviral vectors pseudotyped with VSV-G have been extensively studied in rodents and tropism appears to generally favour neurons rather than glial cells (Jakobsson et al., 2003; Desmaris et al., 2001; Watson et al., 2002), and the *in vitro* sheep neural cultures confirmed this tropism (Linterman et al, 2011). Yet, HIV-1 particles are quite large, approximately 80-100nm in diameter (database on the International Committee on Taxonomy of Viruses, www.ncbi.nlm.nih.gov/ICTVdb) and VSV-G pseudotyped and wild-type HIV-1 particles seem to be the same size (Desmaris et al., 2001), therefore size could strongly limit their free diffusion in the brain. Viruses may achieve only limited spread due to substantial hindrance in the extracellular space (Osten et al., 2006), hence delivery of the lentiviral vectors is not practical for the transduction of large populations of neurons.

Conversely, stereotactic injections which provide a high spatiotemporal control over the injection process can be used to target smaller neuronal populations with distinct functions, such as NSCs within the SVZ, and accordingly surmount the obstacle of limited spread of the virus. It is evident that sheep and human brains are too large and complex to attempt repair of a whole brain, therefore careful targeting of selected cell types and regions is required for therapy to be successful, emphasising the need to specifically direct the injection locale to the SVZ. The extended neurogenesis from NSCs within this region would allow a wider spread of transduced cells within the diseased brain, than would be possible if other regions were targeted. Targeting of this region in soluble lysosomal enzyme defects has been successful, with Liu et al., (2005b) showing that transduced ependyma can express high levels of recombinant protein and serve as a source of enzyme secreted into surrounding CSF and brain parenchyma. The targeting of VSV-G pseudotyped virus to ependymal cells has been previously reported in rodents (Watson et al., 2005). Lentiviral vectors pseudotyped with VSV-G injected into the ventricle of neonatal mouse brains successfully targeted transduction

of the ependymal cells lining the ventricular system and choroid plexus, along the entire rostral-caudal axis of the brain and ventricle. Thus, it is attractive as a method for improving spread of virally transduced cells throughout the brain.

The VSV-G coat binds directly to membrane phospholipids (Burns et al., 1993) therefore viral particles can be endocytosed not only into the cell somata but also into dendrites and axons within the injection area. Whilst it is reported that dendritic uptake of virus and subsequent transport to the soma is inefficient, it is possible (Osten et al., 2006), and intraventricular administration of lentiviral vectors to the lumen of the mouse lateral ventricle has been shown to transduce the ependymal layer throughout the ventricular system (Consiglio et al., 2004). In this study, the spread of the virus through the CSF of the lateral ventricle was considerable, with transduced cells evident along the entire rostral-caudal extent of the ependyma and up to 3mm lateral to the site of injection. Additionally, cell bodies located within the subependymal region were also transduced, indicating endocytosis of the virus at the ventricular surface and transport to the cell soma. The immunohistochemical analysis revealed that some of these transduced cells morphologically resemble NSCs (type B astrocytes). These cells can give rise to transit amplifying cells (type C) which differentiate into migrating neuroblasts (type A) (Lois et al., 1996). This indicates that targeting of the ependyma and SVZ via the CSF of the lateral ventricle may be an efficient method of delivering corrected copies of the *CLN6* gene to NSCs within this region, affecting stem cells *in situ*. Targeting a patient's own neural stem/progenitor cells eliminates the many ethical and host-versus-donor rejection issues associated with similar treatments, such as embryonic stem cell transplants.

It is possible that modifications leading to more accurate targeting of this region could result in a high expression of vector in a greater proportion of NSCs. If the resulting neuroblasts migrate to the cortical regions of the brain most severely affected and involved at the earliest stages of pathogenesis of the disease, then compromised cells within these regions may be replaced with functional cells. This would then circumvent the need to repair all cells, especially if these newly generated neurons are being pulled to where they are most required. This is a very likely situation in the inflammatory brain of affected sheep as there is abundant evidence to support a crucial role of inflammatory induced cytokines in the chemoattraction of NPCs in the diseased brain. As shown in Chapter 3, TNF-α, IL-1β, TGF-β and IL-10 are significantly increased in the affected ovine brain, and it is feasible to consider that the expression of other cytokines such as monocyte chemotactic protein-1 (MCP-1) and stromal cell-derived factor-1 (SDF-1) which can regulate the directed migration of NPCs from the

SVZ (Belmadani et al., 2006; Imitola et al., 2004; Yan et al., 2007), may also be differentially expressed in affected animals. Concentration gradients of chemoattractive and chemorepulsant molecules, such as neuregulin 1, glial cell-derived neurotrophic factor (GDNF) and BDNF may also participate in direction orientated migration of neuroblasts to neurodegenerative regions (Cayre et al., 2009) and effectively disperse corrected cells to the most severely affected cortical regions.

Interestingly, even though ten times more vector was injected into the cisterna magnum than intracortically, there was no evidence of transduced ventricular cells or transduction of any other cell type, demonstrating that this is not a viable route to use for exposure of this vector to the ventricular surface or to other parts of the sheep brain. CSF flows from the lateral ventricles into the third ventricle via the foramina of Monro, and then to the fourth ventricle via the cerebral aqueduct into the brainstem. From there it passes into the cisterna magnum and subarachnoid space, bathing the spinal cord and brain before being returned to the circulation via the arachnoid villi. The extent of incidental labelling of ependymal and subependymal cells lining the lateral ventricles suggest rapid, efficient, transduction of cells, therefore there was probably too little vector left to be effective by the time the CSF had bathed the spinal cord and brain. It is possible that cells may have been transduced along the spinal cord, but this tissue was not analysed and is not a target for these therapies.

This is likely to be a feature of the size of the CNS as well as the vector used. A study of intrathecal delivery of lentiviral vectors to newborn mice resulted in patchy, widely scattered transduction of meninges and secretion of a soluble enzyme into the CSF (Fedorova et al., 2006), and recombinant AAV vectors administered to a mouse model of leptomeningeal metastases resulted in transfected ependymal and subependymal cells throughout the brain (Reijneveld et al., 1999). Evidently the substantially smaller rodent CNS is accessible to transfection via the intrathecal delivery of vectors. Moreover this indicates that reports of positive transgene expression via this route in rodent models of disease cannot be merely adapted to human studies, highlighting the value of large animal models for testing such therapies in a large, complicated CNS and identifying potential hurdles.

This work has provided vital information on aspects of gene therapy in the ovine brain which were successful and highlighted other areas in which modification and further experimentation is required, such as more accurate targeting of NSCs/progenitors within the SVZ or more extensive spread of the virus. A second trial is already underway in which lentiviruses pseudotyped with VSV-G, rabies glycoprotein (RG) or lymphocytic choriomeningitis glycoprotein (LCMV) are being compared for tropism and viral and

transgene spread. In rodents, LV-VSV-G has been shown to display the widest tropism, targeting neurons, astrocytes and progenitor cells (Brooks et al., 2002; Hughes et al., 2002). However, there is little spread away from the injection site due to the large size of the viral particles as well as a low abundance of VSV-G receptor on neural cells. This work revealed the spread of the virus was limited to 2.5mm either side of the injection site within the brain parenchyma which is not sufficient in such a large sized brain. However, the considerable spread of the virus along the ependymal and subependymal region due to the incidental virus present in the lateral ventricle advocates targeting the ependyma via the CSF of the lateral ventricle as an efficient method of delivering virus to NSCs within this region. Hence, animals have been injected directly into the lateral ventricle with LV-VSV-G and it is hoped that the full complement of virus (rather than the incidental presence of virus in this experiment) will greatly increase the proportion of NSCs transduced.

Lentiviruses pseudotyped with RG target neuronal projections (Desmaris et al., 2001; Watson et al., 2002) and single parenchymal injections have been performed. This pseudotype may lead to an increased spread of the virus within the brain, which could lead to gene expression in distal neurons. *In vivo* the LCMV pseudotype targets mouse NPCs (Stein et al., 2005). If this is also true in sheep, injections localised to the SVZ region could potentially result in more accurate and efficient targeting of the persistent NPCs in the SVZ of affected sheep and result in widespread migration of functionally corrected cells. Identification of the most suitable pseudotype will lead to the *CLN6* or *CLN5* coding sequence being cloned into a vector and therapy trials conducted in affected lambs.

5.5 Conclusion

Although few clinical trials have been approved using lentiviral vectors, human gene therapy trials have begun for Batten disease using AAV vectors (section 1.9.4). The well developed sheep models provide an ideal resource to study vector and gene product spread, optimal timing of interventions, and injection site targets to optimise functional effects. Ultimately therapy trials will be conducted in affected lambs. Most children with Batten disease are not diagnosed until they have clinical signs of the disease and significant storage body accumulation. Therefore, it will be important to determine whether storage body accumulation, in association with neurodegeneration and glial activation can be reversed after the disease is already established and to determine if gene therapy can be initiated at a subclinical stage of pathogenesis or if there is a limited time period in which therapy is

required to preserve neuronal function (Griffey et al., 2004). In summary, this study provides the first evidence of lentiviral-mediated gene transfer to the sheep brain, and a strategy with which to test further gene therapy strategies and vectors in NCL.

Chapter 6
General Discussion

6.1 Thesis summary

This thesis aimed to study the role key inflammatory cytokines could play in ovine CLN6 disease pathology, as well as the possibility of cross-cell correction and gene transfer to the ovine brain. Chapter 3 details the quantitative expression of TNF-α, IL-1β, TGF-β and IL-10 mRNA in different brain regions across four ages of affected and control animals. These are key pro-and anti-inflammatory cytokines and it has been postulated that alterations in the expression of some of these inflammatory mediators may be crucial in the development of a detrimental inflammatory cascade. All four cytokines were significantly increased in affected animals compared to age-matched controls at all ages examined, including 6 months of age, before clinical disease symptoms are evident. Surprisingly both TNF-α and IL-10 followed the same pattern of expression, peaking at 18 months before subsequently declining, whereas TGF-β and IL-1β expression remained elevated up to 24 months (Figure 7). Although the reasons for these changes in cytokine expression are unknown, the significant increase in all four cytokines indicates that an abnormal inflammatory response is underway and validates further investigation of the inflammatory cascade in ovine CLN6.

Chapter 4 details the histological and clinical progression of chimeric animals to analyse the effect which normal cells can have on affected cells in the ovine brain and whether normal cells suppress activation in affected cells or vice versa. This study established cross-correction of affected cells by normal cells, with animals consisting of up to 75% affected cells in some brain regions presenting with normal brain volumes, cortical laminar distribution of cells, normal vision, and a lack of glial activation and storage body accumulation, indicating intercellular communication of a corrective factor, despite the fact that CLN6 is an intracellular membrane bound protein. A key finding in this study was persistent neurogenesis along the SVZ of chimeric animals, with newly generated cells observed along white matter tracts and distributed throughout all cortical layers (Figure 18, Figure 19). In contrast newly generated cells in affected animals presented as cellular aggregates within upper cortical layers and suggests that newly generated cells in the chimeras were successfully distributed and integrated in the adult brain, possibly due to a lack of glial activation and associated inflammatory environment. This may be associated with recovering-like brains in a number of chimeric animals and suggests that migration of corrected cells, in combination with a

neurotrophic environment results in newly generated cell survival leading to recovering brain volumes and disease amelioration. Importantly the recovering-like chimeras, especially animal 401/04 which recovered from far below the affected brain volume range, suggest that the pathology is reversible and that not all cells need to be corrected. Some brain regions contained up to 75% affected cells but normal-like brain pathology was evident. The role which glial activation and inflammation have on cell survival in the affected ovine brain is currently unknown. However the evidence for cell survival in the recovering and normal-like chimeras in which minimal glial activation was observed, in contrast to the significant glial activation and increase in cytokine expression evident in affected animals suggests that inflammation is detrimental.

Chapter 5 presents successful lentiviral-mediated gene transfer to the sheep brain. Transductions were stable with expression of GFP protein evident 80 days post injection and no injection associated pathology was observed. Incidental leakage of the virus into the lateral ventricle and subsequent transduction of ependymal and subependymal cells lining the ventricle resulted in GFP expression in cells which morphologically resembled adult NSCs and migrating neuroblasts. Injections directly into the CSF did not result in successful transductions. Hence, this study identified a method by which to target NSCs in the SVZ, a region previously identified in Chapter 4 and in recent studies (Dihanich et al., 2009, article in preparation; Oswald et al., 2008) as an area of extended neurogenesis in affected animals. Targeting of this region would obviate the need for a virus which spreads widely in the brain, as lentiviral vectors can stably integrate into the host cell genome of both dividing and non-dividing cells; hence transduced NSCs could give rise to neuroblasts which also express the corrected gene and migrate to neurodegenerative cortical regions. This in combination with anti-inflammatory therapy could lead to cell survival and contrary to classical beliefs, cross-cell correction of neighbouring cells could occur. In addition, this study identifies sheep as a suitable large animal model for gene therapy trials which could be further extended to other neurological disorders beyond Batten disease.

6.2 Overall discussion

6.2.1 Ovine CLN6, neuroinflammation and neurogenesis

Evidence of extended neurogenesis in affected animals is not unique to this study. Acute neurodegenerative disorders such as epilepsy and stroke consistently show increased levels of neurogenesis (Parent et al., 1997, 2002; Arvidsson et al., 2001, 2002), while there have been

conflicting reports of both increased and decreased neurogenesis in chronic disorders such as AD, PD and HD (Jin et al., 2004; Donovan et al., 2006; Hoglinger et al., 2004; Yoshimi et al., 2005; Baker et al., 2004; Curtis et al., 2003, 2005). Concurrent with the progressive neurodegeneration evident in ovine CLN6, extended neurogenesis along the SVZ and within the cerebral cortex is also a feature of this disease model (see 4.4.2). The factors resulting in extended neurogenesis in neurodegenerative disease and whether or not newly generated neurons survive and become functionally integrated remain unknown. It is possible that alterations in the local microenvironment to resemble conditions seen during development result in an up-regulation of neurogenesis (Sohur et al., 2006). It is also recognized that the plethora of inflammatory and growth factors released by immune cells can be either supportive or detrimental to the different steps in neurogenesis: proliferation, migration, differentiation and survival. Hence, it appears that the outcome may depend on the balance between secreted pro- and anti-inflammatory molecules (Simard and Rivest, 2004; Ekdahl et al., 2009). A study by Ekdahl et al., (2003) revealed that microglia specifically compromise the survival of new neurons but there was no evidence that they suppress cell proliferation or differentiation. Although the newly generated cells in the ovine CLN6 brain will carry the same gene defect and hence self-repair will inevitably fail, the inflammatory environment could expedite this cell fate. This may account for a progressively decreasing brain volume and loss of cortical laminar organisation in affected animals despite the phenomenon of extended neurogenesis.

The newly generated cells present as clusters within the cerebral cortex of affected sheep are presumably consequent to proliferation of NSCs located in the SVZ. The presence of PSA-NCAM positive cells and fibres throughout white matter tracts indicate migration of newly generated cells from the SVZ to cortical regions undergoing neurodegeneration. Molecular cues from the most degenerate brain regions may site-direct migration to these regions, as suggested by studies in human HD brain and mouse models of ischaemia and PD (Curtis et al., 2003; Jin et al., 2003; Yamada et al., 2004). Inflammation induced chemoattraction can play a major role in cell migration but the observed extended neurogenesis in chimeric animals, despite a lack of glial activation, argues against this hypothesis in ovine CLN6. The widespread distribution of newly generated cells to cortical regions in chimeric animals suggests that glial cells may primarily have a detrimental role in cell survival without the benefit of directing cell migration. This suggests that something else associated with CLN6 affected cells upregulates neurogenesis in the diseased brain.

It is known that many cells that express immature neuronal markers, such as PSA-NCAM and DCX do not survive or mature into functionally integrated neurons (Arvidsson et al., 2002; Brown et al., 2003). Hence, although PSA-NCAM staining may reveal increased neurogenesis in affected animals it does not necessarily equate to successful neurogenesis which also requires functional integration and survival of new neurons (Whitney et al., 2009). The loss of neurons as revealed by Nissl staining (Figure 13) and the progressively decreasing brain volume of affected animals (Figure 12), suggests that successful cell replacement does not occur. Findings similar to these have been reported in AD, with increased neurogenesis and PSA-NCAM expression in the hippocampus of patients compared to normal controls (Jin et al., 2004). Furthermore PSA-NCAM and DCX expression were found to increase with increasing disease severity (Jin et al., 2004) similar to the CLN6 ovine model. Despite this increased neurogenesis, progressive cell loss was still observed which suggests that a lack of neurotrophic factors or similar, in combination with a chronic inflammatory response, results in failure of cell integration and survival. The deleterious effect of activated microglia on newly formed neuron survival is likely mediated via the action of cytokines, such as IL-1β, IL-6, TNF-α, NO and ROS (Pocock and Liddle, 2001; Hanisch, 2002; Gebicke-Haerter, 2001; Vallieres et al., 2002), some of which have been shown to be significantly upregulated in the affected brain (Figure 7) even prior to clinical disease manifestation.

Several neurotransmitter systems can also regulate adult CNS neurogenesis. Serotonin plays a clear role and neurogenesis can be increased with serotonin re-uptake inhibitors, which target early progenitor cells (Encinas et al., 2006). Dopamine is known for its effects on neurogenesis, agonists increasing neurogenesis in mouse PD models (Borta and Hoglinger, 2007; Yang et al., 2008). GABA and glutamate appear to play vital roles in the integration of newborn neurons in the adult brain (Ge et al., 2006; Nguyen et al., 2001) and there is evidence for persistent GABAergic (calbindin and calretinin positive) interneuron survival in the affected ovine brain (Oswald et al., 2008), which could act as an attractant for newly generated cells to severely affected brain regions.

Normal brain development is associated with a perinatal wave of gliogenesis which subsequently declines in normal animals by a process of programmed cell death, necessary for the regulation of neuronal and glial cell populations and normal brain development. Alterations in this process as sheep brains exit the developmental phase could result in extended and dysregulated glial activation, or insufficient inhibition of neurogenesis. It is possible that the alteration in some or all of these factors does not occur within the affected brain, enabling extended neurogenesis to continue even at advanced age. However, due to the

inflammatory environment successful completion of neurogenesis and cell replacement is ultimately ill-fated.

6.2.2 Chimeras, neuroinflammation and neurogenesis

If inflammatory factors detrimental to cell survival can be eliminated or dampened down, whilst the mechanisms enhancing cell proliferation and differentiation can be retained then pathological improvement could be accomplished. This appeared to be the situation in the majority of the chimeric animals analysed in Chapter 4, whereby affected cells present without glial activation and in combination with normal cells resulted in enhanced neurogenesis, subsequent cell survival and disease amelioration. The chimeric animals provided a valuable method by which to analyse normal and affected cells side by side within the same *in vivo* environment and the majority of chimeras resembled normal control animals within the histological and clinical parameters analysed. Differing aspects included a recovering brain volume in three animals (Figure 12) and the extended and widespread presence of newly generated cells within the brain (Figure 18, Figure 19). The newly generated cells appeared to mature, integrate and survive in chimeras, resulting in either recovering brain volumes or those which remained within the normal range, despite affected cells being present. Newly generated cells were observed throughout all cortical layers rather than confined to cellular aggregates.

This apparent survival and integration of new cells occurred in the absence of glial activation, suggesting that inflammation in ovine CLN6 which is associated with significant increases in cytokine expression (Chapter 3), is not the causative factor for the up-regulation of neurogenesis. Conversely it suggests that the inflammatory cascade is primarily detrimental and anti-neurogenic. Hence, even if some of the cytokines analysed in Chapter 3 had a pro-neurogenic function, ultimately the combination of other inflammatory mediators present result in a detrimental inflammatory environment and an unsuccessful attempt at brain repair. Cytokine expression was not analysed in the chimeras as the experimental method did not allow for adequately stored tissue for mRNA extraction.

The rate of cell proliferation and genotype of newly generated cells in the chimeric brain could explain the observed changes in brain volume, with some chimeras displaying brain volumes which increased from subnormal to normal levels and some which maintained a normal growth gradient (Figure 12). In addition, cortical thickness measurements and Nissl staining indicated that cellular organisation and migration was normal in recovering and normal-like chimeras (Figure 18, Figure 19). Elucidating the cellular environment essential

for permitting or promoting neurogenesis is a major challenge in understanding the regulation of neurogenesis. In the chimeric brain the damaged and degenerating affected cell populations may still be able to up-regulate neurogenesis within the SVZ and direct cell migration to affected brain regions, but the overall neurodegeneration taking place within the brain would be lower and inflammatory cells would not be activated. Hence survival of newly generated cells occurs.

Due to the method of aggregation chimera production, normal and affected cells were present in the brain prenatally; therefore normal cells may have inhibited the early glial response proposed to be a causative factor in neurodegeneration and pathology in the ovine CLN6 model (Oswald et al., 2005; Kay et al, 2006). It is unclear what role affected glial cells play in initiating neurodegeneration, but it is possible that normal glial cells which would have constituted a portion of the newly generated cells in the chimeric brain, could have contributed to the neurogenic environment that appeared to be present, enabling cell survival. Hence in future therapies integrated anti-inflammatory mechanisms may well be required.

6.2.3 Cross-cell communication and neurotrophic factors

In the chimeric animals, normal cells appeared to alter the fate of affected cells, with most animals displaying a complete lack of storage body accumulation and a normal laminar distribution of cells. Although CLN6 is a membrane bound protein, it may be involved in the processing of secreted factors, such as neurotrophins, which when released from normal cells provide a specific survival or anti-apoptotic signal to affected cells or create a better growth environment able to support continued survival of CLN6-deficient cells. Ultimately, in the chimera brain we do not know whether the affected cells have been present since birth and survived long-term or whether they have been newly generated from affected NSCs. Either way storage accumulation was significantly reduced or completely eliminated and glial activation inhibited, accompanied by a lack of neurodegeneration or neurodegeneration occurring slowly enough for successful neurogenesis to counteract the cell loss.

Neurotrophic factors promote neuronal survival, stimulate axonal growth and play a key role in construction of the normal synaptic network (Yuen et al., 1996; Grimes et al., 1996) during development. In adulthood, they help to maintain neural functions, therefore any alterations in their local synthesis, transport or signalling could adversely affect neuronal survival and lead to neuronal death (Connor and Dragunow, 1998). Neurotrophins bind to their cell surface receptors and can be internalized and retrogradely transported in neurites (Weiss et al., 2003). Nerve growth factor (NGF) and its receptor, tyrosine kinase (Trk) A, enter cells via clathrin

coated pits giving rise to clathrin coated vesicles or "signalling endosomes" (Howe et al., 2001). Studies on the endosomal trafficking of other surface receptors have shown that clathrin coated vesicles move on to become "early endosomes". From here, internalized receptors and ligands can be sorted to recycling endosomes poised to return to the plasma membrane for the re-use of receptors and re-release (and potentially re-use) of ligands. Alternatively, internalized receptors and ligands might be sorted from early endosomes to late endosomes and eventually to lysosomes, where they would be degraded (Weiss et al., 2003). Alterations in the endosomal-lysosomal pathway could be implicated in altered processing and degradation of these factors.

Studies have shown that a loss of neurotrophic support for selective neuronal populations may contribute to the pathology of neurodegenerative diseases including PD, AD, HD and amyotrophic lateral sclerosis (Connor and Dragunow, 1998). Many studies have shown that treatment with neurotrophic factors, including NGF, BDNF, neurotrophins 3 and 4/5, GDNF and IGF, can prevent cell loss. Studies have demonstrated that NGF infusions can reverse the decline in cholinergic neurons and spatial memory defects in aged rat models of AD (Fischer et al., 1987) and in non-human primate brain (Tuszynski et al., 1990, 1991). Chick motor neuron survival was promoted by IGF-1 in a cell culture model of amyotrophic lateral sclerosis (Arakawa et al., 1990), whereas clinical studies found that BDNF increased survival in amyotrophic lateral sclerosis patients (Bradley, 1995). In the LSD Niemann-Pick type C, BDNF and TrkB signalling has been shown to be reduced in affected neurons (Henderson et al., 2000), suggesting that the sorting of this neurotrophin receptor to the lysosomal compartment is impaired.

The commonality of subunit c accumulation in NCL implies that the *CLN* gene products may function in a specific subunit c turnover pathway, disruption of which leads to accumulation (Palmer et al., 1995a, 1997). It has been suggested that the different *CLN* gene products are different components of an oligomeric complex, mutations in which may lead to the altered processing of other factors, other than subunit c. Previous studies have implicated a role for TPP1, which is mutated in CLN2, in the intracellular degradation of neuropeptides, such as neuromedin B and cholecystokinin, which are released by neurons and function as intercellular messengers (Kopan et a., 2004; Warburton et al., 2002). These studies suggested that an absence of TPP1 may result in accumulation of undegraded neuropeptides in the endosomal-lysosomal system, contributing to the pathogenesis of the disease and affecting neuronal viability. The proposed role of CLN6 in pre-lysosomal vesicular transport (Heine et al., 2004a) suggests that the sorting and processing of neurotrophins and their receptors could

be affected in ovine CLN6, resulting in reduced expression of neurotrophins and their receptors, leading to neuronal dysfunction and loss.

Extrapolating which factor(s) are deficient in the ovine CLN6 model and are required for cell survival and cross-correction is a big hurdle but the chimera study strongly indicates that CLN6 is not a cell intrinsic defect but that the processing of soluble factors, such as neurotrophins, could be affected and thus this disease is amenable to cross-correction. Additionally the critical threshold of normal cells required to bring about therapeutic benefit is unknown but it is clear that not all cells need to be corrected. As revealed by these studies some animals with higher affected cell proportions developed better than other animals with smaller affected cell proportions. Hence it is likely that there are critical brain regions or cell types which determine normal development and cell survival. The chimeric study indicates that normal cells can positively affect disease progression and pathology and that some form of cross-cell communication is occurring. Hence gene therapy in ovine CLN6 is worthwhile, as this study suggests that every cell does not need to be replaced. In addition, targeting of NSCs in the SVZ which give rise to neuroblasts that travel to regions of neurodegeneration, working in concert with cross-correction, will extend the zone of therapeutic benefit. This perhaps in combination with anti-inflammatory therapy to target the detrimental role inflammation appears to have on cell survival, may offer therapeutic benefit.

6.3 Future directions

6.3.1 Cytokine expression and the inflammatory cascade

qPCR analysis of cytokine expression in ovine CLN6 did not isolate the critical step in inflammation that needs to be stopped but it does validate the central role that inflammation has been proposed to play in disease pathology (Oswald et al., 2005; Kay et al., 2006). Hence, further investigation of the inflammatory cascade and therapeutic options aimed at preventing or stopping inflammation is warranted.

Future studies could concentrate on increasing the sample size of the studied groups in addition to looking at more time points, specifically including prenatal brains. By 6 months of age significant increases in both pro- and anti-inflammatory cytokines were detected in affected animals compared to controls. Although clinical disease symptoms are not evident by this age glial activation is underway. Hence, a study of cytokine expression at earlier ages, including prenatal ages, would be beneficial for understanding cytokine expression in the normal brain during developmental gliogenic and neurogenic phases. This would indicate

whether cytokine expressions are altered at these ages in affected animals and potentially play a central role in inducing continued glial activation and initiating neurodegeneration in ovine CLN6. For this it is necessary to collect tissue for RNA from both CLN6 and control animals at a wider range of ages including prenatal ages.

As discussed previously, the chimera study indicates that a lack of soluble factors may be central to disease pathology in the affected brain. Due to the central role that neurotrophins play in neuronal survival, as well as evidence for their involvement in other neurodegenerative disorders including LSDs, neurotrophins could be the soluble mediators by which cross-cell communication occurs. Immunohistochemical detection of neurotrophins in the ovine brain would be informative, allowing differences in neurotrophin expression to be revealed. However, this method is not readily amenable to neurotrophin detection in the ovine brain, only a limited number of specific antibodies for ovine neurotrophins being available. However, the production of ruminant specific reagents is constantly improving and should be constantly monitored.

If endosomal-lysosomal processing and sorting of neurotrophic factors or similar, is affected in diseased animals, it is likely to result in the loss of expression of functional proteins or their receptors; hence analysis at the mRNA level is not ideal but does provide an alternative method. A similar study to that of cytokine expression in the ovine brain would still be informative and useful for either validating or eliminating neurotrophins as an area of future research. As mentioned above tissue for RNA is readily available and ovine specific primers for neurotrophins, including BDNF, GDNF, IGF and NGF can be designed in-house and analysed via established qPCR techniques.

Another method is multiplex arrays which could be utilised for analysing a larger number of inflammatory and neurotrophin related genes for primary screening and identifying molecular relationships and networks that can be studied in more detail by qPCR. Whilst there are many sources and types of comprehensive microarrays useful for applications with mouse and human samples, microarrays specifically designed for use with samples from production ruminants are not widely available. Ovine specific microarrays are currently unavailable and cross-species microarray analysis is the only means of examining large scale gene expression changes (Bar-Or et al., 2007). Bovine immune-related cDNA microarrays that hybridize with ovine cDNA are available (Tao et al., 2004; Donaldson et al., 2005) with reports of 91–95% hybridization of sheep cDNA to bovine cDNA and may be an option for the initial screening of some inflammatory mediators.

6.3.2 Chimeric tissue

Although not vital to this study, sufficient chimera tissue is available for further analysis. The location and cell type of normal cells in the brain may be critical for disease amelioration in the chimeras, identification of which would require genotyping of individual cells. This is not currently possible as the CLN6 mutation is unknown but attempts have been made to generate CLN6 specific antibodies. So far attempts have been unsuccessful but studies are ongoing within our lab to generate an antibody. This would allow *in situ* detection of individual cells within a given tissue by indirect immunofluorescence or immunoperoxidase methods making chimeric patterns conspicuous in histological sections and could be performed with double-labelling techniques to identify the genotype of specific cell types, such as microglia or newly generated cells. This would probably be the most informative method for confirming the results and hypotheses proposed in this thesis.

Another possibility is *in situ* hybridization (ISH), to detect specific nucleic acid sequences within cells (John et al., 1969; Gall and Pardue, 1969). Once the mutation for the CLN6 gene is identified, probes raised against the sequence information can be utilised to detect expression within cells. The critical parameters that result in successful completion of this technique requires optimal fixation and storage of tissue, and chimeric tissue available for use has not been specifically fixed for ISH , which could significantly reduce or inhibit ISH quality.

6.3.3 Gene therapy

Building on the results reported here gene therapy trials are currently underway in which lentiviral plasmids containing the *CLN5* and *CLN6* coding sequences with an attached *myc* tag have been injected directly into the cortex and the lateral ventricles of CLN5 and CLN6 affected lambs long before the development of any clinical symptoms. The development of clinical disease will be monitored in these sheep to determine any slowing or absence of disease progression by well established CAT scans of brain volumes and cognitive assays which have recently been established and provide an effective disease index by which to monitor disease progression. These in combination with neurophysiological tests which are currently being established, will allow an assessment of disease progression in animals undergoing current and future therapeutic trials.

Histological examinations will reveal the effectiveness, cell type selection and spread and persistence of transductions in the brain. The well defined pathological presentations of affected animals, including cortical thinning, storage body accumulation, glial activation and

neurogenesis will be examined to determine whether gene therapy is influencing disease pathology and if so, which cell types are transduced to effect these changes. qPCR analysis of cytokine expression in these animals, in combination with the immunohistochemical analysis will reveal whether the presence of functional protein in the brain can influence the inflammatory cascade in disease affected animals and if these changes modify disease pathology. In addition, if studies in affected and control animals implicate a disease associated change in neurotrophin expression, then their expression can be studied in injected animals.

This study will also determine future trial options in the ovine model, including the use of different vectors, such as AAV, and changes in the method of injection. If sufficient transduction of the SVZ and resident NSCs cannot be achieved by the methods trialled than alternative options such as *in vitro* transduction of stem cells and subsequent implantation, or the use of x-ray guided needle placement for more accurate targeting of the SVZ may be required. Anti-inflammatory therapies may also be needed in combination with gene therapy for optimal therapeutic benefit.

6.4 Conclusion

This thesis provides further evidence for an inflammatory role in ovine CLN6 pathogenesis and warrants further investigation especially at prenatal ages to identify whether abnormal cytokine expression is central to the initiation of neurodegeneration. The chimera study indicates that CLN6 is not a cell intrinsic defect and that the processing of soluble factors may be implicated, resulting in cross-cell communication and disease amelioration. This evidence in combination with extended neurogenesis in affected animals, endorses SVZ targeted gene injections as a therapeutic option for ovine CLN6, contrary to the general belief that membrane bound protein defects are not amenable to cross-correction.

Furthermore this study poses questions as to how cross-correction occurs between normal and affected cells in the brain, is CLN6 involved in the processing of some soluble factor such as neurotrophic factors, which can functionally correct neighbouring cells? Furthermore what causes extended neurogenesis in ovine CLN6 and will future therapies targeting this phenomenon also require anti-inflammatory therapy due to the central role which inflammatory mediators appear to play? Continued investigation is required in order to gain a better understanding of all of these facets of the disease, but ultimately this thesis provides a more optimistic therapeutic potential for this form of NCL than had previously been

considered and may warrant similar investigations in other NCLs resulting in presumed membrane bound protein defects.

References

Abdipranoto A, Wu S, Stayte S, & Vissel B. 2008. The role of neurogenesis in neurodegenerative diseases and its implications for therapeutic development. *CNS & Neurological Disorders – Drug Targets* **7**: 187-210.

Aberg MA, Aberg ND, Hedbecker H, Oscarsson J, & Eriksson PS. 2000. Peripheral infusion of IGF-1 selectively induces neurogenesis in the adult rat hippocampus. *Journal of Neuroscience* **20**: 2896-2903.

Abrous DN, Koehl M, & Le Moal M. 2005. Adult neurogenesis: From precursors to network and physiology. *Physiological Reviews* **85**: 523-569.

Aiello C, Terracciano A, Simonati A, Discepoli G, Cannelli N, Claps D, Crow YJ, Bianchi M, Kitzmuller C, Longo D, Tavoni A, Franzoni E, Tessa A, Veneselli E, Boldrini R, Filocamo M, Williams RE, Bertini ES, Biancheri R, Carrozzo R, Mole SE, & Santorelli FM. 2009. Mutations in MFSD8/CLN7 are a frequent cause of variant-late infantile neuronal ceroid lipofuscinosis. *Human Mutation* **30**: E530-540.

Akaneya Y, Takahashi M, & Hatanaka. 1995. Interleukin-1 β enhances survival and interleukin-6 protects against MPP+ neurotoxicity in cultures of fetal rat dopaminergic neurons. *Experimental Neurology* **136**: 44-52.

Akiyama H, Barger S, Barnum S, Bradt B, Bauer J, Cole GM, Cooper NR, Eikelenboom P, Emmerling M, Fiebich BL, Finch CE, Frautschy S, Griffin WS, Hampel H, Hull M, Landreth G, Lue L, Mrak R, Mackenzie IR, McGeer PL, O'Banion MK, Pachter J, Pasinetti G, Plata-Salaman C, Rogers J, Rydel R, Shen Y, Streit W, Strohmeyer R, Tooyoma I, Van Muiswinkel FL, Veerhuis R, Walker D, Webster S, Wegrzyniak B, Wenk G, & Wyss-Coray T. 2000. Inflammation and Alzheimer's disease. *Neurobiology of Aging* **21**: 383-421.

Alexander WS & Hilton DJ. 2004. The role of suppressors of cytokine signaling (SOCS) proteins in regulation of the immune response. *Annual Review of Immunology* **22**: 503-529.

Aloisi F. 2001. Immune function of microglia. *Glia* **36**: 165-179.

Allan SM & Rothwell NJ. 2001. Cytokines and acute neurodegeneration. *Nature Reviews Neuroscience* **2**: 734-744.

Allan SM & Rothwell NJ. 2003. Inflammation in central nervous system injury. *Philosophical Transactions of the Royal Society B: Biological Sciences* **358**: 1669-1677.

Allen MJ, Myer BJ, Khokher AM, Rushton N, & Cox TM. 1997. Pro-inflammatory cytokines and the pathogenesis of Gaucher's disease: Increased release of interleukin-6 and interleukin-10. *Quarterly Journal of Medicine* **90**: 19-25.

Altman J. 1962. Are new neurones formed in the brains of adult mammals? *Science* **135**: 1127-1128.

Arakawa Y, Sendtner M, & Thoenen H. 1990. Survival effect of ciliary neurotrophic factor (CNTF) on chick embryonic motoneurons in culture: Comparison with other neurotrophic factors and cytokines. *Journal of Neuroscience* **10**: 3507-3515.

Arend WP, Ammons JT, & Kotzin BL. 1987. Lipopolysaccharide and interleukin 1 inhibit interferon-gamma-induced Fc receptor expression on human monocytes. *Journal of Immunology* **139**: 1873-1879.

Arsov T, Smith KR, Damiano J, Franceschetti S, Canafoglia L, Bromhead CJ, Andermann E, Vears DF, Cossette P, Rajagopalan S, McDougall A, Sofia V, Farrell M, Aguglia U, Zini A, Meletti S, Morbin M, Mullen S, Andermann F, Mole SE, Bahlo M, & Berkovic SF. 2011. Kufs disease, the major adult form of neuronal ceroid lipofuscinosis, caused by mutations in CLN6. *American Journal of Human Genetics* **88**: 566-573.

Arvidsson A, Kokaia Z, & Lindvall O. 2001. N-methyl-D-aspartate receptor-mediated increase of neurogenesis in adult rat dentate gyrus following stroke. *European Journal of Neuroscience* **14**: 10-18.

Arvidsson A, Collin T, Kirik D, Kokaia Z, & Lindvall O. 2002. Neuronal replacement from endogenous precursors in the adult brain after stroke. *Nature Medicine* **8**: 963-970.

Augestad LB & Flanders WD. 2006. Occurence of and mortality from childhood neuronal ceroid lipofuscinosis in Norway. *Journal of Child Neurology* **21**: 917-922.

Backman CM, Shan L, Zhang YJ, Hoffer BJ, Leonard S, Troncoso JC, Vonsatel P, & Toman TC. 2006. Gene expression patterns for GDNF and its receptors in the human putamen affected by Parkinson's disease: A real-time PCR study. *Molecular and Cellular Endocrinology* **252**: 160-166.

Bader M, Schreiner R, & Wolf E. 2009. Scientific background. In: *Chimeras and Hybrids in Comparative European and International Research* (Taupitz J & Weschka M, eds.), p. 21-32, Springer Dordrecht Heidelberg London New York.

Bae JS, Han HS, Youn DH, Carter JE, Modo M, Schuchman EH, & Jin HK. 2007. Bone marrow-derived mesenchymal stem cells promote neuronal networks with functional synaptic transmission after transplantation into mice with neurodegeneration. *Stem Cells* **25**: 1307-1316.

Baker SA, Baker KA, & Hagg T. 2004. Dopaminergic nigrostriatal projections regulate neural precursor proliferation in the adult mouse subventricular zone. *European Journal of Neuroscience* **20**: 575-579.

Banikazemi M, Bultas J, Waldeck S, Wilcox WR, Whitley CB, McDonald M, Finkel R, Packman S, Bichet DG, Warnock DG, & Desnick RJ. 2007. Agalsidase-beta therapy for advanced Fabry disease: A randomized trial. *Annals of Internal Medicine* **146**: 77-86.

Barak V, Acker M, Nisman B, Kalickman I, Abrahamov A, Zimran A, & Yatziv S. 1999. Cytokines in Gaucher's disease. *European Cytokine Network* **10**: 205-210.

Bar-Or C, Czosnek H, & Koltai H. 2007. Cross-species microarray hybridizations: A developing tool for studying species diversity. *Trends in Genetics* **23**: 200-207.

Barroso I, Benito B, Garcia-Jimenez C, Hernández A, Obregón MJ, & Santisteban P. 1999. Norepinephrine, tri-iodothyronine and insulin upregulate glyceraldehye-3-phosphate dehydrogenase mRNA during brown adipocyte differentiation. *European Journal of Endocrinology* **141**: 169-179.

Barton NW, Brady RO, Dambrosia JM, Di Bisceglie AM, Doppelt SH, Hill SC, Mankin HJ, Murray GJ, Parker RI, Argoff CE, Grewal RJ, & Yu KT. 1991. Replacement therapy for inherited enzyme deficiency-macrophage-targeted glucocerebrosidase for Gaucher's disease. *New England Journal of Medicine* **324**: 1464-1470.

Basu A, Krady J, & Levinson S. 2004. Interleukin-1: A master regulator of neuroinflammation. *Journal of Neuroscience Research* **78**: 151-156.

Batten FE. 1903. Cerebral degeneration with symmetrical changes in the maculae in two members of a family. *Transactions of the Ophthalmological Society of the United Kingdom* **23**: 386-390.

Batten FE. 1914. Family cerebral degeneration with macular change (so-called juvenile form of family amaurotic idiocy. *Quarterly Journal of Medicine* **7**: 444-454.

Baudry M, Yao Y, Simmons D, Liu J, & Bi X. 2003. Postnatal development of inflammation in a murine model of Niemann-Pick type C disease: Immunohistochemical observations of microglia and astroglia. *Experimental Neurology* **184**: 887-903.

Beal MF. 2001. Experimental models of Parkinson's disease. *Nature Reviews Neuroscience* **2**: 325-334.

Beck M. 2007. New therapeutic options for lysosomal storage disorders: Enzyme replacement, small molecules and gene therapy. *Human Genetics* **121**: 1-22.

Beckstead JH. 1994. A simple technique for preservation of fixation-sensitive antigens in paraffin-embedded tissues. *Journal of Histochemistry and Cytochemistry* **42**: 1127-1134.

Belmadani A, Tran PB, Ren D, & Miller RJ. 2006. Chemokines regulate the migration of neural progenitors to sites of neuroinflammation. *Journal of Neuroscience* **26**: 3182-3191.

Ben-Hur T, Ben-Menachem O, Furer V, Einstein O, Mizrachi-Kol R, & Grigoriadis N. 2003. Effects of proinflammatory cytokines on the growth, fate and motility of multipotential neural precursor cells. *Molecular and Cellular Neuroscience* **24**: 623-631.

Bennet MJ, Hosking GP, Gayton R, Thompson G, Galloway JH, & Cartwright IJ. 1988. Therapeutic modification of membrane lipid abnormalities in juvenile neuronal ceroid-lipofuscinosis (Batten disease). *American Journal of Medical Genetics* **5**: 275-281.

Benveniste EN. 1998. Cytokine actions in the central nervous system. *Cytokine and Growth Factor Reviews* **9**: 259-275.

Berchem G, Glondu M, Gleizes M, Brouillet JP, Vignon F, Garcia M, & Liaudet-Coopman E. 2002. Cathepsin-D affects multiple tumor progression steps *in vivo*: Proliferation, angiogenesis and apoptosis. *Oncogene* **21**: 5951-5955.

Bernier PJ, Bedard A, Vinet J, Levesque M, & Parent A. 2002. Newly generated neurons in the amygdala and adjoining cortex of adult primates. *Proceedings of the National Academy of Sciences USA* **99**: 11464-11469.

Beutler E. 2006. Lysosomal storage diseases: Natural history and ethical and economic aspects. *Molecular Genetics and Metabolism* **88**: 208-215.

Bible E, Gupta P, Hofmann SL, & Cooper. 2004. Regional and cellular neuropathology in the palmitoyl protein thioesterase-1 null mutant mouse model of infantile neuronal ceroid lipofuscinosis. *Neurobiology of Disease* **16**: 346-359.

Bielchowsky M. 1913. Über spät-infantile familiäre amaurotische idiotie mit kleinhirnsymptomen. *Deutsch Zeitung der Nervenheilkunde* **50**: 7-29.

Bildfell R, Matwichuk C, Mitchell S, & Ward P. 1995. Neuronal ceroid-lipofuscinosis in a cat. *Veterinary Pathology* **32**: 485-488.

Block ML & Hong JS. 2005. Microglia and inflammation-mediated neurodegeneration: Multiple triggers with a common mechanism. *Progress in Neurobiology* **76**: 77-98.

Block ML, Zecca L, & Hong JS. 2007. Microglia-mediated neurotoxicity: Uncovering the molecular mechanisms. *Nature Reviews Neuroscience* **8**:57-69.

Boediono A, Ooe M, Yamamoto M, Takagi M, Saha S, & Suzuki T. 1993. Production of chimeric calves by aggregation of *in vitro*-fertilised bovine embryos without zonae pellucidae. *Theriogenology* **40**: 1221-1230.

Bonde S, Ekdahl CT, & Lindvall O. 2006. Long-term neuronal replacement in adult rat hippocampus after status epilepticus despite chronic inflammation. *European Journal of Neuroscience* **23**: 965-974.

Bondolfi L, Ermini F, Long JM, Ingram DK, & Jucker M. 2004. Impact of age and caloric restriction on neurogenesis in the dentate gyrus of C57BL/6 mice. *Neurobiology of Aging* **25**: 333-340.

BonDurant RH, McDonald MC, & Trommershausen-Bowling A. 1980. Probable freemartinism in a goat. *Journal of the American Veterinary Medical Association* **177**: 1024-1025.

Borta A & Hoglinger GU. 2007. Dopamine and adult neurogenesis. *Journal of Neurochemistry* **100**: 587-595.

Bosu WT & Basrur PK. 1984. Morphological and hormonal features of an ovine and a caprine intersex. *Canadian Journal of Comparative Medicine* **48**: 402-409.

Bou-Gharios G, Abraham D, & Olsen I. 1993. Lysosomal storage diseases: Mechanisms of enzyme replacement therapy. *Histochemical Journal* **25**: 593-605.

Böyum A. 1968. Isolation of mononuclear cells and granulocytes from human blood. *Scandinavian Journal of Clinical and Laboratory Investigation* **97**: 77-89.

Braak H & Goebel HH. 1979. Pigmentoarchitectonic pathology of the isocortex in juvenile neuronal ceroid lipofuscinosis: Axonal enlargements in layer IIIab and cell loss in layer V. *Acta Neuropathologica* **46**: 79-83.

Bradley WG. 1995. A phase I/II study of recombinant brain derived neurotrophic factor in patients with ALS. *Annals of Neurology* **38**: 971.

Brem G, Tenhumberg H, & Kraublich H. 1984. Chimerism in cattle through micro-surgical aggregation of morulae. *Theriogenology* **22**: 609-613.

Brionne TC, Tesseur I, Masliah E, & Wyss-Coray T. 2003. Loss of TGF-beta1 leads to increased neuronal cell death and microgliosis in mouse brain. *Neuron* **40**: 1133-1145.

Bronson RT, Lake BD, Cook S, Taylor S, & Davisson MT. 1993. Motor neuron degeneration of mice is a model of neuronal ceroid lipofuscinosis (Batten's disease). *Annals of Neurology* **33**: 381-385.

Bronson RT, Donahue LR, Johnson KR, Tanner A, Lane PW, & Faust JR. 1998. Neuronal ceroid lipofuscinosis (nclf), a new disorder of the mouse linked to chromosome 9. *American Journal of Medical Genetics* **77**: 289-297.

Brooks AI, Stein CS, Hughes SM, Heth J, McCray PM, Sauter SL, Johnston JC, Cory-Slechta DA, Federoff HJ, & Davidson BL. 2002. Functional correction of established central nervous system deficits in an animal model of lysosomal storage disease with feline immunodeficiency virus-based vectors. *Proceedings of the National Academy of Sciences USA* **99**: 6216-6221.

Broom MF, Zhou C, Broom JE, Barwell KJ, Jolly RD, & Hill DF. 1998. Ovine neuronal ceroid lipofuscinosis: A large animal model syntenic with the human neuronal ceroid lipofuscinosis variant CLN6. *Journal of Medical Genetics* **35**:717-721.

Brown JP, Couillard-Despres S, Cooper-Kuhn CM, Winkler J, Aigner L, & Kuhn HG. 2003. Transient expression of doublecortin during adult neurogenesis. *Journal of Comparative Neurology* **467**: 1-10.

Bruce AJ, Boling W, Kindy MS, Peschon J, Kraemer PJ, Carpenter MK, Holtsberg FW, & Mattson MP. 1996. Altered neuronal and microglial responses to excitotoxic and ischemic brain injury in mice lacking TNF receptors. *Nature Medicine* **2**: 7788-7794.

Bruere AN, Fielden ED, & Hutchings H. 1968. XX/XY mosaicism in lymphocyte cultures from a pig with freemartin characteristics. *New Zealand Veterinary Journal* **16**: 31-38.

Buckwalter MS & Wyss-Coray T. 2004. Modelling neuroinflammatory phenotypes *in vivo*. *Journal of Neuroinflammation* **1**:10.

Budhia S, Haring LF, McConnell I, & Blacklaws BA. 2006. Quantitation of ovine cytokine mRNA by real-time RT-PCR. *Journal of Immunological Methods* **309**: 160-172.

Burneo JG, Arnold T, Palmer CA, Kuzniecky RI, Oh SJ, & Faught E. 2003. Adult-onset neuronal ceroid lipofuscinosis (Kufs Disease) with autosomal dominant inheritance in Alabama. *Epilepsia* **44**: 841-846.

Burns JC, Friedmann T, Driever W, Burrascano M, & Yee JK. 1993. Vesicular stomatitis virus G glycoprotein pseudotyped retroviral vectors: Concentration to very high titer and efficient gene transfer into mammalian and nonmammalian cells. *Proceedings of the National Academy of Sciences USA* **90**: 8033-8037.

Burrow TA, Hopkins RJ, Leslie ND, Tinkle BT, & Grabowski GA. 2007. Enzyme reconstitution/ replacement therapy for lysosomal storage diseases. *Current Opinions in Paediatrics* **18**: 628-635.

Bustin SA. 2000. Absolute quantification of mRNA using real-time reverse transcription polymerase chain reaction assays. *Journal of Molecular Endocrinology* **25**: 169-193.

Butler JE, Anderson GB, BonDurant RH, Pashen RL, & Penedo MCT. 1987. Production of ovine chimeras by inner cell mass transplantation. *Journal of Animal Sciences* **65**: 317-324.

Butovsky O, Ziv Y, Schwartz A, Landa G, Talpalar AE, Pluchino S, Martino G, & Schwartz M. 2006. Microglias activated by IL-4 or IFN- gamma differentially induce neurogenesis and oligodendrogenesis from adult stem/progenitor cells. *Molecular and Cellular Neuroscience* **31**: 149-160.

Buxton D, Anderson IE, Longbottom D, Livingstone M, Wattegedera S, & Entrican G. 2002. Ovine Chlamydial Abortion: Characterization of the Inflammatory Immune Response in Placental Tissues. *Journal of Comparative Pathology* **127**: 133-141.

Cabrera-Salazar MA, Roskelley EM, Bu J, Hodges BL, Yew N, Dodge JC, Shihabuddin LS, Sohar I, Sleat DE, Scheule RK, Davidson BL, Cheng SH, Lobel P, & Passini MA. 2007. Timing of therapeutic intervention determines functional and survival outcomes in a mouse model of late infantile batten disease. *Molecular Therapy* **15**: 1782-1788.

Cacci E, Ajmone-Cat MA, Anelli T, Biagioni S, & Minghetti L. 2008. *In vitro* neuronal and glial differentiation from embryonic or adult neural precursor cells are differently affected by chronic or acute activation of microglia. *Glia* **56**: 412-425.

Cachon-Gonzalez MB, Wang SZ, Lynch A, Ziegler R, Cheng SH, & Cox TM. 2006. Effective gene therapy in an authentic model of Tay-Sachs-related diseases. *Proceedings of the National Academy of Sciences USA* **103**: 10373-10378.

Cacquevel M, Lebeurrier N, Chéenne S, & Vivien D. 2004. Cytokines in neuroinflammation and Alzheimer's disease. *Current Drug Targets* **5**: 529-534.

Cajal Ry. 1928. *Degeneration and Regeneration of the Nervous System*, Volume 2. p. 750, Haffner Publishing Co. New York, New York, USA.

Cameron HA, Wolley CS, McEwen BS, & Gould E. 1993. Differentiation of newly born neurons and glia in the dentate gyrus of the adult rat. *Neuroscience* **56**: 337-344.

Cameron HA & McKay RD. 2001. Adult neurogenesis produces a large pool of new granule cells in the dentate gyrus. *Journal of Comparative Neurology* **435**: 406-417.

Campbell RM & Peterson AC. 1992. An intrinsic neuronal defect operates in *dystonia musculorum*: A study of *dt/dt* ↔ + / + chimeras. *Neuron* **9**: 693-703.

Cannelli N, Cassandrini D, Bertini E, Striano P, Fusco L, Gaggero R, Specchio N, Biancheri R, Vigevano F, Bruno C, Simonati A, Zara F, & Santorelli FM. 2006. Novel mutations in CLN8 in Italian variant late infantile neuronal ceroid lipofuscinosis: Another genetic hit in the Mediterranean. *Neurogenetics* **7**: 111-117.

Cannelli N, Nardocci N, Cassandrini D, Morbin M, Aiello C, Bugiani M, Criscuolo L, Zara F, Striano P, Granata T, Bertini E, Simonati A, & Santorelli FM. 2007. Revelation of a novel CLN5 mutation in early juvenile neuronal ceroid lipofuscinosis. *Neuropediatrics* **38**: 46-49.

Cannelli N, Garavaglia B, Simonati A, Aiello C, Barzaghi C, Pezzini F, Cilio MR, Biancheri R, Morbin M, Bernardina BD, Granata T, Tessa A, Invernizzi F, Pessagno A, Boldrini R, Zibordi F, Grazian L, & Claps D. 2009. Variant late infantile ceroid lipofuscinoses associated with novel mutations in CLN6. *Biochemical & Biophysical Research Communications* **379**: 892-897.

Caput D, Beutler B, Hartog K, Thayer R, Brown-Shimer S, & Cerami A. 1986. Identification of a common nucleotide sequence in the 3'-untranslated region of mRNA molecules

specifying inflammatory mediators. *Proceedings of the National Academy of Sciences USA* **83**: 1670-1674.

Carlen M, Cassidy RM, Brismar H, Smith GA, Enquist LW, & Frisen J. 2002. Functional integration of adult-born neurons. *Current Biology* **12**: 606-608.

Carmichael ST. 2006. Cellular and molecular mechanisms of neural repair after stroke: Making waves. *Annals of Neurology* **59**: 735-742.

Castaneda JA, Lim MJ, Cooper JD, & Pearce DA. 2008. Immune system irregularities in lysosomal storage disorders. *Acta Neuropathologica* **115**: 159-174.

Cayre M, Canoll P, & Goldman JE. 2009. Cell migration in the normal and pathological postnatal mammalian brain. *Progress in Neurobiology* **88**: 41-63.

Chang M, Cooper JD, Sleat DE, Cheng SH, Dodge JC, Passini MA, Loebel P, & Davidson BL. 2008. Intraventricular enzyme replacement improves disease phenotypes in a mouse model of late infantile neuronal ceroid lipofuscinosis. *Molecular Therapies* **16**: 649-656.

Chao CC, Hu S, Fey WH, Ala TA, Tourtellotte WW, & Peterson PK. 1994. Transforming growth factor beta in Alzheimer's disease. *Clinical and Diagnostic Laboratory Immunology* **1**: 109-110.

Chen R, Fearnley IM, Palmer DN, & Walker JE. 2004. Lysine 43 is trimethylated in subunit c from bovine mitochondrial ATP synthase and in storage bodies associated with Batten disease. *The Journal of Biological Chemistry* **279**: 21883-21887.

Chiasson BJ, Tropepe V, Morshead CM, & van der Kooy D. 1999. Adult mammalian forebrain ependymal and subependymal cells demonstrate proliferative potential but only subependymal cells have neural stem cell characteristics. *Journal of Neuroscience* **19**: 4462-4471.

Chio KS, Reiss U, Fletcher B, & Tappel AL. 1969. Peroxidation of subcellular organelles: Formation of lipofuscin like fluorescent pigments. *Science* **166**: 1535-1536.

Chung S, Ma X, Liu Y, Lee D, Tittiger M, & Ponder KP. 2007. Effect of neonatal administration of a retroviral vector expressing alpha-L-iduronidase upon lysosomal storage in brain and other organs in mucopolysaccharidosis I mice. *Molecular Genetics and Metabolism* **90**: 181-192.

Claussen M, Heim P, Knispel J, Goebel HH, & Kohlschütter A. 1992. Incidence of neuronal ceroid-lipofuscinoses in West Germany: Variation of a method for studying autosomal recessive disorders. *American Journal of Medical Genetics* **42**: 536-538.

Coligan JE, Dunn BM, Ploegh HL, Speicher DW, & Wingfield PT (eds.). 1995. *Current Protocols in Protein Science,* John Wiley & Sons, New York.

Connor B & Dragunow M. 1998. The role of neuronal growth factors in neurodegenerative disorders of the human brain. *Brain Research Reviews* **27**: 1-39.

Conover JC, Doetsch F, Garcia-Verdugo JM, Gale NW, Yancopoulos GD, & Alvarez-Buylla A. 2000. Disruption of Eph/ephrin signaling affects migration and proliferation in the adult subventricular zone. *Nature Neuroscience* **3**: 1091-1097.

Consiglio A, Gritti A, Dolcetta D, Follenzi A, Bordignon C, Gage FH, Vescovi AL, & Naldini L. 2004. Robust *in vivo* gene transfer into adult mammalian neural stem cells by lentiviral vectors. *Proceedings of the National Academy of Sciences USA* **101**: 14835-14840.

Cook RE, Jolly RD, Palmer DN, Tammen I, Broon MF, & McKinnon R. 2002. Neuronal ceroid lipofuscinosis in Merino sheep. *Australian Veterinary Journal* **80**: 292-297.

Cooper JD, Messer A, Feng AK, Chua-Couzens J, & Mobley WC. 1999. Apparent Loss and Hypertrophy of Interneurons in a Mouse Model of Neuronal Ceroid Lipofuscinosis: Evidence for partial response to insulin-like growth factor-1 treatment. *Journal of Neuroscience* **19**: 2556-2567.

Cooper JD. 2003. Progress towards understanding the neurobiology of Battens disease or neuronal ceroid lipofuscinosis. *Current Opinion in Neurology* **16**: 121-128.

Cooper O & Isacson O. 2004. Intrastriatal transforming growth factor alpha delivery to a model of Parkinson's disease induces proliferation and migration of endogenous adult neural progenitor cells without differentiation into dopaminergic neurons. *Journal of Neuroscience* **24**: 8924-8931.

Crow YJ, Tolmie JL, Howatson AG, Patrick WJ, & Stephenson JB. 1997. Batten disease in the west of Scotland 1974-1995 including five cases of the juvenile form with granular osmiophilic deposits. *Neuropediatrics* **28**: 140-144.

Curtis MA, Penney EB, Pearson AG, van Roon-Mom WMC, Butterworth NJ, Dragunow M, Connor B, & Faull RL. 2003. Increased cell proliferation and neurogenesis in the adult human

Huntington's disease brain. *Proceedings of the National Academy of Sciences USA* **100**: 9023-9027.

Curtis MA, Penney EB, Pearson J, Dragunow M, Connor B, & Faull RL. 2005. The distribution of progenitor cells in the subependymal layer of the lateral ventricle in the normal and Huntington's disease human brain. *Neuroscience* **132**: 777-788.

Curtis MA, Kam M, Nannmark U, Anderson MF, Axell MZ, Wikkelso C, Holtas S, van Roon-Mom WM, Bjork-Eriksson T, Nordberg C, Frisen J, Dragunow M, Faull RL, & Eriksson PS. 2007. Human neuroblasts migrate to the olfactory bulb via a lateral ventricular extension. *Science* **315**: 1243-1249.

Das AK, Lu JY, & Hofmann SL. 2001. Biochemical analysis of mutations in plamitoyl-protein thioesterase causing infantile and late-onset forms of neuronal ceroid lipofuscinosis. *Human Molecular Genetics* **10**: 1431-1439.

Das S & Basu A. 2008. Inflammation: A new candidate in modulating adult neurogenesis. *Journal of Neuroscience Research* **86**: 1199-1208.

Deiss LP, Galinka H, Berissi H, Cohen O, & Kimchi A. 1996. Cathepsin D protease mediates programmed cell death induced by interferon-gamma, Fas/APO-1 and TNF-alpha. *EMBO Journal* **15**: 3861-3870.

Dennler S, Goumans MJ, & ten Dijke P. 2002. Transforming growth factor β signal transduction. *Journal of Leukocyte Biology* **71**: 731-740.

Desmaris N, Bosch A, Salaun C, Petit C, Prevost MC, Tordo N, Perrin P, Schwartz O, de Rocquigy H, & Heard JM. 2001. Production and neurotropism of lentivirus vectors pseudotyped with lyssavirus envelope glycoproteins. *Molecular Therapy* **4**: 149-156.

Desnick RJ, Dean KJ, Grabowski GA, Bishop DF, & Sweeley CC. 1980. Enzyme therapy XVII: Metabolic and immunologic evaluation of alpha-galactosidase A replacement in Fabry disease. *Birth Defects Original Article Series* **16**: 393-413.

Desnick RJ. 2004. Enzyme replacement and enhancement therapies for lysosomal diseases. *Journal of Inherited and Metabolic Diseases* **27**: 385-410.

Dihanich S, Palmer DN, Oswald MJ, Williams BP, Schwartz H, Kay GW, & Cooper JD. *In vivo* and *in vitro* evidence for adult neurogenesis in CLN6 sheep. *Proceedings of the 27th International Australasian Winter Conference on Brain Research*, Queenstown, Sept 2009.

Doetsch F, Caille I, Lim DA, Garcia-Verdugo JM, & Alvarez-Buylla, A. 1999a. Subventricular zone astrocytes are neural stem cells in the adult mammalian brain. *Cell* **97**: 703-716.

Doetsch F, Garcia-Verdugo JM, & Alvarez-Buylla A. 1999b. Regeneration of a germinal layer in the adult mammalian brain. *Proceedings of the National Acadamey of Sciences USA* **96**: 11619-11624.

Donaldson L, Vuocolo T, Gray C, Strandberg Y, Reverter A, McWilliam S, Wang Y, Byrne K & Tellam R. 2005. Construction and validation of a bovine innate immune microarray. *BMC Genomics* **6**: 135-156.

Donovan MH, Yazdani U, Norris RD, Games D, German DC, & Eisch AJ. 2006. Decreased adult hippocampal neurogenesis in the PDAPP mouse model of Alzheimer's disease. *Journal of Comparative Neurology* **495**: 70-83.

Drozina G, Kohoutek J, Jabrane-Ferrat N, & Peterlin BM. 2005. Exprssion of MHCII genes. *Current Topics in Microbiology and Immunology* **290**: 147-170.

Du Y & Dreyfus CF. 2002. Oligodendrocytes as providers of growth factors. *Journal of Neuroscience Research* **68**: 647-654.

Dufourny L, Migaud M, Thiery JC, & Malpaux B. 2008. Development of an *in vivo* adeno-associated virus-mediated siRNA approach to knockdown tyrosine hydroxylase in the lateral retrochiasmatic area of the ovine brain. *Journal of Neuroscience Methods* **170**: 56-66.

Dunphy J, Horvath A, Barcham G, Balic A, Bischof R, & Meeusen E. 2001. Isolation, characterisation and expression of mRNAs encoding the ovine CC chemokines, monocyte chemoattractant protein (MCP)-1alpha and -2. *Veterinary Immunology and Immunopathology* **82**: 153-164.

Ehrlich LC, Hu S, Peterson PK, & Chao CC. 1998. IL-10 downregulates human microglial IL-8 by inhibition of NF-kappaB activation. *Neuroreport* **9**: 1723-1726.

Eikelenboom P, Veerhuis R, Scheper W, Rozemuller AJ, van Gool WA, & Hoozemans JJ. 2006. The significance of neuroinflammation in understanding Alzheimer's disease. *Journal of Neural Transmission* **113**: 1685-1695.

Eissner G, Kirchner S, Lindner H, Kolch W, Janosch P, Grell M, Scheurich P, Andreesen R, & Holler E. 2000. Reverse signaling through transmembrane TNF confers resistance to lipopolysaccharide in human monocytes and macrophages 1. *Journal of Immunology* **164**: 6193-6198.

Eissner G, Kolch W, & Scheurich P. 2004. Ligands working as receptors: Reverse signaling by members of the TNF superfamily enhance the plasticity of the immune system. *Cytokine Growth Factor Review* **15**: 353-366.

Ekdahl CT, Claasen JH, Bonde S, Kokaia Z, & Lindvall O. 2003. Inflammation is detrimental for neurogenesis in adult brain. *Proceedings of the National Academy of Sciences USA* **100**: 13632-13637.

Ekdahl CT, Kokaia Z, & Lindvall O. 2009. Brain inflammation and adult neurogenesis: The dual role of microglia. *Neuroscience* **158**: 1021-1029.

Eksandh LB, Ponjavic VB, Munroe PB, Eiberg HE, Uvebrandt PE, Ehiunger BE, Mole SE, & Andreasson S. 2000. Full-field ERG in patients with Batten/Spielmeyer-Vogt disease caused by mutation in the CLN3 gene. *Opthalamic Genetics* **21**: 69-77.

Elleder M, Sokolová J, & Hrebícek M. 1997. Follow-up study of subunit c of mitochondrial ATP synthase (SCMAS) in Batten disease and in unrelated lysosomal disorders. *Acta Neuropathologica* **93**: 379-390.

Elleder M, Lake BD, Goebel HH, Rapola J, Haltia M, & Carpenter S. 1999. Definitions of the ultrastructural patterns found in NCL. In: *The Neuronal Cereoid Lipofuscinoses (Batten Disease)* (Goebel HH, Mole SE, & Lake BD, eds), p. 5-15, IOS Press, Amsterdam.

Encinas JM, Vaahtokari A, & Enikolopov G. 2006. Fluoxetine targets early progenitor cells in the adult brain. *Proceedings of the National Academy of Sciences USA* **103**: 8233-8238.

Eriksson PS, Perfilieva E, Bjork-Eriksson T, Alborn AM, Nordborg C, Peterson DA, & Gage FH. 1998. Neurogenesis in the adult human hippocampus. *Nature Medicine* **4**: 1313-1317.

Escolar ML, Poe MD, Provenzale JM, Richards KC, Allison J, Wood S, Wenger DA, Pietryga D, Wall D, Champagne M, Morse R, Krivit W, & Kurtzberg J. 2005. Transplantation of umbilical-cord blood in babies with infantile Krabbe's disease. *New England Journal of Medicine* **352**: 2069-2081.

Evans MJ & Kaufman MH. 1981. Establishment in culture of pluripotential cells from mouse embryos. *Nature* **292**: 154-156.

Ezaki J, Tanida I, Kanehagi N, & Kominami E. 1999. A lysosomal proteinase, the late infantile neuronal ceroid lipofuscinosis gene (CLN2) product, is essential for degradation of a hydrophobic protein, the subunit c of ATP synthase. *Journal of Neurochemistry* **72**: 2573-2582.

Ezaki J, Takeda-Ezaki M, Koike M, Ohsawa Y, Taka H, Mineki R, Murayama K, Uchiyama Y, Ueno T, & Kominami E. 2003. Characterization of Cln3p, the gene product responsible for juvenile neuronal ceroid lipofuscinosis, as a lysosomal integral membrane glycoprotein. *Journal of Neurochemistry* **87**: 1296-1308.

Fakioglu E, Wilson SS, Mesquita PMM, Hazrati E,& Cheshenko N, Blaho JA, & Heroldi BC. 2008. Herpes Simplex virus downregulates secretory leukocyte protease inhibitor: A novel immune evasion mechanism. *Journal of Virology* **82**: 9337-9344.

Falconer DS & Avery PJ. 1978. Variability of chimeras and mosaics. *Journal of Embryology and Chimeric Morphology* **43**:195-219.

Fearnley IM, Walker JE, Martinaus RD, Jolly RD, Kirkland KB, Shaw GJ, & Palmer DN. 1990. The sequence of the major protein stored in ovine ceroid lipofuscinosis is identical with that of the dicyclohexylcarbodiimide-reactive proteolipid of mitochondrial ATP synthase. *Biochemical Journal* **268**: 751-758.

Fedorova E, Battini L, Prakash-Cheng A, Marras D, & Gusella GL. 2006. Lentiviral gene delivery to CNS by spinal intrathecal administration to neonatal mice. *Journal of Gene Medicine* **8**: 414-424.

Fehilly CB, Willadsen SM, & Tucker EM. 1984a. Interspecific chimerism between sheep and goat. *Nature* **307**: 634-636.

Fehilly CB, Willadsen SM, & Tucker EM. 1984b. Chimeric chimaerism in sheep. *Journal of Reproduction and Fertility* **70**: 347-351.

Ferrer I, Soriano E, Del Rio JA, Alcantara S, & Auladell C. 1992. Cell death and removal in the cerebral cortex during development. *Progress in Neurobiology* **39**: 1-43.

Fischer W, Wictorin K, Björklund A, Williams LR, Varon S, & Gage FH. 1987. Amelioration of cholinergic neuron atrophy and spatial memory impairment in aged rats by nerve growth factor. *Nature* **329**: 65-68.

Fisk R & Storts R. 1988. Neuronal ceroid-lipofuscinosis in Nubian goats. *Veterinary Pathology* **25**: 171-173.

Fossale E, Wolf P, Espinola JA, Lubicz-Nawrocka T, Teed AM, Gao H, Dorotea Rigamonti D, Cattaneo E, MacDonald ME, & Cotman SL. 2004. Membrane trafficking and mitochondrial abnormalities precede subunit c deposition in a cerebellar cell model of juvenile neuronal ceroid lipofuscinosis. *BMC Neuroscience* **5**: 57.

Fox CH, Johnson FB, Whiting J, & Roller PP. 1985. Formaldehyde fixation. *Journal of Histochemistry and Cytochemistry* **33**: 845-853.

Frank-Cannon TC, Alto LT, McAlpine FE, & Tansey MG. 2009. Does neuroinflammation fan the flame in neurodegenerative diseases? *Molecular Neurodegeneration* **4**: 47.

Frantantoni JC, Hall CW, & Neufeld EF. 1969. Hurler and Hunter syndromes: Mutual correction of the defect in cultured fibroblasts. *Science* **162**: 570-572.

Freeman WM, Walker SJ, & Vrana KE. 1999. Quantitative RT-PCR: Pitfalls and potential. *Biotechniques* **26**: 112-122.

Frei K, Lins H, Schwerdel C, & Fontana A. 1994. Antigen presentation in the central nervous system. The inhibitory effect of IL-10 on MHC class II expression and production of cytokines depends on the inducing signals and the type of cell analysed. *Journal of Immunology* **152**: 2720-2728.

Frielingsdorf J, Schwarz K, Brundin P, & Mohapel P. 2004. No evidence for new dopaminergic neurons in the adult mammalian substantia nigra. *Proceedings of the National Academy of Sciences USA* **101**: 10177-10182.

Fritschy JM, Weinmann O, Wenzel A, & Benke D. 1998. Synapse-specific localization of NMDA and GABA (A) receptor subunits revealed by antigen-retrieval immunohistochemistry. *Journal of Comparative Neurology***390**: 194-210.

Frugier T, Mitchell NL, Tammen I, Houweling PJ, Arthur DG, Kay GW, Van Diggelen OP, Jolly RD, & Palmer DN. 2008. A new large animal model of CLN5 neuronal ceroid lipofuscinosis in Borderdale sheep is caused by a nucleotide substitution at a consensus splice site (c.571+1G>A) leading to excision of exon 3. *Neurobiology of Disease* **29**: 306-315.

Gage FH. 2000. Mammalian neural stem cells. *Science* **287**: 1433-1438.

Gagliardi C & Bunnell BA. 2009. Large animal models of neurological disorders for gene therapy. *Institute for Laboratory Animal Research Journal* **50**: 128-143.

Gall JG & Pardue M. 1969. Formation and detection of RNA-DNA hybrid molecules in cytological preparations. *Proceedings of the National Academy of Sciences USA* **63**: 378-383.

Gao H, Boustany RM, Espinola JA, Cotman SL, Srinidhi L, Antonellis KA, Gillis T, Qin X, Liu S, Donahue LR, Bronson RT, Faust JR, Stout D, Haines JL, Lerner TJ, & MacDonald ME. 2002a. Mutations in a novel CLN6-encoded transmembrane protein cause variant neuronal ceroid lipofuscinosis in man and mouse. *American Journal of Human Genetics* **70**: 324-335.

Gao HM, Jiang J, Wilson B, Zhang W, Hong JS, & Liu B. 2002b. Microglial activation-mediated delayed and progressive degeneration of rat nigral dopaminergic neurons: Relevance to Parkinson's disease. *Journal of Neurochemistry* **81**: 1285-1297.

Gao HM, Liu B, Zhang W, & Hong JS. 2003. Novel anti-inflammatory therapy for Parkinson's disease. *Trends in Pharmacological Sciences* **24**: 395-401.

García-Vallejo JJ, Van het Hof B, Robben J, Van Wijk JAE, Van Die I, Joziasse DH & Van Dijk K. 2004. Approach for defining endogenous reference genes in gene expression experiments. *Analytical Biochemistry* **329**: 293-299.

Gardner RL. 1971. Manipulations on the blastocyst. *Advances in the Biosciences* **6**: 279-296.

Garner W & McLaren A. 1974. Cell distribution in chimaeric mouse embryos before implantation. *Journal of Embryology and Experimental Morphology* **32**: 495-503.

Ge S, Goh EL, Sailor KA, Kitabatake Y, Ming GL, & Song H. 2006. GABA regulates synaptic integration of newly generated neurons in the adult brain. *Nature* **439**: 589-593.

Gebicke-Haerter PJ. 2001. Microglia in neurodegeneration: Molecular aspects. *Microscopy Research Techniques* **54**: 47-58.

Giulietti A, Overbergh L, Valckx D, Decallonne B, Bouillon R, & Mathieu C. 2001. An overview of real-time quantitative PCR: Applications to quantify cytokine gene expression. *Methods* **25**: 386-401.

Goebel HH. 1995. The neuronal ceroid-lipofuscinoses. *Journal of Child Neurology* **10**: 424-437.

Goebel HH, Mole SE, & Lake BD (eds.). 1999a. *The Neuronal Ceroid Lipofuscinosis (Batten disease,* IOS Press, Amsterdam.

Goebel HH, Schochet SS, Jaynes M, Bruck W, Kohlschütter A, & Hentati F. 1999b. Progress in neuropathology of the neuronal ceroid lipofuscinoses. *Molecular Genetics and Metabolism* **66**: 367-372.

Goebel HH. 2000. The new nosography of the neuronal ceroid lipofusinoses. *Annals of Pathology* **20**: 479-491.

Goebel HH & Wisniewski KE. 2004. Current state of clinical and morphological features in human NCL. *Brain Pathology* **14**: 61-69. .

Goldman SA & Nottebohm F. 1983. Neuronal production, migration and differentiation in a vocal control nucleus of the adult female canary brain. *Proceedings of the National Academy of Sciences USA* **80**: 2390-2394.

Goldowitz D, Moran TH, & Wetts R. 1992. Mouse chimeras in the study of genetic and structural determinants of behavior. In: *Techniques for the Generic Analysis of Brain and Behaviour* (Goldowitz D, Wahlsten D, & Wimer RE, eds.), pp. 271-290, Elsevier, Amsterdam.

González L, Anderson I, Deane D, Summers C, & Buxton D. 2001. Detection of immune system cells in paraffin wax-embedded ovine tissues. *Journal of Comparative Pathology* **125**: 41-47.

Gould E, Reeves AJ, Graziano MS, & Gross CG. 1999. Neurogenesis in the neocortex of adult primates. *Science* **286**: 548-552.

Gould E, Vail N, Wagers M, & Gross CG. 2001. Adult-generated hippocampal and neocortical neurons in macaques have a transient existence. *Proceedings of the National Academy of Science USA* **98**: 10910-10917.

Grabowski GA, Barton NW, Pastores G, Dambrosia JM, Banerjee TK, McKee MA, Parker C, Schiffmann R, Hill SC, & Brady RO. 1995. Enzyme therapy in type I Gaucher disease: Comparative efficacy of mannose–terminated glucocerebrosidase from natural and recombinant sources. *Annals of Internal Medicine* **122**: 33-39.

Graydon RJ & Jolly RD. 1984. Ceroid-lipofuscinosis (Batten's disease). Sequential electrophysiologic and pathologic changes in the retina of the ovine model. *Investigative Ophthalmology and Visual Science* **25**: 294-301.

Green PD & Little PB. 1974. Neuronal ceroid-lipofuscin storage in Siamese cat. *Canadian Journal of Comparative Medicine* **38**: 207-212.

Greenberg DA & Jin K. 2007. Regenerating the brain. *International Review of Neurobiology* **77**: 1-29.

Grell M, Douni E, Wajant H, Löhden M, Clauss M, Maxeiner B, Georgopoulos S, Lesslauer W, Kollias G, Pfizenmaier K, & Scheurich P. 1995. The transmembrane form of tumor necrosis factor is the prime activating ligand of the 80kDa tumor necrosis factor receptor. *Cell* **83**: 793-802.

Griffey M, Bible E, Vogler C, Levy B, Gupta P, Cooper J, & Sands MS. 2004. Adeno-associated virus 2-mediated gene therapy decreases autofluorescent storage material and increases brain mass in a murine model of infantile neuronal ceroid lipofuscinosis. *Neurobiology of Disease* **16**: 360-369.

Griffey M, Macauley SL, Ogilvie JM, & Sands MS. 2005. AAV2-mediated ocular gene therapy for infantile neuronal ceroid lipofuscinosis. *Molecular Therapy* **12**: 413-421.

Griffin DE. 1997. Cytokines in the brain during viral infection: Clues to HIV-associated dementia. *Journal of Clinical Investigation* **100**: 2948-2951.

Grimes ML, Zhou J, Beattie EC, Yuen EC, Hall DE, Valletta JS, Topp KS, LaVail JH, Bunnett NW, & Mobley WC. 1996. Endocytosis of activated TrkA: Evidence that nerve growth factor induces formation of signaling endosomes. *Journal of Neuroscience* **16**: 7950-7964.

Guarneri R, Russo D, Cascio C, D'Agostino S, Galizzi G, Bigini P, Mennini T, & Guarneri P. 2004. Retinal oxidation, apoptosis and age- and sex-differences in the mnd mutant mouse, a model of neuronal ceroid lipofuscinosis. *Brain Research* **1014**: 209-220.

Hachiya Y, Hayashi M, Kumada S, Uchiyama A, Tsuchiya K, & Kurata K. 2006. Mechanisms of neurodegeneration in neuronal ceroid-lipofuscinoses. *Acta Neuropathologica* **111**: 168-177.

Hackett NR, Redmond DE, Sondhi D, Giannaris EL, Vassallo E, Stratton J, Qiu J, Kaminsky SM, Lesser ML, Fisch GS, Rouselle SD, & Crystal RG. 2005. Safety of direct administration of $AAV2_{CU}$hCLN2, a candidate treatment for the central nervous system manifestations of late infantile neuronal ceroid lipofuscinosis, to the brain of rats and nonhuman primates. *Human Gene Therapy* **16**: 1484-1503.

Hall NA, Jolly RD, Palmer DN, Lake BD, & Patrick AD. 1989. Analysis of dolichyl pyrophosphoryl oligosaccharides in purified storage cytosomes from ovine ceroid-lipofuscinosis. *Biochimica et Biophysica Acta* **993**: 245-251.

Hall NA, Lake BD, Dewji NN, & Patrick AD .1991. Lysosomal storage of subunit c of mitochondrial ATP synthase in Batten's disease (ceroid-lipofuscinosis). *Biochemical Journal* **275**: 269-272.

Haltia M, Rapola P, Santavuori P, & Keränen A. 1973a. Infantile type of so-called neuronal ceroid-lipofuscinosis. Part 2, Morphological and biochemical ctudies. *Journal of the Neurological Sciences* **18**: 269-285.

Haltia M, Rapola P, & Santavuori P. 1973b. Infantile type of so-called neuronal ceroid-lipofuscinosis. Histological and electron microscopic studies. *Acta Neuropathologica* **26**: 157-170.

Haltia M. 2003. The neuronal ceroid-lipofuscinosis. *Journal of Neuropathology and Experimental Neurology* **62**: 1-13.

Hanisch UK. 2002. Microglia as a source and target of cytokines. *Glia* **40**: 140-155.

Harper PA, Walker KH, Healy PJ, Hartley WJ, Gibson AJ, & Smith JS. 1988. Neurovisceral ceroid-lipofuscinosis in blind Devon cattle. *Acta Neuropathologica* **75**: 632-636.

Haskell RE, Hughes SM, Chiorini JA, Alisky JM, & Davidson BL. 2003. Viral-mediated delivery of the late-infantile neuronal ceroid lipofuscinosis gene, TPP-I to the mouse central nervous system. *Gene Therapy* **10**: 34-42.

Haskins M. 2009. Gene therapy for lysosomal storage diseases (LSDs) in large animal models. *Institute for Laboratory Animal Research Journal* **50**: 112-121.

Heese BA. 2008. Current strategies in the management of lysosomal storage diseases. *Seminars in Paediatric Neurology* **15**: 119-126.

Heine C, Koch B, Storch S, Kohlschütter A, Palmer DN, & Braulke T. 2004a. Defective endoplasmic reticulum-resident membrane protein CLN6 affects lysosomal degradation of endocytosed arylsulfatase A. *Journal of Biological Chemistry* **279**: 22347-22352.

Heine VM, Maslam S, Joels M, & Lucassen PJ. 2004b. Prominent decline of newborn cell proliferation, differentiation, and apoptosis in the aging dentate gyrus, in absence of an age-related hypothalamus-pituitary-adrenal axis activation. *Neurobiology of Aging* **25**: 361-375.

Heldmann U, Thored P, Claasen JH, Arvidsson A, Kokaia Z, & Lindvall O. 2005. TNF-alpha antibody infusion impairs survival of stroke-generated neuroblasts in adult rat brain. *Experimental Neurology* **196**: 204-208.

Henderson LP, Lin L, Prasad A, Paul CA, Chang TY, & Maue RA. 2000. Embryonic striatal neurons from niemann-pick type C mice exhibit defects in cholesterol metabolism and neurotrophin responsiveness. *Journal of Biological Chemistry* **275**: 20179-20187.

Herpin A, Lelong C, & Favrel P. 2004. Transforming growth factor-beta-related proteins: An ancestral and widespread superfamily of cytokines in metazoans. *Developmental and Comparative Immunology* **28**: 461-485.

Herrup K & Mullen RJ. 1979. Staggerer chimeras: Intrinsic nature of Purkinje cell defects and implications for normal cerebellar development. *Brain Research* **178**: 443-457.

Herva R, Tyynela J, Hirvasniemi A, Syrjakallio-Ylitalo M, & Haltia M. 2000. Northern epilepsy: A novel form of neuronal ceroid-lipofuscinosis. *Brain Pathology* **10**: 215-222.

Hickey WF. 1999. Leukocyte traffic in the central nervous system: The participants and their roles. *Seminars in Immunology* **11**: 125-137.

Hirsch EC, Hunot S, Damier P, & Faucheux B. 1998. Glial cells and inflammation in Parkinson's disease: A role in neurodegeneration? *Annals of Neurology* **44**: 115-120.

Hobert JA & Dawson G. 2006. Neuronal ceroid lipofuscinoses therapeutic strategies: Past, present and future. *Biochimica et Biophysica Acta* **1762**: 945-953.

Hoglinger GU, Rizk P, Muriel MP, Duyckaerts C, Oertel WH, Caille I, & Hirsch EC. 2004. Dopamine depletion impairs precursor cell proliferation in Parkinson's disease. *Nature Neuroscience* **7**: 726-735.

Houweling PJ, Cavanagh JAL, Palmer DN, Frugier T, Mitchell NL, Windsor PA, Raadsma HW, & Tammen I. 2006. Neuronal ceroid lipofuscinosis in Devon cattle is caused by a single base duplication (c.Gdup662) in the bovine CLN5 gene. *Biochimica et Biophysica Acta* **1762**: 890-897.

Houweling PJ. 2009. The molecular characterisation of large animal models for neuronal ceroid lipofuscinosis. Unpublished PhD thesis, *University of Sydney*, Sydney, Australia.

Howe CL, Valletta JS, Rusnak AS, & Mobley WC. 2001. NGF signaling from clathrin-coated vesicles: Evidence that signalling endosomes serve as a platform for the Ras-MAPK pathway. *Neuron* **32**: 801-814.

Huggett J, Dheda K, Bustin S, & Zumla A. 2005. Real-time PCR normalisation; strategies and considerations. *Genes and Immunity* **6**: 279-184.

Hughes SM, Moussavi-Harami F, Sauter SL, & Davidson BL. 2002. Viral-mediated gene transfer to mouse primary neural progenitor cells. *Molecular Therapy* **5**: 16-24.

Hunot S & Hirsch EC. 2003. Neuroinflammatory processes in Parkinson's disease. *Annals of Neurology* **53**: 49-60.

Idriss HT & Naismith JH. 2000. TNF alpha and the TNF receptor superfamily: Structure-function relationship(s). *Microscopy Research and Technique* **50**: 184-195.

Imitola J, Raddassi K, Park KI, Mueller FJ, Nieto M, Teng YD, Frenkel D, Li J, Sidman RL, Walsh CA, Snyder EY, & Khoury SJ. 2004. Directed migration of neural stem cells to sites of CNS injury by the stromal cell-derived factor 1alpha/CXC chemokine receptor 4 pathway. *Proceedings of the National Academy of Sciences USA* **101**: 18117-18122.

Iosif RE, Ekdahl CT, Ahlenius H, Pronk CJ, Bonde S, Kokaia Z, Jacobsen SE, & Lindvall O. 2006. Tumour necrosis factor receptor 1 is a negative regulator of progenitor proliferation in adult hippocampal neurogenesis. *Journal of Neuroscience* **26**: 9703-9712.

Iosif RE, Ahlenius H, Ekdahl CT, Darsalia V, Thored P, Jovinge S, Kokaia Z, & Lindvall O. 2008. Suppression of stroke-induced progenitor proliferation in adult subventricular zone by tumour necrosis factor receptor 1. *Journal of Cerebral Blood Flow & Metabolism* **28**: 1574-1587.

Itoh S, Itoh F, Goumans MJ, & Tendijke P. 2000. Signaling of transforming growth factor-β family members through Smad proteins. *European Journal of Biochemistry* **267**: 6954-6967.

Ivan CS, Saint-Hilaire MH, Christensen TG, & Milunsky JM. 2004. Adult-onset neuronal ceroid lipofuscinosis type B in an African-American. *Movement Disorders* **20**: 752-754.

Jakobsson J, Ericson C, Jansson M, Björk E, & Lundberg C. 2003. Targeted transgene expression in rat brain using lentiviral vectors. *Journal of Neuroscience Research* **73**: 876-885.

Jansky J. 1908. Dosud nepopsaný pripad familiarni amaurotické idiotie komplikované s hypoplasii mozeckovou. *Sborn Lék* **13**: 165-196.

Jeyakumar M, Thomas R, Elliot-Smith E, Smith DA, van der Spoel AC, d'Azzo A, Perry VH, Butters TD, Dwek RA, & Platt FM. 2003. Central nervous system inflammation is a hallmark of pathogenesis in mouse models of GM1 and GM2 gangliosidosis. *Brain* **126**: 974-987.

Jin K, Zhu Y, Sun Y, Mao XU, Xie L, & Greenberg DA. 2002. Vascular endothelial growth factor (VEGF) stimulates neurogenesis *in vitro* and *in vivo. Proceedings of the National Academy of Sciences USA* **99**: 11946-11950.

Jin K, Sun Y, Xie L, Peel A, Mao XO, Batteur S, & Grenberg DA. 2003. Directed migration of neuronal precursors into the ischemic cerebral cortex and striatum. *Molecular and Cellular Neuroscience* **24**: 171-189.

Jin K, Peel AL. Mao XO, Xie L, Cottrell BA, Henshall DC, & Greenberg DA. 2004. Increased hippocampal neurogenesis in Alzheimer's disease. *Proceedings of the National Academy of Sciences USA* **101**: 343-347.

Jin K, Wang X, Xie L, Mao XO, Zhu W, Wang Y, Shen J, Mao Y, Banwait S, & Greenberg DA. 2006. Evidence for stroke-induced neurogenesis in the human brain. *Proceedings of the National Academy of Sciences USA* **103**: 134198-13202.

Johansson CB, Momma S, Clarke DL, Risling M, Lendahl U, & Frisen J. 1999. Identification of a neural stem cell in the adult mammalian central nervius system. *Cell* **96**: 25-34.

John HA, Birnstiel ML, & Jone KW. 1969. RNA-DNA hybrids at the cytological level. *Nature* **223**: 582-587.

Jolly RD & West DM. 1976. Blindness in South Hampshire sheep: A neuronal ceroid-lipofuscinosis. *New Zealand Veterinary Journal* **24**: 1-23.

Jolly RD, Thompson KG, Murphy CE, Manktelow BW, Bruere AN, & Winchester BG. 1976. Enzyme replacement therapy- An experiment of nature in a chimeric mannosidosis calf. *Pediatric Research* **10**: 219-224.

Jolly RD, Janmaat A, West DM, & Morrison I. 1980. Ovine ceroid-lipofuscinosis: A model of Batten's disease. *Neuropathology and Applied Neurobiology* **6**: 195-209

Jolly RD, Janmaat A, Graydon RJ, & Clemett RS. 1982. Ovine ceroid-lipofuscinosis: The ovine model. In: *Ceroid Lipofuscinoses (Batten disease)* (Armstrong D, Koppang N, & Rider JA, eds.), p. 219-228, Elsevier Biomedical Press, Amsterdam.

Jolly RD, Shimada A, Craig AS, Kirkland KB, & Palmer DN. 1988. Ovine ceroid-lipofuscinosis II: Pathologic changes interpreted in light of biochemical observations. *American Journal of Medical Genetics* **5**: 159-70.

Jolly RD, Shimada A, Dopfmer I, Slack PM, Birtles MJ, & Palmer DN. 1989. Ceroid-lipofuscinosis (Batten's disease): Pathogenesis and sequential neuropathological changes in the ovine model. *Neuropathology and Applied Neurobiology* **15**: 371-383.

Jolly RD, Martinus RD, & Palmer DN. 1992. Sheep and other animals with ceroid-lipofuscinoses: Their relevance to Batten disease. *American Journal of Medical Genetics* **42**: 609-614.

Jolly RD, Palmer DN, Stubbert V, Sutton R, Kelly W, Koppang N, Dahme G, Hartley WJ, Patterson J, & Riis R. 1994. Canine ceroid-lipofuscinoses: A review and classification. *Journal of Small Animal Practice* **35**: 299-306.

Jolly RD & Palmer DN. 1995. The neuronal ceroid-lipofuscinoses (Batten disease): Comparative aspects. *Neuropatholgy and Applied Neurobiology* **21**: 50-60.

Jolly RD, Arthur DG, Kay GW, & Palmer DN. 2002. Neuronal ceroid-lipofuscinosis in Borderdale sheep. *New Zealand Veterinary Journal* **50**: 199-202.

Josephson SA, Schmidt RE, Millsap P, McManus DQ, & Morris JC. 2001. Autosomal dominant Kufs' disease: A cause of early onset dementia. *Journal of the Neurological Sciences* **188**: 51-60.

Kakkis E, McEntee M, Vogler C, Le S, Levy B, Belichenko P, Mobley W, Dickson P, Hanson S, & Passage M. 2004. Intrathecal enzyme replacement therapy reduces lysosomal storage in the brain and meninges of the canine model of MPS I. *Molecular Genetics and Metabolism* **83**: 163-174.

Kaplan MS & Hinds JW. 1977. Neurogenesis in the adult rat: Electron microscopic analysis of light radioautographs. *Science* **197**: 1092-1094.

Kasper D, Planells-Cases R, Fuhrmann JC , Scheel O, Zeitz O, Ruether K, Schmitt A, Poet M, Steinfeld R, Schweizer M, Kornak U, & Jentsch TJ. 2005. Loss of the chloride channel CIC-7 leads to lysosmal storage disease and neurodegeneration. *EMBO Journal* **24**: 1079-1091.

Katz ML, Khan S, Awano T, Shahid SA, Siakotos AN, & Johnson GS. 2005. A mutation in the CLN8 gene in English Setter dogs with neuronal ceroid-lipofuscinosis. *Biochemical and Biophysical Research Communications* **327**: 541-547.

Kaul M. 2008. HIV's double strike at the brain: neuronal toxicity and compromised neurogenesis. *Frontiers in Bioscience* **13**: 2484-2494.

Kay GW, Hughes SM, & Palmer DN. 1999. *In vitro* culture of neurons from sheep with Battens disease. *Molecular Genetics and Metabolism* **67**: 83-88.

Kay GW, Palmer DN, Rezaie P, & Cooper JD. 2006. Activation of non-neuronal cells within the prenatal developing brain of sheep with neuronal ceroid lipofuscinosis (CLN6). *Brain Pathology* **16**: 110-116.

Kay GW, Jay NP, & Palmer DN. 2011. The specific loss of GnRH positive neurons from the hypothalamus of sheep with CLN6 neuronal ceroid lipofuscinosis occurs without glial activation and has only minor effects on reproduction. *Neurobiology of Disease* **41**: 614-623.

Kempermann G, Kuhn HG, & Gage FH. 1997. More hippocampal neurons in adult mice living in an enriched environment. *Nature* **386**: 493-495.

Kida E, Wisniewski KE, & Golabek AA. 1993. Increased expression of subunit c of mitochondrial ATP synthase in brain tissue from neuronal ceroid lipofuscinoses and mucopolysaccharidosis cases but not in long-term fibroblast cultures. *Neuroscience Letters* **164**: 121-124.

Kielar C, Maddox L, Bible E, Pontikis CC, Macauley SL, Griffey MA, Wong M, Sands MS, & Cooper JD. 2007. Successive neuron loss in the thalamus and cortex in a mouse model of infantile neuronal ceroid lipofuscinosis. *Neurobiology of Disease* **25**: 150-162.

Kim YS & Joh TH. 2006. Microglia, major player in the brain inflammation: Their roles in the pathogenesis of Parkinson's disease. *Experimental and Molecular Medicine* **38**: 333-347.

Kim SJ, Zhang Z, Hitomi E, Lee YC, & Mukherjee AB. 2006. Endoplasmic reticulum stress-induced caspase-4 activation mediates apoptosis and neurodegeneration in INCL. *Human Molecular Genetics* **15**: 1826-1834.

Kinjyo I, Hanada T, Inagaki-Ohara K, Mori H, Aki D, Ohishi M, Yoshida H, Kubo M, & Yoshimura A. 2002. SOCS1/JAB is a negative regulator of LPS-induced macrophage activation. *Immunity* **17**: 583-591.

Klenk E. 1939. Beiträge zur Chemie der Lipidosen, Niemann–Picksche Krankheit und amarotische Idiotie. *Hoppe-Seyler Z Physiol Chem* **262**: 128-143.

Knight PA, Pate J, Smith WD, & Miller HRP. 2007. An ovine chitinase-like molecule, chitinase-3 like-1 (YKL-40), is upregulated in the abomasum in response to challenge with the gastrointestinal nematode, Teladorsagia circumcincta. *Veterinary Immunology and Immunopathology* **120**: 55-60.

Koenigsknecht-Talboo J & Landreth GE. 2005. Microglial phagocytosis induced by fibrillar beta-amyloid and IgGs are differentially regulated by proinflammatory cytokines. *Journal of Neuroscience* **25**: 8240-8249.

Kohan R, de Halac IN, Anzolini VT, Cismondi A, Ramirez AMO, Capra AP, & de Kremer RD. 2005. Palmitoyl Protein Thioesterase1 (PPT1) and Tripeptidyl Peptidase-I (TPP-I) are expressed in human saliva. A reliable and non-invasive source for the diagnosis of infantile (CLN1) and late infantile (CLN2) neuronal ceroid lipofuscinosis. *Clinical Biochemistry* **38**: 492-494.

Koike M, Shibata M, Waguri S, Yoshimura K, Tanida I, Kominami E, Gotow T, Peters C, von Figura K, Mizushima N, Saftig P, & Uchiyama Y. 2005. Participation of autophagy in storage of lysosomes in neurons from mouse models of neuronal ceroid lipofuscinosis (Batten disease). *American Journal of Pathology* **167**: 1713-1728.

Koketsu D, Mikami A, Miyamoto Y, & Hisatsune T. 2003. Nonrenewal of neurons in the cerebral neocortex of adult macaque monkeys. *Journal of Neuroscience* **23**: 937-942.

Kominami E, Ezaki J, Muno D, Ishido K, Ueno T, & Wolfe LS. 1992. Specific storage of subunit c of mitochondrial ATP synthase in lysosomes of neuronal ceroid lipofuscinosis (Batten's disease). *Journal of Biochemistry* **111**: 278-282.

Konnai S, Usui T, Ohashi K, & Onuma M. 2003. The rapid quantitative analysis of bovine cytokine genes by real-time RT-PCR. *Veterinary Microbiology* **94**: 283-294.

Kootstra NA & Verma IM. 2003. Gene therapy with viral vectors. *Annual Review of Pharmacology and Toxicology* **43**: 413-439.

Kopan S, U, & Warburton MJ. 2004. The lysosomal degradation of neuromedin B is dependent on tripeptidyl peptidase-I: Evidence for the impairment of neuropeptide degradation in late-infantile neuronal ceroid lipofuscinosis. *Biochemical and Biophysical Research Communications* **319**: 58-65.

Kordower JH, Emborg ME, Bloch J, Ma SY, Chu Y, Leventhal L, McBride J, Chen EY, Palfi S, Roitberg BZ, Brown WD, Holden JE, Pyzalski R, Taylor MD, Carvey P, Ling Z, Trono D, Hantraye P, Déglon N, & Aebischer P. 2000. Neurodegeneration prevented by lentiviral vector delivery of GDNF in primate models of Parkinson's disease. *Science* **290**: 767-773.

Kornack RD & Rakic P. 2001. Generation and migration of new olfactory neurons in adult primates. *Proceedings of the National Academy of Sciences USA* **98**: 4752-4757.

Kornak U, Kasper D, Bosl MR, Kaiser E, Schweizer M, Schulz A, Friedrich W, Delling G, & Jentsch TJ. 2001. Loss of the ClC-7 chloride channel leads to osteopetrosis in mice and man. *Cell* **104**: 205-215.

Krathwohl MD & Kaiser JL. 2004a. Chemokines promote quiescence and survival of human neural progenitor cells. *Stem Cells* **22**: 109-118.

Krathwohl MD & Kaiser JL. 2004b. HIV-1 promotes quiescence in human neural progenitor cells. *Journal of Infectious diseases* **190**: 216-226.

Krzanowska H. 1967. Cell number in relation to heterosis during embryonic growth of mice. *Genetical Research* **10**: 235-240.

Kuan CY, Elliott EA, Flavell RA, & Rakic P. 1997. Restrictive clonal allocation in the chimeric mouse brain. *Proceedings of the National Academy of Sciences USA* **94**: 3374-3379.

Kufs H. 1925. Über eine Spätform der amaurotischen Idiotie und ihre heredofamiliären Grundlagen. *Zentralblatt der Gesamten Neurologischen Psychiatrie* **95**: 169-188.

Kumar S, Boehm J, & Lee JC. 2003. p38 MAP kinases: Key signalling molecules as therapeutic tarets for inflammatory diseases. *Nature Review Drug Discovery* **2**: 717-726.

Kutty RK, Nagineni CN, Kutty G, Hooks JJ, Chader GJ, & Wiggert B. 1994. Increased expression of heme oxygenase-1 in human retinal pigment epithelial cells by transforming growth factor-beta. *Journal of Cellular Physiology* **159**: 371-378.

Kyttälä A, Ihrke G, Vesa J, Schell MJ, & Luzio JP. 2004. Two motifs target Batten disease protein CLN3 to lysosomes in transfected nonneuronal and neuronal Cells. *Molecular Biology of the Cell* **15**: 1313-1323.

Laemmli UK. 1970. Cleavage of structural proteins during the assembly of the head of bacteriophage T4. *Nature* **227**: 680-685.

Lake BD & Cavanagh NPC. 1978. Early-juvenile Batten's disease: A recognisable subgroup distint from other forms of Batten's disease. *Journal of Neurological Sciences* **36**: 265-271.

Lake BD & Hall NA. 1993. Immunolocalization studies of subunit c in late-infantile and juvenile form of Batten disease. *Journal of Inherited Metabolic Disease* **16**: 263-266.

Lake BD, Steward CG, Oakhill A, Wilson J, & Perham TG. 1997. Bone marrow transplantation in late infantile Batten disease and juvenile Batten disease. *Neuropediatrics* **28**: 80-81.

Laywell ED, Rakic P, Kukekov VG, Holland EC, & Steindler DA. 2000. Identification of a multipotent astrocytic stem cell in the immature and adult mouse brain. *Proceedings of the National Academy of Sciences USA* **97**: 13883-13888.

Lee TS & Chau LY. 2002. Heme oxygenase-1 mediates the anti-inflammatory effect of interleukin-10 in mice. *Nature Medicine* **8**: 240-246.

Lee J, Duan W, & Mattson MP. 2002a. Evidence that brain-derived neurotrophic factor is required for basal neurogenesis and mediates, in part, the enhancement of neurogenesis by dietary restriction in the hippocampus of adult mice. *Journal of Neurochemistry* **82**: 1367-1375.

Lee J, Seroogy KB, & Mattson MP. 2002b. Dietary restriction enhances neurotrophin expression and neurogenesis in the hippocampus of adult mice. *Journal of Neurochemistry* **80**: 539-547.

Lerner TJ, D'Arigo KL, Haines JL, Doggett NA, Taschner PE, de Vos N, & Buckler AJ. 1995. Isolation of genes from the Batten candidate region using exon amplification. Batten Disease Consortium. *American Journal of Medical Genetics* **57**: 320-323.

Letterio JJ & Roberts AB. 1998. Regulation if immune responses by TGFβ. *Annual Review of Immunology* **16**: 137-161.

Levi G, Minghetti L, & Aloisi F. 1998. Regulation of prostanoid synthesis in microglial cells and effects of prostaglandin E2 on microglial functions. *Biochimie* **80**: 899-904.

Lichtenstein M, Zimran AC, & Horowitz M. 1997. Cytokine mRNA in Gaucher Disease. *Blood Cells, Molecules, and Diseases* **23**: 395-401.

Lillie F. 1917. The freemartin: A study of the action of sex hormones in the foetal life of cattle. *Journal of Chimeric Zoology* **23**: 371-452.

Lindvall O & Kokaia Z. 2008. Neurogenesis following stroke affecting the adult brain. In: *Adult Neurogenesis* (Gage FH, Kempermann G, & Song H, eds.), p. 549-570, CSHL Press, Cold Spring Harbor, New York.

Linterman KS, Palmer DN, Kay GW, Barry LA, Mitchell NL, McFarlane RG, Black MA, Sands MS, & Hughes SM. 2011. Lentiviral-mediated gene transfer to the sheep brain: Implications for gene therapy in Batten disease. *Human Gene Therapy* In Press, doi: 10.1089/hum.2011.026

Liu YP, Lin HI, & Tzeng SF. 2005a. Tumor necrosis factor-alpha and interleukin-18 modulate neuronal cell fate in embryonic neural progenitor culture. *Brain Research* **1054**: 152-158.

Liu G, Martins I, Wemmie JA, Chiorini JA, & Davidson BL. 2005b. Functional correction of CNS phenotypes in a lysosomal storage disease model using adeno-associated virus type 4 vectors. *Journal of Neuroscience* **25**: 9321-9327.

Loddick SA & Rothwell NJ. 1996. Neuroprotective effects of human recombinant interleukin-1 receptor antagonist in focal cerebral ischaemia in the rat. *Journal of Cerebral Blood Flow and Metabolism* **16**: 932-940.

Lois C & Alvarez-Buylla A. 1994. Long-distance neuronal migration in the adult mammalian brain. *Science* **264**: 1145-1148.

Lois C, Garcia-Verdugo JM, & Alvarez-Buylla A. 1996. Chain migration of neuronal precursors. *Science* **271**: 978-981.

Long SE. 1980. Some pathological conditions of the reproductive tract of the ewe. *Veterinary Record* **106**: 175-177.

Lonka L, Kyttälä A, Ranta S, Jalanko A, & Lehesjoki AE. 2000. The neuronal ceroid lipofuscinosis CLN8 membrane protein is a resident of the endoplasmic reticulum. *Human Molecular Genetics* **9**: 1691-1697.

Lonnqvist T, Vanhanen SL, Vettenranta K, Autti T, Rapola J, Santavuori P, & Saarinen-Pihkala UM. 2001. Hematopoietic stem cell transplantation in infantile neuronal ceroid lipofuscinosis. *Neurology* **57**: 1411-1416.

Lu J, Verkruyse LA, & Hoffman SL. 2002. The effects of lysosomotropic agents on normal and INCL cells provide further evidence for the lysosomal nature of palmitoyl protein thioesterase function. *Bichemica et Biophysica Acta* **1583**: 35-44.

Lucas SM, Rothwell NJ, and Gibson RM. 2006. The role of inflammation in CNS injury and disease. *British Journal of Pharmacology* **147**: S232-S240.

Luckenbill-Edds L. 1997. Laminin and the mechanism of neuronal outgrowth. *Brain Research Reviews* **23**: 1-27.

Lukacs Z, Santavuori P, Keil A, Steinfeld R, & Kohlschütter A. 2003. A rapid and simple assay for the determination of tripeptidyl peptidase (TPP) and palmitoyl protein thioesterase (PPT) in dried blood spots. *Clinical Chemistry* **49**: 509-511.

MacEwan DJ. 2002. TNF ligands and receptors – a matter of life and death. *British Journal of Pharmacology* **135**: 855-875.

Magavi S, Leavitt BR, & Macklis JD. 2000. Induction of neurogenesis in the neocortex of adult mice. *Nature* **405**: 951-955.

Marcum JB. 1974. The freemartin syndrome. *Animal Breeding Abstracts* **42**: 227-242.

Markakis EA & Gage FH. 1999. Adult-generated neurons in the dentate gyrus send axonal projections to field CA3 and are surrounded by synaptic vesicles. *Journal of Comparative Neurology* **406**: 449-460.

Martin JJ. 1991. Adult type of neuronal ceroid lipofuscinosis. *Developmental Neuroscience* **13**: 331-338.

Martin JJ, Gottlob I, Goebel HH, & Mole S. 1999. CLN4: Adult NCL. In: *The Neuronal Ceroid Lipofuscinoses (Batten Disease)* (Goebel HH, Mole SE, & Lake BD, eds.), p. 77-90, IOS Press, Amsterdam.

Martinus RD, Harper PAW, Jolly RD, Bayliss SL, Midwinter GG, Shaw GJ, & Palmer DN. 1991. Bovine ceroid-lipofuscinosis (batten's disease): The major component stored in the DCCD-reactive proteolipid, subunit C, of mitochondrial ATP synthase. *Veterinary Research Communications* **15**: 85-94

Mattiace LA, Davies P, & Dickson DW. 1990. Detection of HLA-DR on microglia in the human brain is a function of both clinical and technical factors. *American Journal of Pathology* **136**: 1101-1114.

Mattson MP, Barger SW, Furukawa K, Bruce AJ, Wyss-Coray T, Mark RJ, & Mucke L. 1997. Cellular signalling roles of TGF beta, TNF alpa and beta APP in brain injury responses ans Alzheimer's disease. *Brain Research Review* **23**: 47-61.

Mayhew IG, Jolly RD, Pickett BT, & Slack PM. 1985. Ceroid-lipofuscinosis (Batten's disease): Pathogenesis of blindness in the ovine model. *Neuropathology and Applied Neurobiology* **11**: 273-290.

Mazzei R, Conforti FL, Magariello A, Bravaccio C, Militerni R, Gabriele AL, Sampaolo S, Patitucci A, Di Iorio G, Muglia M, & Quattrone A. 2002. A novel mutation in the CLN1 gene in a patient with juvenile neuronal ceroid lipofuscinosis. *Journal of Neurology* **249**: 1398-1400.

McGeer P & E McGeer. 2001. Inflammation, autotoxicity and Alzheimer disease. *Neurobiology of Aging* **22**: 799-809.

McGeer EG & McGeer PL. 2007. The role of anti-inflammatory agents in Parkinson's disease. *CNS Drugs* **21**: 789-797.

McNeilly TN, Baker A, Brown JK, Collie D, MacLachlan G, Rhind SM, & Harkiss GD. 2008. Role of alveolar macrophages in respiratory transmission of Visna/Maedi virus. *Journal of Virology* **82**: 1526-1536.

Medd SM, Walker JE, & Jolly RD. 1993. Characterization of the expressed genes for subunit c of mitochondrial ATP synthase in sheep with ceroid lipofuscinosis. *Biochemical Journal* **293**: 65-73.

Mehl E & Jatzkewitz H. 1964. A cerebrosidesulfatase from swine kidney. *Hoppe-Seylers Zeitschrift für Physiologische Chemie* **339**: 260-276.

Meldgaard M, Fenger C, Lambertsen KL, Pedersen MD, Ladeby R, & Finsen B. 2006. Validation of two reference genes for mRNA level studies of murine disease models in neurobiology. *Journal of Neuroscience Methods* **156**: 101-110.

Melville SA, Wilson CL, Chiang CS, Studdert VP, Lingaas F, & Wilton AN. 2005. A mutation in canine CLN5 causes neuronal ceroid lipofuscinosis in Border collie dogs. *Genomics* **86**: 287-294.

Merrill JE & Benveniste EN. 1996. Cytokines in inflammatory brain lesions: Helpful and harmful. *Trends in Neurosciences* **19**: 331-338.

Minagar A, Shapshak P, Fujimura R, Ownby R, Heyes M, & Eisdorfer C. 2002. The role of macrophage/microglia and astrocytes in the pathogenesis of three neurologic disorders: HIV-associated dementia, Alzheimer disease, and multiple sclerosis. *Journal of Neurological Sciences* **202**: 13-23.

Minghetti L. 2005. Role of inflammation in neurodegenerative diseases. *Current Opinion in Neurology* **18**: 315-321.

Mintz B. 1962. Formation of genotypically mosaic mouse embryos. *American Zoologist* **2**: 432.

Mintz B & Palm J. 1969. Gene control of hematopoiesis. I. Erythrocyte mosaicism and permanent immunological tolerance in allophenic mice. *Journal of Experimental Medicine* **129**: 1013-1027.

Mirescu C, Peters JD, Norman L, & Gould E. 2006. Sleep deprivation inhibits adult neurogenesis in the hippocampus by elevating glucorticoids. *Proceedings of the National Academy of Sciences USA* **103**: 19170-19175.

Mitchell WA, Wheeler RB, Sharp JD, Bate SL, Gardiner RM, Ranta US, Lonka L, Williams RE, Lehesjoki AE, & Mole SE. 2001. Turkish variant late infantile neuronal ceroid lipofuscinosis (CLN7) may be allelic to CLN8. *European Journal of Paediatric Neurology* **5**: 21-27.

Mitchison HM, Lim MJ, & Cooper JD. 2004. Selectivity and typers of cell death in the neuronal ceroid ipofuscinoses. *Brain Pathology* **14**: 86-96.

Mizushima N, Ohsumi Y, & Yoshimori T. 2002. Autophagosome formation in mammalian cells. *Cell Structure and Functions* **27**: 421-429.

Mogi M, Harada M, Riederer P, Narabayashi H, Fujita K, & Nagatsu T. 1994. Tumor necrosis factor-alpha (TNF-alpha) increases both in the brain and in the cerebrospinal fluid from parkinsonian patients. *Neuroscience Letters* **165**: 208-210.

Mole SE, Michaux G, Codlin S, Wheeler RB, Sharp JD, & Cutler DF. 2004. CLN6 which is associated with a lysosomal storage disease, is an endoplasmic reticulem protein. *Experimental Cell Research* **298**: 399-406.

Mole SE, Williams RE, & Goebel HH. 2005. Correlations between genotype, ultrastructural morphology and clinical phenotype in teh neuronal ceroid lipofuscinoses. *Neurogenetics* **6**: 107-126.

Mole SE, Williams RE, & Goebel HH (eds.). 2011. *The Neuronal Ceroid Lipofuscinoses (Batten Disease) 2nd edition*, Oxford University Press Inc., New York.

Monje ML, Toda H, & Palmer TD. 2003. Inflammatory blockade restores adult hippocampal neurogenesis. *Science* **302**: 1760-1765.

Montagne A, Grepinet O, Peloille MP, Lantier F, & Lalmanach AC. 2001. Quantification of ovine cytokine gene expression by a competitive RT–PCR method. *Journal of Immunological Methods* **253**: 83-93.

Moore GE, Gerner RE, & Franklin HA. 1967. Culture of normal human leukocytes. *Journal of the American Medical Association* **199**: 519-524.

Moore KW, Vieira P, Fiorentino DF, Trounstine ML, Khan TA, & Mosmann TR. 1990. Homology of cytokine synthesis inhibitory factor (IL-10) to the Epstein-Barr virus gene BCRFI. *Science* **248**: 1230-1234.

Mrak RE & Griffen WS. 2001. Interleukin-1, neuroinflammation and Alzheimer's disease. *Neurobiology of Aging* **22**: 903-908.

Mrak RE & Griffin WS. 2005. Glia and their cytokines in progression of neurodegeneration. *Neurobiology of Aging* **26**: 349-354.

Mullen RJ & Whitten WK. 1971. Relationship of genotype and degree of chimaerism in coat colour to sex ratios and gametogenesis in chimaeric mice. *Journal of Chimeric Zoology* **178**: 165-176.

Mullen RJ. 1977. Site of pcd gene action and Purkinje cell mosaicism in cerebella of chimaeric mice. *Nature* **270**: 245-247.

Mystkowska ET, Ożdżeński W, & Niemierko A. 1979. Factors regulating the degree and extent of chimeric chimaerism in the mouse. *Journal of Embryology and Experimental Morphology* **51**: 217-225.

Nagatsu T & Sawada M. 2006. Cellular and molecular mechanisms of Parkinson's disease: Neurotoxins, causative genes, and inflammatory cytokines. *Cellular and Molecular Neurobiology* **26**: 781-802.

Nakatomi H, Kuriu T, Okabe S, Yamamoto S, Hatono O, KawaharaN, Tamura A, Kirino T, & Nakafuku M. 2002. Regeneration of hippocampal pyramidal neurons after ischemic brain injury by recruitment of endogenous neural progenitors. *Cell* **110**: 429-441.

Naldini L & Verma IM. 2000. Lentiviral vectors. *Advances in Virus Research* **55**: 599-609.

Nawashiro H, Martin D, & Hallenbeck JM. 1997. Inhibition of tumor necrosis factor and amelioration of brain infarction in mice. *Journal of Cerebral Blood Flow and Metabolism* **17**: 229-232.

Neufeld EF & Fratantoni JC. 1970. Inborn errors of mucopolysaccharide metabolism. *Science* **169**: 141-146.

Neufeld EF & Muenzer J. 1995. The mucopolysaccharidoses. In: *The Metabolic Basis of Inherited Disease* (Sriver CR, Beaudet AL, Sly WS, & Valle D, eds.), p. 2465-2494, McGraw Hill, New York.

Neufeld EF. 2004. Enzyme replacement therapy. In: *Lysosomal Disorders of the Brain* (Platt FM & Walkley SV, eds.), p. 327-338, Oxford University Press, USA.

Neumann H. 2001. Control of glial immune function by neurons. *Glia* **36**: 191-199.

Nguyen L, Rigo JM, Rocher V, Belachew S, Malgrange B, Rogister B, Leprince P, & Moonen G. 2001. Neurotransmitters as early signals for central nervous system development. *Cell and Tissue Research* **305**: 187-202.

Nicholas KB & Deerfield DW. 1997. GeneDoc: Analysis and visulaisation of genetic variation. *EMBnet News.*

O'Brien JS, Miller AL, Loverde AW, & Veath ML. 1973. Sanfilippo disease type B: Enzyme replacement and metabolic correction in cultured fibroblasts. *Science* **181**: 753-755.

O'Brien JS & Kishimoto Y. 1991. Saposin proteins: Structure, function, and role in human lysosomal storage disorders. *Federation for American Societies of Experimental Biology* **5**: 301-308.

Ohmi K, Greenberg DS, Rajavel KS, Ryazantsev S, Li HH, & Neufeld EF. 2003. Activated microglia in cortex of mouse models of mucopolysaccharidoses I and IIIB. *Proceedings of the National Academy of Sciences USA* **100**: 1902-1907.

O'Keefe GM, Nguyen VT, & Benveniste EN. 1999. Class II transactivator and class II MHC gene expression in microglia: Modulation by the cytokines TGF-beta, IL-4, IL-13 and IL-10. *European Journal of Immunology* **29**: 1275-1285.

O'Keefe GM, Nguyen VT, Ping Tang LL, & Benveniste EN. 2001. IFNgamma regulation of class II transactivator promoter IV in macrophages and microglia: Involvement of the suppressors of cytokine signaling-1 protein. *Journal of Immunology* **166**: 2260-2269.

Ono K, Tomasiewicz H, Magnuson T, & Rutishauser UB. 1994. N-CAM mutation inhibits tangential neuronal migration and is phenocopied by enzymatic removal of polysialic acid. *Neuron* **13**: 595-609.

Oppenheim RW. 1991. Cell death during development of the nervous system. *Annual Review of Neuroscience* **14**: 453-501.

Osten P, Dittgen T, & Licznerski P. 2006. Lentivirus-based genetic manipulations in neurons *in vivo*. In: *The Dynamic Synpase: Molecular Methods in Ionotropic Receptor Biology* (Kittler JT & Moss SJ, eds.), Taylor & Francis Group, FL, USA.

Ostensen ME, Thiele DL, & Lipsky PE. 1989 Enhancement of human natural killer cell function by the combined effects of tumor necrosis factor alpha or interleukin-1 and interferon-alpha or interleukin-2. *Journal of Biological Response Modifiers* **8**: 53-61.

Oswald MJ, Kay GW, & Palmer DN. 2001. Changes in GABAergic neuron distribution *in situ* and in neuron cultures in ovine (OCL6) Batten disease. *European Journal of Paediatric Neurology* **5**: 135-142.

Oswald MJ, Kay GW, Shemilt SJA, Rezaie P, Cooper JD, & Palmer DN. 2005. Glial activation spreads from specific cerebral foci and precedes neurodegeneration in presymptomatic ovine neuronal ceroid lipofuscinosis (CLN6). *Neurobiology of Disease* **20**: 49-63.

Oswald MJ, Palmer DN, Kay GW, Barwell KJ, & Cooper JD. 2008. Location and connectivity determine GABAergic interneuron survival in the brains of South Hampshire sheep with CLN6 neuronal ceroid lipofuscinosis. *Neurobiology of disease* **32**: 50-65.

Padula AM. 2005. The freemartin syndrome: An update. *Animal Reproduction Science* **87**: 93-109.

Paganelli R, Di lorio A, Patricelli L, Ripani F, Sparvieri E, Faricelli R, Iarlori C, Porreca E, Di Gioacchino M, & Abate G. 2002. Proinflammatoy cytokines in sera of elderly patients with dementia: Levels in vascular injury are higher than those of mild-moderate Alzheimer's disease patients. *Experimental Gerontology* **37**: 257-263.

Paldi A, Nagy A, Markkula M, Barna I, & Dezso I. 1989. Postnatal development of parthenogenetic - fertilized mouse aggregation chimeras. *Development* **105**: 115-118.

Palmer DN, Husbands DR & Jolly RD. 1985. Phospholipid fatty acids in brains of normal sheep and sheep with ceroid-lipofuscinosis. *Biochimica et Biophysica Acta* **834**: 159-163.

Palmer DN, Husbands DR, Winter PJ, Blunt JW, & Jolly RD. 1986a. Ceroid lipofuscinosis in sheep. I. Bis(monoacylglycero)phosphate, dolichol, ubiquinone, phospholipids, fatty acids, and fluorescence in liver lipopigment lipids. *Journal of Biological Chemistry* **261**: 1766-1772.

Palmer DN, Barns G, Husbands DR, & Jolly RD. 1986b. Ceroid Lipofuscinosis in Sheep. II. The major component of the lipopigment in liver, kidney, pancreas and brain is low molecular weight protein. *Journal of Biological Chemistry* **261**: 1773-1777.

Palmer DN, Martinus RD, Barns G, Reeves RD, & Jolly RD. 1988. Ovine ceroid-lipofuscinosis. I. Lipopigment composition is indicative of a lysosomal proteinosis. *American Journal of Medical Genetics* **5**: 141-158.

Palmer DN, Martinus RD, Cooper SM, Midwinter GG, Reid JC, & Jolly RD. 1989a. Ovine ceroid lipofuscinosis: The major lipopigment protein and the lipid-binding subunit of mitochondrial ATP synthase have the same NH_2-terminal sequence. *Journal of Biological Chemistry* **264**: 5736-5740.

Palmer DN, Fearnley IM, Medd SM, Walker JE, Martinus RD, Bayliss SL, Hall NA, Lake BD, Wolfe LS, & Jolly RD. 1989b. Lysosomal storage of the DCCD reactive proteolipid subunit of mitochondrial ATP synthase in human and ovine ceroid lipofuscinoses. *Advances in Experimental Medicine and Biology* **266**: 211-222.

Palmer DN, Fearnley IM, Walker JE, Hall NA, Lake BD, Wolfe LS, Haltia M, Martinus RD, & Jolly RD. 1992. Mitochondrial ATP synthase subunit c storage in the ceroid-lipofuscinoses (Batten Disease). *American Journal of Medical Genetics* **42**: 561-567.

Palmer DN, Bayliss SL, Clifton PA, & Grant VJ. 1993. Storage bodies in the ceroid-lipofuscinoses (Batten disease): Low-molecular-weight components, unusual amino acids and reconstitution of fluorescent bodies from non-fluorescent components. *Journal of Inherited Metabolic Diseases* **16**: 292-295.

Palmer DN, Bayliss SL, & Westlake VJ. 1995a. Batten disease and the mitochondrial ATP synthase subunit c turnover pathway. Raising antibodies to subunit c. *American Journal of Medical Genetics* **57**: 260-265.

Palmer TD, Ray J, & Gage FH. 1995b. FGF-2-responsive neuronal progenitors reside in proliferative and quiescent regions of the adult rodent brain. *Molecular and Cellular Neuroscience* **6**: 474-486.

Palmer DN, Jolly RD, van Mil HC, Tyynelä J, & Westlake VJ. 1997. Different patterns of hydrophobic protein storage in different forms of neuronal ceroid-lipofuscinosis (NCL, Batten disease). *Neuropediatrics* **28**: 45-48.

Palmer DN, Oswald MJ, Westlake VJ, & Kay GW. 2002. The origin of fluorescence in the neuronal ceroid lipofuscinoses (Batten disease) and neuron cultures from affected sheep for studies of neurodegeneration. *Archives of Gerontology and Geriatrics* **34**: 343-357.

Palmer DN & Tammen I. 2011. Large animal models. In: *The Neuronal Ceroid Lipofuscinoses (Batten Disease) 2nd edition* (Mole SE, Williams RE, & Goebel HH, eds.), pp. 284-320, Oxford University Press Inc., New York.

Panicker G, Meadows KS, Lee DR, Nisenbaum R, & Unger ER. 2007. Effect of storage temperatures on the stability of cytokines in cervical mucous. *Cytokine* **37**: 176-179.

Parent JM, Yu TW, Leibowitz RT, Geschwind DH, Sloviter RS, & Lowenstein DH. 1997. Dentate granule cell neurogenesis is increased by seizures and contributes to aberrant reorganization in the adult rat hippocampus. *Journal of Neuroscience* **17**: 3727-3738.

Parent JM. 2002. The role of seizure-induced neurogenesis in epileptogenesis and brain repair. *Epilepsy Research* **50**: 179-189.

Pariset L, Cappuccio I, Ajmone-Marsan P, Bruford M, Dunner S, Cortes O, Erhardt G, Prinzenberg EM, Gutscher K, Joost S, Pinto-Juma G, Nijman IJ, Lenstra JA, Perez T, Valentini A, & Consortium E. 2006. Characterization of 37 breed-specific single-nucleotide polymorphisms in sheep. *Journal of Heredity* **97**: 531-534.

Passini MA, Dodge JC, Bu J, Yang W, Zhao Q, Sondhi D, Hackett NR, Kaminsky SM, Mao Q, Shihabuddin LS, Cheng SH, Sleat DE, Stewart GR, Davidson BL, Lobel P, & Crystal RG. 2006. Intracranial delivery of CLN2 reduces brain pathology in a mouse model of classical late infantile neuronal ceroid lipofuscinosis. *Journal of Neuroscience* **26**: 1334-1342.

Passini MA, Bu J, Fidler JA, Ziegler RJ, Foley JW, Dodge JC, Yang WW, Clarke J, Taksir TV, Griffiths DA, Zhao MA, O'Rioradn CR, Schuchman EH, Shihabuddin LS, & Cheng SH. 2007. Combination brain and systemic injections of AAV provide maximal functional and

survival benefits in the Niemann-Pick mouse. *Proceedings of the National Academy of Sciences USA* **104**: 9505-9510.

Pears MR, Cooper JD, Mitchison HM, Mortishire-Smith RJ, Pearce DA, & Griffin JL. 2005. High resolution 1H NMR-based metabolomics indicates a neurotransmitter cycling deficit in cerebral tissue from a mouse model of Batten disease. *Journal of Biological Chemistry* **280**: 42508-42514.

Pears MR, Salek RM, Palmer DN, Kay GW, Mortishire-Smith RJ, & Griffin JL. 2007. A metabolomic investigation of CLN6 neuronal ceroid lipofuscinosis in affected South Hampshire sheep. *Journal of Neuroscience Research* **85**: 3494-3504.

Peress NS & Perillo E. 1995. Diferential expression of TGF-β 1 ,2, 3isotypes in Alzheimer's disease: A comparative immunohistochemical study with cerbral infarction, aged human and mouse control brains. *Journal of Neuropathology and Experimental Neurology* **54**: 802-811.

Pernthaner A, Cole SA, Morrison L, & Hein WR. 2005. Increased expression of interleukin-5 (IL-5), IL-13, and tumor necrosis factor alpha genes in intestinal lymph cells of sheep selected for enhanced resistance to nematodes during infection with *Trichostrongylus colubriformis*. *Infection and Immunity* **73**: 2175-2183.

Perry VH. 1998. A revised view of the central nervous system micro-environment and major histocompatibilty complex class II antigen presentation. *Journal of Neuroimmunology* **90**: 113-121.

Persaud-Sawin DA, VanDongen A, & Boustany RM. 2002. Motifs within the CLN3 protein: Modulation of cell growth rates and apoptosis. *Human Molecular Genetics* **11**: 2129-2142.

Persaud-Sawin DA & Boustany RM. 2005. Cell death pathways in juvenile Batten disease. *Apoptosis* **10**: 973-985.

Petersen B, Handwerker M, & Huppertz HI. 1996. Neuroradiological findings in classical late infantile neuronal ceroid-lipofuscinosis. *Pediatric Neurology* **5**: 344-347.

Pineda-Trujillo N, Cornejo W, Carrizosa J, Wheeler RB, Munera S, Valencia A, Agudelo-Arango J, Cogollo A, Anderson G, Bedoya G, Mole SE, & Ruiz-Linares A. 2005. A CLN5 mutation causing an atypical neuronal ceroid lipofuscinosis of juvenile onset. *Neurology* **64**: 740-742.

Plata-Salaman CR. 2002. Brain cytokines and disease. *Acta Neuropsychiatrica* **14**: 262-278.

Pocock JM & LiddleAC. 2001. Microglial signalling cascades in neurodegenerative disease. *Progress in Brain Research* **132**: 555-565.

Poët M, Kornak U, Schweizer M, Zdebik AA, Scheel O, Hoelter S, Wurst W, Schmitt A, Fuhrmann JC, Planells-Cases R, Mole SE, Hübner CA, & Jentsch TJ. 2006. Lysosomal storage disease upon disruption of the neuronal chloride transport protein ClC-6. *Proceedings of the National Academy of Sciences USA* **103**: 13854-13859.

Polzin VJ, Anderson DL, Anderson GB, BonDurant RH, Butler JE, Pashens RL, Penedo MCT, & Rowe JD. 1987. Production of sheep-goat chimeras by inner cell mass transplantation. *Journal of Animal Sciences* **65**: 325-330.

Pontikis CC, Cella CV, Parihar N, Lim MJ, Chakrabarti S, Mitchison HM, Mobley WC, Rezaie P, Pearce DA, & Cooper JD. 2004. Late onset neurodegeneration in the Cln3-/- mouse model of juvenile neuronal ceroid lipofuscinosis is preceded by low level glial activation. *Brain Resarch* **1023**: 231-242.

Porter MT, A.L. Fluharty AL, & Kihara H. 1971. Correction of abnormal cerebroside sulfate metabolism in cultured metachromatic leukodystrophy fibroblasts *Science* **172**: 1263-1265.

Porter JC, Messer A, & Peterson A. 1997. The motor neuron degeneration (*mnd*) gene acts intrinsically in motor neurons and peripheral fibroblasts. *Molecular and Cellular Neuroscience* **9**: 185-193

Prehn JH, Bindokas VP, Marcuccilli CJ, Krajewski S, Reed JC, & Miller RJ. 1994. Regulation of neuronal Bcl2 protein expression and calcium homeostasis by transforming growth factor type beta confers wide-ranging protection on rat hippocampal neurons. *Proceedings of the National Academy of Sciences USA* **91**: 12599-12603.

Puri NK, de Kretser T, & Brandon MR. 1987. Monoclonal antibodies to sheep MHC class II molecules recognize all HLA-D or subsets of HLA-D region products. *Human Immunology* **20**: 195-207.

Qasimi P, Ming-Lum A, Ghanipour A, Ong CJ, Cox ME, Ihle J, Cacalano N, Yoshimura A, & Mui AL. 2006. Divergent mechanisms utilized by SOCS3 to mediate interleukin-10 inhibition of tumour necrosis factor alpha and nitric oxide production by macrophages. *Journal of Biological Chemistry* **281**: 6316-6324.

Radonić A, Thulke S, Mackay IM, Landt O, Siegert W, & Nitsche A. 2004. Guideline to reference gene selection for quantitative real-time PCR. *Biochemical and Biophysical Research Communications* **313**: 856-862.

Raivich G, Bohatschek M, Kloss CU, Werner A, Jones LL, & Kreutzberg GW. 1999. Neuroglial activation repertoire in the injured brain: Graded response, molecular mechanisms and cues to physiological function. *Brain Research Reviews* **30**: 77-105.

Ramadan H, Al-Din AS, Ismail A, Balen F, Varma A, Twomey A, Watts R, Jackson M, Anderson G, Green E, & Mole SE. 2007. Adult neuronal ceroid lipofuscinosis caused by deficiency in palmitoyl protein thioesterase 1. *Neurology* **68**: 387-388.

Ramaswami U, Wendt S, Pintos-Morell G, Parini R, Whybra C, Leon Leal JA, Santus F, & Beck M. 2007. Enzyme replacement therapy with agalsidase alfa in children with Fabry disease. *Acta Paediatrica* **96**: 122-127.

Ranta S, Topcu M, Tegelberg S, Tan H, Ustubutun A, Saatci I, Dufke A, Enders H, Pohl K, Alembik Y, Mitchell WA, Mole SE, & Lehesjoki AE. 2004. Variant late infantile neuronal ceroid lipofuscinosis in a subset of Turkish patients is allelic to Northern epilepsy. *Human Mutation* **23**: 300-305.

Regulier E, Pereira de Almeida L, Sommer B, Aebischer P, & Déglon N. 2002. Dose-dependent neuroprotective effect of ciliary neurotrophic factor delivered via tetracycline – regulated lentiviral vectors in the quinolinic acid rat model of Huntington's disease. *Human Gene Therapy* **13**: 1981-1990.

Reijneveld JC, Taphoom MJB, & Voest EE. 1999. A simple mouse model for leptomeningeal metastases and repeated intrathecal therapy. *Journal of Neuro-Oncology* **42**: 137-142.

Reiner A, Del Mar N, Meade CA, Yang H, Dragatsis I, Zeitlin S, & Goldowitz D. 2001. Neurons lacking huntingtin differentially colonize brain and survive in chimeric mice. *Journal of Neuroscience* **21**:7608-7619.

Rider JA & Rider DL. 1988. Batten disease: Past, present and future. *American Journal of Medical Genetics* **5**: 21-26.

Rider JA & Rider DL. 1999. Thirty years of Batten disease research: Present status and future goals. *Molecular Genetics and Metabolism* **66**: 231-233.

Riley LG, Williamson P, Wynn PC, & Sheehy PA. 2008. Lactoferrin decreases primary bovine mammary epithelial cell viability and casein expression. *Journal of Dairy Research* **75**: 135-141.

Robinson TL, Sutherland IA, & Sutherland J. 2007. Validation of candidate bovine reference genes for use with real-time PCR. *Veterinary Immunology and Immunopathology* **115**: 160-165.

Rossant J & Frels WI. 1980. Interspecific chimeras in mammals: Successful production of live chimeras between *Mus musculus* and *Mus caroli*. *Science* **208**: 419-421.

Rota E, Bellone G, Rocca P, Bergamasco B, Emanuellu G, & Ferrero P. 2006. Increased intrathecal TGF-β1, but not IL-12, IFN-γ and IL-10 levels in Alzheimer's disease patients. *Journal of Neurological Sciences* **27**: 33-39.

Rothwell NJ. 1997. Sixteenth Gaddum memorial lecture December 1996. Neuroimmune interactions: The role of cytokines. *British Journal of Pharmacology* **121**: 841-847.

Rothwell N & G Luheshi. 2000. Interleukin 1 in the brain: Biology, pathology and therapeutic target. *Trends in Neurosciences* **23**: 618-625.

Sachs B. 1896. A family form of idiocy, generally fatal and associated with early blindness (amaurotic family idiocy). *New York State Journal of Medicine* **63**: 697-703.

Sakkas D & Vassalli JD. 1993. The preimplantation mammalian embryo. In: *Reproductive Health, Ares-Serono Symposia Series - Frontiers in Endocrinology*, Volume 2 (Campana A, Dreifuss JJ, Sizonenko P, Vassalli JD, & Villar J, eds.), p. 43-54, Ares Serono Symposia Publications, Rome.

Santavuori P, Haltia M, Rapola J, & Raitta C. 1973. Infantile type so-called neuronal ceroid-lipofuscinosis. Part 1. A clinical study of 15 patients. *Journal of the Neurological Sciences* **18**: 257-267.

Santavuori P, Heiskala H, Autti T, Johansson E, & Westermarck T. 1989. Comparison of the clinical courses in patients with juvenile neuronal ceroid lipofuscinosis receiving antioxidant treatment and those without antioxidant treatment. *Advances in Experimental Medicine and Biology* **266**: 273-282.

Sargsyan SA, Monk PN, & Shaw PJ. 2005. Microglia as potential contributors to motor neuron injury in amyotrophic lateral sclerosis. *Glia* **51**: 241-253.

Sastre M, Dewachter I, Rossner S, Bogdanovic N, Rosen E, Borghgraef P, Evert BO, Dumitrescu-Ozimek L, Thal DR, Landreth G, Walter J, Klockgether T, van Leuven F, & Heneka MT. 2006. Nonsteroidal anti-inflammatory drugs repress beta-secretase gene promoter activity by the activation of PPARgamma. *Proceedings of the National Academy of Sciences USA* **103**: 443-448.

Sawada M, Suzumura A, Hosoya M, Marunouchi T, & Nagatsu T. 1999. Interleukin-10 inhibits both production of cytokines and expression of cytokine receptors in microglia. *Journal of Neurochemistry* **72**: 1466-1471.

Schaffer K. 1905. Zur pathogenese der Tay-Sachsschen amaurotischen idiotie. *Neurologisches Zentralblatt* **24**: 386-392, 437-448.

Schägger H. 2006. Tricine–SDS-PAGE. *Nature Protocols* **1**: 16-22.

Schmid H, Cohen CD, Henger A, Irrgang S, Schlöndorff D, & Kretzler M. 2003. Validation of endogenous controls for gene expression analysis in microdissected human renal biopsies. *Kidney International* **64**: 356-360.

Schmittgen TD & Zakrajsek BA. 2000. Effect of experimental treatment on housekeeping gene expression: Validation by real-time, quantitative RT-PCR. *Journal of Biochemical and Biophysical Methods* **46**: 69-81.

Scott P. 1993. Collection and interpretation of cerebrospinal fluids in ruminants. *In Practise* **15**: 298-300.

Shacka JJ & Roth KA. 2007. Cathepsin D deficiency and NCL/Batten disease: There's more to death than apoptosis. *Autophagy* **3**: 474-476.

Sharp J, Wheeler R, Parker K, Gardiner M, Williams R, & Mole S. 2003. Spectrum of CLN6 mutations in variant late infantile neuronal ceroid lipofuscinosis. *Human Mutation* **22**: 35-42.

Sheline YI, Gado MH, & Kraemer HC. 2003. Untreated depression and hippocampal volume loss. *American Journal of Psychiatry* **160**: 1516-1518.

Sheng JG, Griffen WS, Royston MC, & Mrak RE. 1998. Distribution of interleukin-1-immunoreactive microglia in cerebral cortical layers: Implications for neuritic plaque formation in Alzheimer's disease. *Neuropathology and Applied Neurobiology* **24**: 278-283.

Shihabuddin LS & Aubert I. 2010. Stem cell transplantation for neurometabolic and neurodegenerative diseases. *Neuropharmacology* **58**: 845-854.

Siintola E, Topcu M, Kohlschütter A, Salonen T, JoensuuT, Anttonen A, & Lehesjoki A. 2005. Two novel CLN6 mutaions in variant late-infantile neuronal ceroid lipofuscinosis patienst of Turkish origin. *Clinical Genetics* **68**: 167-173.

Siintola E, Partanen S, Stromme P, Haapanen A, Haltia M, Maehlen J, Lehesjoki AE, & Tyynela J. 2006a. Cathepsin D deficiency underlies congenital human neuronal ceroid-lipofuscinosis. *Brain* **129**: 1438-1445.

Siintola E, Lehesjoki AE, & Mole SE. 2006b. Molecular genetics of the NCLs-status and perspectives. *Biochemica et Biophysica Acta* **1762**: 857-864.

Siintola E, Topcu M, Aula N, Lohi H, Minassian BA, Paterson AD, Liu XQ, Wilson C, Lahtinen U, Anttonen AK, & Lehesjoki AE. 2007. The novel neuronal ceroid lipofuscinosis gene MFSD8 encodes a putative lysosomal transporter. *American Journal of Human Genetics* **81**: 136-146.

Simard AR & Rivest S. 2004. Role of inflammation in the neurobiology of stem cells. *Neuroreport* **15**: 2305-2310.

Sims JE. 2002. IL-1 and IL-18 receptors, and their extended family. *Current Opinion in Immunology* **14**: 117-122.

Sjögren T. 1931. Die juvenile amaurotische Idiotie. Klinische und erblichkeitsmedizinsche Untersuchungen. *Hereditas, Lund* **14**: 197-426.

Skorupa AF, Fisher KJ, Wilson JM, Parente MK, & Wolfe JH. 1999. Sustained production of b-glucuronidase from localized sites after AAV vector gene transfer results in widespread distribution of enzyme and reversal of lysosomal storage lesions in a large volume of brain in mucopolysaccharidosis VII mice. *Chimeric Neurology* **160**: 17-27.

Sleat DE, Donnelly RJ, Lackland H, Liu CG, Sohar I, Pullarkat RK, & Lobel P. 1997. Association of mutations in a lysosomal protein with classical late-infantile neuronal ceroid lipofuscinosis. *Science* **277**:1802-1805.

Sleat DE, Lackland H, Wang Y, Sohar I, Xiao G, Li H, & Lobel P. 2005. The human brain mannose 6-phosphate glycoproteome: A complex mixture composed of multiple isoforms of many soluble lysosomal proteins. *Proteomics* **5**: 1520-1532.

Sleat DE, Wang Y, Sohar I, Lackland H, Li Y, Li H, Zheng H, & Lobel P. 2006. Identification and validation of mannose 6-phosphate glycoproteins in human plasma reveal a

wide range of lysosomal and non-lysosomal proteins. *Molecular and Cellular Proteomics* **5**: 1942-1956.

Sleat DE, Zheng H, & Lobel P. 2007. The human urine mannose 6-phosphate glycoproteome. *Biochemica et Biophysica Acta* **1774**: 368-3372.

Smeed JA, Watkins CA, Rhind SM, & Hopkins J. 2007. Differential cytokine gene expression profiles in the three pathological forms of sheep paratuberculosis. *BMC Veterinary Research* **3**: 18.

Smith MC & Dunn HO. 1981. Freemartin condition in a goat. *Journal of the American Veterinary Medical Association* **178**: 735-737.

Smith D, Wallom KL, Williams IM, Jeyakumar M, & Platt FM. 2009. Beneficial effects of anti-inflammatory therapy in a mouse model of Niemann-Pick disease type C1. *Neurobiology of Disease* **36**: 242-251.

Sohur US, Emsley JG, Mitchell BD, & Macklis JD. 2006. Adult neurogenesis and cellular brain repair with neural progenitors, precursors and stem cells. *Philosophical Transactions of the Royal Society B: Biological Sciences* **361**: 1477-1497.

Somlev B, Hansen-Melander E, Melander Y, & Holm L. 1970. XX/XY chimerism in leucocytes of two intersexual pigs. *Hereditas* **64**: 203-210.

Sondhi D, Hackett NR, Apblett RL, Kaminsky SM, Pergolizzi RG, & Crystal RG. 2001. Feasibility of gene therapy for late neuronal ceroid lipofuscinosis. *Archives of Neurology* **58**: 1793-19798.

Sondhi D, Peterson DA, Giannaris EL, Sanders CT, Mendez BS, De B, Rostkowski AB, Blanchard B, Bjugstad K, Sladek JR, Redmond DE, Leopold PL, Kaminsky SM, Hackett NR, & Crystal RG. 2005. AAV2-mediated CLN2 gene transfer to rodent and non-human primate brain results in long-term TPP-I expression compatible with therapy for LINCL. *Gene Therapy* **12**: 1618-1632.

Sondhi D, Peterson DA, Edelstein AM, del Fierro K, Hackett NR, & Crystal RG. 2008. Survival advantage of neonatal CNS gene transfer for late infantile neuronal ceroid lipofuscinosis. *Experimental Neurology* **213**: 18-27.

Sostak P, Theil D, Stepp H. Roeber S, Kretzschmar HA, & Straube A. 2007. Detection of bone marrow-derived cells expressing a neural phenotype in the human brain. *Journal of Neuropathology and Experimental Neurology* **66**: 110-116.

Spielmeyer W. 1905. Über familiären amaurotische idiotie. *Neurologisches Zentralblatt* **24**: 620-621.

Sriram K, Miller DB, & O'Callaghan JP. 2006. Minocycline attenuates microglial activation but fails to mitigate striatal dopaminergic neurotoxicity: Role of tumor necrosis factor-α. *Journal of Neurochemistry* **96**: 706-718.

Stein CS, Martins I, & Davidson BL. 2005. The lymphocytic choriomeningitis virus envelope glycoprotein targets lentiviral gene transfer vector to neural progenitors in the murine brain. *Molecular Therapy* **11**: 382-389.

Steinfeld R, Reinhardt K, Schreiber K, Hillebrand M, Kraetzner R, Brück W, Saftig P, & Gärtner J. 2006. Cathepsin D deficiency is associated with a human neuronal ceroid lipofuscinosis. *Brain* **129**:1438-1445.

Stengel E. 1826. Beretning om et maerkeligt sygdomstilfoelde hos fire sødskende i naerheden af Røraas. *Eyr et medicinsk Tidskrift* **1**: 347-352.

Stephens SA, Brownlie J, Charleston B, & Howard CJ. 2003. Differences in cytokine synthesis by the sub-populations of dendritic cells from afferent lymph. *Immunology* **110**: 48-57.

Stern MS & Wilson IB. 1972. Chimeric studies on the organization of the preimplantation mouse embryo. I. Fusion of asynchronously cleaving eggs. *Journal of Embryology and Experimental Morphology* **28**: 247-254.

Stern MS. 1973. Chimeras obtained by aggregation of mouse eggs with rat eggs. *Nature* **243**: 472-473.

Streit WJ. 1990. An improved staining method for rat microglial cells using the lectin from Griffonia simplicifolia (GSA I-B4). *Journal of Histochemistry and Cytochemistry* **38**: 1683-1686.

Streit WJ & Graeber MB. 1993. Heterogeneity of microglial and perivascular cell populations: Insights gained from the facial nucleus paradigm. *Glia* **7**: 68-74.

Streit WJ, Mrak RE, & Griffin WS. 2004. Microglia and neuroinflammation: A pathological perspective. *Journal of Neuroinflammation* **1**: 14.

Strijbos P & Rothwell NJ. 1995. Interleukin-1 beta attenuates excitatory amino acid-induced neurodegeneration *in vitro*: Involvement of nerve growth factor. *Journal of Neuroscience* **15**: 3468-3474.

Stroemer RP & Rothwell NJ. 1997. Cortical protection by localized striatal injection of IL-1ra following ischemia in the rat. *Journal of Cerebral Blood Flow and Metabolism* **17**: 597-604.

Suzuki T, Higgins PJ, & Crawford DR. 2000. Control selection for RNA quantitation. *Biotechniques* **29**: 332-337.

Suzumura A, Sawada M, Yamamoto H, & Marunouchi T. 1993. Transforming growth factor-beta suppresses activation and proliferation of microglia *in vitro*. *Journal of Immunology* **151**: 2150-2158.

Svennerholm L. 1962. The chemical structure of normal human brain and Tay–Sachs gangliosides. *Biochemical and Biophysical Research Communications* **9**: 436-441.

Sykes M & Sachs DH. 2001. Mixed chimerism. *Philosophical Transactions of the Royal Society B: Biological Sciences* **356**: 707-726.

Szameit S, Vierlinger K, Farmer L, Tuschl H, & Noehammer C. 2008. Microarray-based *in vitro* test system for the discrimination of contact allergens and irritants: Identification of potential marker genes. *Clinical Chemistry* **54**: 525-533.

Tamaki SJ, Jacobs Y, Dohse M, Capela A, Cooper JD, Reitsma M, He D, Tushinski R, Belichenko PV, Salehi A, Mobley W, Gage FH, Huhn S, Tsukamoto AS, Weissman IL, & Uchida N. 2009. Neuroprotection of host cells by human central nervous system stem cells in a mouse model of infantile neuronal ceroid lipofuscinosis. *Stem Cell* **5**: 310-319.

Tammen I, Houweling PJ, Frugier T, Mitchell NL, Kay GW, Cavanagh JAL, Cook RW, Raadsma HW, & Palmer DN. 2006. A missense mutation (c.184C>T) in ovine CLN6 causes neuronal ceroid lipofuscinosis in Merino sheep whereas affected South Hampshire sheep have reduced levels of CLN6 mRNA. *Biochimica et Biophysica Acta* **1762**: 898-905.

Tanaka R, Komine-Kobayashi M, Mochizuki H, Yamada M, Furuya T, Migita M, Shimada T, Mizuno Y, & Urabe T. 2003. Migration of enhanced green fluorescent protein expressing bone marrow-derived microglia/macrophage into the mouse brain following permanent focal ischemia. *Neuroscience* **117**: 531-539.

Tao W, Mallard B, Karrow N & Bridle B. 2004. Construction and application of a bovine immune-endocrine cDNA microarray. *Veterinary Immunology and Immunopathology* **101**: 1-17.

Tarkowski AK. 1961. Mouse chimeras developed form fused eggs. *Nature* **190**: 857-860.

Tarkowski E, Wallin A, Blennow K, & Tarkowski A. 1999. Intracerebral production of tumor necrosis factor-alpha, a local neuroprotective agent, in Alzheimer disease and vascular dementia. *Journal of Clinical Immunology* **19**: 223-230.

Tatton WG, Chalmers-Redman RM, Elstner M, Leesch W, Jagodzinski FB, Stupak DP, Sugrue MM, & Tatton NA. 2000. Glyceraldehyde-3-phosphate dehydrogenase in neurodegeneration and apoptosis signalling. *Journal of Neural Transmission* **60**: 77-100.

Taupin P. 2008. Adult neurogenesis, neuroinflammation and therapeutic potential of adult neural stem cells. *International Journal of Medical Sciences* **5**: 127-132.

Teixeira CA, Espinola J, Huo L, Kohlschütter J, Persaud Sawin DA, Minassian B, Bessa CJP, Guimarães A, Stephan DA, Miranda MCS , MacDonald ME , Ribeiro MG, & Boustany RMN. 2003. Novel Mutations in the CLN6 gene causing a variant late infantile neuronal ceroid lipofuscinosis. *Human Mutation* **21**: 502-508.

Terry RD & Korey SR. 1960. Membranous cytoplasmic granules in infantile amaurotic idiocy. *Nature* **188**: 1000-1002.

Thomas ED, Lochte HL, Lu WC, & Ferrebee JW. 1957. Intravenous infusion of bone marrow in patients receiving radiation and chemotherapy. *New England Journal of Medicine* **157**: 491-196.

Thompson L. 1993. The first kids with new genes. *Time* **141**: 50-53.

Thomson JA, Itskovitz-Eldor J, Shapiro SS, Waknitz MA, Swiergiel JJ, Marshall VS, & Jones JM. 1998. Embryonic stem cell lines derived from human blastocysts. *Science* **282**: 1145-1147.

Tidball JG & St.Pierre BA. 1996. Apoptosis of macrophages during the resolution of muscle inflammation. *Journal of Leukocyte Biology* **59**: 380-388.

Tracey KJ & Cerami A. 1994. Tumor necrosis factor: A pleiotropic cytokine and therapeutic target. *Annual Review of Medicine* **45**: 491-503.

Trono D. 2000. Lentiviral vectors: Turning a deadly foe into a therapeutic agent. *Gene Therapy* **7**: 20-23.

Troost D, Claessen N, van den Oord JJ, Swaab DF, & de Jong JM. 1993. Neuronophagia in the motor cortex in amyotrophic lateral sclerosis. *Neuropathology and Applied Neurobiology* **19**: 390-397.

Turrin NP & Plata-Salamán CR. 2000. Cytokine–cytokine interactions and the brain. *Brain Research Bulletin* **51**: 3-9.

Tuszynski MH, Hoi Sang U, Amaral DG, & Gage FH. 1990. Nerve growth factor infusion in the primate brain reduces lesion-induced cholinergic neuronal degeneration. *Journal of Neuroscience* **10**: 3604-3614.

Tuszynski MH, Hoi Sang U, Yoshida K, & Gage FH. 1991. Recombinant human nerve growth factor infusions prevent cholinergic neuronal degeneration in the adult primate brain. *Annals of Neurology* **30**: 625-636.

Tyynelä J, Palmer DN, Baumann M, & Haltia M. 1993. Storage of saposins A and D in infantile neuronal ceroid liupofuscinosis. *FEBS Letters* **330**: 8-12.

Tyynela J, Suopanki J, Santavuori P, Baumann M, & Haltia M. 1997. Variant late infantile neuronal ceroid-lipofuscinosis: Pathology and biochemistry. *Journal of Neuropathology and Experimental Neurology* **56**: 369-375.

Tyynelä J, Sohar I, Sleat DE, Gin RM, Donnelly RJ, Baumann M, Haltia M, & Lobel P. 2000. A mutation in the ovine cathepsin D gene causes a congenital lysosmal storage disease with profound neurodegeneration. *EMBO Journal* **19**: 2786-2792.

Unsicker K & Krieglstein K. 2000. Co-activation of TGF-beta and cytokine signaling pathways are required for neurotropic functions. *Cytokine Growth Factor Review* **11**: 97-102.

Unsicker K & Krieglstein K. 2002. TGF-betas and their roles in the regulation of neuron survival. *Advances in Experimental Medicne and Biology* **513**: 353-374.

Url A, Bauder B, Thalhammer J, Nowotny N, Kolodziejek J, Herout N, Furst S, & Weissenbock H. 2001. Equine neuronal ceroid lipofuscinosis. *Acta Neuropathologica* **101**: 410-414.

Vallieres L, Campbell IL, Gage FH, & Sawchenko PE. 2002. Reduced hippocampal neurogenesis in adult transgenic mice with chronic astrocyte production of interleukin-6. *Journal of Neuroscience* **22**: 486-492.

Van Diggelen OP, Keulemans JL, Winchester B, Hofman IL, Vanhanen SL, Santavuori P, & Voznyi YV. 1999. A rapid fluorogenic palmitoyl-protein thioesterase assay: Pre- and postnatal diagnosis of INCL. *Molecular Genetics and Metabolism* **66**: 240-244.

Van Diggelen OP, Keulemans JLM, Kleijer WJ, Thoboi S, Tilikete C, & Voznyi YV. 2001. Pre- and postnatal enzyme analysis for infantile, late infantile and adult neuronal ceroid lipofuscinosis (CLN 1 and CLN2). *European Journal of Paediatric Neurology* **5**: 189-192

Vandesomple J, De Preter K, Pattyn F, Poppe B, Van Roy N, De Paepe A, & Speleman F. 2002. Accurate normalization of real-time quantitative RT-PCR data by geometric averaging of multiple internal control genes. *Genome Biology* **3**: 1-11.

van Praag H, Christie BR, Sejnowski TJ, & Gage FH. 1999a. Running enhances neurogenesis, learning, and long-term potentiation in mice. *Proceedings of the National Academy of Sciences USA* **96**: 13427-3431.

van Praag H, Kempermann G, & Gage FH. 1999b. Running increases cell proliferation and neurogenesis in the adult mouse dentate gyrus. *Nature Neuroscience* **2**: 266-270.

Venstrom KA & Reichardt LF. 1993. Extracellular matrix. 2: Role of extracellular matrix molecules and their receptors in the nervous system. *Federation of American Societies for Experimental Biology* **7**: 996-1003.

Vesa J, Hellsten E, Verkruyse LA, Camp LA, Rapola J, Santavuori P, Hofmann SL, & Peltonen L .1995. Mutations in the palmitoyl protein thioesterase gene causing infantile neuronal ceroid lipofuscinosis. *Nature* **376**: 584-587.

Vila M, Jackson-Lewis V, Guégan C, Wu DC, Teismann P, Choi DK, Tieu K, & Przedborski S. 2001. The role of glial cells in Parkinson's disease. *Current Opinion in Neurology* **14**: 483-489.

Vitkovic L, Bockaert J, & Jacque C. 2000. “Inflammtory” cytokines: Neuromodulators in normal brain? *Journal of Neurochemistry* **74**: 457-471.

Viviani B, Bartesaghi S, Corsini E, Corrado L, Galli CL, & Marinovich M. 2004. Cytokines role in neurodegenerative events. *Toxicology Letters* **149**: 85-89.

Vogler C, Levy B, Grubb JH, Galvin N, Tan Y, Kakkis E, Pavloff N, & Sly WS. 2005. Overcoming the blood–brain barrier with high-dose enzyme replacement therapy in murine mucopolysaccharidosis VII. *Proceedings of the National Academy of Sciences USA* **102**: 14777-14782.

Vogt H. 1905. Über familiar amaurotische Idiotie und verwandte Krankheitsbilder. *Monatsschrift der Psychiatrischen Neurologie* **18**: 161-171, 310-357.

von Figura K & Hasilik A. 1986. Lysosomal enzymes and their receptors. *Annual Review of Biochemistry* **55**: 167-193.

Wada R, Tifft CJ, & Proia RL. 2000. Microglial activation precedes acute neurodegeneration in Sandhoff disease and is suppressed by bone marrow transplantation. *Proceedings of the National Academy of Sciences USA* **97**: 10954-10959.

Walkley SU, March PA, Schroeder CE, Wurzelmann S, & Jolly RD. 1995. Pathogenesis of brain dysfunction in Batten disease. *American Journal of Medical Genetics* **57**: 196-203.

Walton NM, Sutter BM, Laywell ED, Levkoff LH, Kearns SM, Marshall GP 2nd, Scheffler B, & Steindler DA. 2006. Microglia instruct subventricular zone neurogenesis. *Glia* **54**: 815-825.

Wang T & Brown MJ. 1999. mRNA quantification by real time TaqMan polymerase chain reaction: Validation and comparison with RNase protection. *Analytical Biochemistry* **269**: 198-201.

Wang Q, Tang XN, & Yenari MA. 2007. The inflammatory response in stroke. *Journal of Neuroimmunology* **184**: 53-68.

Wang D, Zhang W, Kalfa TA, Grabowski G, Davies S, Malik P, & Pan D. 2009. Reprogramming erythroid cells for lysosomal enzyme production leads to visceral and CNS cross-correction in mice with Hurler syndrome. *Proceedings of the National Academy of Sciences USA* **106**: 19958-19963.

Warburton MJ & Bernardini F. 2000. Tripeptidyl-peptidase I deficiency in classical late-infantile neuronal ceroid lipofuscinosis brain tissue. Evidence for defective peptidase rather than proteinase activity. *Journal of Inherited Metabolic Disease* **23**: 145-154.

Warburton MJ & Bernardini F. 2002. Tripeptidyl-peptidase I is essential for the degradation of sulphated cholecystokinin-8 (CCK-8S) by mouse brain lysosomes. *Neuroscience Letters* **331**: 99-102.

Ware CF. 2005. Network communications: Lymphotoxins, LIGHT, and TNF. *Annual Review of Immunology* **23**: 787-819.

Watson DJ, Kobinger GP, Passini MA, Wilson JM, & Wolfe JH. 2002. Targeted transduction patterns in the mouse brain by lentivirus vectors pseudotyped with VSV, Ebola, Mokola, LCMV, or MuLV envelope proteins. *Molecular Therapy* **5**: 528-537.

Watson DJ, Passini MA, & Wolfe JH. 2005. Transduction of the choroid plexus and ependyma in neonatal mouse brain by vesicular stomatitis virus glycoprotein-pseudotyped lentivirus and adeno-associated virus type 5 vectors. *Human Gene Therapy* **16**: 49-56.

Weimer JM, Kriscenski-Perry E, Elshatory Y, & Perace DA. 2002. The neuronal ceroid lipofuscinoses: Mutations in different proteins result in similar disease. *Neuromolecular Medicine* **1**: 111-124.

Weis J, Saxena S, Evangelopoulos ME, & Kruttge A. 2003. Trophic factors in neurodegenerative disorders. *Life* **55**: 353-357.

Weissenbock H & Rossel C. 1997. Neuronal ceroid-lipofuscinosis in a domestic cat: Clinical, morphological and immunohistochemical findings. *Journal of Comparative Pathology* **117**: 17-24.

Weleber RG, Gupta N, Trzupek KM, Wepner MS, Kurz DE, & Milam AH. 2004. Electrographic and clinicopathologic correlations of retinal dysfunction in infantile neuronal ceroid lipofuscinosis (infantile Batten disease). *Molecular Genetics and Metabolism* **83**: 128-137.

Westermarck T, Aberg L, Santavuori P, Antila E, Edlund P, & Atroshi F. 1997. Evaluation of the possible role of coenzyme Q10 and vitamin E in juvenile neuronal ceroid-lipofuscinosis (JNCL). *Molecular Aspects of Medicine* **18**: 259-262.

Westlake VJ, Jolly RD, Bayliss SL, & Palmer DN. 1995a. Immunocytochemical studies in the ceroid-lipofuscinoses (Batten disease) using antibodies to subunit c of mitochondrial ATP synthase. *American Journal of Medical Genetics* **57**: 177-181.

Westlake VJ, Jolly RD, Jones BR, Mellor DJ, Machon R, Zanjani ED, & Krivit W. 1995b. Hematopoietic cell transplantation in fetal lambs with ceroid-lipofuscinosis. *American Journal of Medical Genetics* **57**: 365-368.

Wheeler RB, Sharp JD, Schultz RA, Joslin JM, Williams RE, & Mole SE .2002. The gene mutated in variant late-infantile neuronal ceroid lipofuscinosis (CLN6) and in nclf mutant

mice encodes a novel predicted transmembrane protein. *American Journal of Human Genetics* **70**:537-542.

Whiteland JL, Shimeld C, Nicholls SM, Easty DL, Williams NA, & Hill TJ. 1997. Immunohistochemical detection of cytokines in paraffin-embedded mouse tissues. *Journal of Immunological Methods* **210**: 103-108.

Whitney NP, Eidem TM, Peng H, Huang Y, & Zheng JC. 2009. Inflammation mediates varying effects in neurogenesis: Relevance to the pathogenesis of brain injury and neurodegenerative disorders. *Journal of Neurochemistry* **108**: 1343-1359.

Whitton PS. 2007. Inflammation as a causative factor in the aetiology of Parkinson's disease. *British Journal of Pharmacology* **150**: 963-976.

Williams TJ, Munro RK, & Shelton JN. 1990. Production of inter-species chimeric calves by aggregation of *Bos indicus* and *Bos Taurus* demi-embryos. *Reproduction, Fertilitry and Development* **2**: 385-394.

Williams RE, Lake BD, Elleder M, & Sharp JD. 1999. CLN6 Variant late infantile/early juvenile NCL. In: *The Neuronal Ceroid Lipofuscinosis (Batten disease)* (Goebel HH, Mole SE, & Lake BD, eds.), p. 102-113, IOS Press, Amsterdam.

Williams RE, Aberg L, Autti T, Goebel HH, Kohlschütter A, & Lönnqvist T. 2006. Diagnosis of the neuronal ceroid lipofuscinoses: An update. *Biochemica et Biophysica Acta* **1762**: 865-872.

Wiltrout C, Lang B, Yan Y, Dempsey RJ, & Vemuganti R. 2007. Repairing brain after stroke: A review on post-ischemic neurogenesis. *Neurochemistry International* **50**: 1028-1041.

Wisniewski KE, Kida E, Golabek A, Kaczmarski W, Connell F, & Zhong N. 2001. Neuronal ceroid lipofusinoses: Classification and diagnosis. In: *Batten disease: Diagnosis, Treatment, and Research* (Wisniewski KE & Zhong N, eds.), p. 1-34, Academic Press, San Diego, CA.

Wiznerowicz M & Trono D. 2005. Harnessing HIV for therapy, basic research and biotechnology. *Trends in Biotechnology* **23**: 42-47.

Wong ML & Medrano JF. 2005. Real-time PCR for mRNA quantitation. *BioTechniques* **39**: 75-85.

Woodall CJ, Maclaren LJ, & Watt NJ. 1997. Differential levels of mRNAs for cytokines, the interleukin-2 receptor and class II DR/DQ genes in ovine interstitial pneumonia induced by maedi visna virus infection. *Veterinary Pathology* **34**: 204-211.

Worgall S, Sondhi D, Hackett NR, Kosofsky B, Kekatpure MV, Neyzi N, Dyke JP, Ballon D, Heier L, Greenwald BM, Christos P, Mazumdar M, Souweidane MM, Kaplitt MG, & Crystal RG. 2008. Treatment of late infantile neuronal ceroid lipofuscinosis by CNS administration of a serotype 2 adeno-associated virus expressing CLN2 cDNA. *Human Gene Therapy* **19**: 463-474.

Wraith JE, Clarke LA, Beck M, Kolodny EH, Pastores GM, Muenzer J, Rapoport DM, Berger KI, Swiedler SJ, Kakkis ED, Braakman T, Chadbourne E, Walton-Bowen K, & Cox GF. 2004. Enzyme replacement therapy for mucopolysaccharidosis I: A randomized, double-blinded, placebo-controlled, multinational study of recombinant human alpha-L-iduronidase (laronidase). *Journal of Paediatrics* **144**: 581-588.

Wu JP, McMahon EJ, Matsuda J, Suzuki K, & Matsushima GK. 2001. Expression of immune-related molecules is downregulated in twitcher mice following bone marrow transplantation. *Journal of Neuropathology and Experimental Neurology* **60**: 1062-1074.

Wu YP and Proia RL. 2004. Deletion of macrophage-inflammatory protein 1 alpha retards neurodegeneration in Sandhoff disease mice. *Proceedings of the National Academy of Sciences USA* **101**: 8425-8430.

Wyss-Coray T. 2006. Inflammation in Alzheimer disease: Driving force, bystander or beneficial response? *Nature Medicine* **12**:1005-1015

Wyss-Coray T, Feng L, Masliah E, Ruppe MD, Lee HS, Toggas SM, Rockenstein EM, & Mucke L. 1995. Increased central nervous system production of extracellular matrix components and development of hydrocephalus in transgenic mice overexpressing transforming growth factor-beta1. *American Journal of Pathology* **147**: 53–67.

Yamada M, Onodera M, Mizuno Y, & Mochizuki H. 2004. Neurogenesis in olfactory bulb identified by retroviral labelling in normal and I-Methyl-4-phenyl-1,2,3,6-tetrahydropyridine-treated adult mice. *Neuroscience* **124**: 173-181.

Yan YP, Sailor KA, Lang BT, Park SW, Vemuganti R, & Dempsey RJ. 2007. Monocyte chemoattractant protein-1 plays a critical role in neuroblast migration after focal cerebral ischemia. *Journal of Cerebral Blood Flow and Metabolism* **27**: 1213-1224.

Yanamoto H, Miyamoto S, Tohnia N, Nagata I, Xue JH, & Nakano Y. 2005. Induced spreading depression activates persistent neurogenesis in the subventricular zone, generating cells with markers for divided and early committed neurons in the caudate putamen and cortex. *Stroke* **36**: 1544-1550.

Yang MS, Min KJ, & Joe E. 2007. Multiple mechanisms that prevent excessive brain inflammation. *Journal of Neuroscience Research* **85**: 2298-2305.

Yang P, Arnold SA, Habas A, Hetman M, & Hagg T. 2008. Ciliary neurotrophic factor mediates dopamine D2 receptor-induced CNS neurogenesis in adult mice. *Journal of Neuroscience* **28**: 2231-2241.

Yasukawa H, Misawa H, Sakamoto H, Masuhara M, Sasaki A, Wakioka T, Ohtsuka S, Imaizumi T, Matsuda T, Ihle JN, & Yoshimura A. 1999. The JAK-binding protein JAB inhibits Janus tyrosine kinase activity through binding in the activation loop. *EMBO Journal* **18**: 1309-1320.

Yoshikawa M, Uchida S, Ezaki J, Rai T, Hayama A, Kobayashi K, Kida Y, Noda M, Koike M, Uchiyama Y, Marumo F, Kominami E, & Sasaki S .2002. CLC-3 deficiency leads to phenotypes similar to human neuronal ceroid lipofuscinosis. *Genes to Cells* **7**: 597-605.

Yoshimi K, Ren YR, Seki T, Yamada M, Ooizumi H, Onodera M, Saito Y, Murayama S, Okano H, Mizuno Y, & Mochizuki H. 2005. Possibility for neurogenesis in substantia nigra of parkinsonian brain. *Annals of Neurology* **58**: 31-40.

You Q, Karrow NA, Cao H, Rodriquez A, Mallard BA, & Boermans HJ. 2008. Variation in the ovine cortisol response to systemic bacterial endotoxin challenge is predominantly determined by signalling within the hypothalamic-pituitary-adrenal axis. *Toxicology and Applied Pharmacology* **230**: 1-8.

Yuen EC, Howe CL, Li Y, Holtzman DM, & Mobley WC. 1996. Nerve growth factor and the neurotrophic factor hypothesis. *Brain and Development* **18**: 362-368.

Zaremba J & Losy J. 2001. Early TNF-alpha levels correlate with ischaemic stroke severity. *Acta Neurologica Scandinavica* **104**: 288-295.

Zeman W & Donahue S. 1963. Fine structure of the lipid bodies in juvenile amaurotic idiocy. *Acta Neuropathologica* **3**: 144-149.

Zeman W & Dyken P. 1969. Neuronal ceroid-lipofuscinosis (Batten's disease): Relationship to amaurotic family idiocy? *Pediatrics* **44**: 570-583.

Zeman W, Donahue S, Dyken P, & Green J. 1970. The neuronal ceroid lipofuscinosis (Batten–Vogt syndrome). In: *Handbook of Clinical Neurology* (Vinken PJ & Bruyn GW, eds.), p. 588-679, Elsevier/North-Holland Biomedicul Press, Amsterdam.

Zhang Z, Lee YC, Kim SJ, Choi MS, Tsai PC, Xu Y, Xiao YJ, Zhang P, Heffer A, & Mukherjee AB. 2006. Palmitoyl-protein thioesterase-1 deficiency mediates the activation of the unfolded protein response and neuronal apoptosis in INCL. *Human Molecular Genetics* **15**: 337-346.

Zhao M, Momma S, Delfani K, Carlen M, Cassidy RM, Johansson CB, Brismar H, Shupliakov O, Frisen J, & Janson AM. 2003. Evidence for neurogenesis in the adult mammalian substantia nigra. *Proceedings of the National Academy of Sciences USA* **100**: 7925-7930.

Zhao C, Ling Z, Newman MB, Bhatia A, & Carvey PM. 2007. TNF-α knockout and minocycline treatment attenuates blood-brain barrier leakage in MPTP-treated mice. *Neurobiology of Disease* **26**: 36-46.

Zhong N. 2001. Molecular testing for neuronal ceroid lipofuscinoses. *Advances in Genetics* **45**: 141-158.

Zhu Y, Yang GY, Ahlemeyer B, Pang L, Che XM, Culmsee C, Klumpp S, & Krieglstein J. 2002. Transforming growth factor-beta1 increases bad phosphorylation and protects neurons against damage. *Journal of Neuroscience* **22**: 3898-3909.

Zipp F & Aktas O. 2006. The brain as a target of inflammation: Common pathways link inflammatory and neurodegenerative diseases. *Trends in Neurosciences* **29**: 518-27.

Appendix A

A.1 Zinc salt fixative

12.1g Tris base

0.5g Calcium acetate

pH to 7.0-7.4 in 1L H_2O[1]

5g Zinc chloride

5g Zinc acetate

Store at 4ºC

A.2 RIPA buffer

50mM Tris-HCL, pH 7.4

1% NP-40

0.25% LDS

150mM NaCl

Made up in H_2O[1] and stored at 4°C

A.3 Gel electrophoresis and Western blotting reagents

15% Resolving Gel: 1.9ml 40% acrylamide:bisacrylamide (29:1 w/w)

1.25ml 1.5M Tris pH 8.8

50µl 10% LDS

1.8ml H_2O[1]

25µl 10% ammonium persulphate (APS,Pharmacia Biotech, Uppsala, Sweden)

2.5µl Tetramethylethylenediamine (TEMED, BDH)

4% Stacking Gel:	0.25ml 40% acrylamide:bisacrylamide (29:1 w/w)
	0.63ml 0.5M Tris pH6.8
	25µl 10% LDS
	1.6ml H_2O[1]
	12.5µl 10% APS
	2.5µl TEMED
Electrophoresis Buffer:	25mM Tris
	192mM glycine
	0.1% LDS
Transfer Buffer:	25mM Tris
	192mM glycine
	20% methanol

A.4 10 X TBE

54g Tris base

27.5g Boric acid

20ml 0.5M EDTA pH 8.0

In 1L total H_2O[1]

A.5 SOC medium

2g Bacto-tryptone

0.5g Yeast extract

1ml 1M NaCl

0.25ml 1M KCl

In 97mls H_2O[1]

Autoclaved and cooled to RT

1ml sterilised 2M Mg^{2+} stock

1ml sterilised 2M glucose

Up to 100ml with H_2O[1], pH 7.0

A.6 LB agar

10g NaCl

10g Tryptone

5g Yeast extract

20g Agar

Up to 1L with H_2O[1], pH 7.0

Autoclave

A.7 LB broth + ampicillin

5g NaCl

10g Tryptone

5g Yeast extract

Up to 1L with H_2O[1], pH 7.0

Autoclave

100µg/ml Ampicillin

[1] Water deionised by electrodeionization was used for all experiments described in this thesis.